Theory and Experimental Evaluation of the Super Sweep Spectrum Analyzer

Masao Nagano

Mar. 31, 2008

Supervisor: Prof. Koh-ichiroh Morita

The Graduate University for Advanced

Contents

1 1 Introduction 1

1.1 Spectrum Analyzer ・・・・・・・・・・・・・・・・・・ 1

1.1.1 Backgroun ・・・・・・・・・・・・・・・・・・・・・・ 1

1.1.2 The properties and problems of the sweep method ・・・・・ 2

1.2 History of Spectrum Analyzers ・・・・・・・・・・・・・ 3

1.3 Purposes of this Research ・・・・・・・・・・・・・・・・ 5

1.4 Method ・・・・・・・・・・・・・・・・・・・・・・・・ 5

1.5 Representative result ・・・・・・・・・・・・・・・・・ 6

1.6 Composition of this thesis ・・・・・・・・・・・・・・・ 7

1.7 Glossary ・・・・・・・・・・・・・・・・・・・・・・ 7

1.8 Technical Terms on Spectrum Analyzers ・・・・・・・・・ 9

1.9 Reference ・・・・・・・・・・・・・・・・・・・・・・ 11

2 Review of Sweep-Signal Method ・・・・・・・・・ 13

2.1 Introduction ・・・・・・・・・・・・・・・・・・・・ 13

2.2 Principle of Sweep-Signal Spectrum Analyzers ・・・・・ 14

2.2.1 Outline of Spectrum Analyzers ・・・・・・・・・ 14

2.2.2 Frequency Converter *) ・・・・・・・・・・・・・ 16

2.2.3 Input LPF ・・・・・・・・・・・・・・・・・・・ 17

2.3 Analog signal processing with swept local oscillator ・・・ 18

2.3.1 Frequency converter with Swept Local Oscillator ・・・ 18

2.3.2 Output of IF BPF ・・・・・・・・・・・・・・・・・ 20

2.3.3 Multi Conversion ・・・・・・・・・・・・・・・・・ 22

2.3.4 Restriction of Sweep time ・・・・・・・・・・・・・ 23

2.3.5 Permissible distortion ・・・・・・・・・・・・・・ 25

2.4 Digital IF ・・・・・・・・・・・・・・・・・・・・・ 26

2.4.1 Digital IF method ・・・・・・・・・・・・・・・・・ 27

2.4.2 Quadrature Detection ・・・・・・・・・・・・・・・ 28

2.4.3 Digitized IF Signal with Swept Local oscillator ・・・・ 30

2.4.4 Base Band Signal ・・・・・・・・・・・・・・・・・ 32

2.5 Analysis of Sweep Spectrum analyzer ・・・・・・・・・ 36

2.5.1 Spectrum Analyzer as Pseudo Fourier Transformer ・・・ 36

2.5.2 Restriction of sweep rate ・・・・・・・・・・・・・・ 39

2.5.3 Gauss Function as Resolution Filter ・・・・・・・・・ 43
2.5.4 Simulation of Over-Swept response ・・・・・・・・・・ 47
2.5.5 Analog Gaussian Filter ・・・・・・・・・・・・・・ 50
2.5.6 Resolution Bandwidth ・・・・・・・・・・・・・・ 51
2.5.7 Response against two tone Signals ・・・・・・・・・・ 54
2.6 Other Properties of Sweep Spectrum Analyzers ・・・・・ 57
2.6.1 Shape Factor ・・・・・・・・・・・・・・・・・・ 57
2.6.2 Time Domain measurement ・・・・・・・・・・・・・ 58
2.6.3 Noise level and Resolution Bandwidth ・・・・・・・・ 61
2.6.4 Zero Carrier ・・・・・・・・・・・・・・・・・・ 64
2.7 Bandwidth of Signals and Resolution Filters ・・・・・・・ 65
2.7.1 Signal under the measurement ・・・・・・・・・・・ 65
2.7.2 Observed signal ・・・・・・・・・・・・・・・・・ 65
2.7.3 Discussion: ・・・・・・・・・・・・・・・・・・ 71
2.7.4 Conclusion ・・・・・・・・・・・・・・・・・・ 73
2.8 Sweep method and FFT method ・・・・・・・・・・・・ 75
2.8.1 Digital IF method ・・・・・・・・・・・・・・・・ 75
2.8.2 FFT ・・・・・・・・・・・・・・・・・・・・・ 75
2.8.3 Frequency resolution (RBW) in FFT ・・・・・・・・ 77
2.8.4 Bandwidth of the processed signal and dynamic range ・・ 78
2.8.5 Ripple on the spectrum ・・・・・・・・・・・・・・ 79
2.8.6 DC Response in FFT method ・・・・・・・・・・ 80
2.9 Multiple-FFT Measurement ・・・・・・・・・・・・・ 81
2.9.1 Outline of the measurement ・・・・・・・・・・ 81
2.9.2 Sweep Rate ・・・・・・・・・・・・・・・・・・ 81
2.9.3 Actual Measurement Time ・・・・・・・・・・・・・ 83
2.9.4 Demerit of the FFT Method ・・・・・・・・・・ 85
2.10 Summary ・・・・・・・・・・・・・・・・・・・・・ 86
2.11 Reference ・・・・・・・・・・・・・・・・・・・・ 88

3 Theory and System of Super Sweep Method ・・・ 89

3.1 Introduction ・・・・・・・・・・・・・・・・・・・・ 88
3.2 Theory of super sweep method ・・・・・・・・・・・・ 88
3.2.1 Back ground of super sweep method ・・・・・・・・・・ 88
3.2.2 Mathematical model of super sweep method ・・・・・ 88
3.2.3 Implementation of Super Sweep method ・・・・・・ 92
3.3 Signal Processing of Super Sweep Method ・・・・・・ 94
3.3.1 Inspection of Super Sweep Method ・・・・・・ 94

3.3.2 Inspection of negative chirp filter ・・・・・・ 95
3.3.3 Gauss function as negative chirp filter ・・・・・・ 99
3.3.4 Practical negative chirp filter ・・・・・・・・・・ 100
3.3.5 Maximum Sweep rate ・・・・・・・・・・・・・・ 101
3.4 Complex filter and Display ・・・・・・・・・・・・・・ 103
3.5 Summary ・・・・・・・・・・・・・・・・・・・・・・ 104
3.6 Reference ・・・・・・・・・・・・・・・・・・・・・・ 104

4 Experiments of new method ・・・・・・・・・・ 105
4.1 Introduction ・・・・・・・・・・・・・・・・・・・・・ 105
4.2 Experimental system ・・・・・・・・・・・・・・・・・ 105
4.2.1 Overview of the system ・・・・・・・・・・・・・・・ 105
4.2.2 Signal flow of the system ・・・・・・・・・・・・・・ 107
4.2.3 External view of the system ・・・・・・・・・・・・・ 108
4.2.4 Chain of filters ・・・・・・・・・・・・・・・・・ 110
4.2.5 Implementation of the Gaussian filter ・・・・・・・・・ 111
4.2.6 Sampling in the frequency domain ・・・・・・・・・ 112
4.2.7 Setting Up Parameters ・・・・・・・・・・・・・・・ 113
4.2.8 Coefficients of Negative Chirp Gaussianl Filters ・・・ 115
4.2.9 Span and Sweep time Corresponding to Plotted *1/k* ・・・ 115
4.2.10 Discrete Integral to obtain a Spectrum ・・・・・・・ 118
4.3 Property and Configuration of DDC (GC4016) ・・・・・・・ 120
4.3.1 Outline of Digital Down Converter Channels ・・・・・・ 120
4.3.2 CIC Filter ・・・・・・・・・・・・・・・・・・・・ 121
4.3.3 Distribution Arithmetic (DA) method FIR Filter ・・・・ 123
4.3.4 Apportionment of Decimation ・・・・・・・・・・・ 124
4.3.5 Coefficients of FIR filters ・・・・・・・・・・・・・ 124
4.4 Specification of the experimental system ・・・・・・・・・・ 128
4.5 Summary ・・・・・・・・・・・・・・・・・・・・・・ 129
4.6 Reference ・・・・・・・・・・・・・・・・・・・・・・ 129
4.7 Appendix: Latency: ・・・・・・・・・・・・・・・・ 129

5 Result and Discussion ・・・・・・・・・・・・・・ 131
5.1 Introduction ・・・・・・・・・・・・・・・・・・・・・ 131
5.2 Measured Spectrums ・・・・・・・・・・・・・・・・・ 131
5.2.1 Sample of measurements ・・・・・・・・・・・・・ 131
5.2.2 The way to verify the over sweep response ・・・・・・・ 134
5.2.3 The way to estimate the 3dB bandwidth of a peak ・・・・ 134

5.2.4 Estimation of the peak Level ・・・・・・・・・・ 134
5.3 Result ・・・・・・・・・・・・・・・・・・・・・・・・ 138
5.3.1 Numerical result ・・・・・・・・・・・・・・・・・・・ 138
5.3.2 Result of the Peak level reduction ・・・・・・・・・・ 141
5.3.3 Result of the broadening of RBW ・・・・・・・・・・ 143
5.4 Discussion ・・・・・・・・・・・・・・・・・・・・・・ 135
5.4.1 Peak level Reduction ・・・・・・・・・・・・・・ 145
5.4.2 Broadening of the resolution bandwidth ・・・・・・・ 145
5.4.3 Total consideration of the maximum sweep rate ・・・・・ 145
5.5 Summary ・・・・・・・・・・・・・・・・・・・・・・ 146
5.6 Reference ・・・・・・・・・・・・・・・・・・・・・・ 146

6 Additional discussions ・・・・・・・・・・・・・・・ 147
6.1 Introduction ・・・・・・・・・・・・・・・・・・・・ 147
6.2 Required condition for fast sweep ・・・・・・・・・・ 147
6.2.1Operation time ・・・・・・・・・・・・・・・・・・・ 147
6.2.2 Operation time of each sample of a spectrum ・・・・・・ 148
6.2.3 Required performance of the operation ・・・・・・・ 150
6.2.4 Relation between the IF bandwidth and the sampling frequency 151
6.2.5 Implementation of the fast complex filter ・・・・・・・ 152
6.3 Display of new method ・・・・・・・・・・・・・・・ 154
6.4 Filter margin and synchronization of frequency ・・ 156
6.4.1 Over view of latency and synchronization of the system ・・ 156
6.4.2 Margin corresponding to chain of filters ・・・・・・・ 156
6.4.3 Synchronization between spectrums and ramp signals ・・ 158
6.5 Response of the IF filter ・・・・・・・・・・・・・・・・ 160
6.6 Super Sweep Method and Chirp Z-Transform ・・・・・・・ 161
6.6.1 Theoretical Background ・・・・・・・・・・・・・・ 161
6.6.2 Numerical Analysis ・・・・・・・・・・・・・・・・ 164
6.6.3 Numerical Analysis of a Sweep Method ・・・・・・・ 167
6.7 Response against two-tone signals ・・・・・・・・・・ 169
6.8 Influence of the noise ・・・・・・・・・・・・・・・・ 172
6.8.1 Noise in Spectrum Analyzers ・・・・・・・・・・・ 172
6.8.2 Phase Noise of the local oscillator ・・・・・・・・・・ 172
6.8.3 Noise in the IF signal ・・・・・・・・・・・・・・・ 174
6.9 Examples of Spectrums ・・・・・・・・・・・・・・・・ 177
6.9.1 RBW 1Hz ・・・・・・・・・・・・・・・・・・・・・ 177
6.9.2 RBW 100Hz ・・・・・・・・・・・・・・・・・・・・ 178

6.9.3 RBW 1kHz ・・・・・・・・・・・・・・・・・・・・ 179
6.9.4 RBW 100kHz ・・・・・・・・・・・・・・・・・・・・ 180
6.10 View of spurious peaks ・・・・・・・・・・・・・・・・ 182
6.11 Comparison of the methods ・・・・・・・・・・・・・・・・ 185
6.12 Reference ・・・・・・・・・・・・・・・・・・・・ 187

7 Application in Radio Astronomy ・・・・・・・・・・・・ 189
7.1 Introduction ・・・・・・・・・・・・・・・・・・・・ 189
7.2 Improvement of SNR against sweep method ・・・・・・・・ 190
7.3 Observation of W49N ・・・・・・・・・・・・・・・・・・・・ 196
7.3 Comparison against FFT method , Observation of W49N ・・・ 196
7.4 Observation of Methanol Maser at Yamaguchi ・・・・・・・ 201
7.5 Discussion for Observations of 7.2, 7.3 and 7.4 ・・・・・・・ 203
7.6 Chirp Z-Transform System of GREAT ・・・・・・・ 204
7.7 Characteristic of each method ・・・・・・・・・・・ 206
7.7.1 Maximum sweep rate ・・・・・・・・・・・・・・・・ 206
7.7.2 Sample data on a spectrum ・・・・・・・・・・・・・・ 207
7.7.3 Product of Receptive Bandwidth and Aquisition-Time ・・・ 208
7.8 Conclusion ・・・・・・・・・・・・・・・・・・・・ 211
7.9 Reference ・・・・・・・・・・・・・・・・・・・・ 212

8 Conclusions ・・・・・・・・・・・・・・・・・・・・ 213
8.1 Conclusion ・・・・・・・・・・・・・・・・・・・・・・ 213
8.2 The representative contributions ・・・・・・・・・・ 214
8.3 Reference ・・・・・・・・・・・・・・・・・・・・・・ 215

9 List of Publications ・・・・・・・・・・・・・・ 216

List of Tables

2.1 Peak Level Reduction vs. Normalized Sweep Rate ・・・・・・・・・ 49
2.2 Broadening of Rbw against Normalized Sweep Rate ・・・・・・・・・ 50
2.3 Specification of signal in Fig.2.32~2.35 ・・・・・・・・・・・・・ 65
2.4 Characteristics of Windows ・・・・・・・・・・・・・・・・・ 77
2.5-a: Results of Type A (Rohde&Schwaltz FSU in 2006) ・・・・・・・・・ 85
2.5-b: Results of Type B (Agilent ESA in 2006) ・・・・・・・・・・・・ 85
2.6 Characteristics of each methods ・・・・・・・・・・・・・・・・ 87

4.1 Principal parameters under the experiments ・・・・・・・・・・ 114
4.2 Normalized sweep rate 1/k and the SPAN and Sweep time
RBW of all conditions are 300Hz ・・・・ 117
4.3 Apportionment of Decimation ・・・・・・・・・・・・ 124
4.4 Coefficient of CFPR filters ‘cfir_68’ (21TAP) ・・・・・・・・・ 125
4.5 The Coefficient of the PFPR filter ‘pfir_68’ (63TAP) ・・・・・・ 125
4.6 Primary specification of the experimental system ・・・・・・・・ 128

5.1 Results of *S1* ・・・・・・・・・・・・・・・・・・・・・ 138
5.2 Results of *S2* ・・・・・・・・・・・・・・・・・・・・・ 139
5.3 Results of conventional spectrum analyzer (*Cnv*), R3264 ・・・・・・ 140
5.4 Peak Level Reduction vs. Normalized sweep rate ・・・・・・・・・ 141
5.5 1/k : Peak Level reduction corresponds to -0.1dB ・・・・・・・・・ 142
5.6 Broadening of RBW vs. Normalized sweep rate *1/k* ・・・・・・・・ 143
5.7 1/k corresponds to *Rbw'/Rbw=1.1* ・・・・・・・・・・・・・・ 144

6.1 Operation time of the experimental system (DSP complex filter) ・・・ 148
6.2 Operation time of the experimental system (complex filter of the DDC) 153
6.3 Experimental conditions of Fig.6.12 ・・・・・・・・・・・・・ 169
6.4 Comparisons of spectrum measurement methods ・・・・・・・・ 185
7.1 Conditions of Measurements ・・・・・・・・・・・・・・・・ 191
7.2 SNR against Integral time ・・・・・・・・・・・・・・・・・ 194
7.3 Standard deviations against Integral times ・・・・・・・・・・・ 169

List of Figures

1.1 Example of a over sweep-rate response ・・・・・・・・・・・・ 3
1.2 Comparison of a sweep rate between the sweep method and the super sweep method ・・ 6
1.3 Samples of display of a spectrum analyzer ・・・・・・・・・・・・・ 10

2.1 Block Diagram of a Classic Sweep Spectrum Analyzer ・・・・・・ 15
2.2 Block Diagram of a Frequency Converter ・・・・・・・・・・・・・ 17
2.3 Frequency around a mixer ・・・・・・・・・・・・・・・・・ 17
2.4 Frequencies of signals around a mixer with the swept local ・・・・・・ 19
2.5 Time-Frequency diagram around a mixer with the swept local ・・・ 21
2.6 Multi frequency converter ・・・・・・・・・・・・・・・・・・・ 22
2.7 Response of an RBW filter measuring CW signal ・・・・・・・・ 24
2.8 Examples of over sweep-rate responses ・・・・・・・・・・・・・ 25
2.9 Block Diagram of sweep spectrum analyzers with digital IF ・・・・・・ 15
2.10 Detail of digital IF section ・・・・・・・・・・・・・・・・・ 27
2.11 Quadrature Detection in Frequency Domain ・・・・・・・・・ 30
2.12 Digitized IF signal with swept local oscillator: $S_{IF}(t)$ ・・・・・・ 32
2.13 Quadrature Detected IF Signal through a wide band LPF: $S_B(t)$ ・・ 33
2.14 Quadrature Detected IF Signal through a RBW Filter : $S_{B\_RBW}(t)$ ・・ 34
2.15 Spectrum Extracted from a Signal $S_{B\_RBW}(t)$ ・・・・・・・・・ 34
2.16 Signal Flow of Sweep Spectrum analyzers with Digital IF system ・・ 35
2.17 Simplified Block Diagram of Sweep Spectrum Analyzers with Digital IF 36
2.18 Conceptual diagram of sweep time and rate ・・・・・・・・・・・ 40
2.19 Example of over swept-rate response ・・・・・・・・・・・・ 41
2.20 Power spectrum under over-sweep ・・・・・・・・・・・・・・・ 42
2.21 Simulation of the integral Eq.(2.47-b) : Response of Gaussian filter against chirped base band signal
(a) SPAN=10kHz, RBW=1kHz, T_S =20msec ,Peak level = -0.10dB, 1/k=0.5 45
(b) SPAN=10kHz,RBW=1kHz, T_S =4msec, Peak level = -1.73dB, 1/k=2.5 45
(c) SPAN=1 k Hz, RBW=1 k Hz, T_S =2msec, Peak level = -0.1dB, 1/k=0.5 46
2.22 Peak Level Reduction vs. Normalized Sweep Rate ・・・・・・・・ 47
2.23 Broadening of *Rbw* vs *1/k* ・・・・・・・・・・・・・・・・ 48

2.24 Spectrums of two Tone signals ・・・・・・・・・・・・・・・・ 53
2.25 Base Band Signals and Spectrum against two-tone Signal
Span=10kHz, Rbw=1kHz, Sweep Time=20mse
(a) Spectrums of two signals, ⊿f=1500Hz ・・・・・・・・・・・・・・ 55
(b) Spectrums of two signals, ⊿f=1330Hz ・・・・・・・・・・・・・・ 55
(c) Spectrums of two signals, ⊿f=1000Hz ・・・・・・・・・・・・・・ 56
(d) Spectrums of two signals, ⊿f=800Hz ・・・・・・・・・・・・・・ 56
2.26 Shape factor (Bandwidth selectivity) ratio of 60dB and 3dB bandwidth 58
2.27 Time domain measurement ・・・・・・・・・・・・・・・・・ 59
2.28 Spectrum of Dynamical Signal ・・・・・・・・・・・・・・・・ 60
2.29 Equivalent Noise Bandwidth (ENBW) of a resolution filter ・・・・・・ 61
2.30 Relation between noise level and RBW
(a) Observed noise level changes as $10\log(Rbw_1 / Rbw_0)$ ・・・・・ 63
(b) low level signal and RBW ・・・・・・・・・・・・・・ 63
2.31 Zero Carrier ・・・・・・・・・・・・・・・・・・・・・・・ 64
2.32 Measurement of wideband signals with RBW 1MHz ・・・・・・・ 67
2.33 Measurement of wideband signals with RBW 100kHz ・・・・・・・ 68
2.34 Measurement of wideband signals with RBW 1kHz ・・・・・・・ 69
2.35 Measurement of wideband signals with SPAN 200kHz ・・・・・・・ 71
2.36 Convolution of FM signal and RBW filter ・・・・・・・・・・ 72
2.37 Dynamics of FM modulation and the RBW filters ・・・・・・・・・・ 74
2.38 Example of Block diagram of an FFT method ・・・・・・・・・・ 75
2.39 Concept of FFT ・・・・・・・・・・・・・・・・・・・・・・・ 76
2.40 Example of a Scallop Loss ・・・・・・・・・・・・・・・・・ 78
2.41 Bandwidth of processed signal in seep method and FFT method ・・ 79
2.42 Ripples on Spectrums in FFT method ・・・・・・・・・・・・・・ 80
2.43 Jointed Spectra by Step Sweep method ・・・・・・・・・・・・・ 82
2.44 Sweep rate Against *Rbw* ・・・・・・・・・・・・・・・・・・ 84
2.45 Ripple on a Spectrum by Step Sweep method ・・・・・・・・・・ 86

3.1 Diagram of our Experimental System ・・・・・・・・・・・・ 93
3.2 Overview of Digital Down Converter (DDC) ・・・・・・・・・・・ 93
3.3 Base band signal in sweep method ・・・・・・・・・・・・・・ 95
3.4 Product of Chirped base band signal and negative chirp function ・・・ 97

3.5 Gaussian Filter: RBW=300Hz ・・・・・・・・・・・・・・・・・ 98
3.6 Gaussian Filter(RBW=300Hz) $g_n(t)$ as a Negative chirp filter ・・・・・・99
3.7 Time limited Gausian filter ・・・・・・・・・・・・・・ 100
3.8 Frequency response for χ=*2.6* and *3.0* ・・・・・・・・・・・・ 101
3.9 Response time and the frequency range of a negative chirp filter ・・・・ 102
3.10 Signal Flow of a Complex filter ・・・・・・・・・・・・・・・ 103

4.1 Overview of Our Experimental System ・・・・・・・・・・・・ 106
4.2 Real Panel view of our Experimental System ・・・・・・・ 106
4.3 Over view of Signal Flow of our Experimental System ・・・・・・・ 107
4.4 Over view of the Experimental System ・・・・・・・・・・・・ 108
4.5 Internal view of DSP Unit ・・・・・・・・・・・・・・・・・ 109
4.6 Internal block diagram of the DSP Unit ・・・・・・・・・・・・ 109
4.7 Chain of Band Limit Filters ・・・・・・・・・・・・・・・ 111
4.8 Figure of a Gauss filter (dB) and Minimum Sampling Rate ・・・・・・・ 112
4.9 Sampling Rate of a spectrum data ・・・・・・・・・・・・・・・・ 113
4.10-a Coefficients of the Gaussianl Filter of *S1*
$\sigma = Span / T_S = 40 \cdot 10^3 / 0.1 = 4 \cdot 10^5$ ・・・・・・・・・・・・・ 113
4.10-b Coefficients of the Gaussianl Filter of *S2*
$\sigma = Span / T_S = 40 \cdot 10^3 / 0.03 = 1.33 \cdot 10^6$ ・・・・・・・・・・・・・ 113
4.11 Discrete Integral to extract a Spectrum ・・・・・・・・・・・・・ 119
4.12 Down Converter Channels ・・・・・・・・・・・・・・・・・ 120
4.13 CIC Decimation Filter ・・・・・・・・・・・・・・・・・・・・ 121
4.14 CIC Filter Frequency Response for N=4,M=1,R=7 and fc=1/8 ・・・・・・ 122
4.15 Frequency Response of CIC Filter around zero frequency ・・・・・・ 122
4.16 Illustrated algorithm of an FIR filter ・・・・・・・・・・・・・ 123
4.17 Concept of FIR filter in DA method ・・・・・・・・・・・・・・ 123
4.18 Figure of ‘cfir_68’ (21TAP) ・・・・・・・・・・・・・・・・・ 126
4.19 Figure of ‘pfir_68’ (63TAP) ・・・・・・・・・・・・・・・・・ 126
4.20 Frequency response of CFIR with PFPR ・・・・・・・・・・・・・ 127

5.1 (a) Spectrums with various *1/k* of Sweep method ・・・・・・・・・ 132
5.1 (2) Spectrums with various *1/k* of Super Sweep method ・・・・・・・・ 133
5.2 Three point data that decide the 3dB bandwidth, *Rbw*’ ・・・・・・ 135
5.3 Three points around the peak ・・・・・・・・・・・・・・・・・ 137

5.4 Peak Level Reduction vs. Normalized sweep rate ・・・・・・・ 142
5.5 Broadening of the RBW vs. 1/k ・・・・・・・・・・・・・・・ 144

6.1 Interval of frequency and time between each sample of a spectrum 149
6.2 Relation between IF filter and sampling frequency ・・・・・・・・ 151
6.3 Complex filter using DA FIR filter of DDC:GC4016 ・・・・・・・・・・
152
6.4 Multi trace Display on PC ・・・・・・・・・・・・・・・・・ 155
6.5 Artificial Analog trace Display of R3264 ・・・・・・・・・ 155
6.6 Chain of Filters and its Latency ・・・・・・・・・・・・・・・ 156
6.7 Latency and Margin for a Filter ・・・・・・・・・・・・・・・ 157
6.8 Synchronization on abscissa ・・・・・・・・・・・・・・・・ 159
6.9 Signal flow of Spectrum analyzers by FFT method ・・・・・・・ 160
6.10 Spectrum of FFT method with IF frequency response ・・・・・ 160
6.11 Concept of Chirp Z-Transform ・・・・・・・・・・・・・・・ 162
6.12 (a) Spectrum by Super Sweep Method (SdB),
Gaussian Filter (g) And Base Band signal (I and Q) ・・・・ 164
6.12 (b) I and Q part of the Spectrum in (a) ・・・・・・・・・・・・ 165
6.12 (c) Transition of phase of Spectrum in (a) : $\tan^{-1}(Q/I)$ of (b) ・・・・ 165
6.12 (d) Differentiation of phase in (b) ・・・・・・・・・・・・・・ 166
6.12 (e) Second differentiation of phase in (b) ・・・・・・・・・・・・ 166
6.13 (a) Spectrum by Sweep Method (SdB),
Gaussian Filter (g) and Base Band signal (I and Q) ・・・・・ 167
6.13 (b) Transition of phase of Spectrum of (a) ・・・・・・・・・ 168
6.13 (c) Second differentiation of phase in (b) ・・・・・・・・・ 168
6.14 (a) Spectrums of two signals, ⊿f=1500Hz, Sweep Time 2msec ・・・・ 170
6.14 (b) Spectrums of two signals, ⊿f=1000Hz, Sweep Time 2msec ・・・・ 170
6.14 (c) Spectrums of two signals, ⊿f=1500Hz, Sweep Time 10msec ・・・・ 171
6.14 (d) Spectrums of two signals, ⊿f=1000Hz, Sweep Time 10msec ・・・ 171
6.15 Model of noise of spectrum analyzers ・・・・・・・・・・・・ 172
6.16 Phase noise of Sweep Spectrum Analyzers ・・・・・・・・・・・ 173
6.17 Deformed diagram of our experimental system ・・・・・・・・・ 174
6.18 Obtained Spectrums using Super Sweep Method ・・・・・・・・・ 175
6.19 Noise of IF signal and Spectrum ・・・・・・・・・・・・・・・・ 176

6.20 Spectrum with RBW 1Hz ・・・・・・・・・・・・・・・・・ 177
6.21 Spectrum with RBW 100Hz and 1kHz, SPAN100kHz ・・・・・ 178
6.22 (a) Spectrum with RBW 1kHz , SPAN4MHz ・・・・・・・・・ 179
6.22 (b) Spectrum with RBW 1kHz , SPAN400kHz ・・・・・・・・・ 180
6.23 (a) Spectrum with RBW 100kHz , SPAN 1GHz ・・・・・・・・・ 181
6.23 (b) Spectrum with RBW 100kHz , SPAN 100MHz ・・・・・・・・・ 181
6.24 (a) Spectrum measured by R3264 ・・・・・・・・・・・・ 182
6.24 (b) Spectrum measured by Super sweep method ・・・・・・・・・ 183
6.24 (c) Over lay of Spectrums of (a) and (b) ・・・・・・・・・・・・ 183
6.25 Time/Frequency Diagram of IF signal and resolution filter ・・・・・ 184

7.1 System for estimating SNR ・・・・・・・・・・・・・・・・ 191
7.2 (a) Measured Spectrum using sweep spectrum analyzer with AVG 3 191
7.2 (b) Spectrum measured with AVG 30 ・・・・・・・・・・・・・・・ 192
7.3 (a) Spectrum measured using the super sweep method with AVG 73 ・・ 193
7.3 (b) Spectrum measured using Super sweep method with AVG 732 ・・・ 193
7.4 SNR against Integral time ・・・・・・・・・・・・・・・・・・・ 194
7.5 Standard deviations against Integral times ・・・・・・・・・・・・ 195
7.6 Spectrum of Hydrogen Maser of W49N ・・・・・・・・・・・・・ 196
7.7 (a) Spectrum measured using Super sweep method ・・・・・・・・・ 197
7.7 (b) Spectrum measure with 3.4 sec integral ・・・・・・・・・・・・ 198
7.7 (c) Spectrum measured with 29.4 sec integral ・・・・・・・・・・・・ 199
7.8 SNR against Average time length ・・・・・・・・・・・・・ 200
7.9 Signal raised by methanol maser of 9.67GHz. ・・・・・・・・・ 201
7.10 Same signal with Fig.7.9 measure by Super sweep method ・・・・・ 202
7.11 Astronomical requirements
on spectral resolution and bandwidth ・・・・・ 204
7.12 Diagram of SOFIA-GREAT-CTS spectrometer ・・・・・・・・・ 205
7.13 Output of SAW compressor of SOFIA-GREAT-CTS spectrometer ・・・・ 205
7.14 Adaptive Configuration Corresponding to the Measurement Condition 206
7.15 Time Frequency Diagram of Measured Spectrum
and Processing Bandwidth: Real-Time FFT Method ・・・・・ 209
7.16 Time Frequency Diagram of Measured Spectrum
and Processing Bandwidth: Sweep Method ・・・・・・・・ 209

7.17 Time Frequency Diagram of Measured Spectrum
and Processing Bandwidth: Super Sweep Method ・・・・・・・・・ 210
7.18 Super Sweep with very wide-band *Flt* ・・・・・・・・・・・・・ 211

Acknowledgements

I express my appreciation to Prof. Noriyuki Kawaguchi for kind consulting, for his encouragement and efforts to introduce this thesis to PhD justification stage of Graduate University of Advanced Studies. I acknowledge Prof. Koh-ichiro Morita, who gave me precious advices. Pof. Yoshihiro Chikada gave me important suggestion, which recommended me to clear up the relationship between the methods of chirp-Z transform and the super sweep. Due to this suggestion, I could upgrade a quality of this thesis. I thank Prof. M.Fujishita, who was a student of doctor class when I was an undergraduate student (G4) of A-Lab. of Nagoya University, and taught me fundamentals of Fourier transform and interferometer. I requested Prof. Fujishita to be a member of judging committee. I thank him for accepting the request. I thank to Dr. S.Iguchi, Dr. H.Hanada and Dr. S.Tuboshita for gracious advices. I also thank Mr.Hara and Mr.Kijima for their support; they are members of Mizusawa VELA Observatory of NAOJ. I would like to thank Dr.K.Fujisawa and Dr.K.Wajima for their supports to use 32m antenna of Yamaguchi.

I thank Dr.M.Sone for supporting this research from the early stage. I could not start this research without a support from him. I also thank Mr.T.Onodera, who had been my partner until he finished his master course.

I should thank all the people of SKY-Ware Co, President T.Shinhama, Mr.H.Motomatsu, Mr.K.Kamii and Mr.H.Mikami. This research work was made using the measurement instrument system ‘Algo-Chest’. It was produced by SKY-Ware Co. under my plan.

Author thank President K.Tanaka Micronix Co. for giving an opportunity to develop spectrum analyzers and to apply the new method.

Chapter 1
Introduction

This thesis introduces ‘Super-Sweep method’; it is a new method of sweep-signal spectrum analysis, which give high-speed measurements. Since spectrum analyzers developed in 1960’s, they have been improved over years, but their fundamental method of it has not changed. Especially, sweep-signal spectrum analyzers have a property whose sweep rate is restricted, which is in inverse proportional to the square of the frequency resolution and the restriction has not been improved. We intended to break the restriction and made an experiment system that achieved a fast sweep measurement.

1.1 Spectrum Analyzer

1.1.1 Background

This thesis suggests ‘Super-Sweep method’, which is a new method of a spectrum analysis, which improved a sweep rate of the analysis drastically.

A Sweep spectrum analyzer is measurement instrument that measures electronic signals in the frequency domain and provides spectrums. This analyzer is very useful and necessary for developing and testing radio communication devices or instruments. Especially, it is the most convenient instrument to measure the Radio Frequency (RF) signal. In recent years, wireless communication technologies have progressed rapidly. In radio astronomy, a sweep spectrum analyzer is commonly used as a receiving system. The analyzer is desired to measure a wider band, with finer resolution, in a wider dynamic range in a time as short as possible.

Sweep spectrum analyzers have representative characteristics as follows [1][2][[3][4].

1) The measurement time (i.e. the sweep time) is inversely proportional to the square of the resolution bandwidth (*Rbw*). For example, in the case that the measurement frequency band (*Span*) is 1MHz, *Rbw* is 10kHz and 1 kHz, the sweep time is 0.2sec and 20 sec, respectively.

2) The noise level of measured spectrum is proportional to the *Rbw*. It requires narrower *Rbw* to obtain a spectrum with lower noise level, but it demands longer sweep time.

3) The analyzer has sensitivity for one frequency at one instant. The analyzer presents the spectrum as a persistence of vision or a trace. In the case that the sweep time is long, the analyzer cannot follow dynamical changes of the spectrum.

To overcome above characteristic, some types of the analyzers employ the 'Digital IF filter'. The HP3588 produced by Hewlett-Packerd Inc. is one of them and achieves the measurement speed in maximum four times faster than a conventional analyzer by estimating and correcting distortions of the spectrum [5].

The FFT method is another way to overcome the characteristics. The FFT method achieves a fast measurement with fine resolution (e.g. with *Rbw* is narrower than 10kHz). But this method is not suitable for measurement of wideband span and resolution (e.g. with *Rbw* wider than 10kHz or 30kHz). In these conditions, the sweep method is suitable at the point of measurement time, cost and other specifications such as dynamic range [6]. In the FFT method, the frequency span of one measurement is narrower than the Nyquist frequency of the AD/C. To measures frequency span wider than the Nyquist frequency, we have to measure multiple times by stepping up the tuning frequency and join the results. The number of the measurement increases in proportion to the ratio of the span per the Nyquist frequency.

The difference of characteristics between the sweep method and FFT method is not only the measurement rate but also some other characteristics. These methods have merit and demerit respectively. We should use them selectively in accordance with the purpose. The relation and difference will be described in section 2.8.

1.1.2 Properties and problems of the sweep method

A sweep spectrum analyzer is the most convenient instrument to observe a Radio Frequency (RF) signal. But it has imperfectness as a Fourier transformer. In this method, the sweep time T_S is restricted as

$$T_S \geq k_0 \frac{Span}{Rbw^2}, \qquad (1.1)$$

where k_0 is a constant value, which is 2~3 experimentally, ***Span*** is a measured frequency bandwidth, and ***Rbw*** is a resolution bandwidth. In the case that the T_S is too short against the restriction, the measured spectrum has some distortion (it is shown in Fig.2.8). Typically, three types of the distortion exist,

1) Resolution expansion: An expansion of the frequency resolution (*Rbw*),
2) Level reduction: A reduction of the peak level,
3) Frequency shift: A shift of the spectrum toward higher frequency.

We called these phenomenon 'over sweep-rate response', which are described in chapter 2. And they appear on the spectrum except when the sweep time is infinity. In some conventional spectrum analyzers, the level reduction of 0.1dB is permitted maximally, and the value k_0 of Eq.(1.1) is decided corresponding to the reduction 0.1dB [1] [2][3][4].

One example of the 'Frequency shift' is shown in Fig.1.1, where *Span* and *Rbw* is 20kHz and 1kHz, respectively. There are two spectrums, the sweep time of the bold line is 60msec and it of the thin line is 10sec. The sweep time 60msec is longer 20msec than the typical value corresponding to Eq.(1.1). We can see that the bold line, which is shifted to right side.

Sweep spectrum analyzer has a characteristic that it cannot measure without any distortion. We have to use it finding a compromise between the accuracy and measurement time. One of the compromises is Eq.(1.1).

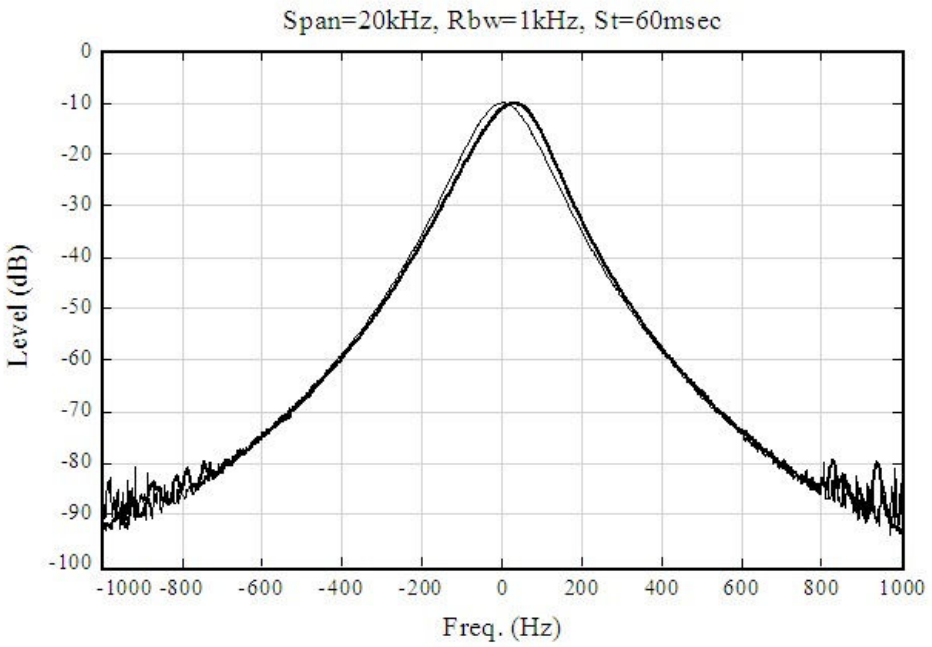

Fig.1.1 Example of an over sweep-rate response

Span=20kHz, *Rbw*=1kHz,
The bold line: Sweep Time 60msec; typical (automatically)
The thin line : Sweep Time 10sec; very slow (manual)

1.2 History of Spectrum Analyzers

The first sweep spectrum analyzer was developed by Hewlet-Packard Co (*HP*). in 1960's [7]. Until 1970's, the sweep spectrum analyzers were made by analog circuit technology. Those displays were CRTs, and spectrums were shown as persistence of its luminescent screen. In 1974, M.Engelson (Tektronix, Inc.) wrote the book [1]; "Modern Spectrum Analyzer Theory and Applications". In this book, M.Engelson systematized technologies of spectrum analyzers.

In 1978, *HP* Co produced the spectrum analyzer HP8568A, whose operation was controlled with microprocessors. HP8568A had a digital storage display.

In the first half of 1980's, other factories (such as ADVANTEST and Tektronix Inc.) produced spectrum analyzers that were controlled with microprocessors and had digital storage display. These analyzers had A/D converter that digitized the final spectrum signal into the digital data, and we could obtain the average of the spectrum. In this decade, "GP-IB" (called "HP-IB" too) became popular for most measurement instruments. Then most spectrum analyzers could communicate with a computer by these interfaces and we could include spectrum analyzers in automatic measurement

system. In these years, spectrum analyzers of FFT method became popular. The FFT method uses to measure a low frequency signal such as 100kHz or under. They were made by almost digital signal processing technologies.

From the second half of 1980's, the technologies of the digital signal processing were introduced into sweep spectrum analyzers. The HP8560 series (produced by HP. Co.) and the R3265 series (produced by ADVANTEST Co.) had digital resolution filter that were narrower than 300Hz or 100Hz. They were some application of the FFT method and these operations were done by regular microprocessors such as 68000.

In the last of 1980', HP. Co. produced the analyzer HP3588 [8]. This analyzer was epoch-making instrument. It was the first analyzer which had an LSI of a digital filter and digital signal processor in a sweep spectrum analyzers. But characteristics of operation and performance differed a lot from those of other sweep spectrum analyzer. HP3588 was considered not to be accepted by many RF and analog engineers.

Since 1990's, the primary technology of a radio communication became digital, and technologies of spectrum analyzers were forced to adapt itself to the technology. Many spectrum analyzers had functions of digital modulation analyses. Technologies of digital signal processing were introduced into spectrum analyzers actively in these years.

In the middle of 1990's, Tektronix Inc. produced the "Real Time Spectrum Analyzer series", which had powerful processor and measured spectrums by the FFT method. This analyzer made a new category of spectrum analyzer.

In 2000's, Agilent Technology Co. produced PSA series spectrum analyzers. It was a sweep spectrum analyzer. All of their RBW filters were made by digital filters.

As described above paragraphs, in the history of spectrum analyzers, the technology of the digital signal processing have been introduced from its backend to the front-end. At present, the highest classes of spectrum analyzers are mainly made by digital signal processing technology such as PSA series [9]. In this kind of analyzers, the method to achieve first measurement of fine RBW was FFT method, and the principle of sweep method was not changed from the appearance of the analyzers. The FFT method has some demerits against the sweep method, and most spectrum analyzers to measure RF signal are made by the sweep method at present.

1.3 Purposes of this Research

We investigated the process of the sweep spectrum analysis and the FFT method. And research the optimized application of these methods.

This thesis suggested the 'Super Sweep method' to improve the characteristics described in section 1.1. This method intends to make the analyzer operate with faster sweep rate arbitrarily than a conventional method in principal.

The new method is the third way to measure spectrums following the sweep and the FFT, and has eliminated the demerit of the sweep method and has several merits as compared with the sweep and the FFT method.

Practically, we cannot obtain the Fourir transform perfectly using any of those methods. The conventional sweep spectrum analysis and FFT method are artificial methods to observe the spectrum. The new method may be one of the artificial methods, but at least it eliminated some restriction of the sweep method and has some merit that the FFT method does not have.

1.4 Method

We analyzed the new method, and made a model of the system, which was implemented the new method. We researched the fundamental model and designed the experimental system that achieved the new method.

1. We analyzed the sweep method and the FFT method as a conventional way and represented the sweep method as a mathematical model. It was fundamental research to invent the new method. We investigated that the cause of the over sweep-rate response was the chirp phase factor in the IF signal (see section 2.5).
2. We considered the mathematical model of the super sweep method, which improved the sweep method. The new method achieved the fast sweep using the negative chirp filter, which canceled the chirp phase factor of the IF signal and rejected the almost case of the over sweep-rate response.
3. We researched the model of the signal processing of the new method and what devices were suitable to implement the new method.
4. We designed and implemented the experimental system, which achieved the new method. This thesis reported the description of the process. The experimental system included the conventional spectrum analyzer as a RF down converter. We designed and made a digital signal processing (DSP) unit, which processed the IF signal that is one output of the spectrum analyzer (see section 4.2). The back-end system, which displays a spectrum and worked as a man-machine interface, was build with a PC. We measured the peak level and to observed resolution bandwidth by changing the normalized sweep rate (see Eq.(1.3)), and plotted the result.
5. We reported the result of the experiments and verified that the new method achieved the fast measurement against the conventional method.

6. There were many topics about the new method such as devices to operate the new method, the analysis the chain of the filter and relation between the Chirp Z-transform etc. In Chapter 6, these topics were discussed.
7. The comparison among the three methods of merit and demerit is described in this thesis.

1.5 Representative result

We verified the theory of the new method, in which the sweep rate σ is

$$\sigma \le Rbw \times (Flt / \chi), \qquad (1.2)$$

where *Flt* is the bandwidth that we could process on the resolution filter, and χ is a constant value from 2.5 to 4.0. In the case that the *Flt* is enough wider than the *Rbw*, we can obtain a fast sweep rate as we desire. The sweep rate of the new method against the normalized sweep rate *1/k* is shown in Fig.1.2. The value *1/k* is defined in Chapter 2 as

$$1/k = \frac{Span}{T_S \times Rbw^2} = \frac{\sigma}{Rbw^2} \ . \qquad (1.3)$$

The sweep rate of the sweep method is in inversely proportion to the square of the *Rbw*. In the new method, it is in proportion of the product of *Rbw* and *Flt*. Especially, at the narrower *Rbw* the new method had large advantages.

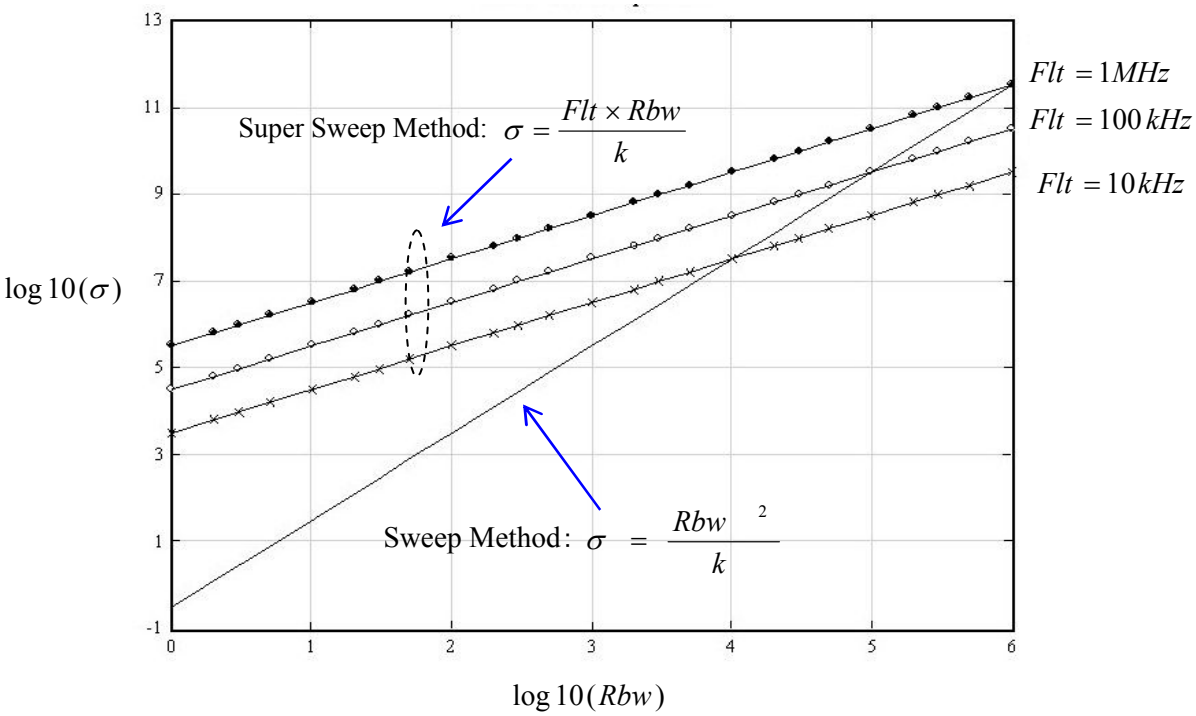

Fig.1.2 Comparison of a sweep rate between the sweep method and the super sweep method

The unit of σ and *Rbw* is Hz

1.6 The Composition of this thesis

In Chapter 2, we summarized the characteristics of a sweep spectrum analyzer and analyzed the mathematical model of the analyzer, and the digital IF method is described which was a base of the new method. And we described about the FFT method too.

In Chapter 3, we described the theory and the implementation of the 'Super Sweep method'. We invented a 'negative chirp filter' with a complex digital filter, and examined that the filter allowed the spectrum analyzer to measure any times faster in principle.

In Chapter 4, we reported a development of the experiment system to prove the theory of the Super Sweep method, and got the results that achieved 30 times faster measurements than traditional sweep spectrum analyzer.

In Chapter 5, we discuss the result, and improve that the new method allowed a sweep spectrum analyzer to operate faster in accordance with system condition in theoretically.

In Chapter 6, the additional discussion is done. The new method has several interesting property.

In Chapter 7, Applications in the radio astronomy are reported. Some characteristics are investigated. One of them was the SNR when the analyzer measure low power signal as measured signals in radio astronomy. Author observed radio signals of some astronomical body using radio telescopes, our experimental system, sweep spectrum analyzers and the built-in FFT system of the telescope. And we compared the SNR of the three methods.

Chapter 8 are the conclusions.

1.7 Glossary

English

$f_{IN}(t)$	Input (measured) signal
$f_{IN\_A}(t)$	The analytic signal of $f_{IN}(t)$
f_S	The Sampling frequency of the Analog Digital Converter (AD/C)
$g(t)$	The impulse response of the Gaussian filter
$G(\omega)$	The frequency response of the Gaussian filter
I	In-phase factor
Log AMP	Logarithmic amplifier
$S_B(t)$	Base band signal
$S_{B\_RBW}(t)$	Base band signal through the RBW filter
$S_{IF}(t)$	Intermediate Frequency (IF) signal
$S_{IF\_A}(t)$	The analytic signal of $S_{IF}(t)$

$S_1(t)$	1st local IF signal
R_S	The rate of the sweep rate against a traditional sweep method, Defined by Eq.(3.35).
T_S	Sweep time as a parameter
$T_{S\_\min}$	The minimum sweep time
$P(\omega)$	Power spectrum
Q	Quadrate factor
k_0	A coefficient decided by the impulse response of the resolution filter. It decided from the response time of the resolution filter such as *k/Rbw*.
1/k	Normalized sweep rate. Defined by Eq.(2.40)

Greek

ω	Radian frequency
ω_B	Radian frequency of the base band signal $S_B(t)$
ω_{IF}	Radian frequency of the IF signal $f_{IF}(t)$
ω_{IN}	Radian frequency of the input signal $f_{IN}(t)$
ω_0	Radian center (at t=0) frequency of the local oscillator
ω_l	Radian frequency of the signal generated by the local oscillator $l(t)$
σ	Sweep rate (Hz/sec) $\sigma = k\frac{Span}{Rbw^2}$
$\sigma_{\max}$	Maximum sweep rate
$\triangle$	frequency difference

Acronyms

AD/C	Analog to digital converter
ATT	Attenuator
CZT	Chirp-Z Transform
CTS	Chirp-Z Transform Spectrometer
IF	Intermediate Frequency
IF BPF	IF band pass filter
LPF	Low pass filter
RBW	Resolution bandwidth described in section 2.5.6 As a condition of conventional spectrum analyzer
Rbw	RBW as a parameter

RBW filter	The IF BPF whose bandwidth is narrowest and decides the frequency resolution of the spectrum.
Rbw'	observed *Rbw* as a parameter
SPAN	Frequency span; the frequency range that we desire as a spectrum.
Span	SPAN as a parameter
St	Sweep Time

Name of conventional instruments:

FSU: The spectrum analyzer produced by Rhode-Schwartz Inc.

R3264: The spectrum analyzer produced by ADVANTEST Co.

PSA: The spectrum analyzer produced by Agilent Technology Co.

1.8 Technical Terms on the Spectrum Analyzer

An example of a spectrum analyzer's display is shown in Fig.1.3. There are some special terms used in a spectrum analyzer corresponding to the parameter on the display of the spectrum, which are indicated by numbers with a circle

① **Center frequency** ,(**CF**) indicates the center frequency of the display scale.

② **Span** (**SPAN**) is the frequency bandwidth of the measurement, corresponding to the difference between **Start** (left end of the scale: ②') and the **Stop** (right end of the scale: ②").

②' Start (START or STT). It is the start frequency of the scale, the frequency of the left end of the scale.

②" Stop (STOP or STP). It is the stop frequency of the scale, the frequency of the right end of the scale.

③ **Reference Level**. (**RL**). It is the level top of the scale, usually indicated by the unit dBm.

④ Level per division; It is the level difference of each vertical scale grid, usually indicated such as '****dB/**'.

⑤ **Marker**,(**MK** or **MKR**). It is a mark that indicates the frequency and the level of the position of the spectrum that selected by the operator of the analyzer.

⑥ **Video Bandwidth** (**VBW**). It is the bandwidth of the filter that is set up after the power detector of the spectrum.

⑦ **Sweep Time** (**ST** or **Ts**). It is the time that the sweep needs the from Start to Stop frequency.

⑧ **Attenuator** (**ATT**). It is a attenuator that is implemented RF front end.

⑨ **Resolution bandwidth** (**RBW** or Rbw). It is the frequency resolution bandwidth that decides the resolution of the spectrum.

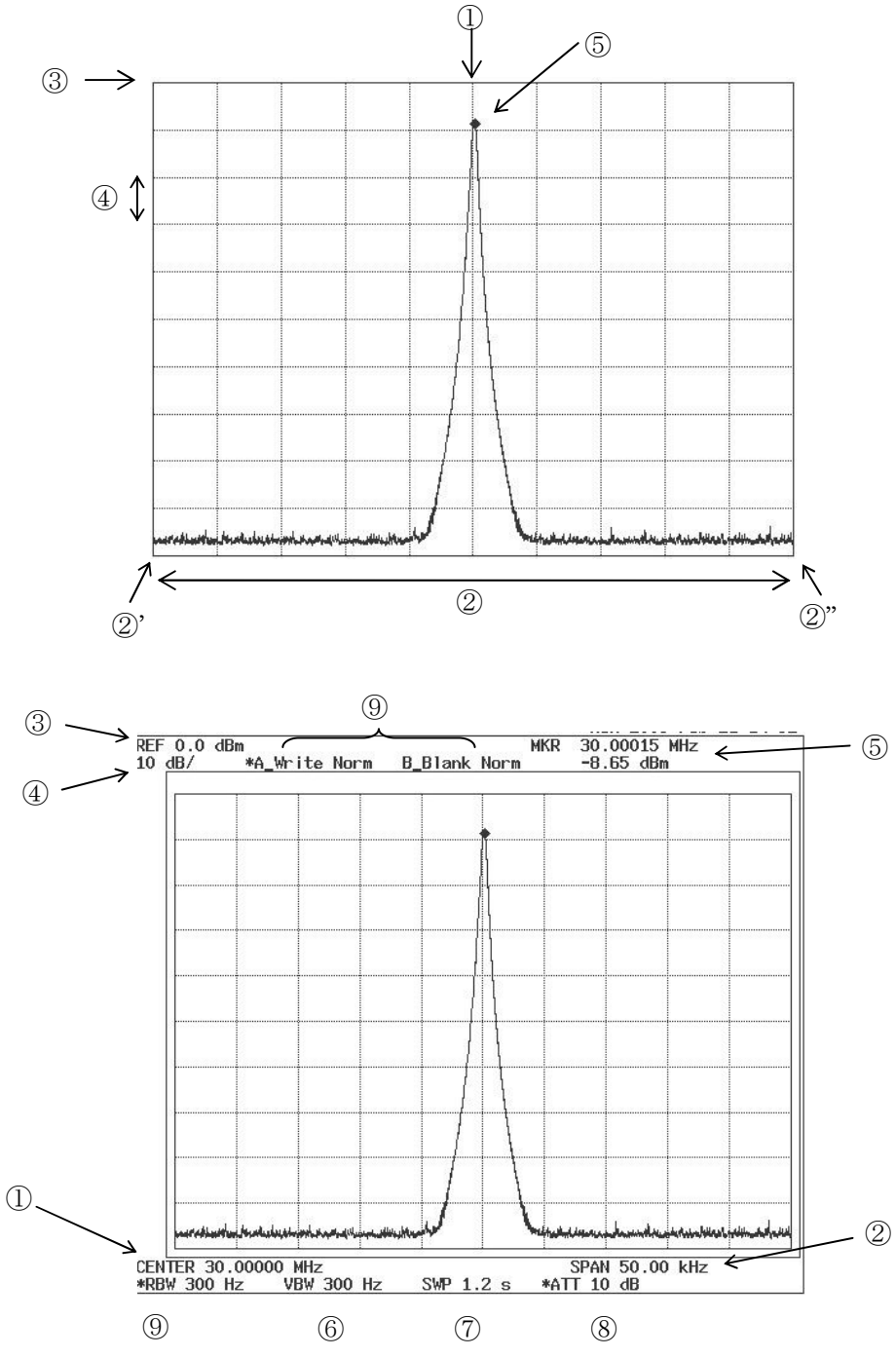

Fig. 1.3 Samples of display of a spectrum analyzer

1.9 Reference

[1] Morris Engelson “Spectrum Analyzer Theory and Applications” Artech House publishers Oct. 1974

[2] Masao Nagano “Signal Processing of Sweep Spectrum Analyzer” S^2PATJ vol.3, No.4 Dec. 2000 pp.17-24

[3] George D. Tsakiris “Resolution of a spectrum analyzer under dynamic operations” Rev. Sci. Instrum., Vol.48, No.11, Nov. 1977 pp.1414-1419

[4] R.A.Witte “Spectrum and Network measurement”, 1993 Prentice-Hall,Inc

[5] Kirsten C. Carlson “A 10-Hz-to-150-MHz Spectrum Analyzer with a Digital IF Section” Hewlett-Packard Journal June 1991

[6] “Spectrum Analyzer R&S FSU Specifications”, Version 10.00, May 2006, Rhode & Schwaltz GmbH & Co. KG

[7] Home Presentation Resources Collection Time line Technology News:
“Spectrum Analyzer - Signal Analyzer”
http://www.hpmemory.org/wb_pages/wall_b_page_04.htm

[8] Kirsten C. Carlson “A 10-Hz-to-150-MHz Spectrum Analyzer with a Digital IF Section” Hewlett-Packard Journal June 1991

[9] Dan Strassberg, “Spectrum analyzers measure faster and more accurately”, EDN, 11/23/2000

Chapter 2

Review of Sweep-Signal Method

2.1 Introduction

The theoretical backgrounds of the sweep spectrum analyzer are well summarized in the references [1][2][3]. In this chapter, we present detailed analysis of the method on the signal processing.

Section 2.2 shows the outline of the sweep spectrum analyzer. Section 2.3 describes the principal theory of the sweep method. Section 2.4 describes the digital IF method as an improvement of the sweep method. Section 2.5 shows the mechanism of the sweep method as the digital signal processing. Section 2.6 describes a few important characteristics of the sweep method. Section 2.7 investigates the property of the resolution filter in case of measuring the FM modulated signal. Section 2.8 describes the some characteristics of the FFT method. And section 2.9 concludes this section.

The description of this chapter introduces the fundamental of the new method, which is described in chapter 3.

2.2 Principle of Sweep-Signal Spectrum Analyzers

This section describes the structure and the properties of the conventional sweep spectrum analyzer. Section 2.2.1 describes the outline, section 2.2.2 will describe about a frequency down converter, and section 2.2.3 describe the function of the LPF.

2.2.1 Outline of Spectrum Analyzers

A simplified block diagram of a traditional sweep spectrum analyzer is shown in Figure 2.1. This kind of analyzers consists of many components as follows [1].

- LPF
- ATT & Pre-AMP
- Frequency Converters
- Log AMP
- Detector
- Video Filter
- AD/C

- 'LPF' (low pass filter) prevents the mixer from receiving higher frequency signal than the system cannot process. A function of the LPF is described in section 2.2.3.
- 'ATT' (attenuator) is used to degrease the power of the input signal, in the case that the power of the input signal is too large. And ATT is used to reduce the noise power of the input.
- Usually sweep spectrum analyzers have multiple 'Frequency converters'. They consist of a mixer, a local oscillator and a band pass filter and output of IF (Intermediate Frequency) signal '$S_{IF}(t)$'. It is described in section 2.2.2.
- The 'Log Amp' converts the amplitude of the $S_{IF}(t)$ logarithmically.
- The 'Detector' detects the output of the Log Amp with AM detection.
- The 'Video Filter' limits the bandwidth of the detected signal and outputs the envelope of the $S_{IF}(t)$. In the classic sweep spectrum analyzer with analog displays, this signal was used to drive the vertical deflection plate of the CRT directly. Hence the signal is called 'Video signal'. Most spectrum analyzers since 1980s digitizes the Video signal with the 'AD/C', AD converter, and the spectrum is displayed by a digitized display.
- The digitized data is put into memory of the 'Display system', which is controlled by a microcomputer or other control devices. The Display shows the Video signal as the 'Power Spectrum: $P(\omega)$'.

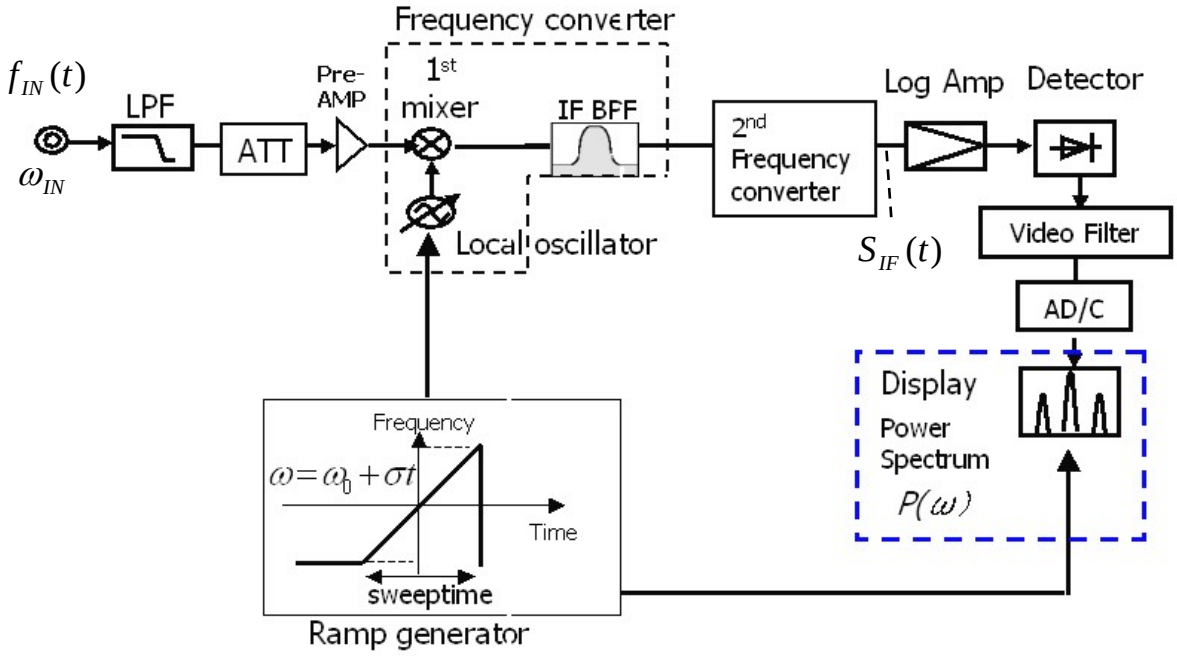

Figure 2.1 Block Diagram of Classic Sweep Spectrum Analyzer

2.2.2 Frequency Converter *)

A block diagram of the Frequency converter is shown in Fig.2.2, which consists of three elements, a mixer, a local oscillator and an IF BPF (IF Band Pass Filter). The most important element is the mixer, which operates as a multiplier and makes the products of the input signal and the local oscillator as an analog circuit.

In the case that the frequency of the input signal and the local oscillator is ω_{IN} and ω_l, respectively, the mixer produce the two signals whose frequency are $\omega_{IN}+\omega_l$ and $|\omega_{IN}-\omega_l|$. This operation corresponds to Eq.(2.1), which is one of the formulas about the trigonometric function [4].

$$\cos(A)\times\cos(B)=\frac{1}{2}\left[\cos(A+B)+\cos(A-B)\right]. \qquad (2.1)$$

And the output of the mixer includes two feed through factor of ω_{IN} and ω_l. These frequencies around the mixer are shown in Fig.2.3.

The 'IF BPF' permits only one signal, usually $\omega_{IN}+\omega_l$ or $|\omega_{IN}-\omega_l|$ to be outputted from the converter. The output of the IF BPF is called 'IF (Intermediate Frequency) signal'.

In the case that the input signal $f_{IN}(t)$ is explained as;

$$f_{IN}(t)=A(t)\cos(\omega_{IN}t+\theta(t)), \qquad (2.2)$$

the output will be

$$S_{IF}(t)=A(t)\cos((\omega_{IN}+\omega_l)t+\theta(t)) \qquad (2.3\text{-a})$$

$$\text{or}\quad S_{IF}(t)=A(t)\cos(|\omega_{IN}-\omega_l|t+\theta(t)), \qquad (2.3\text{-b})$$

where *A(t)* is the amplitude and θ *(t)* is the phase factor. The Frequency converter transform frequency only, and influences on other factors such as *A(t)* and θ*(t)*. Equation (2.3-a) and (2.3-b) can be explained by

$$S_{IF}(t)=\mathrm{Re}[A(t)\exp[j((\omega_l+\omega_{IN})t+\theta(t))]] \qquad (2.4\text{-a})$$

$$\text{or}\quad S_{IF}(t)=\mathrm{Re}[A(t)\exp[j((\omega_l-\omega_{IN})t+\theta(t))]]. \qquad (2.4\text{-b})$$

The frequency $\omega_{IN}+\omega_l$ or $|\omega_{IN}-\omega_l|$ is generally called 'Intermediate frequency' or simply 'IF'.

*) note: Sometimes a frequency converter is called another name such as down converter, frequency down converter, RF down converter and converter.

2.2.3 Input LPF

The discussion of last section has the assumption that the frequency of the input signal is under the frequency ω_{IN_max} which is lower than the lowest frequency of the local oscillator ω_{l_mn}. In the case that another signal exists and its frequency ω_{IN}' satisfies the following equation

$$\omega_{IN}'-\omega_l = \omega_l - \omega_{IN}, \qquad (2.5)$$

we cannot distinguish the frequency ω_{IN} from ω_{IN}'. To avoid this trouble, the input signal is passed through the LPF shown in Fig.2.1. The frequency ω_{IN_max} is the cut-off frequency of the LPF.

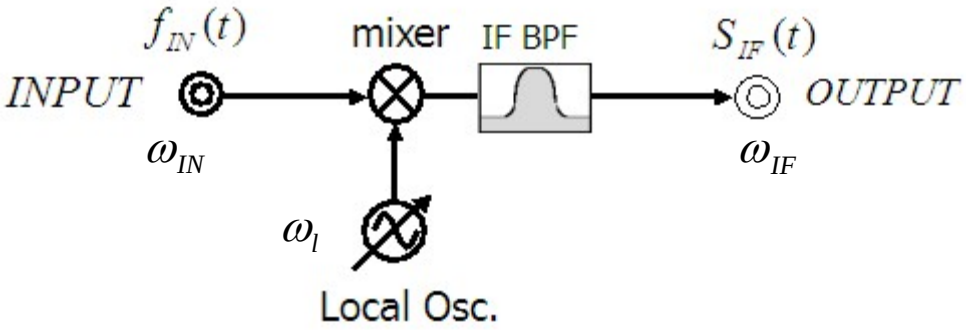

Figure 2.2 Block Diagram of a Frequency Converter

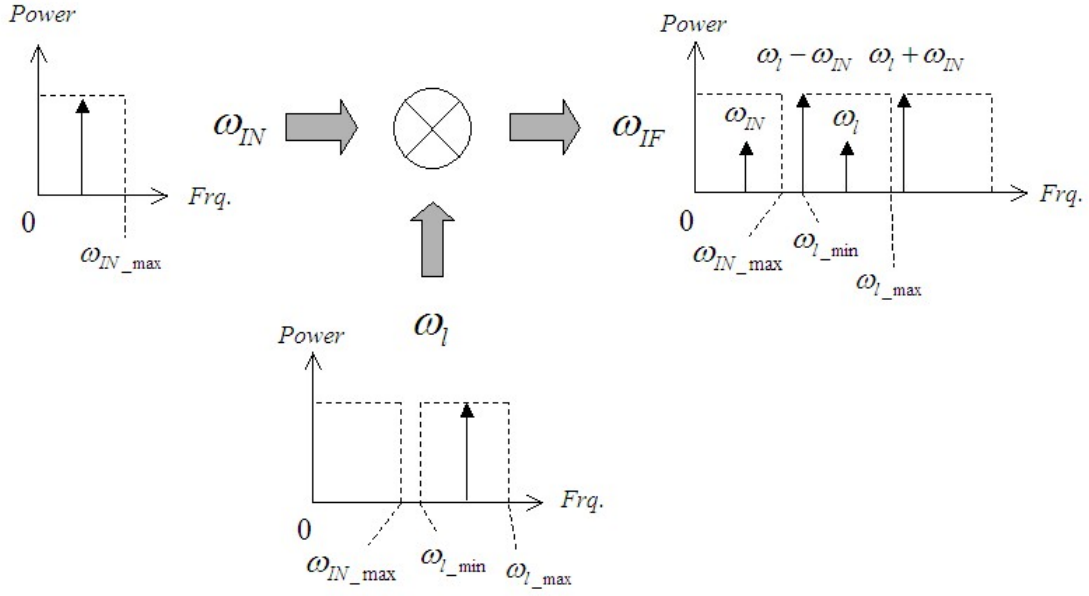

fin=2GHz, fl=6GHz, fl-fin=4GHz, fl+fin=8GHz

Fig. 2.3 Frequency around a mixer

2.3 Analog signal processing with swept local oscillator

The qualitative discussion on the frequency converters with swept local oscillator is given in this section.

2.3.1 Frequency converter with Swept Local Oscillator

In the condition that the local oscillator does not sweep and generate a CW signal, the system shown in Fig.2.2 operates as a general radio receiver. On the other hand, a sweep spectrum analyzer is provided with a characteristic that the local oscillator generates a sweeping signal. The frequency of output signal of the frequency converter is shown in Fig.2.4.

We assumed the system that is under the condition itemized as follows.

・The input is CW signal for simplification.

・The maximum and minimum frequency of the input signal is $\omega_{IN\_\max}$ and $\omega_{IN\_\min}$.

・The minimum and maximum frequencies of the local oscillator, $\omega_{l\_\max}$ and $\omega_{l\_\min}$ which is defined as;

$$\omega_{l\_\max} \geq \omega_l \geq \omega_{l\_\min} \qquad (2.6)$$

$$\omega_{l\_\max} - \omega_{l\_\min} = \omega_{IN\_\max}. \qquad (2.7)$$

・The frequency of the input signal is restricted by the input LPF as

$$\omega_{IN\_\max} \geq \omega_{IN}. \qquad (2.8)$$

・The frequency of the local oscillator is higher than the frequency of the input.

$$\omega_{l\_\min} \geq \omega_{IN\_\max} \qquad (2.9)$$

・ 'T_S' is defined as the sweep time. The local oscillator generates the signal ω_l within the sweep time periodically. The time '*t*' is considered periodically as

$$T_S \geq t \geq 0. \qquad (2.10)$$

Then the converter generates two signals, $\omega_l + \omega_{IN}$ and $\omega_l - \omega_{IN}$, which are indicated in blue and red square in Fig. 2.4, respectively.

In the case that ω_{IN} equals to $\omega_{IN\_\min}$, $\omega_{IN} + \omega_l$ and $\omega_l - \omega_{IN}$ are same frequency, and traced by the line '①' in Fig.2.4. Similarly, ω_{IN} equals to $\omega_{IN\_\max}$ they are traced by '②' and '③' respectively.

In the case of $\omega_{IN} = \omega_{IN\_\min}$, the frequency $\omega_{IN} + \omega_l$ equals to $\omega_{l\_\max}$ at $t = T_S$, which is indicated as the point 'L' in Fig.2-4.

In the case that $\omega_{IN} = \omega_{IN\_\max}$, the frequency $\omega_l + \omega_{IN}$ equals to $\omega_{l\_\max}$ at $t = 0$, which is indicated as the point 'H' in blue. In the case that ω_{IN} is $(\omega_{IN\_\max} + \omega_{IN\_\min})/2$, the frequency $\omega_l + \omega_{IN}$ equals $\omega_{l\_\max}$ at $t = T_S/2$, which is indicated as the point 'M' in blue. In the case that $\omega_{IN} = \omega_{IN\_\min}$, $\omega_l + \omega_{IN}$ equals $\omega_{l\_\max}$ at $t = T_S$, which is indicated by 'L' in blue.

Similarly for the signal $\omega_l - \omega_{IN}$, the points corresponding to $\omega_l - \omega_{IN} = \omega_{l\_\min}$ are indicated as 'L','M' and 'H' in red which are arranged in reverse order to those of $\omega_{IN} + \omega_l$.

In the case that we configure the IF BPF whose center frequency equals $\omega_{l\_\min}$ or $\omega_{l\_\max}$, we can obtain the power corresponding to the any frequency of ω_{IN}, and we can know the time when the power come in corresponds to the frequency ω_{IN}.

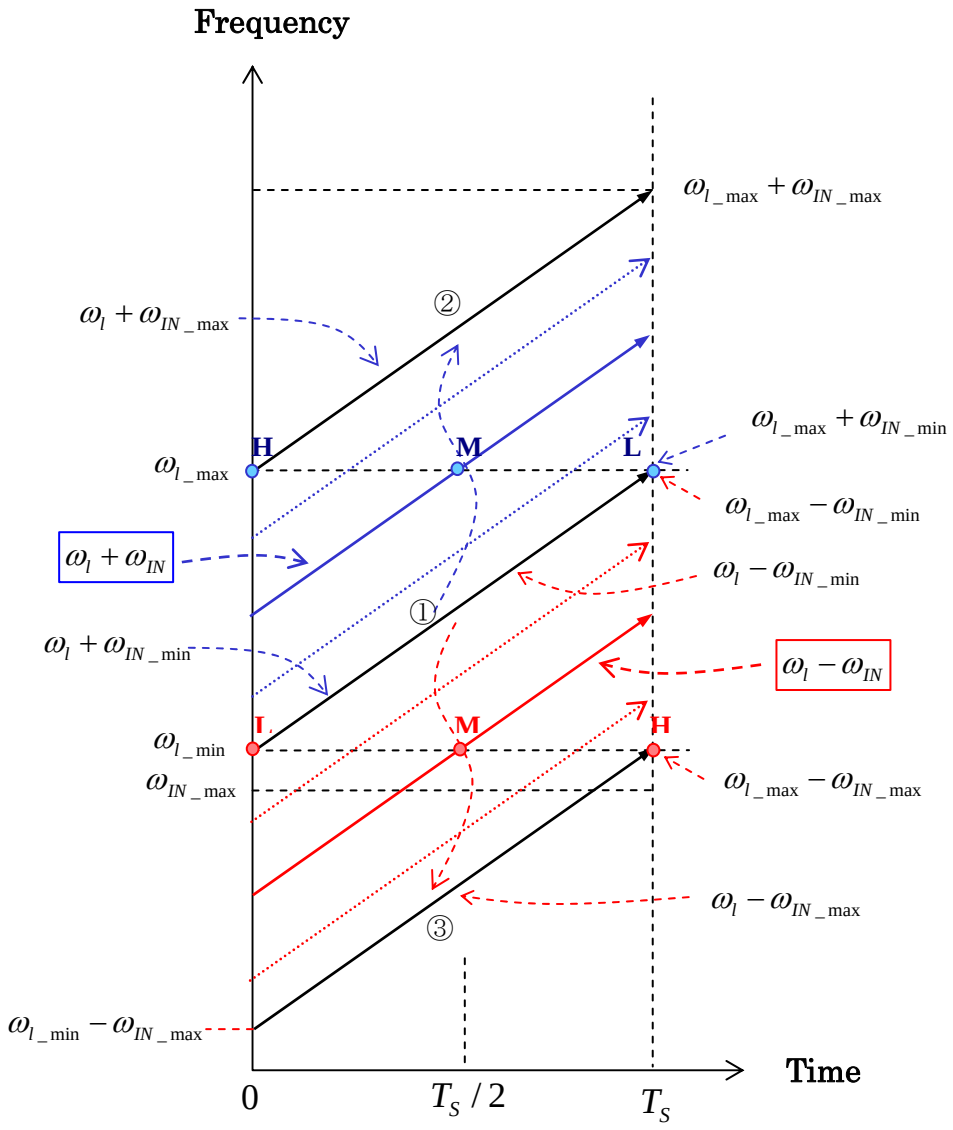

Fig. 2.4 Frequencies of signals around a mixer with the swept local

2.3.2 Output of IF BPF

The time-frequency diagram of the signal around the frequency converter with the swept local oscillator (see Fig.2.2) is shown in Fig.2.5. Where, the input signal is assumed as a single CW signal, the condition of the system is similar to that in the last section, and the center frequency of the IF BPF: ω_{IF} is set to $\omega_{l\_\min}$ (see Fig.2.4).

When the frequency of the mixer's output is around $\omega_{l\_\min}$, the output of the IF BPF has a power. The frequency ω_{IF} is generally called as 'Intermediate Frequency' or 'IF frequency'.

The abscissa of Fig2.5 indicates the time and the ordinate indicates the frequency. The each graphs of the Fig.2.5 is itemized as follows.

- (a) shows the frequency of the input signal ω_{IN} against time. The input signal is $f_{IN}(t)$, which is assumed a single CW signal.
  In his figure and (b) and (c), the ordinate indicates frequency.
- (b) shows the frequency of the local oscillator whose frequency is swept from ω_{l_START} to ω_{l_STOP}. These parameters satisfy the next equation.

$$\omega_{l\_\max} \geq \omega_{l\_STOP} > \omega_{l\_START} \geq \omega_{l\_\min}$$

- (c) shows the frequency of the mixer's output, $\omega_{mix\_out} = \omega_l - \omega_{IN}$ *) and the pass band of the IF BPF which is $\omega_{IF} = \omega_{l\_\min}$. '*h(t)*' is the impulse response of the IF BPF. The frequency response of IF BPF is drawn as a graduated horizontal bar. By selecting the frequency ω_{l_START} and ω_{l_STOP} adequately, the line of ω_{mix_out} clothes the path band of the IF BPF around the time $t = T_S / 2$.
- (d) shows the output of the IF BPF as $S_{IF}(t)$. In this figure, the ordinate indicates a voltage. The horizontal line indicates a voltage 0 V. Where $S_{IF}(t)$ has a significant value around the time $t = T_S / 2$.
- (e) shows the power of the $S_{IF}(t)$. The unit of ordinate is dBm. We can consider $S_{IF}(t)$ is a spectrum of the input signal $f_{IN}(t)$.

In the case that the input signal $f_{IN}(t)$ is another type of signal, such as modulated or multi CW signal etc, we can observe the spectrum of $f_{IN}(t)$ as a distribution of the spectrum.

In summary, for a sweep spectrum analyzer we should chose the IF frequency higher than the maximum frequency of the input signal $\omega_{IN\_\max}$ which corresponds to the cut-off of the LPF front of the mixer. The frequency of the local oscillator should be tuned from the IF frequency to the 'IF frequency+ $\omega_{IN\_\max}$' [1].

Note *): The most sweep spectrum analyzers employ the frequency of the mixer's output to be $\omega_l - \omega_{IN}$.

2007.03.14　1 回目推敲, 2007.04.26, 2007.08.19

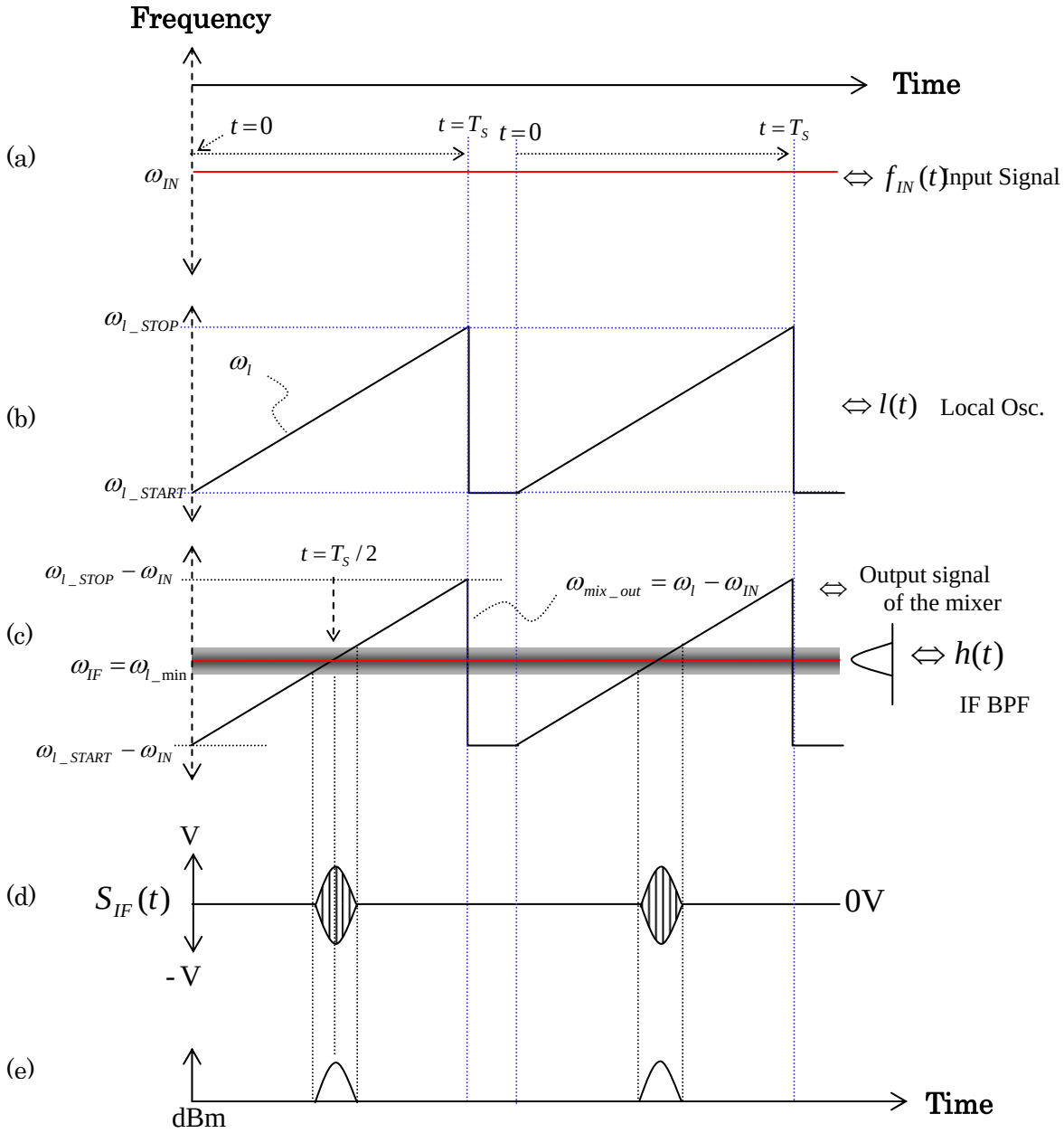

Fig. 2.5 Time-Frequency diagram around a mixer with the swept local

2.3.3 Multi Conversion

Usually, spectrum analyzers have multiple frequency converters. Usually, they are called 1st, 2nd, and 3rd converter from the front end of the input side. This section describes why spectrum analyzers have multiple down converters.

The frequency of the 1st local oscillator in the most modern spectrum analyzer is approximately 4GHz to measure wide frequency range. The frequency resolution of the spectrum, which is obtained by the system in Fig.2.5, is decided by the bandwidth of the IF BPF. Some spectrum analyzer have the resolution 1kHz; others, 10Hz; still others, 1Hz. It is difficult to achieve such a narrow filter at the center frequency 4GHz. Therefore most spectrum analyzers typically have three or four stages of frequency converters [1]. The example of a multi stage of the frequency converter is shown in Fig.2.6. This example has three stages and the 3rd IF frequency is 21.4 MHz. Most spectrum analyzers have this IF frequency, 21.4 MHz and has the IF BPF as a resolution filter on this frequency.

Usually, the IF BPF on the 21.4MHz IF is called 'Resolution Bandwidth Filter', 'RBW BPF' or 'RBW filter', which decides the frequency resolution of the measure spectrum [1][2].

Note) The IF frequency of many FM radio receivers are 21.4MHz, and we can get the filter whose band pass is 21.4MHz with reasonable price. It is one of the reasons that the IF frequency of spectrum analyzers are 21.4MHz.

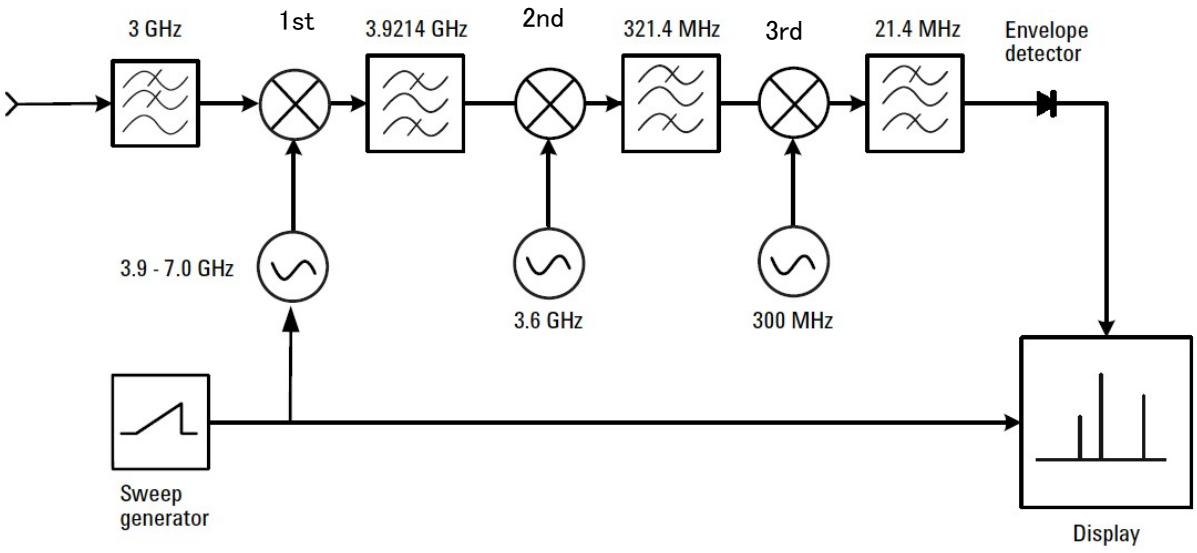

Fig. 2.6 Multi frequency converter (Referred Figure 2.5 of [1])

2.3.4 Restriction of Sweep time

A response of a RBW filter is illustrated in Figure 2.7, where the horizontal axis indicates both time and frequency. The measured signal is a CW, '*Rbw*' is the 3dB bandwidth of the RBW filter; 'T_S' is the sweep time; 'Span' is the measurement frequency range which equals $\omega_{l\_STOP} - \omega_{l\_START}$; and '$\Delta T$' is the time corresponding to the response of the RBW filter, which is explained as

$$\Delta T = T_S \times \frac{Rbw}{Span}. \qquad (2.11)$$

A sweep spectrum analyzer obtains the spectrum from the response of the RBW filter. Any filters require a finite time to charge and discharge, and the time length are inversely proportional to its bandwidth [1]. Then ΔT has a restriction explained by next equation.

$$\Delta T \geq \frac{k_0}{Rbw}, \qquad (2.12)$$

where k_0 is a constant of proportionality. Equation (2.12) can be modified by replacing ΔT as the right side of Eq.(2.11).

$$T_S \times \frac{Rbw}{Span} \geq \frac{k_0}{Rbw}. \qquad (2.13)$$

It is modified as

$$T_S \geq k_0 \frac{Span}{Rbw^2}. \qquad (2.14)$$

In the most sweep spectrum analyzers, the value of 'k_0' are in the range from two to three.

In the case that T_S is shorter than the time of Eq.(2.14), the peak-level of the spectrum will be reduced as shown in Fig.2.8, where *Span* and *Rbw* of the all spectrums equal to 50 kHz and 300 Hz respectively. The sweep times T_S of 'A' to 'F' is 2.0sec, 1.2sec, 500msec, 100msec, 50msec and 20msec, respectively. Especially, 'B' is a 'AUTO' which is configured by Eq.(2.14). The peak level is reduced and the width of the peak is expanded corresponding to the sweep rate, $Span/T_S$. We call this phenomenon 'over sweep-rate response'.

In the most conventional sweep spectrum analyzers, the value of k_0 is decided by a condition that the level reduction is about 0.1dB [2]. Actually, the difference level of peaks between A and B in Fig.2.8 was 0.13dB.

In summary, sweep spectrum analyzer has a restriction on its sweep time and sweep rate.

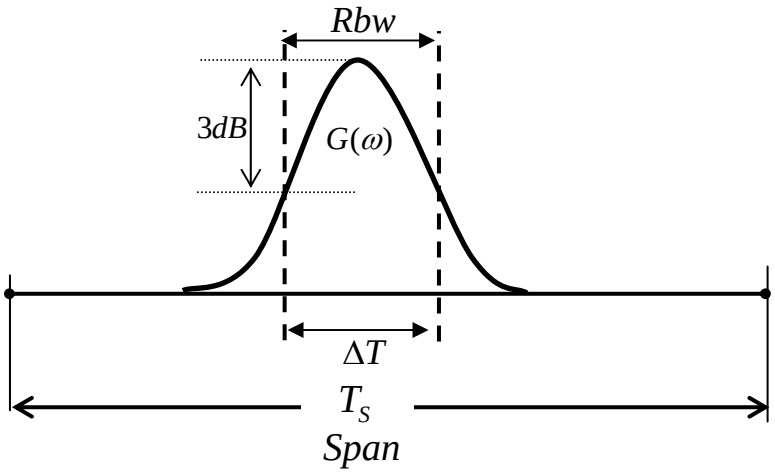

Fig 2.7 Response of an RBW filter measuring CW signal

2.3.5 Permissible distortion

The theory of level reduction is described in section 2.5. By the theory, we cannot measure a spectrum without any reduction. We have to use the analyzer permitting the level reduction, which is about 0.1dB [1][2].

Sweep spectrum analyzers have a property that the spectrum is shifted to the right side corresponding to the charge and discharge time of the RBW filter. Figure 2.8 shows the shifts that corresponds to the frequencies of the peaks as follows

$$\textit{Shift time} = T_S \times \{(\textit{frequency of the peak}) - (\textit{center frequency})\}/\textit{Span}\ .$$

As the results, all of the shift times were approximately 2.2msec, which are 0.66 of the inverse of the *Rbw*= 300Hz.

In the case that the sweep time is longer than the condition of Eq.(2.14), as far as we observe the spectrum with our eyes, the shift and the level reduction is negligible obstruction.

2007.04.26, 2008.08.19

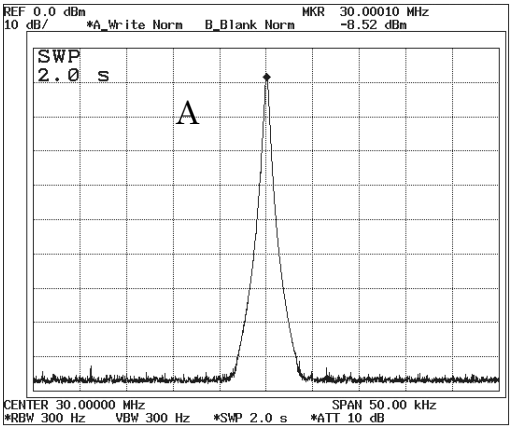

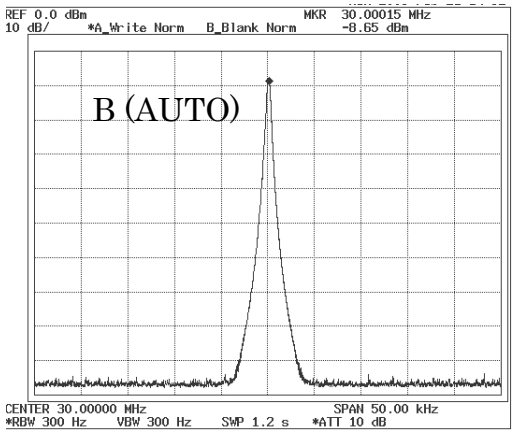

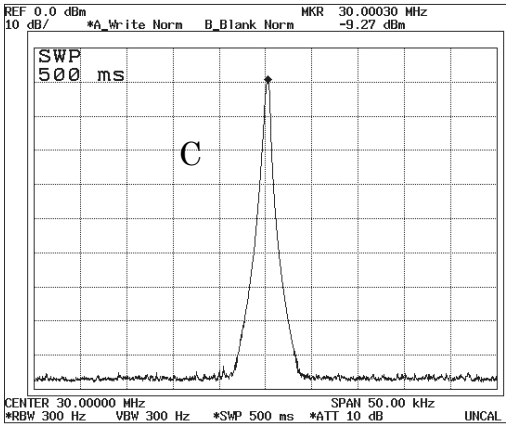

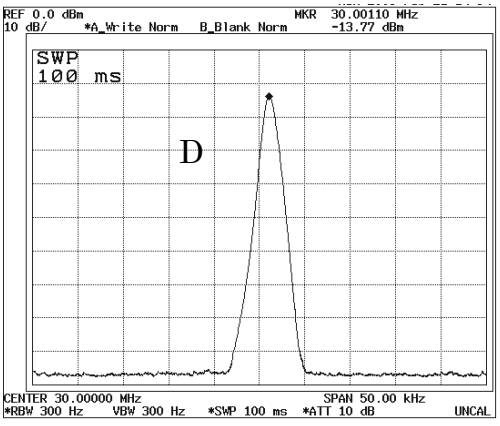

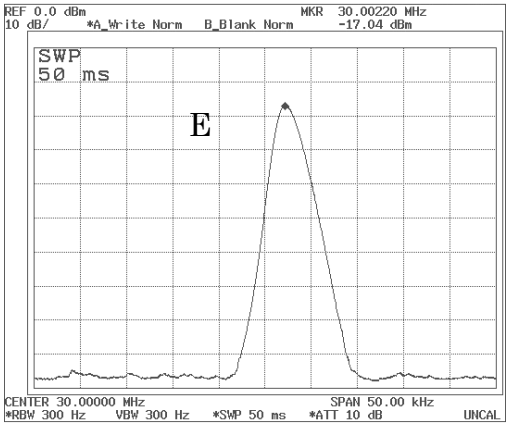

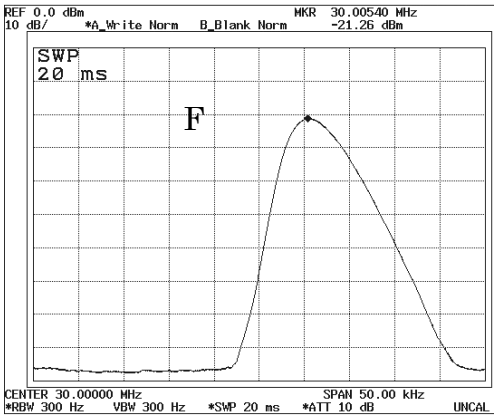

Span=50kHz, Rbw=300Hz

Fig 2.8 Examples of over sweep-rate responses

2.4 Digital IF

The qualitative property of the sweep spectrum analyzer is described in section 2.2. The systems described in section 2.2 and 2.3 were analog type only. This section describes a ‘digital IF method’. We considered that introducing the digital IF method is appropriate to describe the property of the analyzers mathematically.

2.4.1 Digital IF method

The block diagram of Fig.2.9 suggests an example of the spectrum analyzer which has both analog and digital IF method. In the both method, the spectrum is measured as a changing power of the signal, ‘ $S_{IF}(t)$ ’, which is called as 'Intermediate frequency signal', or simply 'IF signal'. It is passed through the ‘IF BPF’ of the 3rd down converter whose center of the pass band is fixed, as described in section 2.3.

In analog IF method, the IF signal is passed through the ‘LOG AMP’ and the power is detected by the ‘Detector’, and the ‘Video Filter’ reduced the bandwidth of the detected power, they are described in section 2.2. The ‘Peak Detector’ and the ‘Sampler’ pick up the extracted power at each interval, which is 1/500~1/4000 of the sweep time synchronized with the ‘Ramp signal’. The AD/C digitized the sampled power. Then the sampling frequency is satisfied 10kHz or 50kHz to detect the power.

In digital IF method, the AD/C digitizes the IF signal directory. In some early type of this method, the frequency of the IF signal were configured as the range under 10kHz and the sampling frequency were 20k or 30kHz. And a calculation of FFT (Fast Fourier transform) is used to obtain a spectrum [1].

In recent years (such as since 2000s), we can use high-speed AD/C with 14bit and digitize the 21.4MHz IF signal directly. In this thesis, the early type is not discussed. We will discuss about the type that has high-speed AD/C and signal processing devises. Figure 2.10 shows one example of a digital IF section which has high-speed AD/C and DDC (Digital Down converter described in chapter 4) and the DSP (may be any computer device). The details of the digital-IF method will be described, in following sections.

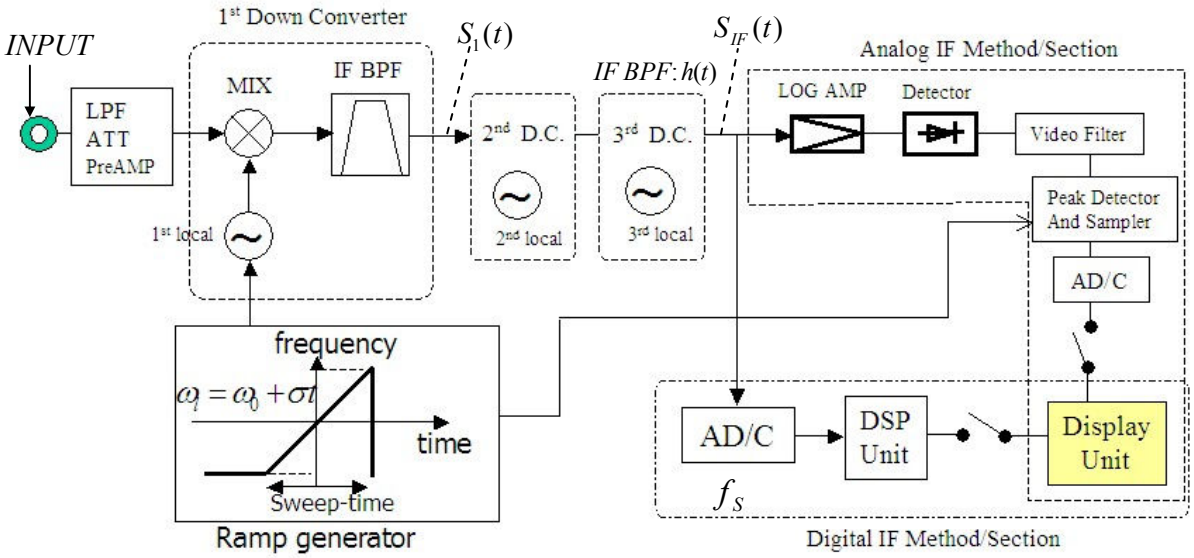

Fig. 2.9 Block Diagram of sweep spectrum analyzers with digital IF

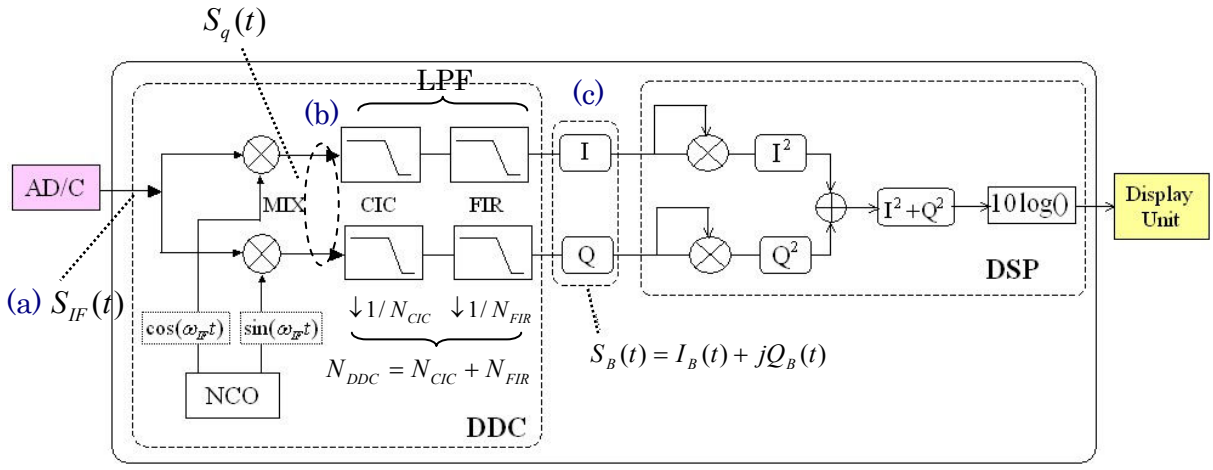

Fig. 2.10 Detail of digital IF section

2.4.2 Quadrature Detection

The digital IF section of Fig.2.10 has some stages, (a), (b), and (c). The signal of (a) is the output of the AD/C and the digitized signal of final analog IF and explained as a real signal,

$$S_{IF}(t) = A(t)\cos(\omega_{IF}\, t + \theta(t)), \qquad (2.15)$$

where *A(t)* is the amplitude, $\theta(t)$ is the phase factor and ω_{IF} is the IF frequency. The spectrum of this signal is shown in (a) of Fig.2.11.

The signal $S_{IF}(t)$ is inputted into the DDC (Digital Down Converter) drawn in Fig.2.10 and enclosed by the dotted square. The DDC operates as a 'Quadrature detector' for the input, and output a 'Base Band Signal'. The 'NCO', numerical controlled oscillator generates two signals, $\cos(\omega_{IF}\, t)$ and $-\sin(\omega_{IF}\, t)$. The two mixers make the product of the signal $S_{IF}(t)$ multiplied $\cos(\omega_{IF}\, t)$ and $-\sin(\omega_{IF}\, t)$ digitally. The signal line whose mixer is linked with $\cos(\omega_{IF}\, t)$ is called '*I*-ch', '*I* part' or '*I*' simply. Similarly, the part linked with $\sin(\omega_{IF}\, t)$ is called '*Q*-ch', '*Q* part' or '*Q*'.

The *I* part at the point (b) is given by

$$I_q(t) = A(t)\cos(\omega_{IF}\, t + \theta(t)) \times \cos(\omega_{IF}\, t), \qquad (2.16\text{-a})$$

it is modified as

$$I_q(t) = \tfrac{1}{2} A(t)\{\cos(2\,\omega_{IF}\, t + \theta(t)) + \cos(\theta(t))\}. \qquad (2.16\text{-b})$$

Similarly, the *Q* part is

$$\begin{aligned} Q_q(t) &= A(t)\cos(\omega_{IF}\, t + \theta(t)) \times (-\sin(\omega_{IF}\, t)) \\ &= \tfrac{1}{2} A(t)\{\sin(2\omega_{IF}\, t + \theta(t)) + \sin(\theta(t))\} \end{aligned}. \qquad (2.16\text{-c})$$

We can consider that the signal $I_q(t)$ and $Q_q(t)$ as a complex signal,

$$S_q(t) = I_q(t) + jQ_q(t), \qquad (2.17)$$

where *j* is an imaginary unit. We can consider a negative frequency in the signal $S_q(t)$.

A system that generates the signal $S_q(t)$ is called a 'quadrature detector'. We call sometimes the quadrature detector that includes the LPF of the DDC.

In Fig.2.11 the sampling frequency of the AD/C is f_s, and the frequency of the IF signal is regarded around $f_s/4$. Then, the angular frequency $2\omega_{IF}$ is a Nyquist frequency (equals to $2\pi f_s/2$) at the stage of (a) and (b). The spectrum of the signal whose frequency is higher than the Nyquist frequency turns around to the negative Nyquist frequency such as the 'Image' of (b) in Fig.2.11.

The signal $S_q(t)$ is inputted into the LPF, which consists of CIC and FIR filters as shown in Fig.2.10. The characteristic about the CIC and FIR are described in chapter 4 and [5]. In the case that the image factor is rejected by the LPF, the passed through signals $S_B(t)$ is given by

$$S_B(t) = \frac{1}{2} A(t)\{\cos\theta(t) + j\sin\theta(t)\}. \qquad (2.18\text{-a})$$

This signal $S_B(t)$ can be considered an analytic signal, whose real part and imaginary part is a pair of Hilbert transform [6], and it can be written as

$$S_B(t) = \frac{1}{2} A(t) \exp[j\theta(t)] = I_B(t) + jQ_B(t) \qquad (2.18\text{-b})$$

This signal has the amplitude $A(t)$ and phase factor $\theta(t)$ of the input signal Eq.(2.2),

$$f_{IN}(t) = A(t)\cos(\omega_{IN} t + \theta(t)),$$

and the IF signal Eq.(2.15)

$$S_{IF}(t) = A(t)\cos(\omega_{IF} t + \theta(t))$$

The analog and digital down-converters, discussed in the above section, rejects the carrier frequency from the input signals, and output the type of the signal $S_B(t)$ that is generally called a **base band signal**.

We can consider that the signal $f_{IN}(t)$ and $S_{IF}(t)$ are real parts of an analytic signal. And we can define the analytic signals as

$$f_{IN\_A}(t) = A(t) \times \exp[j(\omega_{IN} t + \theta(t)] \qquad (2.19\text{-a})$$

$$S_{IF\_A}(t) = A(t) \times \exp[j(\omega_{IF} t + \theta(t))]. \qquad (2.19\text{-b})$$

The base band signal is made by rejecting the carrier frequency from $f_{IN\_A}(t)$ and $S_{IF\_A}(t)$.

The frequency range of $S_B(t)$ is limited by the LPF, and we can reduce the sampling frequency. Usually, the DDC has a function to reduce the rate, which is called **decimation** and the rate of decimation is usually integer. The CIC and FIR filter has the function whose decimation rate is N_{CIC} and N_{FIR}, independently. The total decimation rate N_{DDC} is sum of them, $N_{DDC} = N_{CIC} + N_{FIR}$.

The decimation of (c) from (b) of Fig.2.11 is two, where the Nyquist frequency is $f_s/4$. If any signal whose frequency is from $f_s/4$ to $f_s/2$ or from $-f_s/4$ to $-f_s/2$, some aliasing signals appear in the signal $S_B(t)$ [6]. These aliasing signals are drawn as the gray area and linked by the dotted arrow lines in (b). Usually the LPF reduces the level of the signal whose frequency is higher than its cut off frequency, and output the signal whose frequency area is around 0Hz reducing the aliasing signal, and the area is shown as '*Flt*' in (c). In the case that the DDC is used as a radio receiver, the *Flt* should be wider than the bandwidth of the received signal.

(a) Real IF signal

$S_{IF}(t)$

(b) Base Band signal with image-factors

$S_q(t)$

(c) Decimated Base Band signal without image-factor

$S_B(t)$

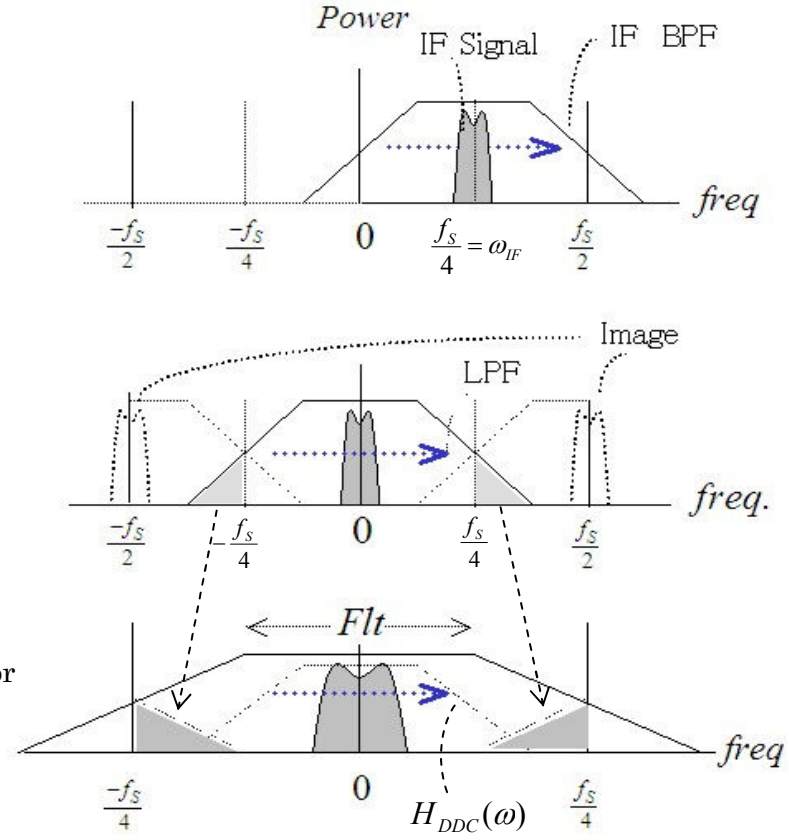

Fig. 2.11 Quadrature Detection in Frequency Domain

2.4.3 Digitized IF Signal with Swept Local oscillator

The local oscillator of sweep spectrum analyzers generates the sweep signal *l(t)*, which is explained as

$$l(t) = \exp\left[j(\pi \cdot \sigma t^2 + \omega_0 t + \theta_0)\right], \qquad (2.20)$$
$$-T_S/2 \le t \le T_S/2$$

where, t is a time, σ is the sweep rate, ω_0 is the frequency at $t=0$, θ_0 is an initial phase, and T_S is the sweep time. The sweep rate σ is decided by Span and the Sweep time.

$$\sigma = \frac{Span}{T_S} \qquad (2.21)$$

In the case that the input signal is explained as Eq.(2.2),

$$f_{IN}(t) = A(t)\cos(\omega_{IN}\, t + \theta(t))\,,$$

the output of the 1st down converter $S_1(t)$ (see Fig.2.9) can be considered as next equation by the discussion of section 2.2.2 and 2.2.3.

$$\begin{aligned} S_1(t) &= a \times A(t) \times \mathrm{Re}\left[\exp[j(-\omega_{IN} t + \theta(t))] \times l(t)\right] \\ &= a \times A(t) \times \mathrm{Re}\left[\exp[j(\pi\sigma t^2 + (\omega_l - \omega_{IN})t + \theta(t) + \theta_0)]\right] \end{aligned} \qquad (2.22)$$

where 'a' is a gain that is adequate vale which is decided by the system condition.

The IF signal, input of the AD/C is a same signal with the input signal except for the carrier frequency.

$$S_{IF}(t) = a' \times A(t) \times \mathrm{Re}\left[\exp[j(\pi\sigma t^2 + \omega_{IF}\, t + \theta(t) + \theta_0)]\right], \qquad (2.23\text{-a})$$

where *a'* is a constant which corresponds to the gain of the down converters, and ω_{IF} is assumed as $\omega_{IF} = \omega_l - \omega_{IN}$.

In equation 2.23-a, it is assumed that the bandwidths of the IF BPF of all down converters (e.g. Fig. 2.11) are sufficiently wider than the bandwidth of the signal. Practically, the effect of the IF BPF should be consider and Eq.(2.23-a) is rewritten as

$$S_{IF}(t) = h(t) * \left\{a' \times A(t) \times \mathrm{Re}\left[\exp[j(\pi\sigma t^2 + \omega_{IF}\, t + \theta(t) + \theta_0)]\right]\right\}, \qquad (2.23\text{-b})$$

where $h(t)$ is the impulse response of the all IF BPF, and ω_{IF} is the center frequency of IF BPF. Actually, the $h(t)$ is almost the response of the narrowest IF BPF, usually it is an IF BPF of the last down converter. In Fig.2.9, it is BPF of the 3rd down converter. In Equation (2.23-b), as the absolute value of the *t* becomes larger, value of the frequency becomes higher. And the amplitude of $S_{IF}(t)$ is reduced when |t| is larger.

Figure 2.12 is the example of a digitized IF signal, which is computed from Eq.(2.23-b), where ω_{IF} equals to 21.4MHz, $\theta(t)$ and θ_0 equal to zero for simplification, Span equals 8MHz and Sweep time equals 0.2msec. The abscissa indicates not only time, but also frequency. The current frequency ω of $S_{IF}(t)$ is define as the differential of the phase of Eq.(2.23-b), which can be explained as

$$\omega = \omega_{IF} + 2\pi\sigma t\,, \qquad (2.24)$$

where σ is decided by Eq.(2.21).

The amplitude of the signal is reduced around the left and right side corresponding to the frequency response of the filter $h(t)$.

In Fig.2.12, the bandwidth of $h(t)$ was approximately 8MHz. We can obtain the spectrum of $f_{IN}(t)$ by detecting the power of this signal with this bandwidth. But, it need narrower band pass filter to obtain higher resolution spectrum. It can be achieved by the signal processing on the digitized IF signal, which is described on the following sections.

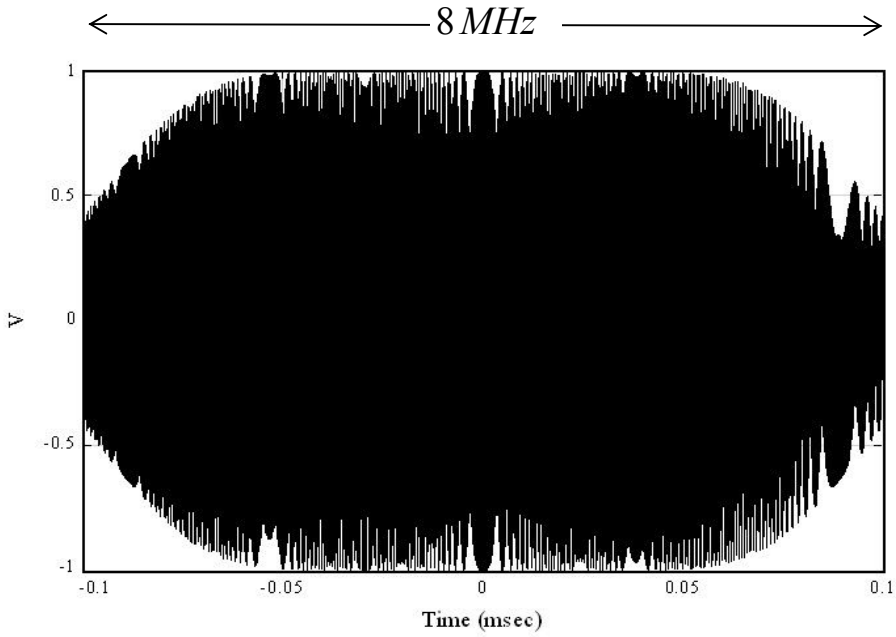

Fig. 2.12 Digitized IF signal with swept local oscillator: $S_{IF}(t)$

Measured signal was CW, *Span*=8MHz, T_S =0.2msec, IF Bandwidth≒8MHz

2.4.4 Base Band Signal

In the spectrum analyzer with a digital IF system such as shown in Fig.2.9 or 2.10, the IF signal $S_{IF}(t)$ is passed through the AD/C and DDC, and converted into the base band signal, which is represented as $S_B(t)$, Eq.(2.18-b). The example of the base band signal $S_B(t)$ is shown in Fig.2.13, which is converted from the IF signal $S_{IF}(t)$, Eq.(2.23-b) and Fig.2.12.

The NCO of the DDC generates $\cos(\omega_{IF}\, t)$ and $-\sin(\omega_{IF}\, t)$. The IF frequency factor ω_{IF} is rejected, and the signal $S_B(t)$ is explained as

$$S_B(t) = h_{DDC}(t) * \left\{ a'' \times A(t) \times \exp[\, j(\pi \sigma t^2 + \theta(t) + \theta_0)] \right\}, \qquad (2.25)$$

where *a"* is a constant corresponds to a gain of the system, $h_{DDC}(t)$ is a impulse response of the LPF implemented in the DDC. Usually, the bandwidth of $h_{DDC}(t)$ is narrower than *h(t) in* Eq.(2.23-b). The frequency response of $h_{DDC}(t)$ is drawn in Fig.2.11 (c) as $H_{DDC}(\omega)$. Where, the 3dB bandwidth of the $H_{DDC}(\omega)$, $h_{DDC}(t)$ is configured as 4MHz.

The frequency of $S_B(t)$ is a differentiation of the phase factor of Eq.(2.25), it is explained as

$$\omega_B = 2\pi\sigma t + \frac{d}{dt}\theta(t). \quad (2.26\text{-a})$$

In Figure 2.13, $\theta(t)$ and $\theta_0(t)$ are assumed to be zero for a simplification, and the time *t* equals zero at the center. Equation (2.26-a) is rewritten as

$$\omega_B = 2\pi\sigma t. \qquad (2.26\text{-b})$$

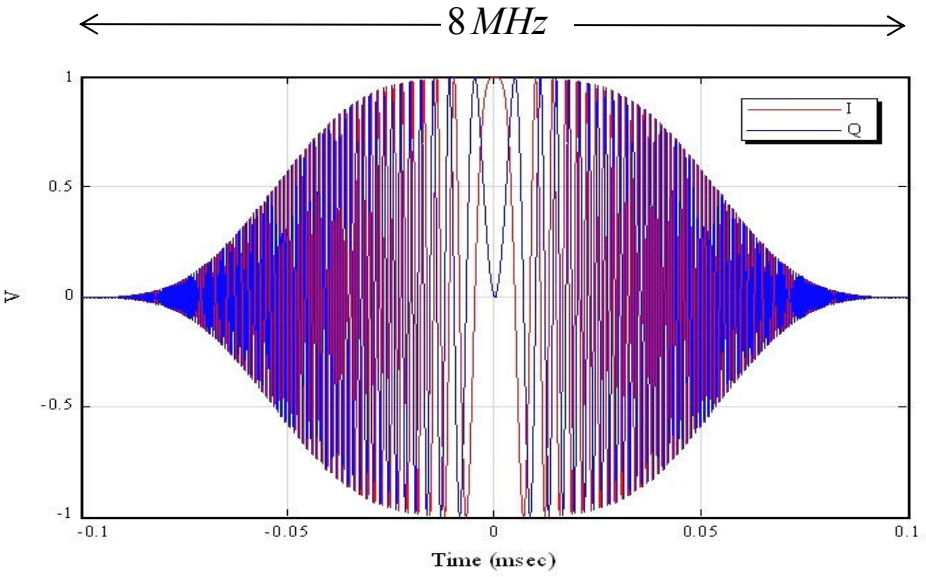

Fig. 2.13 Quadrature Detected IF Signal through a wide band LPF: $S_B(t)$

Measured signal was CW, *Span*=8MHz, T_S =0.2msec, Bandwidth≒4MHz

The frequency ω_B is 0Hz when t equals zero. If we convolute the narrower LPF on the signal $S_B(t)$, we can extract the part around 0Hz as shaper impulse, as shown in Fig.2.14. Now, we define that the narrow LPF is a '**RBW filter**' and the output signal is $S_{B\_RBW}(t)$. In the case that the frequency of the input signal is $\omega_{IN} \pm \delta\omega$, the frequency of the base band signal is

$$\omega_{B\delta} = 2\pi\sigma t \pm \delta\omega . \qquad (2.27\text{-a})$$

The time t_0 at which $\omega_{B\delta}$ equals zero can be explained as

$$t_0 = \mp \frac{\delta\omega}{2\pi\sigma t} . \qquad (2.27\text{-b})$$

This time t_0 is corresponding to the frequency $\delta\omega$, and $\delta\omega$ can be explained as

$$\delta\omega = \mp 2\pi\sigma t_0 . \qquad (2.27\text{-c})$$

Whether plus or minus of the double sign, depends on the system configuration described in section 2.2.

The abscissa of Fig.2.13 and 2.14 indicates both time and frequency. We can obtain the power spectrum by computing the square sum of the real part and the imaginary part of $S_{B\_RBW}(t)$, whose example is shown in Fig.2.15.

The spectrum is obtained by following equation.

$$F(\omega) = 10\log\left(S_{B\_RBW}(t)\right) = 10\log\left(I(t)^2 + Q(t)^2\right) \qquad (2.28)$$

where *I(t)* and *Q(t)* is the real part and imaginary part of $S_{B\_RBW}(t)$.

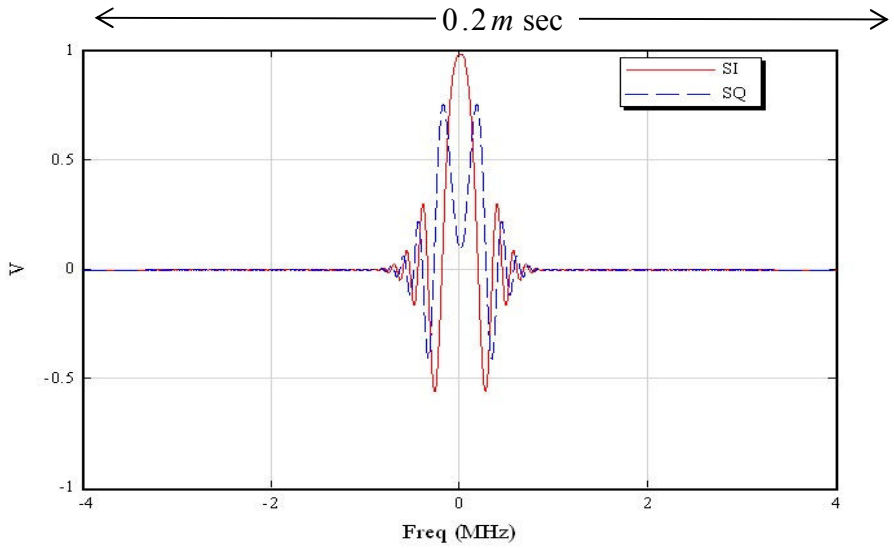

Fig. 2.14 Quadrature Detected IF Signal through a RBW Filter : $S_{B\_RBW}(t)$

Measured signal was CW, *Span*=8MHz, T_S =0.2msec, *Rbw*=300kHz

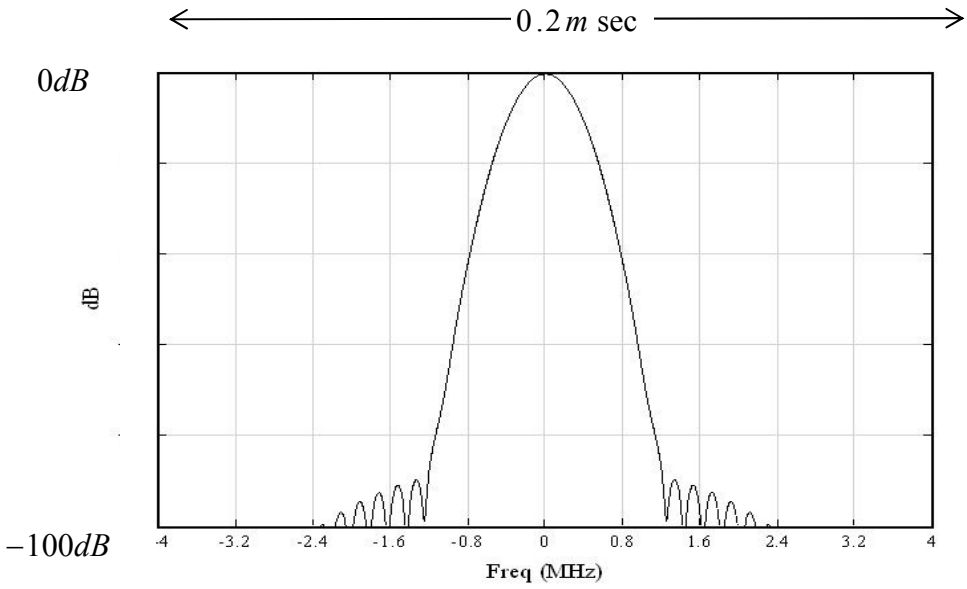

Fig. 2.15 Spectrum Extracted from a Signal $S_{B\_RBW}(t)$

Measured signal was CW, *Span*=8MHz, T_S =0.2msec, *Rbw*=300kHz

The deformed signal flow of the sweep spectrum analyzer that includes the digital IF system is shown in Fig.2.16, where the all signals are assumed analytic signals. The down converter indicates as the total function of all analog and all digital.

The input signal $f_{INPUT\_A}(t)$ includes the carrier frequency factor $\exp[j(\omega_{IN}t)]$, which is removed by the down converter. The down converter attaches the chirp factor $\exp[j(\sigma t^2)]$ on the signal. The base band signal keep the factor $A(t)$ and $\theta(t)$. The RBW filter extracts the part of the signal whose frequency is around 0Hz. The spectrum is obtained as the square sum of real part and imaginary part of $S_{B\_RBW}(t)$.

In conventional sweep spectrum analyzer, the IF BPF: RBW filter, extracts the spectrum. It is not efficient to replace this processing in a digital. In this case we must keep the sampling frequency corresponding to the IF frequency. On the other hand, in the case we convert the IF signal into the base band signal, we can reduce the sampling frequency according to the pass band of the LPF. The reduction of the sampling frequency is called **decimation** [5]. We can obtain the spectrum with minimum size of the data by the decimation.

More consideration about the signal processing to obtain the spectrum will be done in section 2.5.

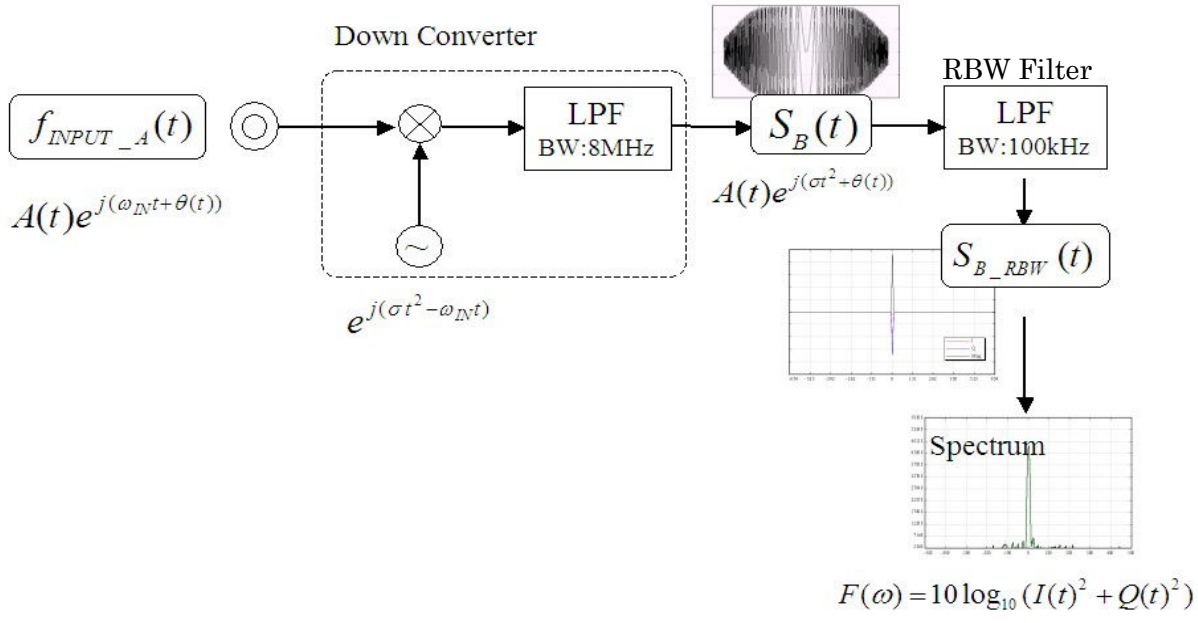

Fig. 2.16 Signal Flow of a Sweep Spectrum analyzers with Digital IF system

2.5 Analysis of Sweep Spectrum analyzer

The fundamental and qualitative analysis was given in section 2.2~2.4. This section describes the mathematical analysis of the sweep spectrum analyzer.

2.5.1 Spectrum Analyzer as Pseudo Fourier Transformer

A simplified block diagram of a sweep spectrum analyzer is shown in Fig.2-17 [2][3]. Actually, sweep spectrum analyzers have two or three down converters with a mixer, a local oscillator and an IF BPF. In this section, the down converters are figured as one for a simplification. By the discussion, section 2.2 and 2.3, we can down convert the input signal $f_{IN}(t)$ (whose frequency is ω_{IN}) to the base band signal (0Hz), and we can express the signals as analytic signals.

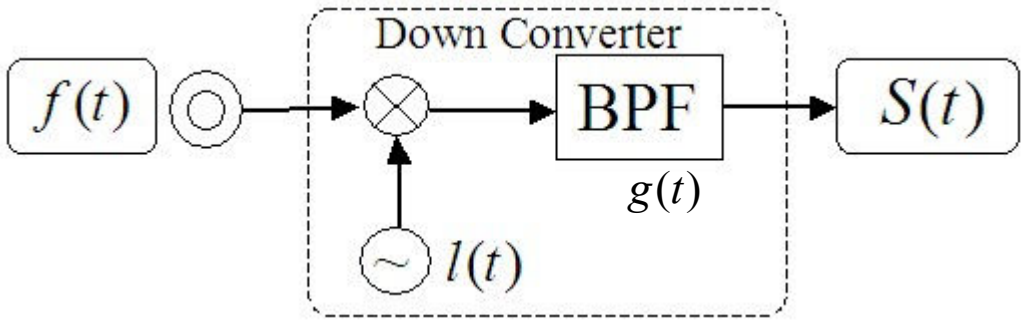

Fig. 2.17 Simplified Block Diagram of a Sweep Spectrum Analyzers with Digital IF

The 'Down Converter' converts the input signal $f(t)$ to the base band signal. The frequency of the local oscillator swept over the frequency band, '*Span*' with some sweep rate. The *Span* is a frequency band we desire to measure for the spectrum. Mathematical expressions of the $f(t)$ and $S(t)$ are given with the following equations,

$$f(t) = a(t)\exp[\, j\omega_s t\,] \qquad (2.29\text{-a})$$

$$S(t) = g(t) * \{f(t) \times l(t)\}, \qquad (2.29\text{-b})$$

where *a(t)* is time variations in amplitude and phase of a signal under the measurement, which is often called 'a base band signal'. And ω_s is the angular frequency. We assume *f(t)* is a band limited complex signal. The impulse response of the 'IF BPF' is expressed by *g(t)*, which is not a complex but a real function. The '*' denotes the operation of a convolution. The *l(t)* is a signal

generated by a local oscillator of which frequency is swept at the sweep rate denoted by σ. It can be expressed as

$$\left.\begin{aligned} l(t) &= \exp\left[-j(\pi\cdot\sigma t^2+\omega_0 t+\theta_0)\right], \\ &-T_S/2 \le t \le T_S/2, \end{aligned}\right\} \quad (2.30\text{-a})$$

where 't' is time, 'θ_0' is the initial phase, 'ω_0' is the angular frequency of the oscillator at *t=0* and the σ is the sweep rate (Hz/sec). The sweep in the frequency is repeated every cycle with the duration, T_s seconds over the SPAN band, *Span*, so that the sweep rate can be written as

$$\sigma = Span/T_S. \qquad (2.30\text{-b})$$

In every sweep cycle, the measured power spectrum is shown on a display, repeatedly.
By substituting Eq.(2.30-a) into Eq.(2.29-b), we can derive a complete expression for *S(t)* as

$$S(t) = g(t) * \left\{ f(t)\times\exp[-j(\pi\cdot\sigma t^2+\omega_0 t+\theta_0)] \right\}, \qquad (2.31\text{-a})$$

and rewrite as

$$S(t) = \int_{-\infty}^{\infty} g(\tau) f(t-\tau)\times\exp\left\{-j\left(\pi\cdot\sigma(t-\tau)^2+\omega_0(t-\tau)+\theta_0\right)\right\} d\tau \qquad (2.31\text{-b})$$

It is modified as

$$S(t) = \exp[-j(\pi\sigma t^2+\omega_0 t+\theta_0)]\int_{-\infty}^{\infty} g(\tau)\times a(t-\tau)\times\exp\left\{j\left(\omega_s(t-\tau)-(\pi\sigma\tau^2-2\pi\sigma\tau t-\omega_0\tau)\right)\right\} d\tau$$

$$= \exp[-j(\pi\sigma t^2+\omega_0 t+\theta_0)]\cdot\exp[j\omega_s t]\int_{-\infty}^{\infty} g(\tau)a(t-\tau)\times\exp\left\{-j\left(\pi\sigma\tau^2-2\pi\sigma t\tau+(\omega_s-\omega_0)\tau\right)\right\} d\tau$$

$$\cdots\cdots\cdots\cdots\cdots (2.31\text{-c})$$

where *f(t)* is substituted with Eq.(2.29-a). In the case that the sweep rate $\sigma = 0$, Eq.(2.31-c) is written as

$$S_0(t) = \exp[j\{(\omega_s-\omega_0)t-\theta_0\}] = \int_{-\infty}^{\infty} g(\tau)r(\tau)\times\exp\left\{-j(\omega_s-\omega_0)\tau\right\} d\tau, \qquad (2.32)$$

where $S_0(t)$ is a signal of *S(t)* with $\sigma = 0$, and the time t is a independent variable to the integration, and $r(\tau)$ is defined as

$$r(\tau) \equiv a(t-\tau). \qquad (2.33)$$

The integral in Eq.(2.32) is a Fourier transform against the τ on a product of $g(\tau)$ and $r(\tau)$, and $S_0(t)$ is written as

$$\left.\begin{aligned} S_0(t) = \exp[\, &j((\omega_s-\omega_0)t-\theta_0)] \\ &\times\{G(\omega_s-\omega_0) * R(\omega_s-\omega_0)\}, \end{aligned}\right\} \quad (2.34)$$

where $G(\omega)$ and $R(\omega)$ is the Fourier transform of $g(\tau)$ and $r(\tau)$. It is possible to express the $R(\omega)$ by a theory of the Fourier transform as follows [7].

$$R(\omega) = \exp[-j\omega t] \times A(-\omega) \qquad (2.35)$$

where *A(ω)* is the Fourier transforms of a(τ), and Eq.(2.34) is modified as

$$S_0(t) = \exp[-j\theta_0] \times \{G(\omega_0 - \omega_s) * A(\omega_s - \omega_0)\}. \qquad (2.36\text{-a})$$

The function *g(t)* is a real signal. Then $G(-\omega) = G^*(\omega)$ and $|G(\omega_s - \omega_0)| = |G(\omega_0 - \omega_s)|$, where $G^*(\omega)$ is the complex conjugate of $G(\omega)$.

In the case that we focus the magnitude of Eq.(2.36-a) only, Eq.(2.36-a) can be rewritten as

$$|S_0(t)| = |G^*(\omega_0 - \omega_s) * A(\omega_0 - \omega_s)|, \qquad (2.36\text{-b})$$

and can be considered as an amplitude spectrum $A(\omega_0)$ which is convolved with $G(\omega_0)$.

In the case that the sweep rate σ is sufficiently small that can be assumed zero, the frequency $\omega_0 - \omega_s$ can be replaced by ω as

$$\omega(t) = 2\pi\sigma t + \omega_0 - \omega_s, \qquad (2.36\text{-c})$$

where $2\pi\sigma t + \omega_0$ is the differential of the phase factor of Eq.(2.30-a). Then Eq.(2.36-b) is replaced by

$$|S_0(t)| = |G^*(\omega(t)) * A(\omega(t))|. \qquad (2.36\text{-d})$$

From Equation (2.29) we can see the relation $F(\omega(t)) = A(\omega(t) - \omega_s)$ and

$$A(\omega(t)) = F(\omega(t) + \omega_s), \qquad (2.36\text{-e})$$

where $F(\omega)$ is the Fourier transform of *f(t)*. Then Eq.(2.36-d) is modified as

$$|S_0(t)| = |G^*(\omega(t)) * F(\omega(t) + \omega_s)|. \qquad (2.36\text{-f})$$

This equation stands only for the σ sufficiently small. The restriction on the sweep rate is discussed in the next section.

The above equations represent that a sweep spectrum analyzer is a Fourier transformer which gives the Fourier components at any frequency ω as the convolution of $F(\omega)$ and $G(\omega)$. Theoretically, if $G(\omega)$ was the delta function $\delta(\omega)$, Eq. (2.36-f) was the true Fourier transform of *f(t)*. Most spectrum analyzers have $G(\omega)$ defined by RBW filters, instead of $\delta(\omega)$. And they measure spectrum with a limited sweep rate.

The RBW is a significant parameter of a spectrum analyzer and is defined as a half power (3dB) bandwidth of a RBW filter. The RBW filter decides the frequency resolution of the measurements as expressed in Eq.(2.36-e).

2.5.2 Restriction of sweep rate

The sweep spectrum analyzer measures spectrum by a restricted sweep rate which is theoretically given in [3][7][8], and summarized in this section.

Usually, the characteristic of the RBW filter, $g(t)$ can be expressed as a Gaussian function whose frequency response is $G(\omega)$, shown in the following equation,

$$G(\omega) = \exp\left[-\frac{\ln 2}{(\pi \cdot Rbw)^2} \omega^2 \right], \qquad (2.37)$$

where *Rbw* is the 3dB bandwidth of $G(\omega)$ expressed in Hz, whereas ω in radians. Next two equations show the restriction of sweep rate and sweep time corresponds to the *Rbw*.

$$\sigma_{\max} = \frac{Span}{T_{s\_\min}} = \frac{Rbw^2}{k_0} [Hz/\sec], \qquad (2.38)$$

$$T_{S\_\min} = \frac{Span}{\sigma_{\max}} = \frac{Span \cdot k_0}{Rbw^2} [\sec], \qquad (2.39)$$

where $\sigma_{\max}$ is the maximum sweep rate, $T_{S\_\min}$ is the minimum sweep time, 'Span' is a frequency SPAN, and k_0 is constant which is defined experimentally 2~3 [3][2]. Here we defined the variable '*1/k*' as the 'Normalized sweep rate', which is explained by following equation [8].

$$\frac{1}{k} = \frac{Span}{T_S \times Rbw^2} = \frac{\sigma}{Rbw^2}, \qquad (2.40)$$

with the restricted of $1/k \le 1/k_0$.

The characteristic $G(\omega)$ can be observed as a frequency response of $S_0(t)$, Eq.(2.36-f) in the case that $F(\omega)$ is δ function (*f(t)* is a CW signal). The example of $G(\omega)$ is shown in Fig.2.18, where the abscissa indicates both time and frequency. The time ΔT corresponds to *Rbw* as $\Delta T = T_S \cdot Rbw / Span$.

In the case that *1/k* is larger than $1/k_0$, the value σ in Eq.(2.31-c) becomes so large that it can no more be disregarded as zero and Eq(2.32)~(2.36-f) could not be established. In the case that the sweep rate is too high beyond the limit, so that the peak level of the measured spectrum is reduced and the bandwidth is broadened. This property is called 'over swept-rate response' [10]. Several authors [3][2][11] have investigated the phenomenon theoretically and experimentally. This thesis describes only the results as following three topics.

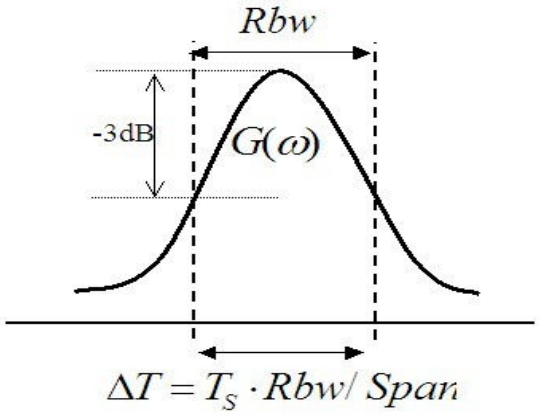

Fig. 2.18 Conceptual diagram of sweep time and rate

1) The peak level reduction:

$$\frac{A'}{A} = \left\{ 1 + \left(\frac{2}{\pi} \ln 2 \right)^2 \left(\frac{1}{k} \right)^2 \right\}^{-\frac{1}{4}}, \qquad (2.41)$$

where *A* is the amplitude of the signal at *1/k* equals to zero, and *A'* is the measured amplitude of the signal. In most conventional sweep spectrum analyzer, the value of k_0 is decided to make the reduction 0.1dB [1]-[3].

2) The broadening of the resolution bandwidth:

$$\frac{Rbw'}{Rbw} = \left\{ 1 + \left(\frac{2}{\pi} \ln 2 \right)^2 \left(\frac{1}{k} \right)^2 \right\}^{\frac{1}{2}}, \qquad (2.42)$$

where *Rbw* is configured value and *Rbw'* is the observed value.

An example of the over swept-rate response is shown in Fig.2-19. The solid and dashed lines indicate the response of the resolution filter for the *1/k* equals 0.5 and 5.0. Some kinds of spectrum analyzers have RBW filters implemented by the digital IF method. They estimate and correct the distortion of Eq.(2.41) and (2.42), and achieve its sweep rate 2~4 times faster than the conventional one [10].

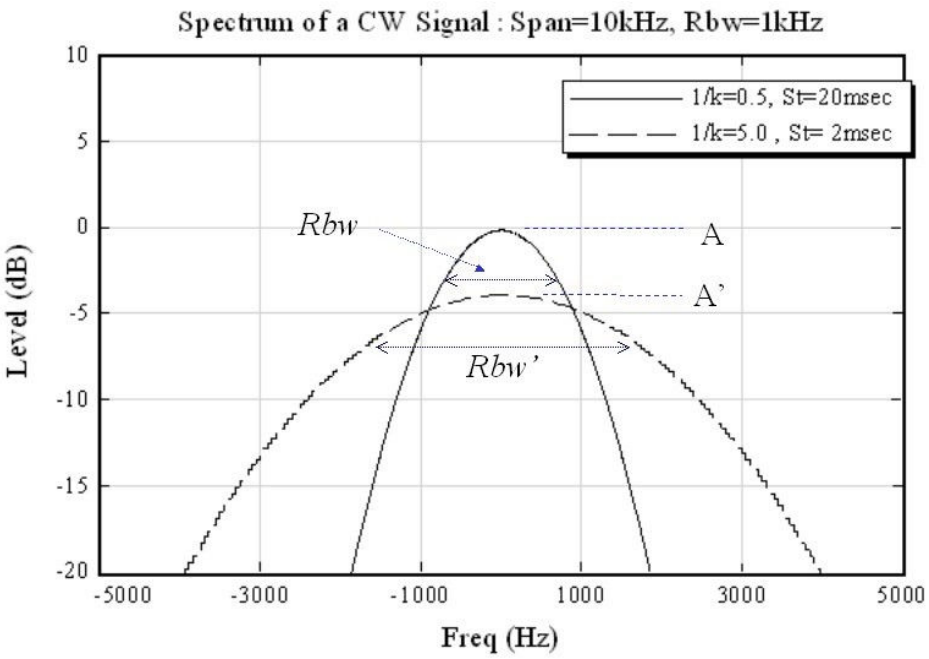

Fig. 2.19 Example of over swept-rate response

3) The Peak shift:

In the case that the RBW filter is an analog filter. The measured spectrum has frequency shift, $\Delta\omega$ by the latency of the filter response [11].

$$\Delta\omega = 2\pi \times (1/k) \times Rbw^{2} \times \Delta t \,, \qquad (2.43)$$

where $\Delta\omega$ is shifted radian frequency of the peak, and Δt is the delay of the RBW filter response.

Figure 2.20 shows the samples of spectrum whose *1/k* equals 0.5, 10 and 50. The over sweep-rate response occurs on 1/k=10 and 50. The response of digital filter is symmetrical on the frequency axis, and we can forecast and correct this latency.

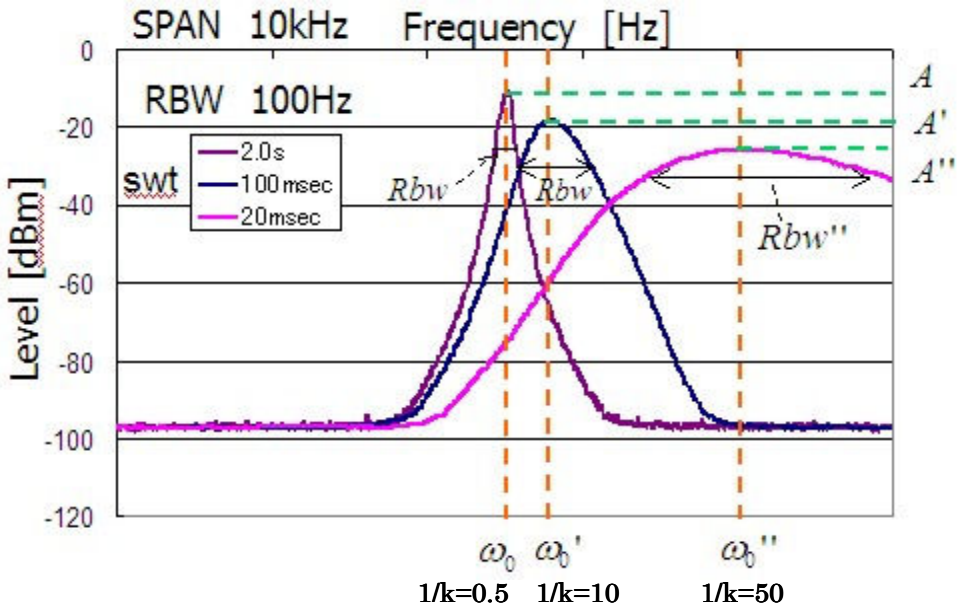

Fig. 2.20 Power spectrum under over-sweep

2.5.3 Gauss Function as Resolution Filter

Usually, Gauss filter is chosen as the characteristics of the resolution filter in a sweep spectrum analyzer by the reason as follows [1][11].

1. Well distinction for two signals (well shape factor)
2. Quick response for the sweep signal

In this thesis, the impulse response of a Gaussian filter is explained by $g(t)$ whose frequency response is $G(\omega)$, they are expressed by [12]

$$g(t) = \exp\left[-\frac{t^2}{a^2} + j\omega_{IF} \right], \qquad (2.44\text{-a})$$

$$G(\omega) = a\sqrt{\pi}\,\exp\left[-\frac{1}{2}a^2(\omega - \omega_{IF})^2 \right]. \qquad (2.44\text{-b})$$

When *Rbw* is the 3dB bandwidth, $G(\omega)$ is given by

$$G\left(\omega_{IF} \pm \frac{Rbw}{2} \right) = \frac{1}{2} G(\omega_{IF}). \qquad (2.45)$$

From this equation, '*a*' is introduced as follows.

$$a^2 = \frac{2\ln 2}{(\pi \cdot Rbw)^2}. \qquad (2.46)$$

In the sweep spectrum analyzer, the Gaussian filter receive the chirp signal as expressed in Eq.(2.31-a) (see section 2.5.1).

$$S(t) = l(t) \int_{-\infty}^{\infty} g(\tau) f(t-\tau) \times \exp\left\{ j\left(\pi\sigma\,\tau^2 - 2\pi\sigma\,t\tau - \omega_0 \tau \right) \right\} d\tau,$$

where *S(t)* is the output of the Gaussian filter, *l(t)* is the output of the local oscillator, *f(t)* is the input signal.

When *f(t)* is CW signal, such as

$$f(t) = \exp[-j\omega_0 t], \qquad (2.47\text{-a})$$

S(t) and its magnitude are explained as next equations by modifying Eq.(2.31-c).

$$\begin{aligned} S(t) &= g(t) * \left\{ f(t) \times \exp[\; j(\pi \cdot \sigma\, t^2 + \omega_0 t + \theta_0)] \right\} \\ &= g(t) * \left\{ \exp[\; j(\pi \cdot \sigma\, t^2 + \theta_0)] \right\} \end{aligned} \qquad (2.47\text{-b})$$

$$
\begin{aligned}
|S(t)| &= \left| \int_{-\infty}^{\infty} \exp[-\tau^2/a^2] \times \exp[j\omega_0(t-\tau)] \times \exp\left\{ j\left(\pi\sigma\,\tau^2 - 2\pi\sigma\, t\tau - \omega_0\tau\right)\right\} d\tau \right| \\
&= \left| \int_{-\infty}^{\infty} \exp[-\tau^2/a^2] \times \exp[j\omega_0 t] \times \exp\left\{ j\left(\pi\sigma\,\tau^2 - 2\pi\sigma\, t\tau\right)\right\} d\tau \right| \quad , \qquad \text{(2.47-c)} \\
&= \left| \int_{-\infty}^{\infty} \exp[-\tau^2/a^2] \times \exp\left\{ j\left(\pi\sigma\,\tau^2 - 2\pi\sigma\, t\tau\right)\right\} d\tau \right|
\end{aligned}
$$

It is very difficult to solve this integration analytically. We simulated this equation as shown in Fig. 2.21(a) and (b). In the figures, the red and blue lines is *I(t)* and *Q(t)* that is real and imaginary part of

$$f(t) \times \exp[\, j(\pi \cdot \sigma t^2 + \omega_0 t + \theta_0)] = \exp[\, j(\pi\sigma t^2)]\,. \qquad (2.48)$$

Each of them is one part of the convolution of Eq.(2.47-b). The green line indicates $g(t)$ that is another part of the convolution. For these three signals, the ordinate is 1 to -1 for the full vertical scale. The black line indicates $|S(t)|$ whose ordinate is 0 to –100dB in the full vertical scale.

In Figure 2.21, the abscissa indicates both time and frequency, time corresponds to the sweep time that is 20msec in (a) and 4msec in (b), frequency corresponds to the *Span* that is commonly 10kHz. And both of the *Rbw* are 1kHz. The peak level of $S(t)$ in (a) and (b) is –0.10dB and –1.73dB, respectively. The observed RBW, *Rbw'* is 1.0kHz and 1.6kHz, respectively. But, the figures of $S(t)$ are both parabolic lines, i.e. they are Gauss function.

Figure 2.21(c) is corresponding to the part of Fig.(a), which is magnified around the center (t =0sec and frequency = 0Hz). Its *Span* equals 1kHz. And the sweep time equals 2msec, which corresponds to 2/Rbw. This relation among *Span*, *Rbw*, and sweep time is corresponding to Eq.(2.40) whose *k* equals 2.0.

$\theta(t)$ of (c) indicates 'atan(Q/I)'. $\theta(t)$ is zero at the center and $-\pi/2$ at the start point and stop point of (c). The differentiation of the phase factor of Eq.(2.48) is the frequency, $2\pi\sigma t$. The changing of the phase and frequency within the period of (c) is very slow, and the integration of Eq.(2.47-b) and (2.47-c) almost same as the case that σ equals zero. But the integration is reduced against the σ which is non zero. If the σ is larger and larger, the value of the integral will be reduced.

We can consider that the cause of the reduction (the over sweep-rate response) is the operation of the filter against the chirp signal.

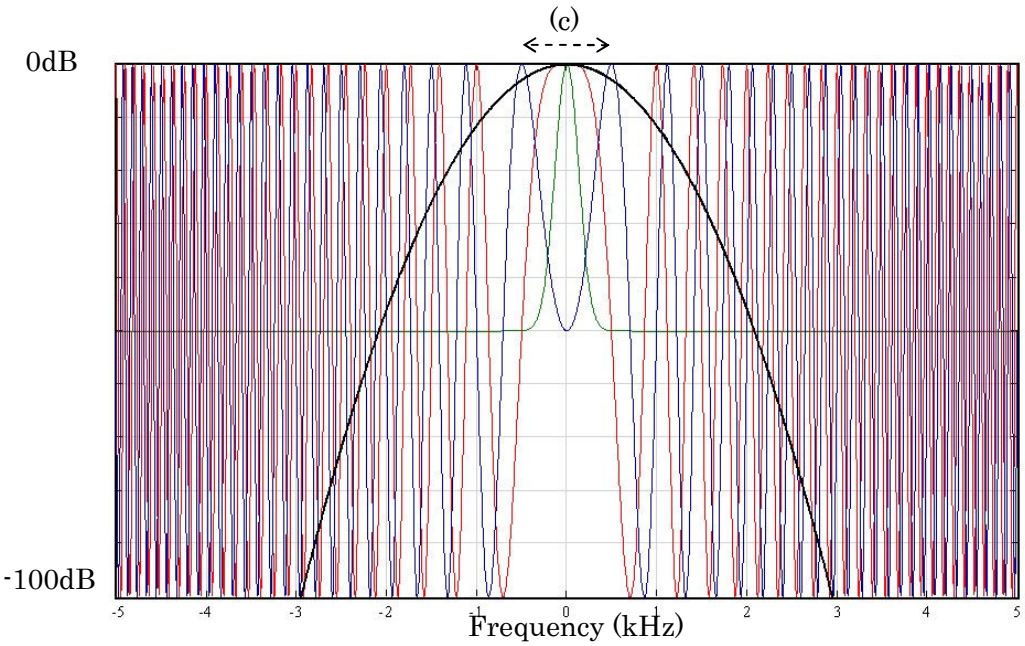

Fig. 2.21 (a) Base Band signal and Spectrum

SPAN=10kHz, RBW=1kHz, T_S =20msec ,Peak level = -0.10dB, 1/k=0.5

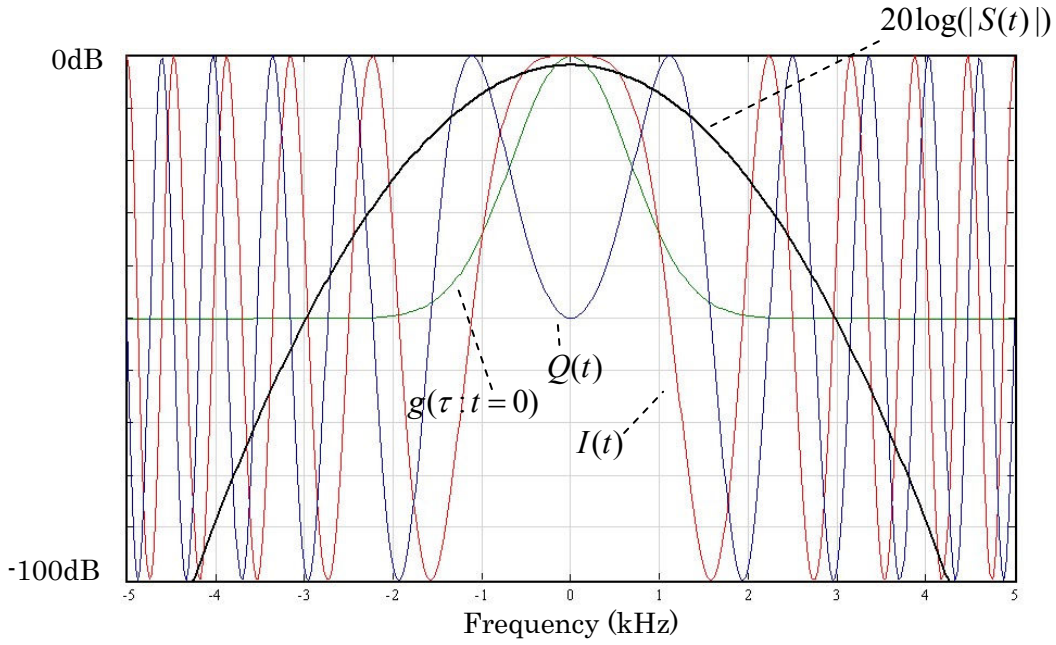

Fig.2.21 (b) Base Band signal and Spectrum:

SPAN=10kHz, RBW=1kHz, T_S =4msec, Peak level = -1.73dB, 1/k=2.5

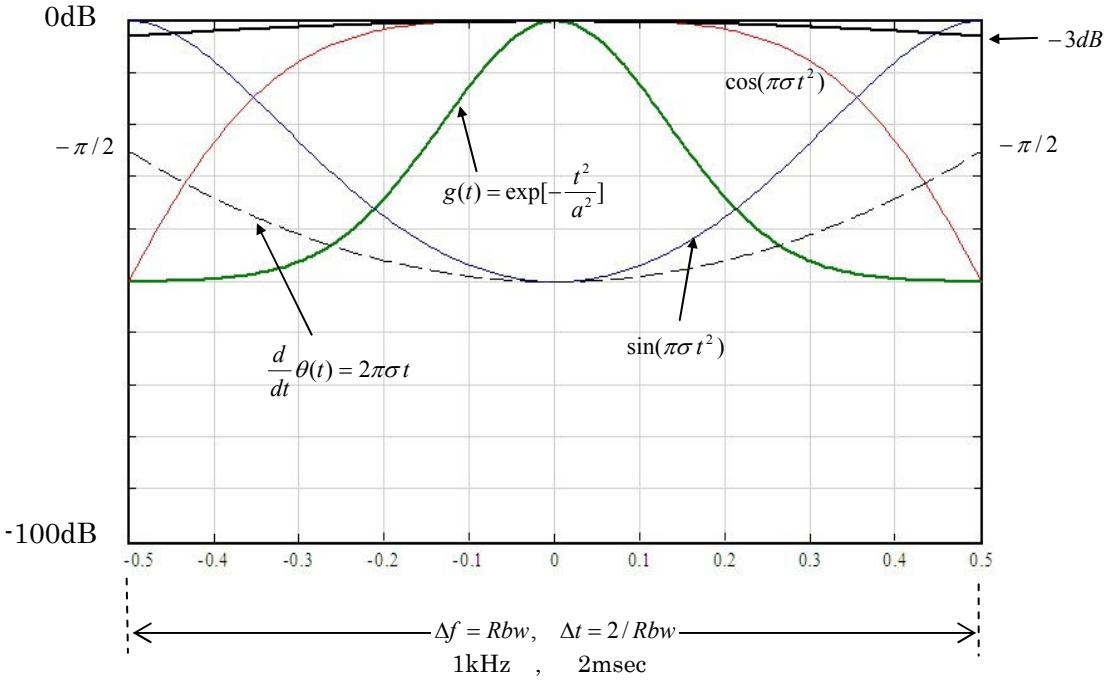

Fig.2.21 (c) SPAN=1kHz, RBW=1kHz,
T_S =2msec, Peak level = -0.1dB, 1/k=0.5

Fig. 2.21 Simulation of the integral Eq.(2.47-b) :
Response of Gaussian filter against chirped base band signal

2.5.4 Simulation of Over Swep-Rate response

The plotted peak level reduction against the normalized sweep rate *1/k* is shown in Fig.2.22 and Table 2.1, where *1/k* is defined by Eq.(2.40). The line of '*Theory*' was the plot of Eq.(2.41), and the line 'R3264' was obtained by using a spectrum analyzer R3264, produced by Advantest Co. We got these data by measuring a CW signal and plotting the peak level. The *Span* and *Rbw* of All plots were 2kHz and 30Hz, respectively. We changed the 1/k by changing the sweep time T_S, which is shown in Table2.1. The line of 'Siml' was obtained by the numeric analysis, which operated the integral of Eq.(2.47-c) and detected the peak levels. Figure 2.21 is the one example of the analysis.

The plotted broadening of the *Rbw* against the *1/k* is shown in Fig.2.23 and Tabl 2-2. The line of '*Theory*' was the plot of Eq.(2.42). The line of 'Siml' was obtained by the same analysis of Fig.2.21 and 2.22 by measuring the observed *Rbw*, *RBw'* as shown in Fig.2.19. In Figure 2.23, we did not plot the line 'R3264', for the large distortion of the spectrum and insufficient resolution of the display with R3264.

The line 'R3264' in Fig.2-22 is lower than the simulation and model, for the reason that the RBW filter of R3264 is not ideal Gaussian filter.

The both lines 'Siml' in Fig.2.22 and 2.23 almost correspond to '*Theory*'. Then we confirmed that the over sweep-rate response exist in the digital IF method as Eq.(2.41) and (2.42).

By the result of Fig.2.22, the value of 1/*k* that made the reduction 0.1dB was 0.5. And the reduction at *k=2* was 0.14dB. The general permitted peak reduction is 0.1dB [1]. The value k_0 in Eq.2.12 to Eq.2.14 is decided that make the reduction 0.1dB.

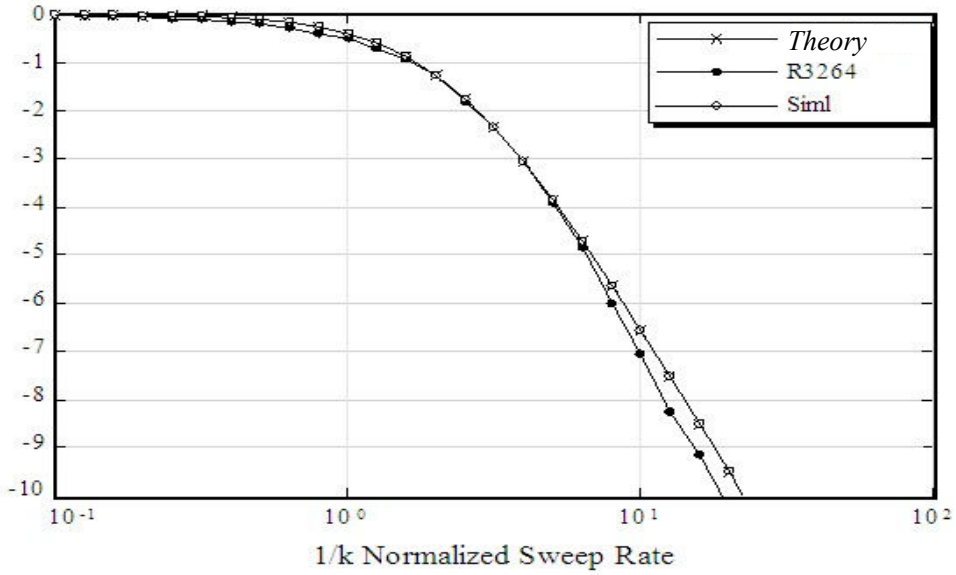

Fig. 2.22 Peak Level Reduction vs. Normalized Sweep Rate

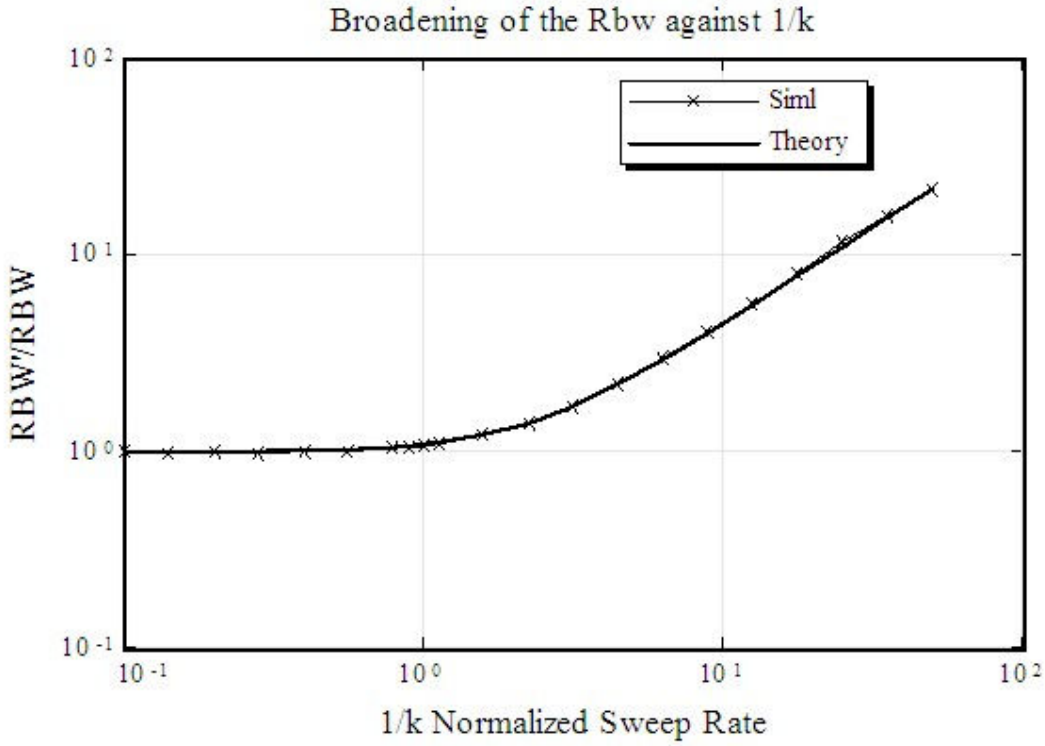

Fig. 2.23 Broadening of *Rbw* vs *1/k*

Table 2.1 Peak Level Reduction vs. Normalized Sweep Rate

1/k	*Theory*	R3264	Siml	T_S
0.100	0.00	0.000	−0.004	22.2
0.126	−0.01	−0.016	−0.007	17.7
0.158	−0.01	−0.032	−0.011	14.0
0.200	−0.02	−0.042	−0.017	11.1
0.251	−0.03	−0.077	−0.027	8.85
0.316	−0.04	−0.097	−0.042	7.03
0.398	−0.07	−0.142	−0.066	5.58
0.501	−0.10	−0.197	−0.10	4.43
0.631	−0.16	−0.273	−0.16	3.52
0.794	−0.25	−0.404	−0.25	2.80
1.00	−0.39	−0.504	−0.39	2.22
1.26	−0.58	−0.722	−0.58	1.78
1.58	−0.86	−0.918	−0.87	1.40
2.00	−1.25	−1.25	−1.25	1.11
2.51	−1.74	−1.80	−1.74	0.885
3.16	−2.35	−2.33	−2.35	0.703
3.98	−3.06	−3.05	−3.06	0.558
5.01	−3.85	−3.91	−3.85	0.443
6.31	−4.71	−4.84	−4.71	0.352
7.94	−5.62	−6.01	−5.62	0.280
10.0	−6.56	−7.04	−6.56	0.222
12.6	−7.52	−8.25	−7.52	0.177
15.8	−8.49	−9.14	−8.49	0.140
20.0	−9.47	−10.21	−9.48	0.111
25.1	−10.46	−11.58	−10.47	0.88
31.6	−11.46	−12.18	−11.46	0.070
39.8	−12.45	−13.52	−12.46	0.056
50.1	−13.45	−14.50	−13.45	0.044

Table 2.2 Broadening of Rbw against Normalized Sweep Rate

1/k	Siml	*Theory*
0.1	1	1
0.14	0.98	1
0.2	1	1
0.28	0.98	1.01
0.4	1	1.02
0.56	1.01	1.03
0.79	1.05	1.06
0.89	1.06	1.07
1	1.08	1.09
1.12	1.1	1.12
1.58	1.22	1.22
2.24	1.41	1.41
3.16	1.72	1.72
4.47	2.24	2.21
6.31	3.04	2.96
8.91	4.11	4.06
12.59	5.78	5.64
17.78	8.21	7.91
25.12	11.79	11.13
35.48	16.07	15.69
50.12	22.11	22.14

2.5.5 Analog Gaussian Filter

In the case that the RBW filter is digital filter, the response of the filter keeps the property as a Gauss function. But when the filter is an analog filter, the response does not keep in a fast sweep as shown in Fig.2.8. Many analog-Gaussian filters are designed by Bessel method in 4^{th} or 5^{th} order; these are not ideal Gauss filter [11]. The peak reductions of them are generally larger than the theory as shown in Fig.2.22 and Table 2.1.

By the result of 'R3264' in Fig.2.22, the value of k, which made the peak reduction 0.1dB, was about 3.1 (1/k=0.32). And the reduction at k=2 was 0.2dB.

Many conventional spectrum analyzer which has analog RBW filters configure is configured whose k_0 is larger than 2 (see Eq.(2.28) and (2.29)).

2.5.6 Resolution Bandwidth

In a spectrum analyzer, a resolution bandwidth (RBW) is defined by the minimum frequency that distinguishes two signals as two signals on a measured spectrum.

In the case that the frequency between the two signals is larger than the RBW, the peaks of the spectrum are observed distinctively as shown in Fig.2.24 (a), where the difference of two signals is 1.5×RBW. On the other hand, in the case that the difference is narrower than the RBW, the two signals are observed as one peak, it is shown in Fig.2.24(b), where the frequency difference is 0.9 ×RBW.

For a single CW signal, the spectrum is observed as a figure of an RBW filter explained by Eq.(2.36-c). For two CW signals whose level are equal and the frequency are $\omega_0 + \Delta$ and $\omega_0 - \Delta$, the Fourier transform of the signal $F(\omega)$ is explained by

$$F(\omega) = \delta(\omega_0 + \Delta) + \delta(\omega_0 - \Delta), \tag{2.49}$$

and the measured spectrum $S(\omega)$ is explained as

$$\begin{aligned} S(\omega) &= F(\omega) * G(\omega) \\ &= G(\omega - \omega_0 + \Delta) + G(\omega - \omega_0 - \Delta). \end{aligned} \tag{2.50}$$

To distinguish the signals, $S(\omega)$ must have a dip between two signals, and its differentiation $dS(\omega_0)/d\omega$ must be zero at $\omega = \omega_0$, and the second differentiation, $d^2S(\omega_0)/d\omega^2$ must be larger than zero, i.e. $S(\omega)$ must have a minimum value at $\omega = \omega_0$.

It is assumed for a simplification that ω_0 is zero, and

$$G(\omega) = \exp[-\alpha^2\omega^2]. \tag{2.51}$$

Then, Equation (2.50) can be rewrote as

$$S(\omega) = \exp[-\alpha^2(\omega + \Delta)^2] + \exp[-\alpha^2(\omega - \Delta)^2]. \tag{2.52}$$

The differentiation of $S(\omega)$ is explained as

$$\frac{dS(\omega)}{d\omega} = -2\alpha^2\left[(\omega + \Delta) \times \exp[-\alpha^2(\omega + \Delta)^2] + (\omega - \Delta) \times \exp[-\alpha^2(\omega - \Delta)^2]\right]. \tag{2.53}$$

Substitute zero for ω, and take it zero as follows.

$$\frac{dS(0)}{d\omega} = -2\alpha^2\left[\Delta \times \exp[-\alpha^2\Delta^2] - \Delta \times \exp[\alpha^2\Delta^2]\right] = 0. \tag{2.54}$$

And second differentiation is

$$\begin{aligned} \frac{d^2S(\omega)}{d\omega^2} = -2\alpha^2 \{&(1 - 2\alpha^2(\omega + \Delta)^2) \times \exp[-\alpha^2(\omega + \Delta)^2] \\ &+ (1 - 2\alpha^2(\omega - \Delta)^2) \times \exp[-\alpha^2(\omega - \Delta)^2]\} \end{aligned} \tag{2.55}$$

By substituting zero for ω,

$$\left.\begin{aligned}\frac{d^2S(0)}{d\omega^2} &= -2\alpha^2\left[(1-2\alpha^2\Delta^2)\times\exp[-\alpha^2\Delta^2]+(1-2\alpha^2\Delta)^2)\times\exp[-\alpha^2\Delta^2]\right] \\ &= -4\alpha^2\left[(1-2\alpha^2\Delta^2)\exp[-\alpha^2\Delta^2]\right]\end{aligned}\right\} \quad (2.56)$$

To keep Eq.(2.56) larger than zero, Δ must be

$$\Delta > \frac{1}{\alpha\sqrt{2}}. \qquad (2.57\text{-a})$$

From Eq.(2.44-b), (2.46) and (2.51),

$$\alpha^2 = \frac{1}{2}a^2 = \frac{\ln 2}{(\pi \cdot Rbw)^2}, \qquad (2.57\text{-b})$$

then α is substituted as

$$\alpha = \frac{\sqrt{\ln 2}}{(\pi \cdot Rbw)}. \qquad (2.57\text{-c})$$

In the case that the unit of the frequency of *Rbw* is Hz, Eq.(2.57-c) is divided by 2π, and then

$$\alpha = \frac{2\sqrt{\ln 2}}{Rbw}. \qquad (2.57\text{-c})$$

Therefore Eq.(2.55) is rewritten as

$$\Delta > \frac{Rbw}{\sqrt{8\ln 2}} \cong 0.425\,Rbw, \qquad (2.58\text{-a})$$

$$2\Delta \geq 0.85 Rbw. \qquad (2.58\text{-b})$$

In the case that the difference of the two signals is larger than 0.85Rbw, we can distinguish the two signals. Figure 2.24(c) was obtained by the simulation, where $2\Delta = 1.0Rbw$. There are tree arrows, the center arrow indicates $S(0)$ and both side arrows indicate $S(\Delta), S(-\Delta)$. The wave around the center was caused by the beat note between the two signals. In the case that Δ was wider than 0.85*Rbw*, the peak level of the center was lower than the both sides and we can distinguish two signals. The description of the simulation is described in the next section.

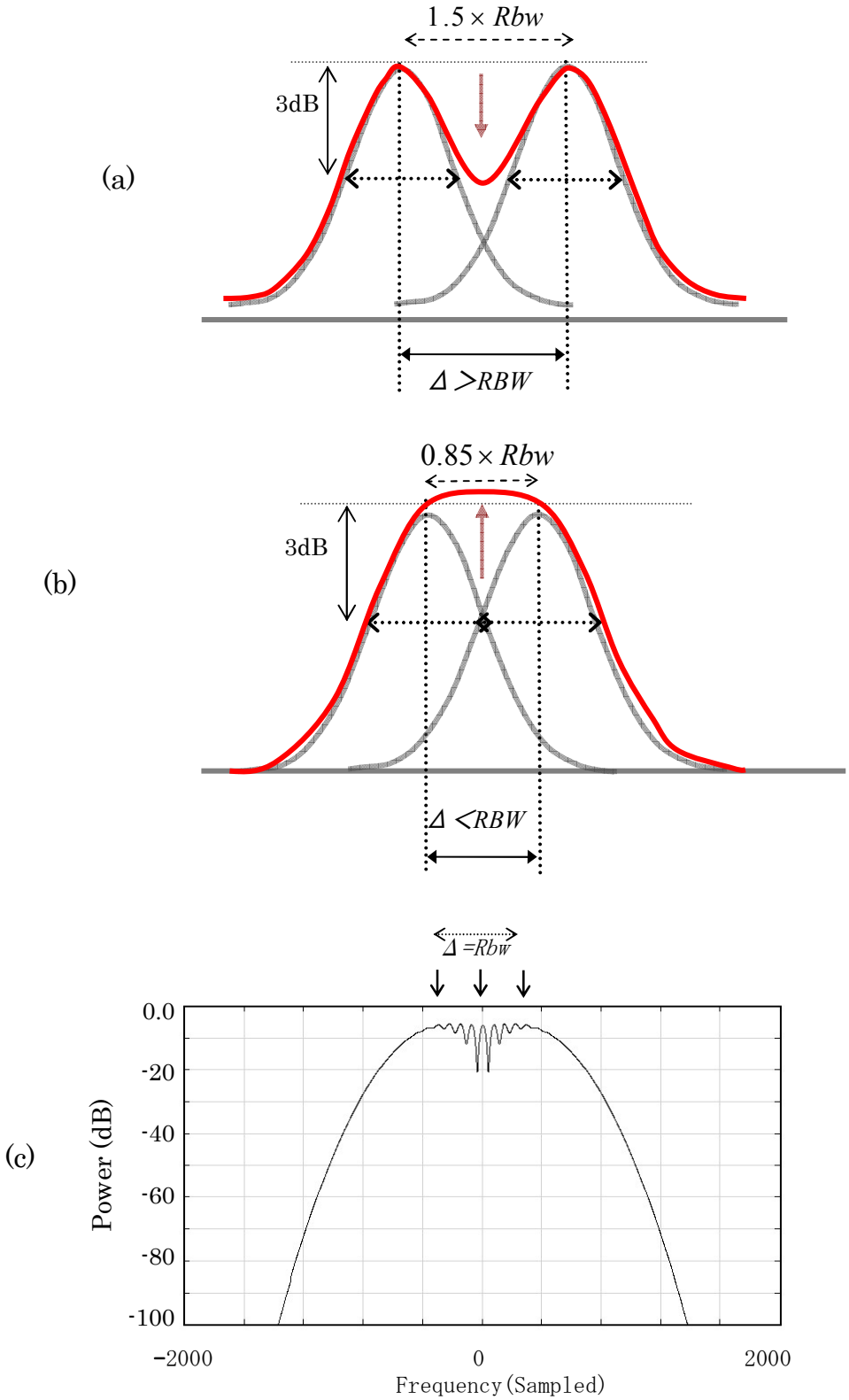

Fig.2.24 Spectrums of two Tone signals

2.5.7 Response against two tone Signals

Last section describes the response of the Gauss filter against a two-tone signal in frequency domain. This section describes it in time domain by a simulation.

We simulated the two-tone signal explained by

$$f(t) = \frac{1}{2}\left(\exp[-j(\omega_0 t + \Delta \times t + \theta_0)] + \exp[-j(\omega_0 t + \Delta \times t)]\right), \tag{2.59}$$

where Δ is the difference of the frequency between the two-tone.

We can obtain the spectrum *S(t)* by substituting Eq.(2.59) for *f(t)* in Eq.(2.47-b) as follows.

$$\begin{aligned} S(t) &= g(t) * \left\{ f(t) \times \exp[\, j(\pi \cdot \sigma t^2 + \omega_0 t)] \right\} \\ &= g(t) * (1/2)\left\{\exp[\, j(\pi \cdot \sigma t^2 + \Delta t + \theta_0)] + \exp[\, j(\pi \cdot \sigma t^2 - \Delta t)]\right\} \end{aligned} \tag{2.60}$$

The signal explained in the '{}' and the spectrum, *10log|S(t)|* is shown in (a)~(d) of Fig.2.25.

The conditions of each Fig.2.25 were as follows. The sampling frequency was 200kHz. The abscissa of each figure indicates both time and frequency. The full scale of the Span is 10kHz and the sweep time was 20msec. The RBW was 1kHz.

In all Figures ((a) to (d)), the green lines indicate the Gauss filter. The red lines indicate I part, and the blue lines indicate Q part of the base band signal of Eq.(2.59), respectively. The bold black lines indicate the spectrums $S(t)$ that are indicated with dB unit as $20\log(S(t))$. The top level of each screen is 0dB, which corresponds to $S(t)$ equals 1.0, and the bottom corresponds to –100dB. $S(t)$ is indicated as two lines. θ_0 of one line is zero and θ_0 of another is π. The wave of $S(t)$ around the center was caused by the beat note, and the phase of the beat corresponds to θ_0.

Each figure from (a) to (d) had different Δ. In (a) and (b) Δf was 1500Hz and 1330Hz, respectively. There were two peaks on $S(t)$, which was marked with arrows. In (c) Δ was 1000Hz that was equal RBW. There were not obvious peak. Two arrows indicate the signal frequency, where the levels were almost flat. In (d) Δ was 800Hz, there were not obvious peak. The maximum peak existed around the center. In the case that Δf was narrower than RBW, two signals were not resolved.

In the case that the initial phase θ_0 was zero, we had a peak at the center, but when θ_0 was π, we had deep dip at the center. We could not get the obvious threshold of the Δ to distinct the two-tone peaks, but the threshold exists between *Rbw* and 1.33*Rbw*.

2007.04.29

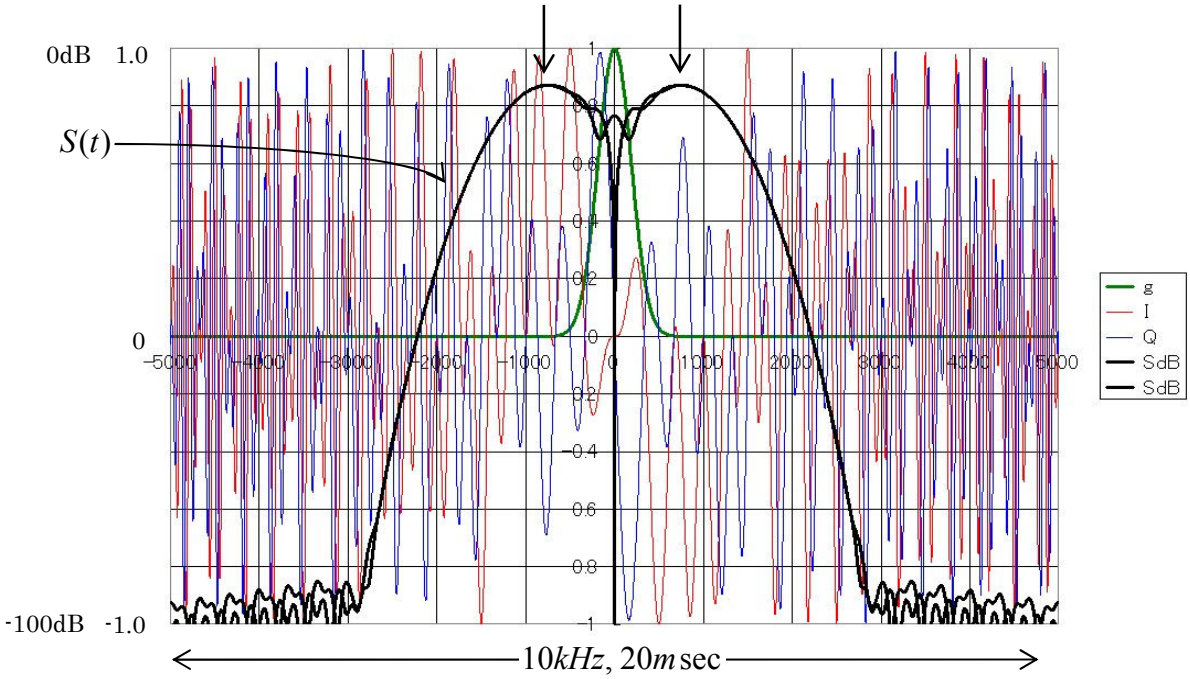

Fig.2.25 (a) Spectrums of two signals, ⊿f=1500Hz

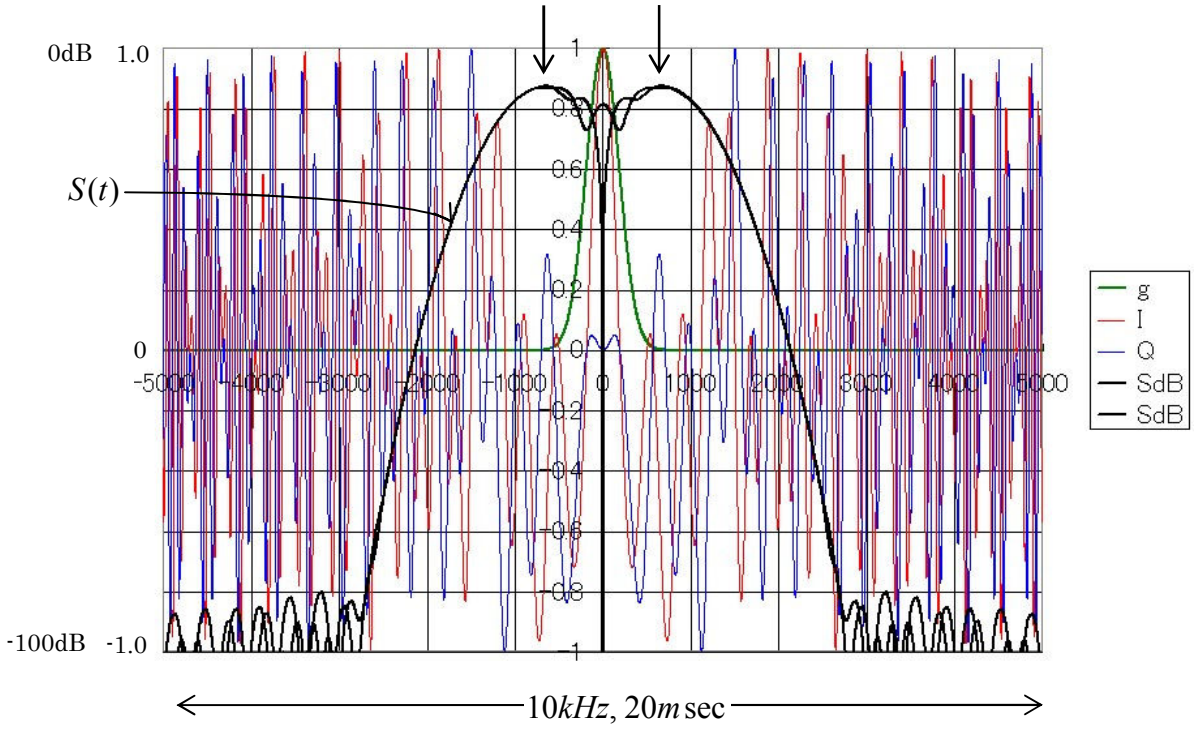

Fig.2.25 (b) Spectrums of two signals, ⊿f=1330Hz

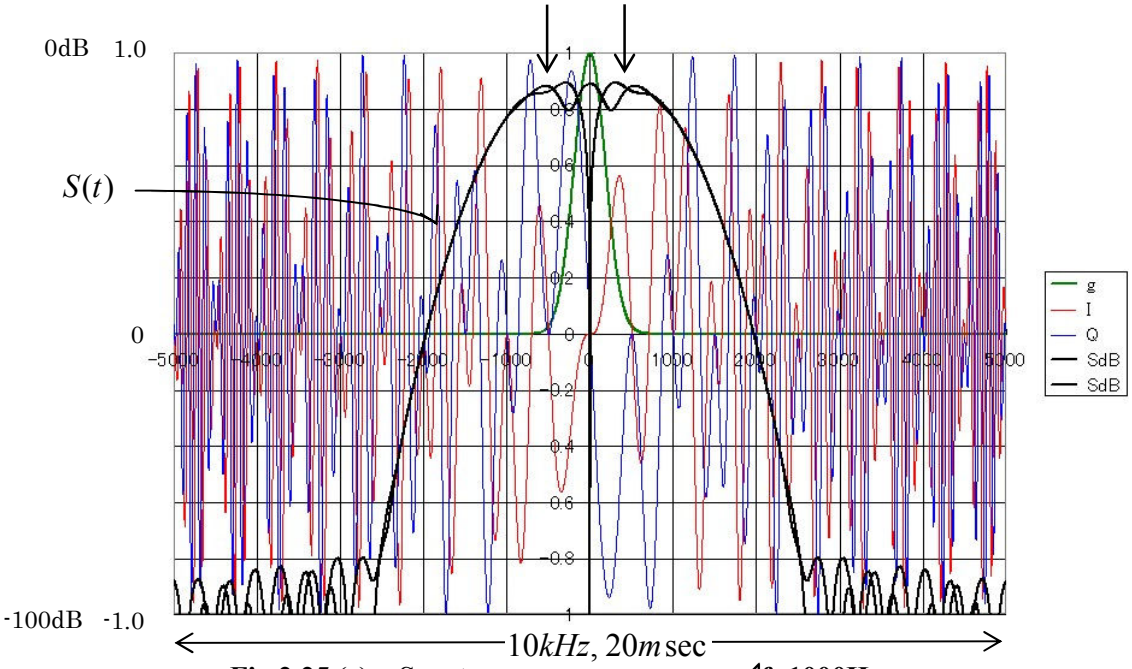

Fig.2.25 (c) Spectrums of two signals, ⊿f=1000Hz

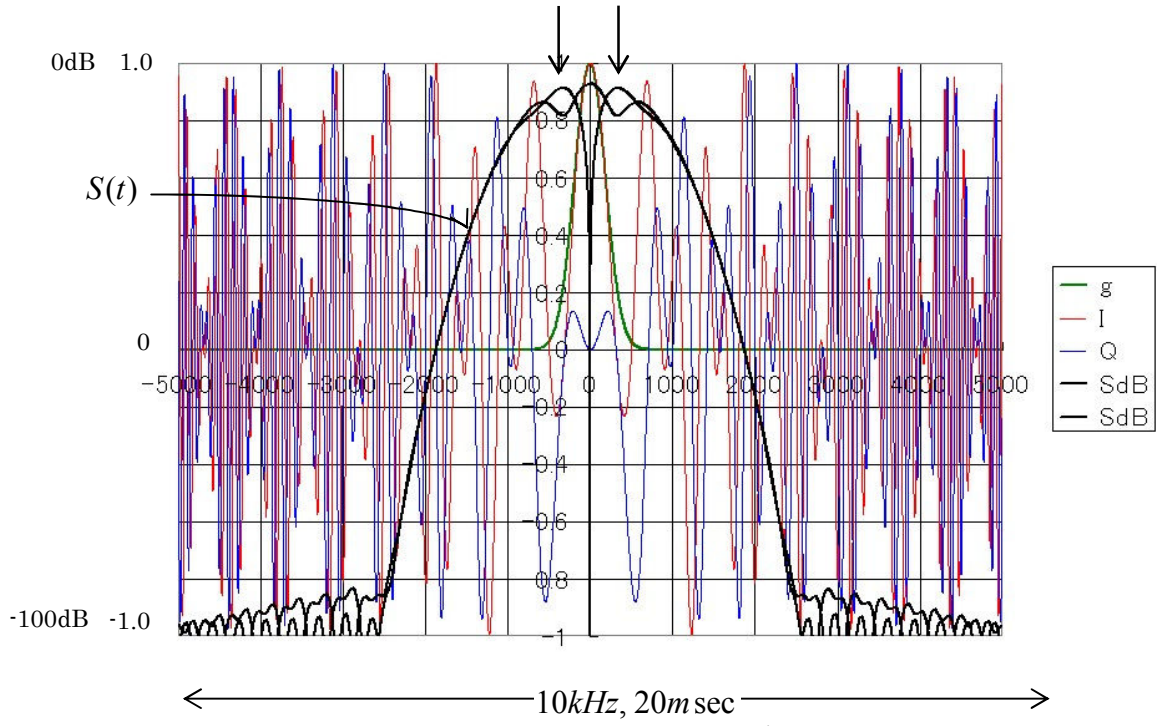

Fig.2.25 (d) Spectrums of two signals, ⊿f=800Hz

Fig.2.25 Base Band Signals and Spectrum against two-tone Signal
Span=10kHz, Rbw=1kHz, Sweep Time=20msec

2.6 Other Properties of Sweep Spectrum Analyzers

Until last section, fundamental theories of a spectrum analyzer have described. It may be simple, but the whole system of a spectrum analyzer consists of many parts. The properties of each part have significant influence on the result of measurements. This thesis does not describe the all, but this section describes about some properties that has large relationship with the theme of this thesis.

2.6.1 Shape Factor

In last section, some analyses were described haw the RBW filter distinct the two signals of same level. In the case to distinct two signals unequal in their level, not only resolution but also the shape of the filter decides the resolution that distinct the two signals. To detect the lower signal, the filter skirts must be under the lower signal [1].

Many corporations who product spectrum analyzers use a parameter, '**shape factor**' to indicate the shape of the resolution filter [1]. The shape factor is defined as the ratio of 60dB and 3dB bandwidth of the filter. It is also called **bandwidth selectivity.**

An example for the comparison between an analog and digital resolution filter is shown in Fig.2-26. They were spectrums measured CW signal, where **a** and **b** indicated the shape of the analog and the digital filter. The shape factor of the analog filter was 12.7. The shape of digital filter is 4.47 and it is almost a parabola for it is a logarithm of the Gauss function. And the shape factor was almost same to a mathematical calculation as follows.

The frequency response of Gaussian filter is explained as [4][8],

$$G(\omega) = -\alpha\omega^2 . \qquad (2.61)$$

The shape factor R_{SF} is explained as

$$R_{SF} = \frac{\omega_{-60}}{\omega_{-3}} = \frac{\sqrt{60/\alpha}}{\sqrt{3/\alpha}} = \sqrt{60/3} = 4.47 , \qquad (2.62)$$

where ω_{-3} and ω_{-60} are the value of ω at $G(\omega)$ was –3dB and –60dB. It is a special future of a digital Gaussin filter whose R_{SF} is independent from α and constantly 4.47. Digital IF methods are excellent in a shape factor against an analog method.

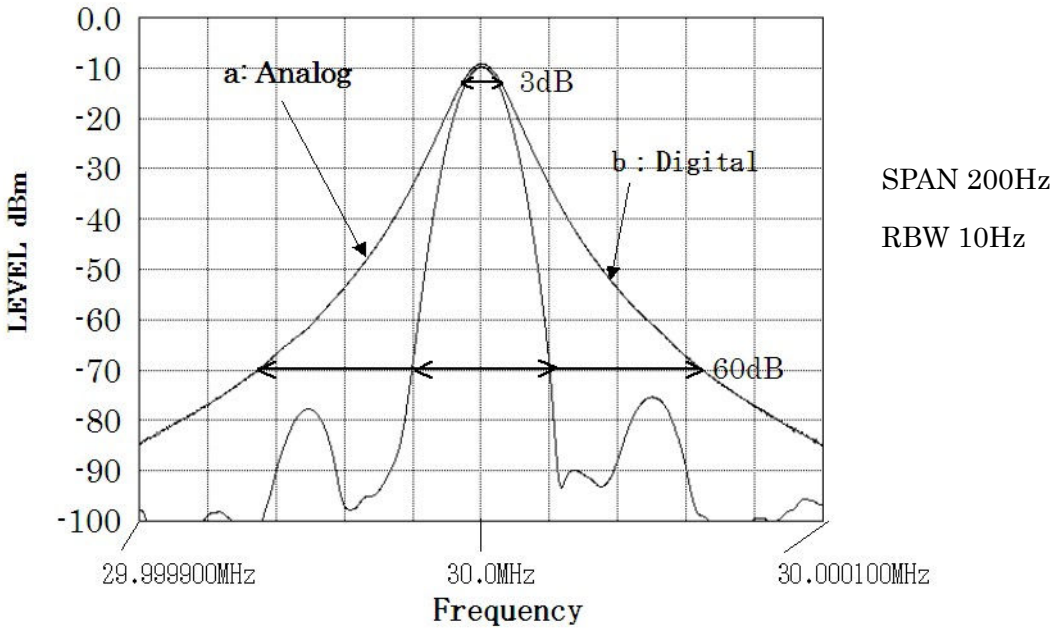

Fig. 2.26 Shape factor (Bandwidth selectivity)
ratio of 60dB and 3dB bandwidth

2.6.2 Time Domain measurement

The abscissas of sweep spectrum analyzers indicate not only frequency but also time as described in section 2.3 and 2.4. In the case that its span equals zero, the abscissa indicate only a time.

A sample screen of an oscilloscope is shown in Fig.2-27 (a), whose ordinate indicate a voltage. Figure 2-27(b) shows a zero span measurement of a spectrum analyzer. Its ordinate of (b) indicates a power (Watt). These may be like together, but the substances of the measurement are different.

These screens measured same signal, $A(t)\cos(\omega t)$, where A is a amplitude and ω is the radial frequency. The oscilloscope shows it as instantaneous figure. But in (b), we watch it as only A(t). In many case, the carrier frequency ω is not significant information to analyze the signal. It is reasonable to measure the signal with removed the carrier frequency.

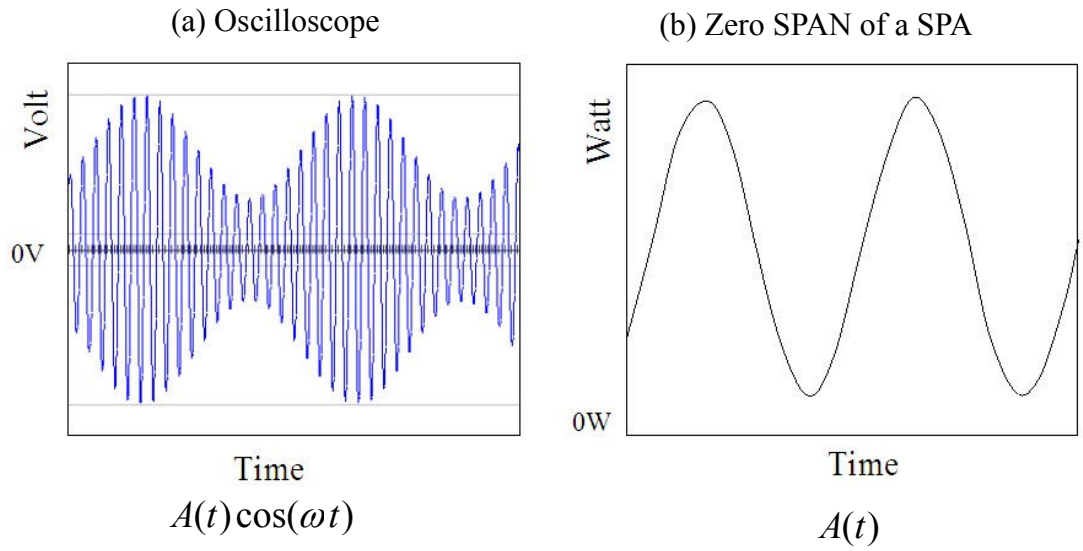

Fig 2.27 Time domain measurement

In the case that the RBW is relatively larger against the SPAN, or the SPAN is narrower, the spectrum is more similar to it obtained by a zero span measurement. One sample of a spectrum that observed a TDMA (Time Domain Multi Access) signal is shown in Figure 2.28, which is PDC (digital mobile phone: second generation of mobile phones) signal. The power envelope the signal is intermittent signal with some interval. The bandwidth of the signal is 21kHz. In Figure 2.28 (a), the RBW is 10kHz, and the spectrum represents the TDMA burst. By changing the sweep time we can observe the interval of the burst. A wideband RBW has sharp resolution in the time domain.

In Figure 2.28 (b), the RBW is 1kHz, the spectrum does not represents the burst, because the RBW is too narrow to response the burst signal.

By above discussion, the relation between the resolution of frequency and time is a trade-off. The relation is a kind of the ‘uncertainty principle’.

The ratio of RBW to SPAN decides which property of the abscissa is significant time or frequency. In the case that the ratio of RBW/SPAN is larger, the abscissa mainly time. On the other hand, in the case that the ratio is smaller, it is mainly frequency.

A sweep spectrum analyzer can configure the ratio, RBW/SPAN with fine step by changing the *Span* and the sweep time. By changing the ratio we can obtain many information from the measured signal.

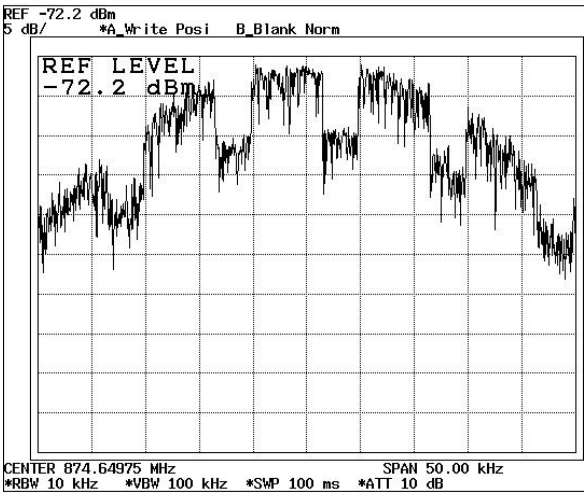

(a) Wide RBW

SPAN	50kHz
RBW	10kHz
Swp Time	100msec

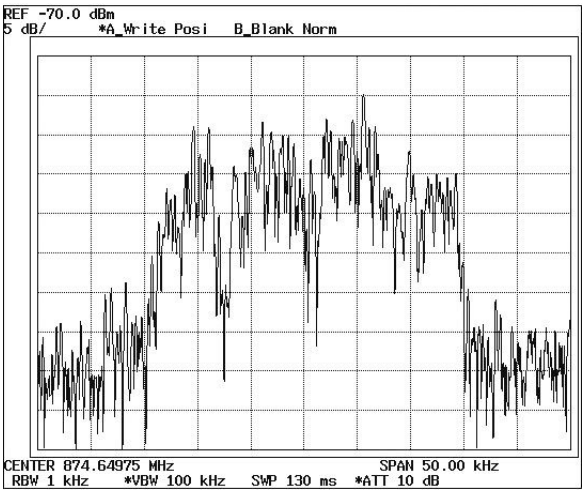

(b) Narrow RBW

SPAN	50kHz
RBW	1kHz
Swp Time	130msec

Fig.28 Spectrum of Dynamical Signal

2.6.3 Noise level and Resolution Bandwidth

A spectrum analyzer has a noise on its several stage, and we cannot measure a signal whose level is under the noise. In some case, the noise is an interference of the measurement. In another case, the noise is an object of the measurement. Sometimes we measure a signal like noise such as CDMA (Code Domain Multiple Access) signal.

We observe a spectrum as a convolution of $F(\omega)$ and $G(\omega)$, which is explained by Eq.(2.36-c),

$$|S_0(t)| = |F(\omega) * G(\omega)|.$$

If $F(\omega)$ is an ideal white-nose, $S_0(t)$ is assumed as [1][2],

$$|S_0(t)| = N_0 \int_0^\infty G(\omega)\, d\omega, \qquad (2.63)$$

where N_0 (Watt/Hz) is the noise power density per one Hz. The noise is included in the input signal and generated within the spectrum analyzer itself. The integral can be replaced by

$$G_0 \cdot B_{ENBW} = \int_0^\infty G(\omega)\, d\omega \qquad (2.64)$$

where G_0 is the gain and B_{ENBW} is the equivalent noise bandwidth of the resolution filter, respectively. Figure 2.29 shows the relation between $G(\omega)$ and B_{ENBW}.

$S_0(t)$ is assumed 'observed noise power', P_N. Then Equation (2.63) can be replaced by

$$P_N = S_0(t) = N_0 \cdot G_0 \cdot B_{ENBW} \qquad (2.65)$$

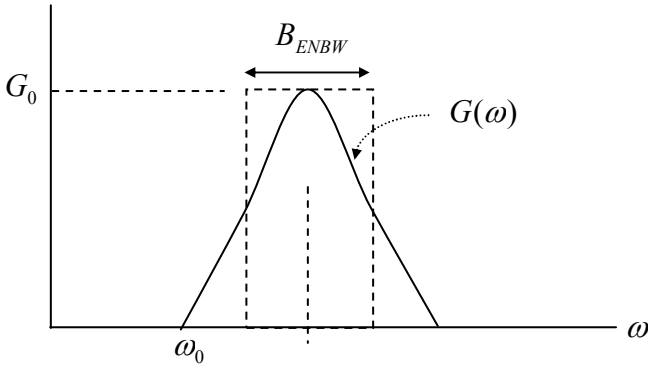

Fig.2.29 Equivalent Noise Bandwidth (ENBW) of a resolution filter

The observed noise power P_N is in proportion of resolution bandwidth *Rbw*. In the case we measure the noise by different bandwidth, the ratio of the observed noise level P_V (dB) is

$$P_V = 10\log(Rbw_1 / Rbw_0) \qquad (2.67)$$

where Rbw_1 and Rbw_0 is the *Rbw* of each measurement.

The example of the noise level variance is shown in Figure 2.30-(a). The one spectrum is measure by RBW=1MHz and another is 100kHz. The difference of the noise level is approximately 10dB. For continuous wave (CW) signal, we can get better S/NR (signal to noise ratio) using the narrower resolution bandwidth.

An example measuring low-level signal is shown in Fig.2.30-(b). The level of the measured signal is -90dBm. The RBW of the upper line is 1MHz and lower one is 10kHz. The VBW* (video bandwidth: see 2.2.1) of upper line is 1kHz and it of lower one is 3kHz. The upper line has narrower deviation of the noise by narrower VBW. The peak of the signal is shown at the center of lower line. In the upper line, the peak is not shown.

The RBW decides the noise level and the VBW decrease the deviation of the noise. We should select the bandwidth of these filters corresponding to the characteristics of the measured signal.

'Pre-detection filter' is a filter whose bandwidth is narrowest before the power detector [2]. Usually, it is the RBW filter. **'Post-detection filter'** is implemented after the detector [2], it decides the deviation of the detected power.

In the FFT method (see section 2.8), pre-detection filter is according with the window function and post-detection filter is according with the averaging of the spectrum.

* Note : VBW* (video bandwidth)

The VBW is the cutoff frequency (3 dB point) of on adjustable low pass filter, which is implemented after the detector. In digital IF method, it accords with the LPF processing after the detecting power by computing the square sum of the real part and the imaginary part of the signal *S(t)*. In the case that the video filter does not exist, the VBW equals to the RBW.

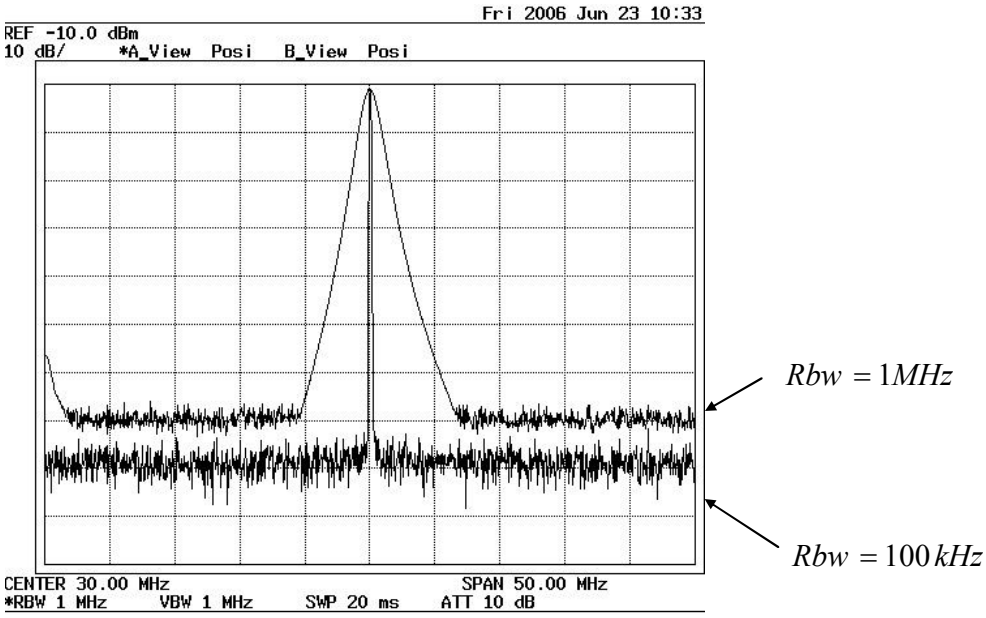

(a) Observed noise level changes as $10\log(Rbw_1 / Rbw_0)$

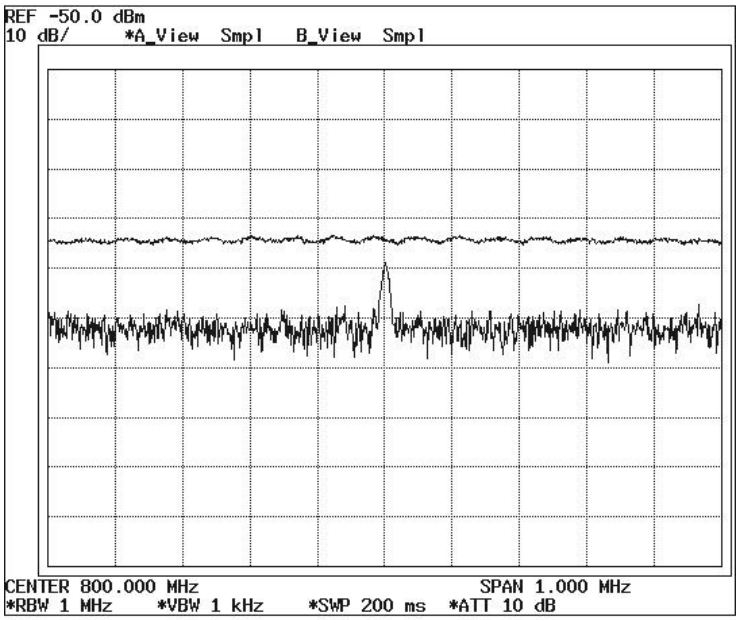

Signal level : -90dBm
SPAN: 1MHz

Upper : RBW 1MHz, VBW 1kHz

Lower : RBW 10kHz, VBW=3kHz

(b) low level signal and RBW

Fig.2.30 Relation between noise level and RBW

2.6.4 Zero Carrier

Sweep spectrum analyzers cannot measure a signal whose frequency is lower than an RBW. By the discussion of section 2.3.2, the 1st IF frequency of the most sweep-spectrum analyzers is lowest frequency of the local oscillator $\omega_{l\_\min}$, and the frequency of the 1st mixer's output is $\omega_l - \omega_{IN}$. (ω_l is the frequency of the local oscillator, $\omega_{l\_\min}$ is the minimum frequency of the local oscillator and ω_{IN} is the frequency of the input (measured) signal.)

Even if we have no input signal, the mixer output a signal whose frequency is ω_l, which is called 'local feed thorough'. We observe the peak whose frequency was zero at any time. In the case that the frequency of the input signal is zero ($\omega_{IN} = 0$), we cannot distinguish whether the signal is not exist or the frequency is zero. The peak is called 'DC response' or 'Zero Carrier' [2] *).

The figure of the peak of the Zero Carrier accords with the *Rbw* filter. We cannot observe the signal whose frequency is lower than the *Rbw*. This is one demerit of a sweep spectrum analyzer. The example of the Zero Carrier is shown in Fig.2.31.

*) Actually, the input signal is accepted through an AC connection at the RF front-end of analyzers. Then, the analyzers have not a sensibility to DC signals.

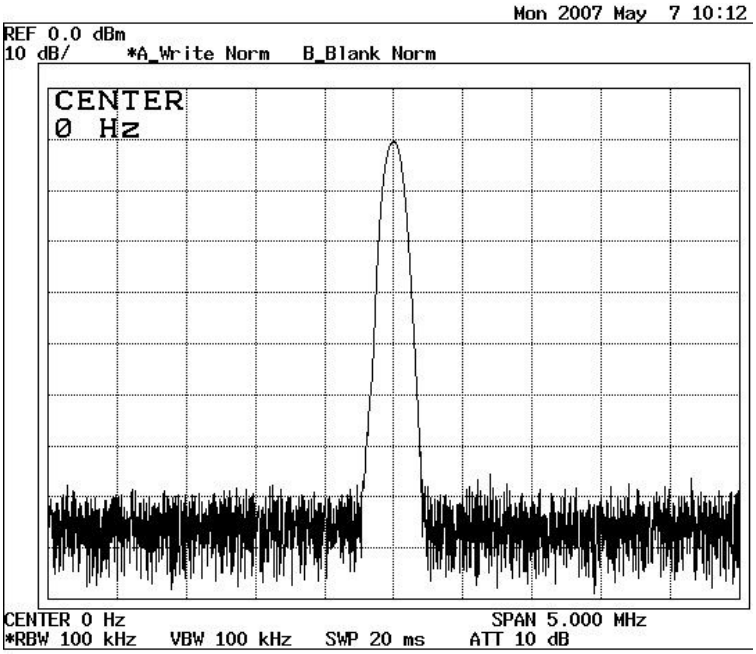

Fig.2.31 Zero Carrier

2.7 Bandwidth of Signals and Resolution Filters

We cannot obtain an ideal Fourier transform of any signals without infinite acquisition time. Therefore, spectrum analyzers have resolution filter and measures spectrum with restricted sweep rate. Until last section, we assumed the measured signal was CW for simplify. In this section, we examine measurements of wideband signals.

2.7.1 Signal under the measurement

Figure 2.32~2.35 are samples of wideband signals measured by a sweep spectrum analyzer. The signal is frequency modulated (FM) signal generated by a manufactured signal generator (SG), and the signal is explained as follows,

$$f(t) = A_c \sin\left(\omega_c t - \frac{\Delta\omega}{\omega_m} \cos(\omega_m t) \right), \qquad (2.68)$$

where A_c is the amplitude of the signal, ω_c is the carrier frequency , $\Delta\omega$ is the frequency deviation, ω_m is the modulation frequency [13], and these parameters are shown in Table 2.3. The bandwidth of the modulated signal was approximately 1.1MHz.

Table2.3 Specification of signal in Fig.2.32~2.35

Symbol	Value	Description
A_c	0.224 Volt	Amplitude, in 50 Ω circuit. The power is –60dBm
ω_c	860.945 MHz	Carrier frequency
$\Delta\omega$	530 kHz	Frequency deviation
ω_m	10 kHz	Modulation frequency,

2.7.2 Observed signal

The all (a) of Fig.2.32~2.34 show the shapes of the RBW filters, they were obtained by measuring a CW signal whose level were –60dBm. Their power was the same to the modulated signals. The all (b) show the spectrum with each RBW, and (c) show the trace measured by zero-span mode. The all figures show the spectrums measured with RBW 30kHz for the reference. The bandwidth of the measured signal is approximately 1.1MHz.

Figure 2.32 (a) shows the figure of the RBW filter 1MHz, and the span was 2MHz. The difference of the level between the center and the both side right and left was approximately 10dB.

Figure.2.32 (b) shows the spectrum with the span was 2MHz and the sweep time was 200msec. The frequency resolution was very coarse and the trace was similar to the wave of the zero-span. The trace had many ripples that were cased by a response of both time domain and frequency domain. The peak power of (b) was almost –60dBm. The level down was approximately 3dB on the both side start and stop of the scale.

Figure (c) shows the trace by zero-span mode whose sweep time was 200 μ sec. The interval of the ripple was 50 μ sec that was according with the twice of the modulation frequency 10kHz.

Figure 2.33 shows the results measured with RBW 100kHz whose bandwidth is approximately 10% against the measured signal as shown in Figure (a).

Figure (b) is the spectrum, whose envelope is simile to the spectrum of RBW 30kHz. The level of the spectrum was higher than the spectrum measured by RBW 30kHz. The spectrum seems to have many sideband lobs; they were not side lobes but the response of the power in time domain. The frequency interval of each side lobes was 10kHz as shown in Fig.2.35, but the RBW 100kHz was not enough to resolve them.

Figure (c) shows the trace of zero-span by the same condition with Fig.2.32 except for the RBW. The interval of the ripple was 50 μ sec, and the level deviation was larger than it of Fig.2-32, whose bottom was almost the noise floor. The peak level is corresponding to the level of center in Fig.(b), which is –64dBm.

Figure 2.34 shows the results measured with RBW 1kHz whose bandwidth is approximately 0.1% against the measured signal as shown in Fig. (a).

Figure (b) is the spectrum, which is observed asymmetrically. The reason of the asymmetry considered for the insufficient resolution of digitizing on the display. In the measurement of narrower span, the levels of the sideband lobes ware symmetrically as shown in Fig.2.35 (b). This spectrum consists of many side lobes. Their level and frequency ware static. Each interval of them was 10kHz, which accords with modulation frequency of the FM.

Figure (c) shows the trace of zero-span whose level is –83dBm, almost flat and approximately 20dB lower than the peak level of Fig.2.33 (c). The ratio 20dB is considered as the rate of RBW between Fig.2.33 and 2.34.

Figure 2.35 are results measured the signal of Fig.2.33~2.35 with span equals 200kHz. Each figure (a), (b-1) and (c) has different RBW, which are 100kHz, 10kHz and 1kHz, respectively.

The level of the trace (a) was dynamically changed. It was the response of the time domain as shown in Fig.2.33 (c). On the other hand, the trace (c) was static. The frequency resolution (RBW) of (c) was enough fine to show the side lobes. In the case that the RBW was narrower than 3kHz, the level of each lobes did not change. The level in (a) were approximately 20dB higher than (b-1) and (c).

The spaces between each lobe were filled with beat notes, and the period of the beats were 100 μ second as shown in (b-2). But in the case that the RBW was wider than 30kHz, the period was 50 μ sec as shown in Fig.2.33(c).

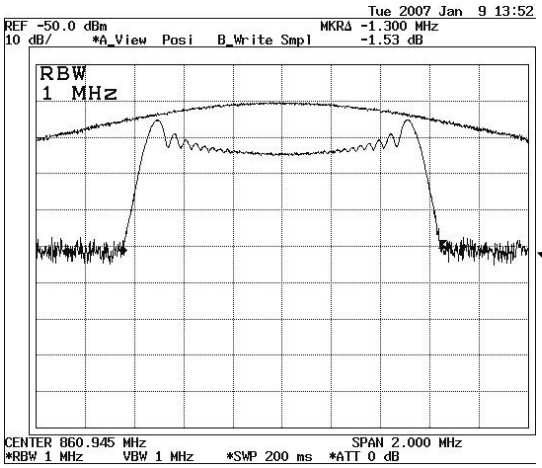

(a)

Figure of RBW 1MHz

Spectrum measured with RBW 30kHz

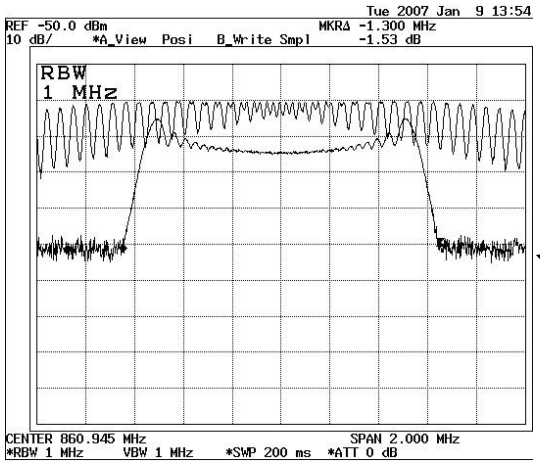

(b)

Spectrum by RBW 1MHz

Spectrum measured with RBW 30kHz

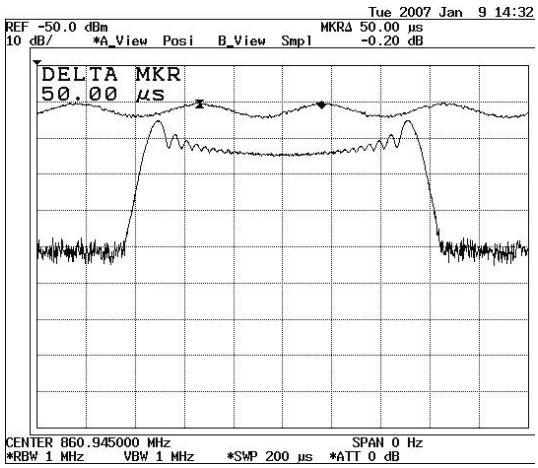

(c)

Zero span trace by RBW 1MHz
The cycle of the ripple was 50 μ sec

Spectrum measured with RBW 30kHz

Fig.2.32 Measurement of wideband signals with RBW 1MHz

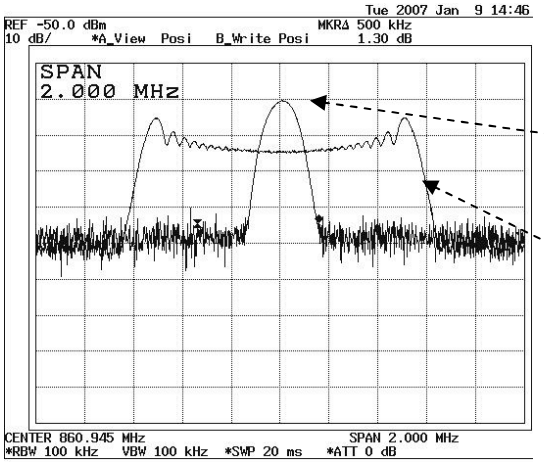

(a)

Figure of RBW 100kHz

Spectrum measured with RBW 30kHz

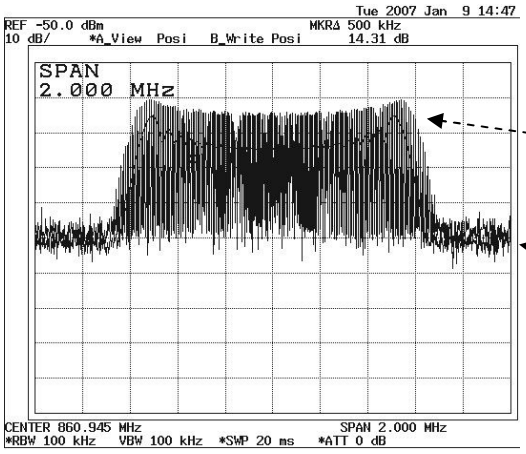

(b)

Spectrum by RBW 100kHz

The spectrum measured with RBW 30kHz is behind the front spectrum.

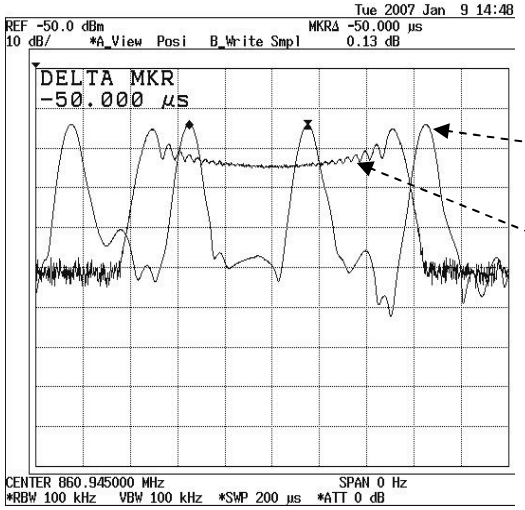

(c)

Zero span trace by RBW 100kHz

The cycle of the ripple was 50 μ sec

Spectrum measured with RBW 30kHz

Fig.2.33 Measurement of wideband signals with RBW 100kHz

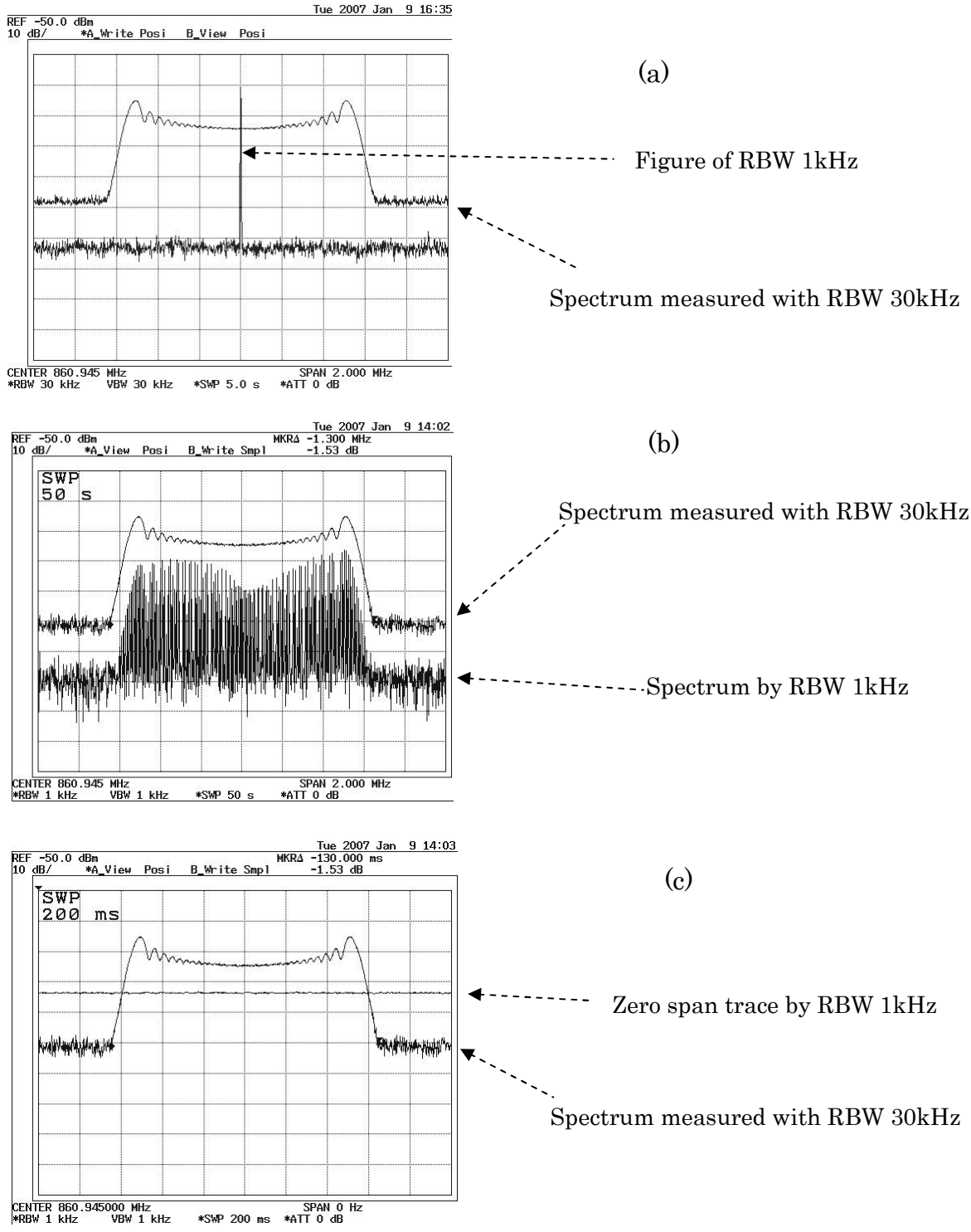

Fig.2.34 Measurement of wideband signals with RBW 1kHz

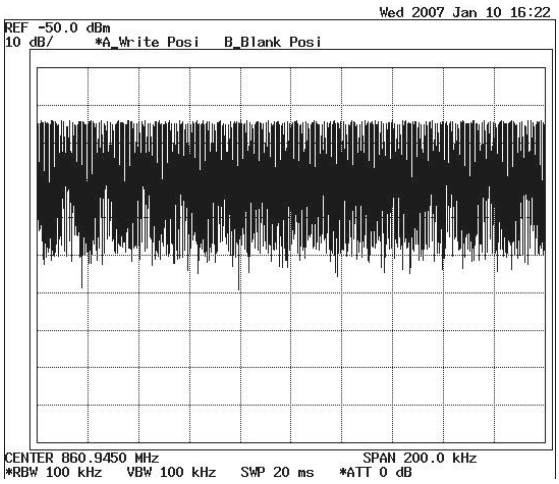

(a) RBW 100kHz

The trace is shown as many teeth of a saw. Their level and frequency are dynamically changing with the cycle of 50 μ sec as shown Fig.2-33(c).

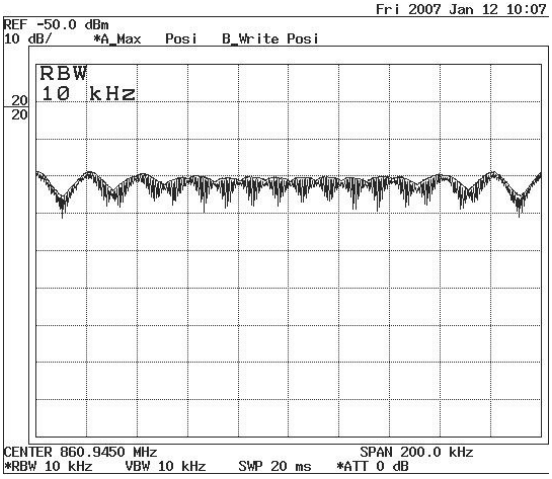

(b-1) RBW 10kHz

Gently undulating sideband lobs are shown. Each interval of them are 10kHz which is modulation frequency.

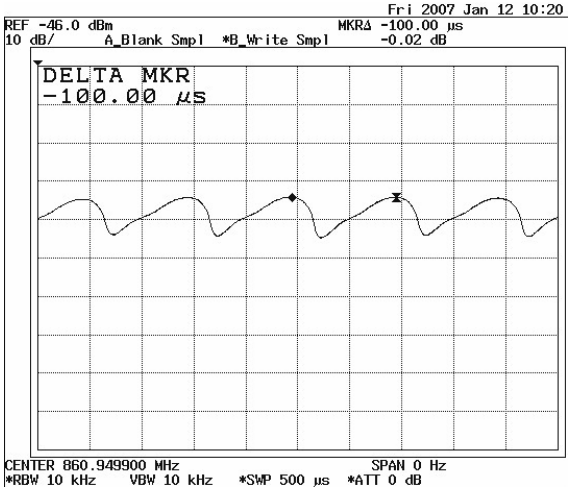

(b-2)

The spaces between each lobes are filled with beat notes. The period of the beats were 100 μ sec.

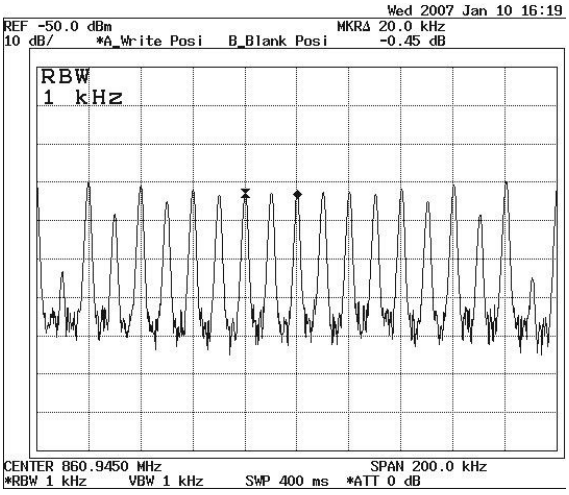

(c) RBW 1kHz

Many sideband lobs are shown. Their level and frequency are static. Each interval of them are 10kHz.

Fig.2.35 Measurement of wideband signals with SPAN 200kHz

2.7.3 Discussion:

Sweep spectrum analyzers show a spectrum of the signal, *f(t)* as a trace which is explained by the Eq.(2.36-c), $|S_0(t)| = |F(\omega) * G(\omega)|$. It can be explained as

$$\begin{aligned} |S_0(t)| &= |F(\omega) * G(\omega)| \\ &= \int_{-\infty}^{\infty} \mathrm{F}(\tau)\mathrm{G}(\omega - \tau)\mathrm{d}\tau \end{aligned} \tag{2.69}$$

The FM signal measured in this section, Eq.(2.68) can be rewrote as [14],

$$f(t) = A_c \sum_{n=-\infty}^{\infty} J_n(m)\cos(\omega_c + n\omega_m)t, \tag{2.70-a}$$

where *m* is a modulation index,

$$m = \frac{\Delta\omega}{\omega_m}, \tag{2.70-b}$$

$J_n(m)$ is the Bessel function of the first kind of order n and argument m. The signal $f(t)$ was a set of some CW signals whose frequency interval was ω_m, 10kHz. The bandwidth was approximately 1.1MHz and the number of the sideband lobes is about 110.

The concept of the convolution of the FM signal and the RBW filter, which is explained by Eq.(2.69) is shown in Fig. 2.36. In the case that the bandwidth of the RBW filter is narrower than 10kHz, the RBW filters accepts one side lobe and the integral of Eq.(2.69) took same level. On the other hand, in the case that the bandwidth was wider than 10kHz, the number of the side lobes accepted by the filter was in proportion to the RBW.

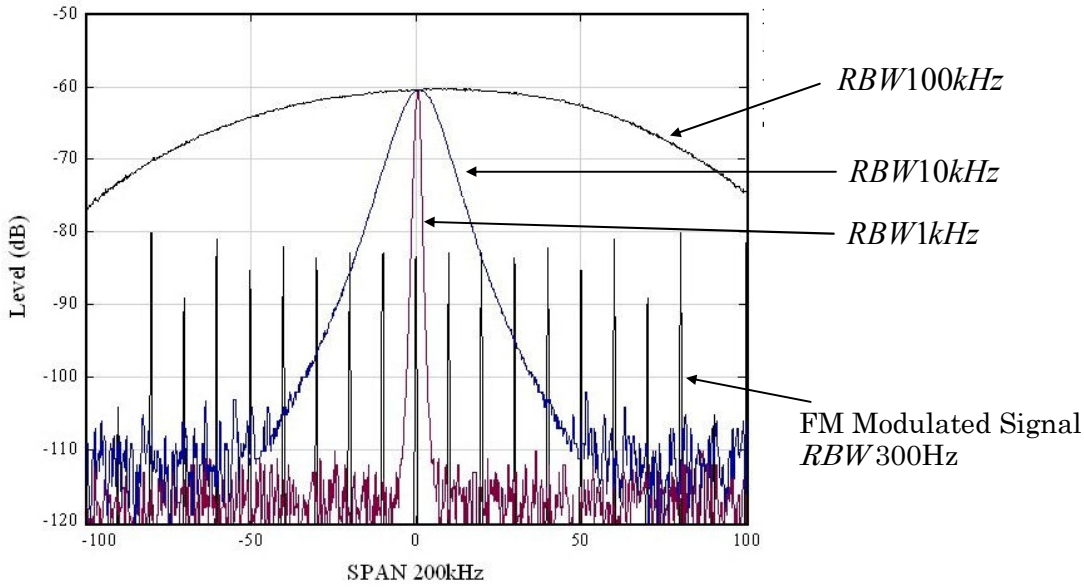

Fig.2.36 Convolution of FM signal and RBW filter

Although the model explained by Eq.(2.69) is a static model, we can consider the FM modulation as a dynamical model, which is shown in Fig.2.37. The instantaneous frequency of an FM modulated signal such as Eq.(2.68) dynamically changes. In the condition Table 2.1, the frequency changes 10,000 times in one second.

The spectrum under side of Fig.2.37 shows the concept of the instantaneous and the max-hold spectrum of the signal. The upper side figure shows the dynamical change of the frequency of the signal against the time. The time length of the graph is 2m second (-0.001sec to 0.001sec). And in the upper left side, the impulse responses of the RBW filters, RBW 100kHz and 1kHz, are shown.

The time length of the impulse response of RBW 100kHz and 1kHz was 0.02msec and 2msec (see section 2.5.3), respectively. The time length of RBW filter, 100kHz is shorter than the period of the modulation frequency (10kHz), then the filter can response the instantaneous frequency of the signal. It is fact that the instantaneous frequency always lies in the range 1.06MHz, which is indicated as a frequency deviation in the Fig.2.37. In the case that RBW is 100kHz, we could observe that the RBW filter responded the instantaneous frequency as shown in Fig.2.33 (c).

On the other hand, the time length of RBW 1kHz filter is very long than the period. The filter cannot response against the instantaneous changing of the frequency. The output of the filter is almost static. And the spectrum obtained by RBW 1kHz has only energy at all specific frequency explained by Eq.(2.70-a) and has no energy at any where else.

The all spectrums obtained by different RBW are correct, but they measured by different conditions. A wide RBW has low frequency resolution, but has high resolution in time. And a narrow RBW has high frequency resolution and has low resolution in time. It is one kind of the uncertainty principle as next equation.

$$\Delta f \times \Delta t = \text{constant} \tag{2.71}$$

where Δf and Δt are resolution of each domain of RBW filters.

2.7.4 Conclusion

This section described that spectrums show different result corresponding to different conditions. An RBW is the most significant parameter to decide the condition. The abscissa of a sweep spectrum analyzer has a property that indicates a time. In the case that the RBW is wider against the span, the trace indicates the instantaneous response rather than frequency. A narrow RBW give us static spectrum, which are more similar to the Fourier transform of the signal.

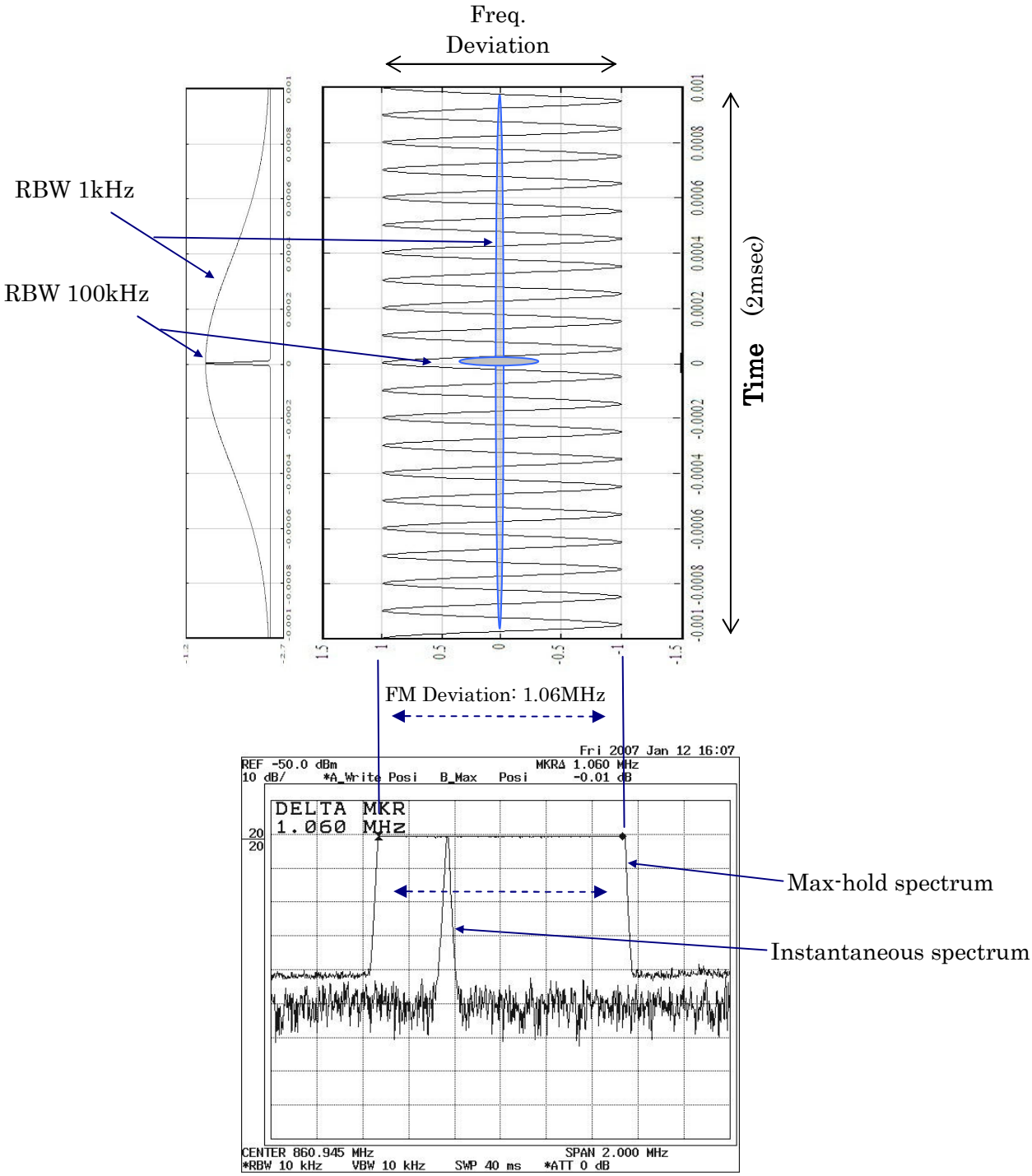

Fig.2.37 Dynamics of FM modulation and the RBW filters

2.8 Sweep method and FFT method

This section describes properties of FFT method and differences between the sweep method and the FFT method.

2.8.1 Digital IF method

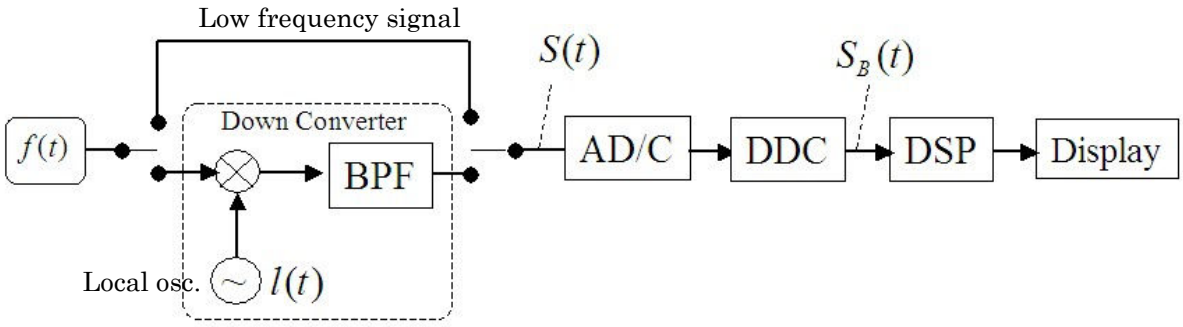

Fig.2.38 Example of Block diagram of an FFT method

There are two kinds of the spectrum analyzer that employs the FFT (Fast Fourier Transform) method. One has the 'down-converter', which converts an RF signal into an IF signal, which is digitized by an AD/C. Another has not the down-converter, the AD/C accept the input signal directly. The concepts of both types are shown in Figure 2.38. To measure the signal whose frequency is under the Nyquist frequency the down-converter is not needed.

In the method with the down converter, the local oscillator of the down converter is fixed tuned (not sweeping). The band-pass filter (BPF) does not decide the resolution of the spectrum, but limit the bandwidth of the signal. This band limitation prevents the aliasing (the folding of out-of-band signals into the AD/C sampled data). The Fourier transform is done by the FFT prosessing, which is computed in the DSP.

2.8.2 FFT

The description about the FFT is given by [7][15] and other many documents. The principle form of Fourier transform is expressed following equation.

$$F(\omega) = \int_{-\infty}^{\infty} f(t) \cdot e^{-j\omega t} dt \qquad (2.72)$$

This equation requires the integration time to take from minis infinite to infinite, but it is impossible. In the FFT method, the integration time is limited as a window function, *g(t)*. The measured signal *f(t)* is multiplied by *g(t)* and *f(t)* ×*g(t),* which is called 'windowed function'. The measured signal is assumed to repeat infinitely as the windowed function.

The outline of the FFT method is shown in Fig.2.39, where $f(t)$ and $g(t)$ is a measured signal and the window function, and T_W is the time length of the window function. By the theory, the Fourier transform of a product of two functions is a convolution of the transforms of the two functions in the frequency domain as follows [7].

$$s(t) = f(t) \times g(t) \qquad (2.73\text{-a})$$

$$S(\omega) = F(\omega) * G(\omega) \qquad (2.73\text{-b})$$

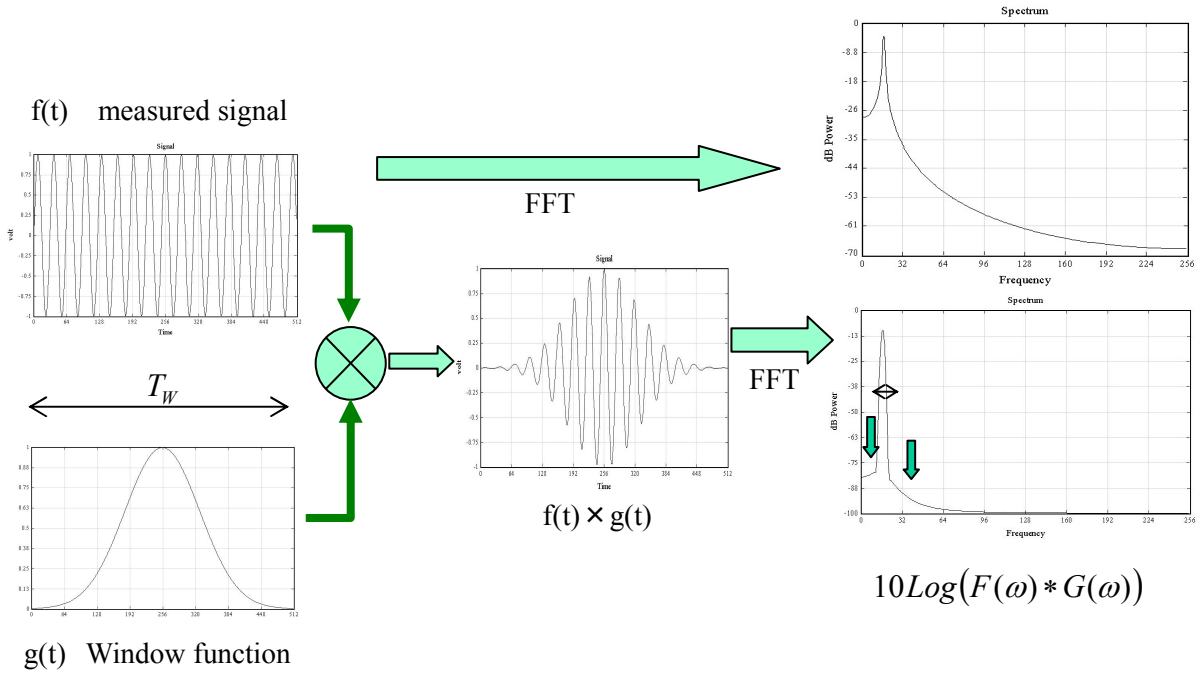

Fig.2.39 Concept of FFT

The FFT is a kind of discrete Fourier transform. In this method, $f(t)$ and $g(t)$ is transformed into discrete forms as,

$$f[i] = f(i \times \Delta t), \qquad (2.74\text{-a})$$

$$g[i] = g(i \times \Delta t). \qquad (2.74\text{-b})$$

$$f_W[i] = f[i] \times g[i], \qquad (2.74\text{-c})$$

$$\Delta t = 1/f_s, \quad i = 0 \sim N-1,$$

where f_S is the sampling frequency, N is the size of the window. And the Fourier transform, $S(\omega)$ is expressed as,

$$S[k] = \sum_{n=0}^{N-1} f_W[n] \cdot \exp[-j(2\pi / N)nk], \qquad (2.75\text{-a})$$

$$\omega = 2\pi\Delta f \cdot k, \quad \Delta f = f_S /(2N), \qquad (2.75\text{-b})$$

where k is a desecrated frequency as a number of bin (display sample). The spectrum $S[k]$ is statistical which is averaged within the time T_W. The abscissa has no factor of a time. The resolution of the time corresponds to T_W, which is defined by

$$T_W = \frac{1}{f_s}(N-1) \qquad (2.75\text{-c})$$

2.8.3 Frequency resolution (RBW) in FFT

In the FFT method, the window function operates as a resolution filter. The frequency resolution is dependent on the window function as Eq.(2.73-b). Table 2.2 gives the specifications of typical window functions [15]. In the sweep spectrum analyzer, the 3dB bandwidth (Rbw) is given as a number of bins.

An example of enlarged peak of a spectrum is shown in Figure 2.40, where the small circles indicate sample points of desecrated spectrum such as expressed Eq.(2.75-a) and (2.75-b), and the solid line indicates the continuous spectrum $S(\omega)$. In Figure 2.40 (a), one sample of $S[k]$ corresponds to the peak of $S(\omega)$. On the other hand, in (b), $S[k]$ has no sample at the peak and we observe the peak level lower than the true peak. The 'Scallop Loss' of Table 2.4 indicates the worst loss.

Some solution to prevent the Scallop Loss is suggested. One solution is a employing a flat top window and other is interpolation of the spectrum $S[k]$ [16].

Table 2.4 Characteristics of Windows (referred by [15])

Window function	Operation Mathematical formula	3.0 dB Bandwidth, RBW (bin)	Scallop Loss (dB)	Highest side lobe Level (dB)
Rectangle	$w_R[i] = \begin{cases} 1, & i = 0 \sim N-1 \\ 0, & i < 0, N \le i \end{cases}$	0.89	3.92	-13
Hanning	$w_h[i] = w_r[i](1 - \cos(2\pi j / N))$	1.20~1.86	0.86~2.1	-23 ~ -47
Gauss	$w_g[i] = w_r[i] \cdot \exp[-i^2 / a^2]$ $a^2 \equiv 4\ln 2/(f_s \pi \cdot Rbw)^2$	1.33~1.79	0.94~1.69	-42~ -59

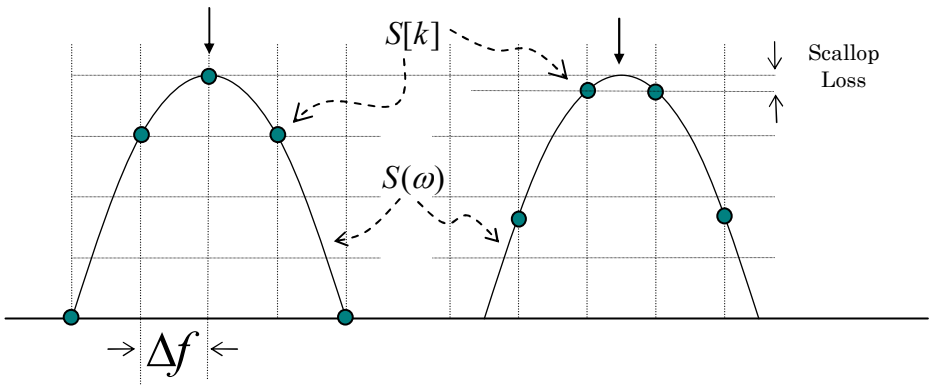

(a) Catching the peak (b) Causing the Scallop

Fig. 2.40 Example of Scallop Loss

2.8.4 Bandwidth of the processed signal and dynamic range

In the sweep spectrum analyzer, the RBW filter limits the bandwidth of the input signal finally. In the FFT method, the bandwidth corresponds to the Nyquist frequency of the AD/C, which is generally enough wider than the frequency resolution (*Rbw*). The difference of the two methods is shown in Figure 2.41.

In the case that the measured signal is multi tone such as

$$f_{mlt}(t) = \sum_{i=0}^{n-1} a_i \cdot \cos(\omega_i t + \theta_i), \qquad (2.76)$$

where a_i is a amplitude of each tone, and θ_i is the initial phase, the maximum instantaneous amplitude $A_{\max}$ is expressed by

$$A_{\max} \le \sum_{i=0}^{n-1} a_i \ . \qquad (2.77)$$

This value $A_{\max}$ is dependent on the each phase θ_i. The gain in front of the ADC should be controlled to prevent the clipping corresponding to the maximum amplitude. Generally, this amplitude becomes larger according with the bandwidth of the signal. On the other hand, in the sweep method, the signal in front of the AD/C, is band limited, and we take the gain in front of the ADC take larger than the FFT method. At the point of the bandwidth of signal that is received by an AD/C, the sweep method has an advantage against the FFT method.

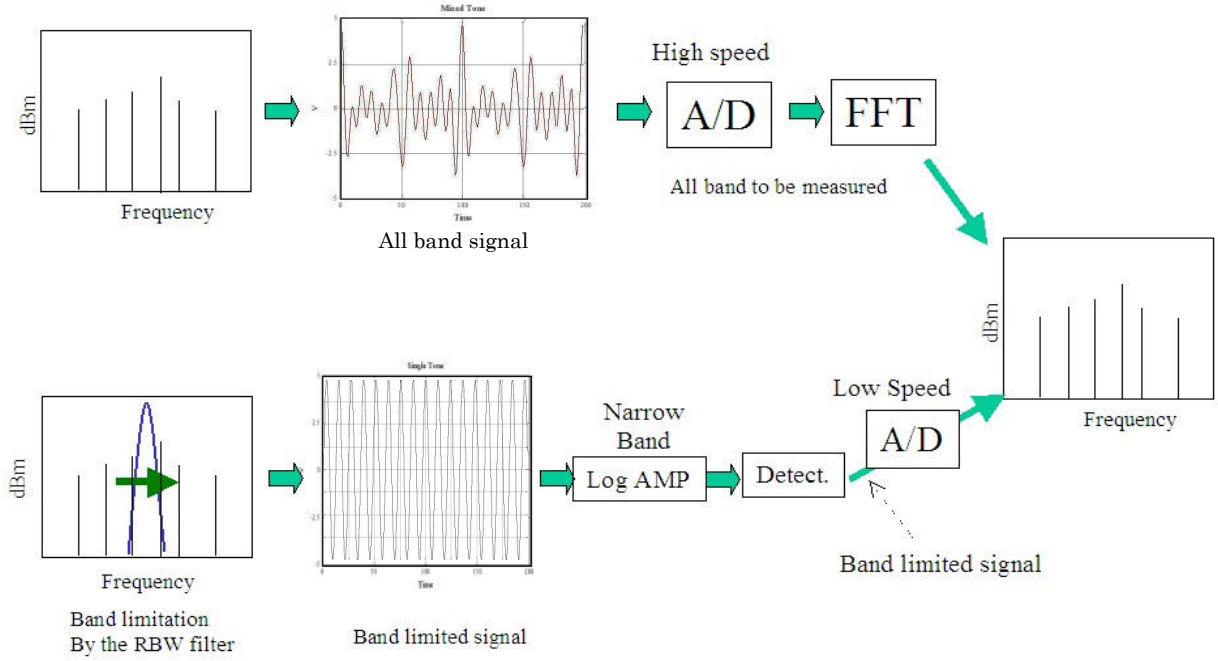

Fig.2.41 Bandwidth of processed signal in seep method and FFT method

2.8.5 Ripple on the spectrum

The spectrum measured by the FFT method that has a down converter (as shown Fig.2.38) may include a ripple that is caused by a frequency response of the IF BPF. An example of frequency response of an IF filter is shown in Figure 2.42 (a), which is obtained by a chirped signal passed thorough the one of the IF filters in R3264 (produced by ADVANTEST Co.). And the figure (b) illustrates the spectrum, which is assumed obtained from the signal (a).

Although, in the sweep method, the frequency response of the IF filter is observed as a convolution factor against the spectrum $F(\omega)$. In the FFT method, the frequency response of the IF filter, $R(\omega)$ is observed as the ripple of the spectrum given by

$$S(\omega) = R(\omega) \cdot \{F(\omega) * G(\omega)\}. \qquad (2.78)$$

We considered that this phenomenon was cased by the non-sweep of the local oscillator.

We must correct the ripple or design the IF BPF have low ripple to obtain a exact spectrum, or approve the ripple.

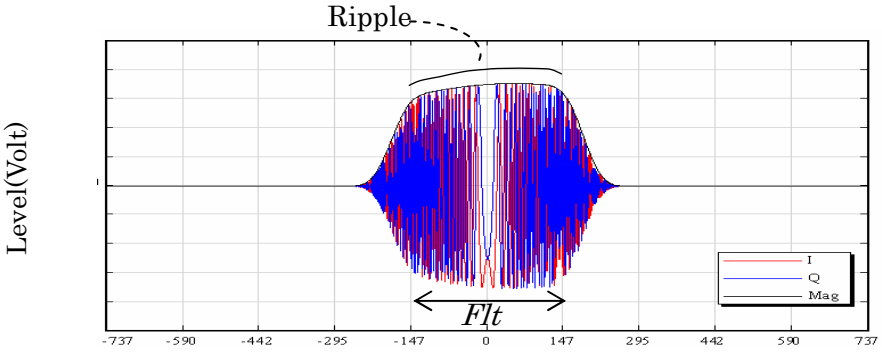

Chirped signal passed thorough the IF BPF

(a) Frequency response of an IF filter

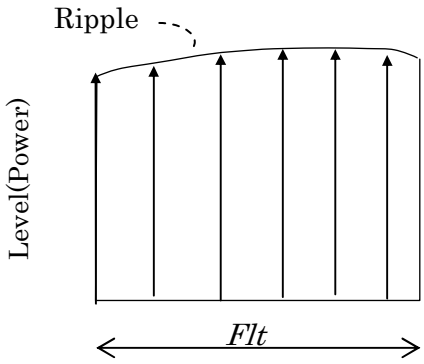

(b) The spectrum with a ripple

Fig 2.42 Ripples on Spectrums in FFT method

2.8.6 DC Response in FFT method

In the FFT method with the down converter, the DC response (see 2.6.4) exists by the same reason with the sweep method. But in the FFT method without the down converter, the DC response caused by the local feed thorough does not exist, but the spectrum of the DC is observed as the peak at 0Hz that is true value of the spectrum. The FFT method is the most popular method to measure low frequency signals.

2.9 Multiple-FFT Measurement

2.9.1 Outline of the measurement

The frequency span obtained by the FFT method with down converter is narrower than the bandwidth of the IF BPF. The block diagram of the FFT method is shown in Fig.2.43 (a). The bandwidth is defined as '*Flt*' that is shown in Fig.2.42. In the case that the desired frequency span is wider than the *Flt*, some spectrum analyzers employ the 'Step sweep method' or 'Multiple-FFT Measurement' [19], which is described as follows.

(1) The frequency of the local oscillator is increased with an interval time T_W (second) or more by a step. The frequency is explained as

$$\omega_{lk} = \omega_{l1} + k \times Flt \qquad (2.79)$$

where k is the number of the step, ω_{lk} is the frequency of *k-th* step and ω_{l1} is the first frequency of the local oscillator. The transition of the frequency against the time is shown in Fig.2.43 (b).

(2) The IF signal (output of the BPF) whose interval is T_W, is digitized by the A/D converter 'AD/C' and stored in the memory 'MEM'. The signal is transformed into the spectrum by the FFT processing.

(3) The part of the spectrum obtained by (2) whose frequency range corresponds to the *Flt* is extracted, see Fig.2-43 (b) and (c).

(4) The operation (1) to (3) is repeated until that the desired span of the spectrum is obtained. The results of multiple FFT are concatenated to provide the spectra for a desired span, see Fig.2.34 (d).

By this method, we can measure a spectrum with any span, as we desire. This method is called 'multiple FFT method'.

2.9.2 Sweep Rate

The sweep rate of the multiple-FFT measurement was considered as follows.

In this method, the local oscillator does not sweep and we considered the sweep rate as the span band that obtained within one second. To consider the sweep rate, we did not consider the operation time of the DSP, response time of the oscillator, and other factor which dependent on the condition of the system.

The acquisition time of one FFT, T_W corresponds to the time length of the window function. It is given by

$$T_W = \frac{k_W}{Rbw} \quad , \; k_W = 2.5 \sim 3.5 \, , \qquad (2.80)$$

where the window function is assumed Gauss. The value of k_W is experimentally decided by [16] or [17]. The span obtained by one FFT is *Flt*. Then the sweep rate is assumed as

$$\sigma = \frac{Flt}{T_W} = \frac{1}{k_W} Flt \cdot Rbw . \qquad (2.81)$$

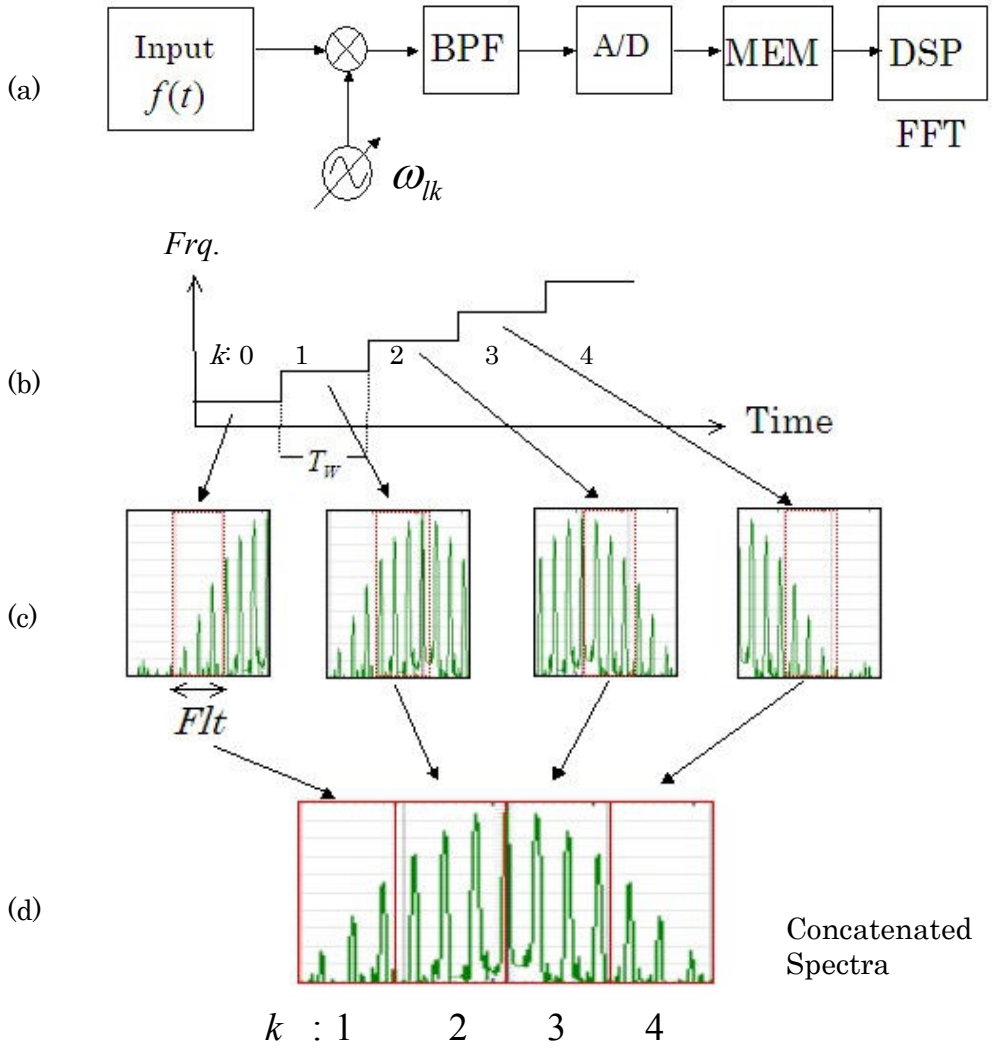

Fig 2.43 Jointed Spectra by Step Sweep method

The rate between *Flt* and *Rbw* will be known by section 4.2.5 as follows.

$$Flt \geq 5.8 \times Rbw \qquad (2.82)$$

We considered the relation between the sampling frequency F_S and *Flt* as follows (section 6.2.4 will describe a discussion about this).

$$F_S \geq (Flt + Bwd), \qquad (2.83\text{-a})$$

where *Bwd* is the bandwidth of desired dynamic range such as 100dB down bandwidth. In the case that the filter is digital, the *Bwd* is assumed roughly twice of the *Flt*. Then Eq.(2.83-a) can be rewrote as

$$F_S \geq 3 \times Flt, \qquad (2.83\text{-b})$$

and

$$Flt \leq \frac{F_S}{3}, \qquad (2.83\text{-c})$$

The relation between F_S and *Rbw* is considered by Eq.(2.82) and (2.83-a~c).

$$F_S \geq 17.4 \times Rbw, \text{ or } \quad Rbw \leq F_S / 17.4 \qquad (2.84)$$

The sweep rate is explained by substituting Eq.(2.83-c) in to Eq.(2.81) as

$$\sigma \geq \frac{1}{k_W} Flt \cdot Rbw = \frac{1}{k_W} \frac{F_S}{3} Rbw = 0.095 \cdot F_S \cdot Rbw, \qquad (2.85)$$

where k_W is 3.5. As a result, the sweep rate is in proportion to the product of F_S and *Rbw*.

2.9.3 Actual Measurement Time

The sweep rate against the Rbw with the sampling frequency 100MHz and 200kHz, which is computed by Eq.(2.85), is shown in Fig.2.44. The rate of sweep method is drawn in the figure for a comparison.

In actual system, the overall measurement time is including a processing time, local switching time and other several factors [19]. Therefore, the actual sweep rate is given by

$$\begin{aligned} \sigma &= \frac{Span}{\text{Total Processing Time}} \\ &= \frac{Span}{(\text{int}(Span / Flt) + 1) \times \{\max(T_P, k_W / Rbw + T_{SLO})\}}, \end{aligned} \qquad (2.86)$$

where T_P is the processing time of the FFT, T_{SLO} is the local switching time. If the processing time is shorter than the acquisition time, it has almost no influence to the measurement time.

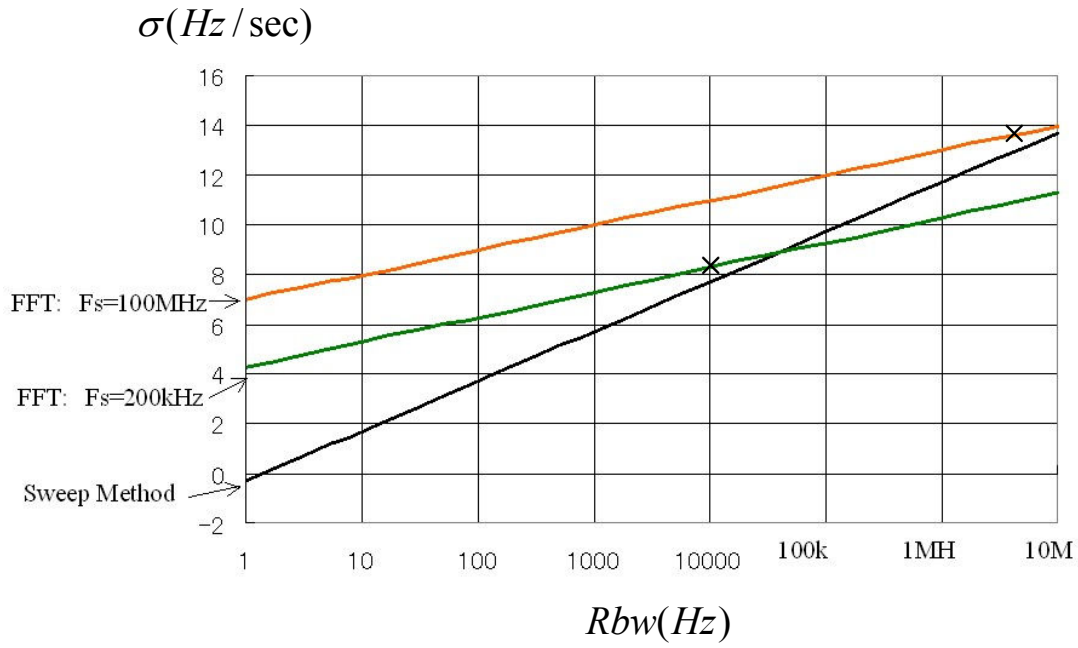

Fig 2.44 Sweep rate Against *Rbw*

FFT: Computed by Eq.(2.85)

Sweep: Computed by Eq.(2.38)

x : Indicate the point that Rbw=(Sampling frequency)/17.4

We cannot achieve the FFT with the Rbw by the sampling frequency.

The sweep rate of the sweep method is in inverse proportion to square of *Rbw*, but the rate of the FFT method, Eq.(2.86) is in inverse proportion to *Rbw*. It is expected that the FFT method can achieve faster sweep rate at narrower *Rbw*. But the wider *Rbw* requires faster sampling rate, shorter the window time T_W , and shorter operation time. The symbols 'x' in Fig.2.44 indicates the value of *Rbw* that is '(Sampling frequency)/17.4'. By the discussion of Eq.(2.84), we cannot achieve the FFT with the *Rbw* larger than the point of 'x'. We have a point that the processing time T_P becomes larger than the window time T_W . And we have the point of *Rbw* that the FFT method is not faster than the sweep method.

We investigated the measurement time of two conventional types of spectrum analyzers. We measured the measurement time including operation time or other all-processing against each *Rbw* using a stopwatch, where the span was set enough wider than the *Rbw*.

The result of type A is shown in Table 2.5-a. This type of analyzer has the FFT method of *Rbw* from 1Hz to 10kHz. It was until *Rbw* 1kHz that the sweep rate was faster than the sweep method. The result of type B is shown in Table 2.5-b. It was until *Rbw* 100Hz that the sweep rate was faster than the sweep method. The difference of achieved sweep rate of the two types was approximately 7 times. The two types assumed to have different processor.

Table 2.5-a: Results of Type A (Rohde&Schwaltz FSU in 2006)

RBW	σ : Sweep Method (for Reference)	σ : FFT method	Ratio against the sweep method
1Hz	0.5Hz/sec	3.75kHz/s	7500
10Hz	50Hz/sec	37.5kHz/s	750
100Hz	5kHz/sec	375kHz/s	75
1kHz	0.5MHz/sec	3MHz/s	6
10kHz	50MHz/sec	10MHz/s	0.2

Table 2.5-b: Results of Type B (Agilent ESA in 2006)

RBW	σ : Sweep Method (for Reference)	σ : FFT method	Ratio against the sweep method
1Hz	0.5Hz/sec	500Hz/s	1000
10Hz	50Hz/sec	500Hz/s	100
100Hz	5kHz/sec	50kHz/s	10
300Hz	45kHz/sec	27kHz/s	0.6

By the result of above discussion, it considered that the maximum *Rbw* that achieves faster sweep rate than the analog method is dependent on the performance of the signal processor. It is important to take optimized configuration that takes a balance between the performances AD/C, DSP and other parts of the system.

2.9.4 Demerit of the FFT Method

As described in section 2.8.5 and Fig.2.42, the spectrum obtained by the FFT method has some ripple corresponding to the characteristic of the IF BPF. In the step sweep (multiple-FFT) method, the ripple will appear on the each spectrum as shown in Fig.2.45. It is difficult to make the IF BPF that has perfectly flat pass band. It is more realistic to take an equalization of the IF BPF than to make it with flat pass band.

There are not continuities on the time between each result of the FFT. In the case we measure a dynamic signal, some gaps may exist between the each result of the FFT.

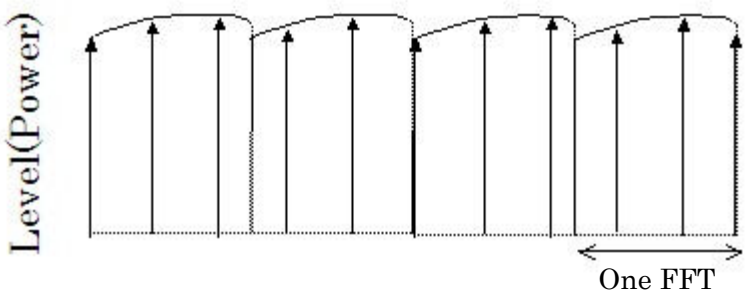

Fig 2.45 Ripple on a Spectrum by Step Sweep method

2.10 Summary

This chapter described the theory and property of the sweep spectrum analyzer. It is a kind of pseudo-Fourier transformer. In sweep method, the spectrum $S(\omega)$ is obtained as a convolution of Fourier transform of the signal $F(\omega)$ and frequency response of the resolution filter $G(\omega)$, which is given by

$$S(\omega) = F(\omega) * G(\omega).$$

The sweep time is in proportional to the *Span* and in inversely proportional to the square of resolution bandwidth (*Rbw*) as next equation.

$$T_S \geq k_0 \frac{Span}{Rbw^2},$$

where k_0 is 2~3 experimentally.

The abscissa of spectrums obtained by sweep spectrum analyzer indicates not only frequency but also time. The resolution of the frequency and the time is under a binding of the uncertainty principal.

$$\Delta f \times \Delta t = constant \qquad (2.87)$$

The sweep spectrum analyzer can change the condition of the measurement such as the *Rbw* and the sweep time. We can obtain variable result by changing the condition, and we can estimate the Fourier transform of the signal $F(\omega)$. On the other hand, in the FFT method, the abscissa has not factor of time. The sweep method has an advantage at the point of variety measurement condition against the FFT method.

The sweep spectrum analyzer is a narrowband system as described in section 2.8. It is conformity to measure with wider dynamic range.

Table 2.6 concludes the characteristic of each method.

Some report about the FFT method is described in [1][2][17][18].

Table 2.6 Characteristics of each methods

Category	Merit	Demerit
Sweep Method	・Measuring RF signal, up to μ wave ・Wideband measuring 3GHz to 8GHz ・Wide dynamic range	・Slow speed at narrow RBW ・Around DC (0Hz) is observed as Zero carrier
FFT method With no down converter	・Low frequency from 0Hz ・Time domain measurement by same instrument system ・Transient phenomenon	・The dynamic range is dependent on the AD/C ・System performance is dependent on the processor
FFT method With down converter	・High speed with narrow RBW ・Well shaping factor of RBW filter	・Wide band measurement over 100MHz ・The IF filter response appears on the spectrum.
Digital Oscilloscope (Time domain)	・Transient phenomenon	・Difficult to measure multi tone signal
Digital Oscilloscope (Frequency domain)	・Low cost	・Low dynamic range

2.11 Reference

[1] Agilent Technologies, Spectrum Analysis Basics, Application Note 150, August 2,2006

[2] R.A.Witte “Spectrum and Network measurement”, 1993 Prentice-Hall,Inc

[3] Morris Engelson “Spectrum Analyzer Theory and Applications” Artech House publishers Oct. 1974

[4] 岩波数学公式Ⅱ 級数・フーリエ解析 森口・宇田・一松 1957 岩波書店

[5] Masao Nagano “The first signal processing device for digital radio communications”, S^2PATJ vol.4, No.2, June 2001 pp23-30

[6] Alan.V.Oppenheim, “Digital Signal Processing”, 1975, Prentice Hall

[6-2] Alan.V.Oppenheim, “Signal And System”, 1983, Prentice Hall

[7] E.Oran Brigham, “The Fast Fourier Transform”, Prentice-Hall,Inc.,1974

[8] Masao Nagano “Signal Processing of Sweep Spectrum Analyzer” S^2PATJ vol.3, No.4 Dec. 2000 pp.17-24

[9] Masao Nagano “Spectrum Analyzer of Super Sweep IF Filter” S^2PATJ vol.4, No.2, June 2001 pp23-30

[10] Kirsten C. Carlson “A 10-Hz-to-150-MHz Spectrum Analyzer with a Digital IF Section” Hewlett-Packard Journal June 1991

[11] George D. Tsakiris “Resolution of a spectrum analyzer under dynamic operations” Rev. Sci. Instrum., Vol.48, No.11, Nov. 1977 pp.1414-1419

[12] Y.Kagawa “Analog/Digitsl Filter”, Science Press, Inc. Tokyo Japan ,1981

[13] F.R.Connor “Modulation Second Edition”, Edward Arnold (Publishers) Ltd. 1982

[14] B.P.Lathi “Communication Systems”, McGraw-Hill Book Co.Ltd. 1977, p158

[15] F.J.Harris “On the Use of Windows for Haramonic Analysis”, Proceedings of the IEEE, Vol66, No.1, Jan, 1978

[16] Masao Nagano “The IF filter of a Spectrum Analyzer using FFT” S^2PATJ vol.4, No.1, March 2001 pp20-27

[17] M.Nagano “The spectrum analyzer understanding from the signal processing”, Interface, Sep.2005, CQ publish Co. Tokyo Japan.

[18] M.Nagano “The spectrum analyzer understanding from the signal processing”, Interface, Aug.2005, CQ publish Co. Tokyo Japan.

[19] Agilent Technologies, Performance Spectrum Analyzer Series Swept and FFT Analysis, Application Note 5980-3081, Oct 5,2004

Chapter 3

Theory and System of Super Sweep Method

3.1 Introduction

Chapter 2 described the reason why sweep spectrum analyzers have the restriction of the sweep rate. This chapter describes the principle of the super sweep method that was introduced in [5]. This method made a breakthrough in the restriction of the sweep method, which is described in section 2.5.2.

Section 3.2 described the mathematical description of the super sweep method and the fundamental concept of the implementation.

Section 3.3 describes the signal processing of the super sweep method using the model, which is described in section 3.2. In this section we inspect the negative chirp operation by numerical analyses, and describe the Gaussian filter as the negative chirp filter and analyze the maximum sweep rate of the method.

In section 3.4, an implementation of the complex filter is considered.

3.2 Theory of super sweep method

3.2.1 Back ground of super sweep method

In this chapter or later, we assumed that the described system was made by the digital IF method, which was illustrated by Fig.2-10, 2-11 and 2-12 in section 2.4.

In section 2.5, we investigated the restriction and 'over sweep-rate response' of the sweep rate in sweep spectrum analyzers. The phenomenon is caused because the resolution filter accepts the chirped IF signal. The over sweep-rate response exists whenever the sweep rate σ was not zero. Figure 2.21 (a) and (c) show the reduction 0.1dB, which was permitted condition generally.

In Fig.2.21(c), the transition of the phase against the Gaussian filter was so small that the transition was assumed almost stop within the time length of the Gaussian filter. In a hypothesis that we set up, we could obtain the spectrum without the peak level reduction by canceling the phase factor of the base band signal before the resolution filter process.

3.2.2 Mathematical model of super sweep method

In this section, we assumed that the measured signal was a CW signal for simplification. The super sweep method was one of methods to approximate the Fourier transform. By the theory of

linearity on Fourier transform, we could apply the result, which was proved for a CW signal, to a general signal as a sum of CW signals.

In the system described in Fig.2.17, the IF signal *S(t)* had a chirped phase factor: $\pi\sigma t^2$, which was described in Eq.(2.31a)~(2.31c). This factor caused the imperfect of the Fourier transform. We intended to cancel the chirped phase factor using a complex filter as follows. The super sweep method introduced a complex filter that had a negative chirp factor. The impulse response of the filter was expressed by

$$g_n(t) = g(t)\exp[\, j\pi\sigma t^2\,]. \qquad (3.1)$$

By replacing $g(t)$ with above $g_n(t)$ in Eq.(2.31-a), Eq.(2.29-b) is modified as

$$S_n(t) = g_n(t) * \{f(t)\times l(t)\}, \qquad (3.2)$$

where $S_n(t)$ is modified IF signal. This equation can be modified as

$$\left.\begin{aligned} S_n(t) &= \{g(t)\exp[\, j\pi\sigma t^2\,]\} * \{f(t)\times\exp[-j(\pi\sigma t^2+\omega_0 t+\theta_0)]\} \\ &= \int_{-\infty}^{\infty}\{g(\tau)\cdot\exp[\, j\pi\sigma\tau^2\,]\} \\ &\qquad \times\{f(t-\tau)\exp[-j(\pi\sigma(t-\tau)^2+\omega_0(t-\tau)+\theta_0)]\}d\tau \\ &= \exp[-j(\pi\sigma t^2+\omega_0 t+\theta_0)] \\ &\qquad \times\int_{-\infty}^{\infty} g(\tau)f(t-\tau)\times\exp[j(2\pi\sigma t+\omega_0)\tau\,]\,d\tau \end{aligned}\right\} \qquad (3.3)$$

There are no terms that included τ^2 in the exponential function. The filter $g_n(t)$, 'a negative chirp filter' cancels the terms. Equation (3.3) is now modified as

$$S_n(t) = l(t)\int_{-\infty}^{\infty} g(\tau)f(t-\tau)\times\exp[j\omega(t)\tau]\,d\tau\,, \qquad (3.4)$$

where ω(t) is defined as

$$\omega(t) = 2\pi\sigma\, t + \omega_0\,. \qquad (3.5)$$

Then, Eq.(3.4) can be written by substituting $f(t-\tau)$ with Eq.(2.29).

$$\left.\begin{aligned} S_n(t) &= l(t)\exp[\, j\omega_s t]\times\int_{-\infty}^{\infty} g(\tau)a(t-\tau)\times\exp[-j(\omega_s-\omega(t))\tau]\,d\tau \\ &= l(t)\exp[\, j\omega_s t]\times\int_{-\infty}^{\infty} g(\tau)\cdot r(\tau)\times\exp[-j(\omega_s-\omega(t))\tau]\,d\tau\,, \end{aligned}\right\} \qquad (3.6)$$

where $r(\tau)$ is $a(t-\tau)$.

It is possible to replace the integration of Eq.(3.4) with the product of the Fourier transforms of $g(t)$ and $r(\tau)$ as follows.

$$S_n(t) = l(t)\exp[\, j\omega_s t]\times\{G(\omega_s-\omega(t)) * R(\omega_s-\omega(t))\}\,, \qquad (3.7)$$

where $G(\omega)$ and $R(\omega)$ is a Fourier transform of $g(\tau)$ and $r(\tau)$. By the characteristic of the Fourier transform, $R(\omega)$ can be expressed as follows [1].

$$R(\omega(t)) = \exp[-j\omega(t)t] \times A(-\omega(t)), \quad (3.8)$$

where $A(\omega)$ is the Fourier transform of $a(\tau)$. Thus Eq.(3.7) is modified as

$$S_n(t) = l(t) \times \exp[j\omega(t)t] \times \{G(\omega_s - \omega(t)) * A(\omega(t) - \omega_s)\}. \quad (3.9\text{-a})$$

By Eq(2.36-e),

$$A(\omega(t)) = F(\omega(t) + \omega_s), \quad (3.9\text{-b})$$

and g(t) is a real signal. Then

$$G(-\omega) = G^*(\omega), \quad (3.9\text{-c})$$

where $G^*(\omega)$ is the complex conjugate of $G(\omega)$. The Eq.(3.9-a) can be written as

$$S_n(t) = l(t) \times \exp[j\omega(t)t] \times \{G^*(\omega(t) - \omega_s) * F(\omega(t))\}. \quad (3.9\text{-d})$$

In the case that we focus the magnitude of Eq.(3.9-d), it can be written as

$$|S_n(t)| = |G^*(\omega(t) - \omega_s) * F(\omega(t))|. \quad (3.10)$$

Although, the conventional sweep method requires that the sweep rate equals to zero to obtain spectrum as a convolution with RBW filter (see section 2.5.1 and Eq.(2.36-c)). But Eq.(3.10) indicates that we can obtain a spectrum even if the sweep rate σ is not zero. It is an effect of the filter represented by Eq.(3.1) that have the negative chirp factor. We named the filter represented by Eq.(3.1) '**negative chirp filter'**. And we named the new method, in which this filer is used, **'super sweep method'**.

3.2.3 Implementation of Super Sweep method

In this section, we introduce the hardware in which the super sweep method was implemented. The super sweep method inversed the chirp factor of the signal, and was a complex signal processing system.

An example of a diagram, implemented the super sweep method, is shown in Fig.3.1. It was almost similar to the system described in section 2.4 "Digital IF". It was exactly the same as the system that excludes the 'Analog IF method' from Fig.2.9. The 'RF Down Converter' had a local oscillator that generated a sweep signal *l(t)*, Eq.(2.30),

$$l(t) = \exp\left[j\left(\pi \cdot \sigma t^2 + \omega_0 t + \theta_0\right)\right], \qquad (3.11)$$

and had the mixer and the IF BPF as shown in Fig.2.9. It converted the 'INPUT' signal into the 'IF Signal', *S(t)*. The A/D converter: 'AD/C' digitized the IF Signal which had efficient sampling frequency corresponding to the bandwidth of the IF signal. The output of the AD/C was transferred to the Digital Down Converter (DDC).

The overview of the DDC is shown in Fig.3.2. The DDC converted the digitized IF signal into the 'Base Band Signals',

$$S_B(t) = I_b(t) + jQ_b(t)\,. \qquad (3.12)$$

The function of the DDC is described in section 2.4. In Figure 3.2, the decimation rate of the 'Decimation LPF' was N_D. This rate was decided corresponding to the resolution bandwidth (*Rbw*); the decision-making process is described in the later section. The outputs of the decimation LPF were the 'Base Band Signal', $S_B(t)$, which were inputted into the 'Complex Filter'. The negative chirp filter was implemented as this filter. The output of this filter was the signal $S_n(t)$ which was described in section 3.2.2. $S_n(t)$ was transferred into the 'Display'. The Display was a sub-system which displays the $S_n(t)$ as a spectrum. The detail of signal processing and the each part is described in the following sections.

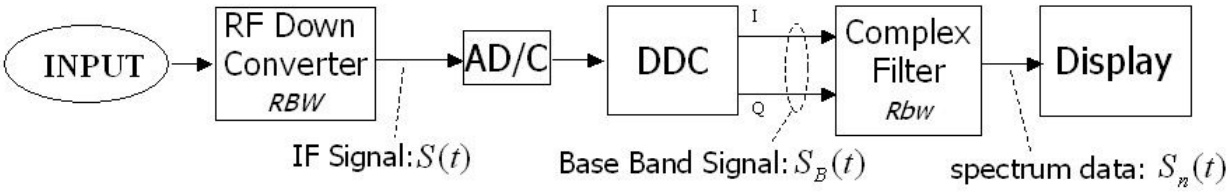

Fig. 3.1 Diagram of our Experimental System

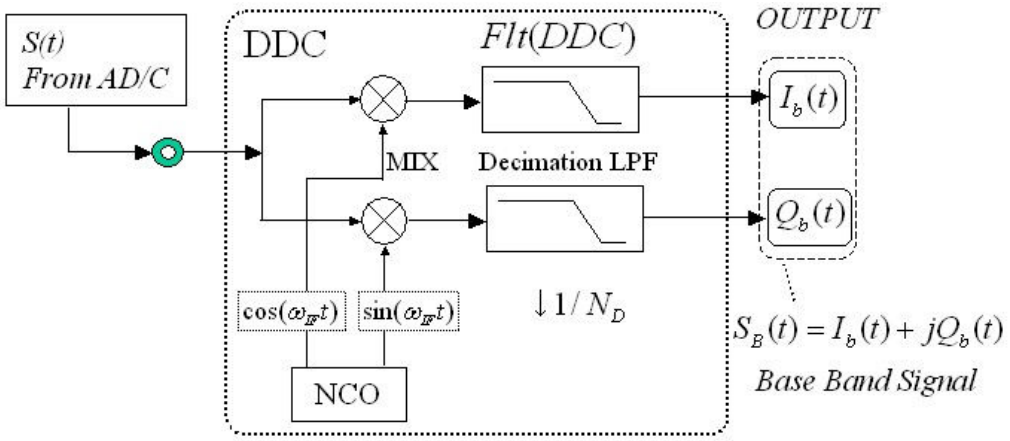

Fig. 3.2 Overview of Digital Down Converter (DDC)

3.3 Signal Processing of Super Sweep Method

This section inspected the theory of the super sweep method, which was introduced in section 3.2. This section described the signal processing of the system shown in Fig.3.1. The measured signal in this section was considered to be a CW, for simplification.

3.3.1 Inspection of Super Sweep Method

The Base Band Signal, output of the DDC, in Fig.3.2 has the same formula with Eq.(2.31-a).

$$S_B(t) = h(t) * \left\{ f(t) \times \exp[\, j(\pi \cdot \sigma t^2 + \omega t + \theta_0)] \right\}, \qquad (3.13)$$

where *h(t)* is the total impulse response of the RF Down converter and the DDC, and ω is the center frequency of the local oscillator in the RF down converter.

In the case that $f(t)$ is a CW signal, $f(t)$ is given by

$$f(t) = a \times \exp[\, j\omega t], \qquad (3.14)$$

where '*a*' is the amplitude and ω is the angular frequency. Then the signal $S_B(t)$ is written as

$$S_{B\_CW}(t) = h(t) * \left\{ a \times \exp[\, j(\pi\sigma t^2 + \theta_0)] \right\}, \qquad (3.15)$$

An example of $S_{B\_CW}(t)$ is shown in Fig.3.3. The two lines of the figure are a real and an imaginary part of the signal, $I_b(t)$ and $Q_b(t)$, respectively. The envelope of $S_{B\_CW}(t)$ is corresponding to the frequency response of $h(t)$. In Fig.3.3, the frequency of $S_{B\_CW}(t)$ at *t=0* is *0Hz*. The time, at which the frequency equals to 0Hz, generally changes corresponding to ω.

In the case that the frequency of the $f(t)$ equals to $\omega + \Delta\omega$, Eq.(3.15) is written as

$$S_{B\_CW}(t) = h(t) * \left\{ a \times \exp[\, j(\pi\sigma t^2 + \Delta\omega t + \theta_0)] \right\}. \qquad (3.16)$$

And when the frequency equals to zero, the time Δt is given by

$$\Delta t = -\Delta\omega/(2\pi\sigma). \qquad (3.17)$$

It is modified as;

$$\Delta\omega = -2\pi\sigma \times \Delta t. \qquad (3.18)$$

We can obtain the frequency of $f(t)$ from this equation. The abscissa of Fig.3.3 indicates the time progress and also indicates the frequency.

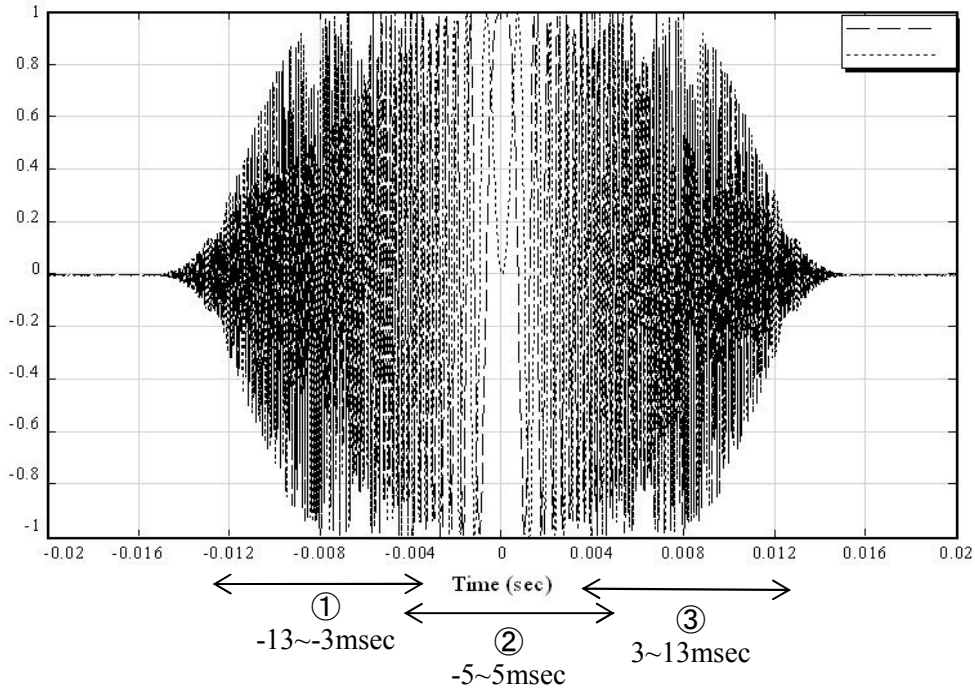

Fig. 3.3 Base band signal in sweep method

3.3.2 Inspection of negative chirp filter

An example of the base band signal prior to the negative chirp filter is shown in Figure 3.3. In Fig.3.3, *Span* was 40kHz, *Rbw* was 300Hz, sweep time was 40msec, amplitude '*a*' was one, and the plotting sampling frequency was 10kHz. The signal was computed by Eq.(3.15) with the following process.

The sweep rate σ was,

$$\sigma = Span / T_S = 40 \cdot 10^3 / (40 \cdot 10^{-3}) = 10^6, \qquad (3.19)$$

and $h(t)$ was so designed that the 3dB bandwidth was 20kHz. Equation (3.15) was modified as

$$S_{B\_CW}(t) = h(t) * \left\{ \exp[\, j\pi\sigma\, t^2] \right\}, \qquad (3.20)$$

where *a* and θ_0 were assumed to be one and zero for simplification. $S_{B\_CW}(t)$ was band limited chirp signal. In traditional method, σ should be,

$$\sigma = \frac{Span}{T_S} \le \frac{Span}{k \dfrac{Span}{Rbw^2}} = \frac{1}{k} Rbw^2 = 4.5 \cdot 10^4, \qquad (3.21)$$

where T_S is given by Eq.(2.14) and *k* is 2.0. The rate Eq.(3.19) was 22.25 times faster than a conventional method.

The signals shown in Fig.3.3 are typical base band signal of sweep spectrum analyzers, whose frequency is chirped. The signals are digitized; therefore we can cancel the chirp factor by computing.

If the bandwidth of $h(t)$ is wide enough, it can be assumed to be δ function, and $S_{B\_CW}(t)$: Eq.(3.20) can be assumed to be as the following equation.

$$S_{B\_CW}(t) = \exp[\, j\pi\sigma\, t^2] \qquad (3.22\text{-a})$$

We defined a function $u(t)$ as

$$u(t) = \begin{cases} 0 & |t| > 5m\sec \\ \exp[-j\pi\sigma t^2] & |t| \le 5m\sec \end{cases}. \qquad (3.22\text{-b})$$

And we defined the product of $u(t)$ and $S_{B\_CW}(t)$ with time lag τ, $S_u(t)$ as,

$$\left.\begin{aligned} S_u(t) &= u(t) \times S_{B\_CW}(t-\tau) \\ &= \exp[-j\pi\sigma t^2] \times \exp[\, j\pi\sigma (t-\tau)^2] \\ &= \exp[\, j\pi\sigma(-2t\tau + \tau^2)]. \end{aligned}\right\} \qquad (3.22\text{-c})$$

When |t|>5msec, $S_u(t)$=0.

The frequency of $S_u(t)$ is dependent on the time lag τ. When τ=8msec, 0msec and -8msec, $S_u(t)$ was ①, ② and ③ of Fig.3.4, respectively. These were corresponding to ①, ② and ③ of Fig.3.3. The frequency of ① and ③ were constant and ② was a small change which could be assumed in the range of a quantum error of the digitizing.

Through the above discussion, we inspected that the chirp factor of the signal $S_{B\_CW}(t)$ could be canceled.

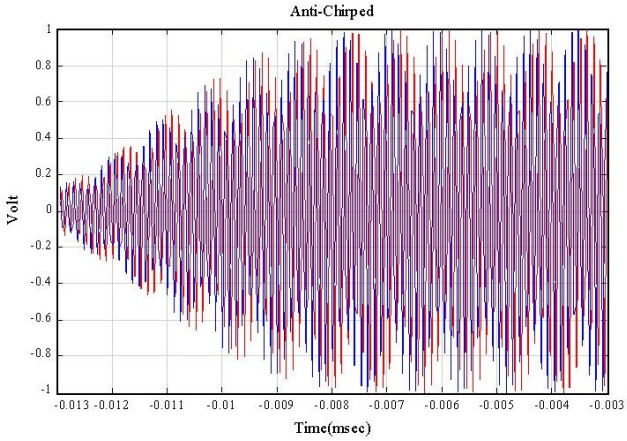

① τ =-8 msec

The frequency is -8kHz.

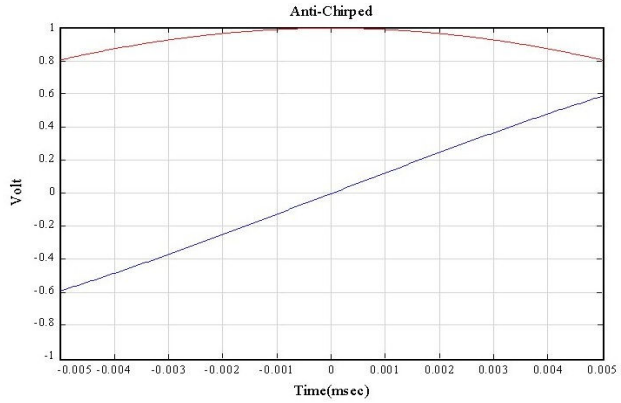

② τ = 0 msec

The phase is changed from -1/5 π (-36deg) to 1/5 π (36deg). The frequency is 0.002Hz.

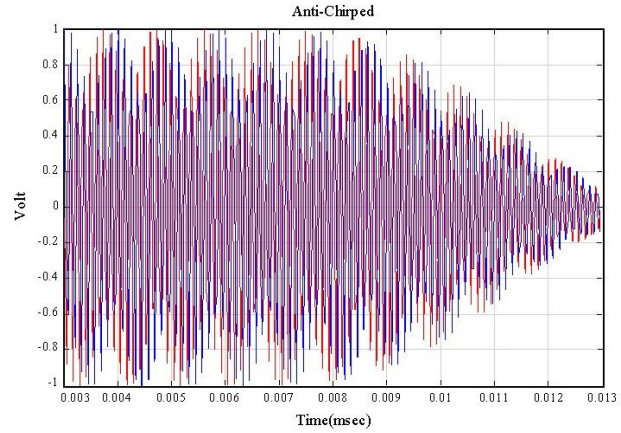

③ τ = 8 msec

The frequency is 8kHz.

Fig.3.4 Product of Chirped base band signal and negative chirp function

Figure 3.5 shows the impulse response of the Gaussian filter $g(t)$ at RBW 300Hz. The abscissa scale is fitted to Fig.3.4. $g(t)$ is expressed by the following equation (see section 2.5.3).

$$g(t) = \exp\left[-\frac{(\pi \cdot Rbw)^2}{2\ln 2} t^2\right] \qquad (3.23)$$

We defined the integral for the product of $g(t)$ and $S_u(t)$ as 'P' which is a spectrum of $f(t)$, given by

$$\left.\begin{aligned} P &= \int_{-0.005}^{0.005} g(t) \cdot S_u(t) dt \\ &= \int_{-0.005}^{0.005} g(t) \cdot u(t) S_{B\_CW}(t-\tau) dt \\ &= g_n(t) * S_B\_CW(t) \\ &= g_n(t) * \{f(t) \cdot l(t)\}. \end{aligned}\right\} \qquad (3.24)$$

Where P can be assumed as a spectrum $S_n(t)$, Eq.(3.2). Equation (3.24) means that P equals the convolution of negative chirp filter and chirped base band signal, Eq.(3.2). The operation of the super sweep method is represented by Eq.(3.24).

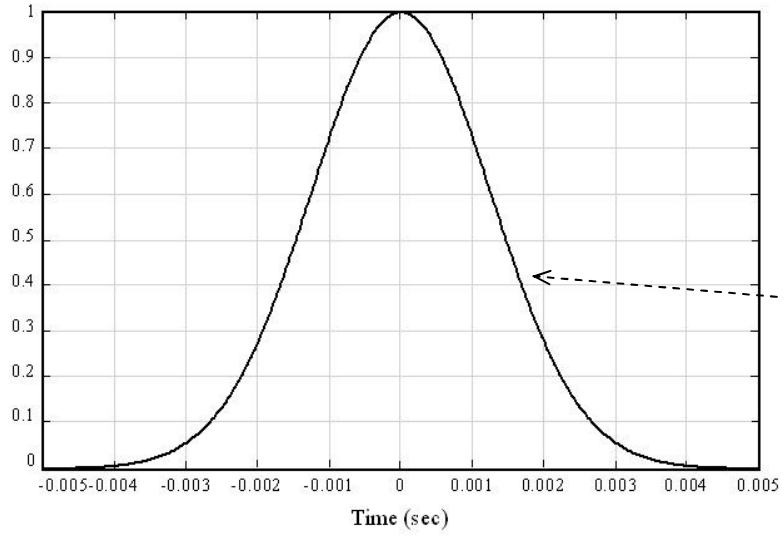

The impulse response of the Gaussian Filter for RBW=300Hz

$$g(t) = \exp\left[-\frac{(\pi \cdot Rbw)^2}{2\ln 2} t^2\right]$$

Fig.3.5 Gaussian Filter: RBW=300Hz

3.3.3 Gauss function as negative chirp filter

The negative chirp filter $g_n(t)$, Eq.(3.1) is a kind of low pass filter. We can extract the time Δt, Eq.(3.17) and the peak power of the base band signal $S_B(t)$, Eq.(3.13) from the convolution of $g_n(t)$ and $S_B(t)$. And we can obtain the frequency and power of the signal $f(t)$.

The Gaussian filter is usually chosen for the RBW filter of a spectrum analyzer [2][3][4]. The following equation shows an example of a negative chirp filter modified from Eq.(3.1).

$$g_n(t) = \exp\left[-\frac{(\pi \cdot Rbw)^2 t^2}{2\ln 2}\right] \times \exp[j(-\pi\sigma t^2)]. \qquad (3.25)$$

The relation between *Rbw* and the above function is described in [3][5]. In the case that σ equals to zero, the Fourier transform of $g_n(t)$ corresponds to $G(\omega)$ of Eq.(2.37).

$$G(\omega) = \exp\left[-\frac{\ln 2}{(\pi \cdot Rbw)^2}\omega^2\right],$$

An example of the negative chirp filter is shown in Fig.3.6 whose condition is fitted with Fig.3.3~3.5 (RBW=300Hz, Span=20kHz, Sweep time=40msec). It is a complex function and consists of the real part and imaginary part as follows.

$$I_g(t) = \mathrm{Re}[g_n(t)] \qquad (3.26\text{-a})$$

$$Q_g(t) = \mathrm{Im}[g_n(t)] \qquad (3.26\text{-b})$$

In Figure 3.6, Gauss function $g(t)$ is added as an envelope of $g_n(t)$.

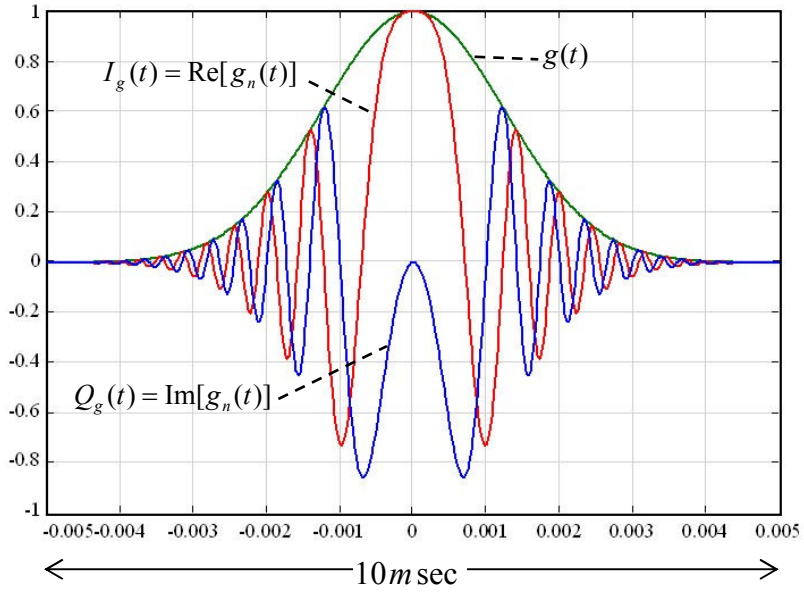

Fig.3.6 Gaussian Filter(RBW=300Hz) $g_n(t)$ as a Negative chirp filter

3.3.4 Practical negative chirp filter

The time in the Eq.(3.25) has no limit, therefore it is defined from minus infinity to infinity. The amplitude of Eq.(3.25) approaches zero when $|t|$ is infinity. Actually, the $|t|$ is limited as a digital filter. We defined the time limit T_G as follows.

$$T_G = \chi / Rbw \quad , \tag{3.27}$$

where χ is a constant. The filter function $g_n(t)$ is defined within the specified time as follows.

$$|t| \leq T_G / 2 \tag{3.28}$$

We defined the time-limited function $g_{nL}(t)$, which is product of $g_n(t)$ and the function of $\mathrm{Rect(t)}$ shown in Fig.3.7, and it is represented as follows.

$$g_{nL}(t) = g_n(t) \times \mathrm{Rect(t)}, \tag{3.29}$$

where

$$\mathrm{Rect(t)} = \begin{cases} 0 \cdots |t| > T_G / 2 \\ 1 \cdots |t| \leq T_G / 2 \end{cases}. \tag{3.30}$$

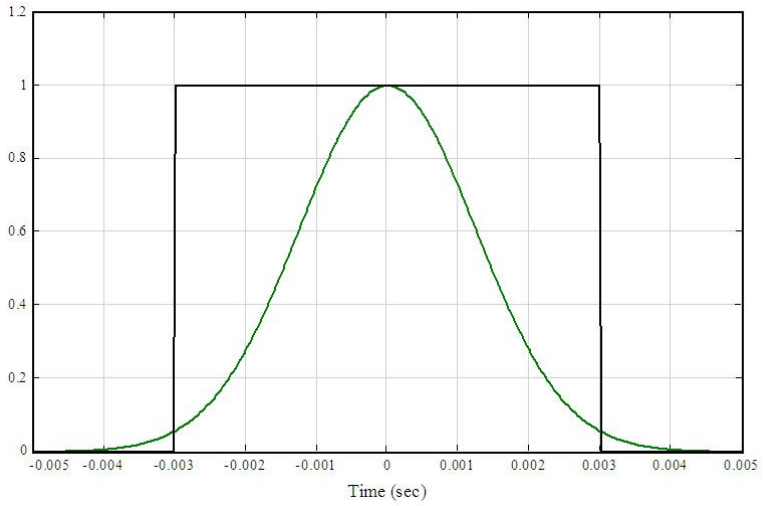

Fig. 3.7 Time limited Gausian filter

The Fourier transform of $\mathrm{Rect(t)}$ is known as sinc function and Dirichelet kernel $\mathrm{D}(\omega)$ [6].

$$\mathrm{D}(\theta) = \exp\left[j\frac{\theta}{2} \right] \frac{\sin\left(\frac{N\theta}{2} \right)}{\sin\left(\frac{\theta}{2} \right)} \quad , \theta = 2\pi \frac{\omega}{\omega_S}, \quad \omega_S = 2\pi f_S \, , \tag{3.31-a}$$

where f_S is the sampling frequency of input signal of the negative chirp filter, N is the tap number of the filter and θ is the normalized frequency. We modified Eq. (3.31-a) by scaling θ with ω.

$$\mathrm{D}(\omega) = \exp\left[j\frac{\omega}{2} \right] \frac{\sin(N\omega/2)}{\sin(\omega/2)} \quad . \qquad (3.31\text{-b})$$

The Fourier transform of $g_{nL}(t)$, $G_{nL}(\omega)$ is convolution of $g_n(t)$ and Rect(t).

$$G_{nL}(\omega) = G(\omega) * D(\omega) \qquad (3.32)$$

The Fourier transform of a Gauss function is also Gauss function itself. Figure 3.8 shows the examples of frequency responses of these filters, in which χ equals 2.6 and 3.0. In the case that χ is smaller, the frequency response has larger side lobes. It requires χ to be 2.6~3.0 and above, to reduce the side lobe level -75 ~ -100 dB from its peak level, as shown in Fig.3.8. Practically, the level of side lobes is decided by the combination of the χ and the sampling rate.

We should inspect the property of the filter for each measurement condition.

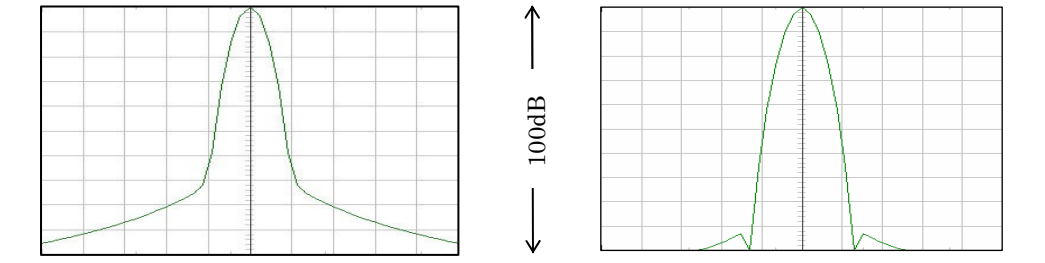

(a) $T_G = 2.6 / Rbw$ (b) $T_G = 3.0 / Rbw$

Fig. 3.8 Frequency response for χ=2.6 and 3.0

3.3.5 Maximum Sweep rate

In the case that the sweep rate is σ, the negative chirp filer sweeps the frequency Δf within the time T_G, as shown in Fig.3.9.

$$\Delta f = \sigma \cdot T_G = \sigma \cdot \chi / Rbw \quad . \qquad (3.33)$$

In Figure 3.9, the bandwidth of the base band signal is denoted as '*Flt*', which is defined 3dB bandwidth of the *h(t)* described in Eq.(3.13). If the *Flt* is narrower than the Δf, the integration of Eq.(3.4) does not operate completely. Then the *Flt* should be wider than the Δf as follows.

$$Flt \geq \Delta f = \sigma \cdot \chi / Rbw \quad . \qquad (3.34\text{-a})$$

From this inequality, the maximum sweep rate, $\sigma_{\max\_s}$ can be written as the next equation.

$$\sigma_{\max\ S} = Rbw \times (Flt / \chi) \, . \qquad (3.34\text{-b})$$

Dividing Eq.(3.34-b) by Eq.(2.38) that is maximum sweep rate in the conventional method, we define a new parameter R_s as follows.

$$R_s \equiv \frac{\sigma_{\max\_S}}{\sigma_{\max}} = \frac{k_0}{\chi} \times \frac{Flt}{Rbw} \qquad (3.35)$$

This parameter R_s indicates the fastness of the super sweep method against the conventional method. And it is in proportion to *Flt/Rbw*, because k_0 and χ are constants.

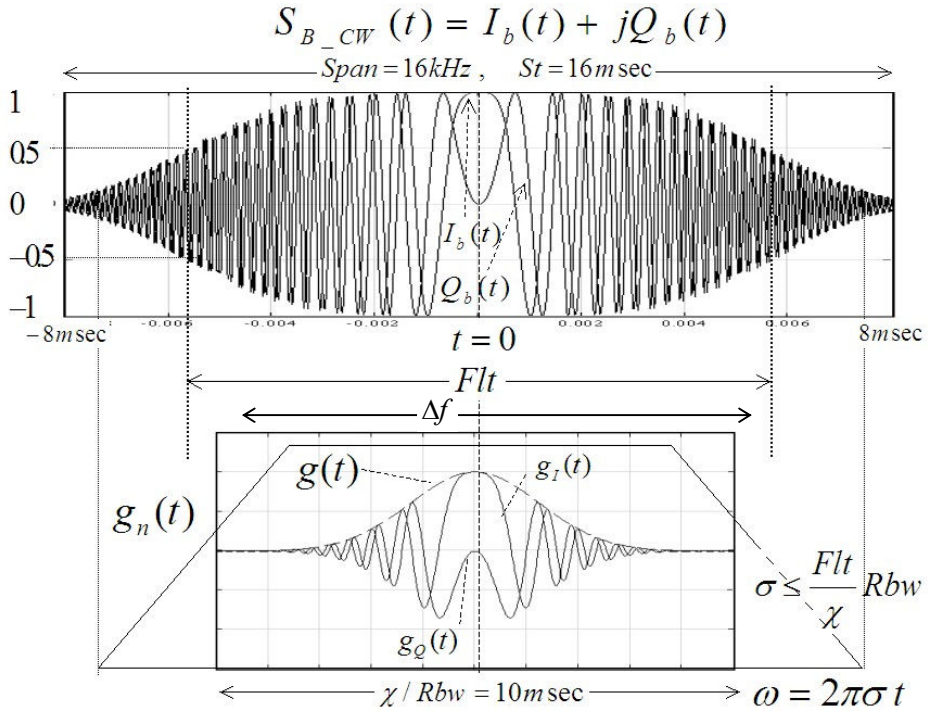

Fig. 3.9 Response time and the frequency range of a negative chirp filter

3.4 Complex filter and Display

Figure 3.10 is rewritten diagram of Fig.3.1, in which 'Complex filter' and 'Display' are emphasized in the details. The base band signal $S_B(t)$, Eq.(3.13) is inputted into the complex filter. This filter (which is enclosed by the dotted square) has four convolutions, two additions and one subtraction and produces the signal: '$I_S(t)+Q_S(t)$' as follows

$$\begin{aligned} I_S + jQ_S &= S_B(t) * g_n(t) \\ &= (I_b + jQ_b) * (g_I + jg_Q) \\ &= (I_b * g_1 - Q_b * g_Q) + j(Q_b * g_I + I_b * g_Q), \end{aligned} \tag{3.36}$$

where $g_I(t)$ and $g_Q(t)$ is the real part and imaginary part of $g_n(t)$.

The output is the complex spectrum signal and followed by the 'Display'. Square-sum of $I_S(t)$ and $Q_S(t)$ is the power spectrum, usually expressed in unit dB. The power spectrum $S_{dB}(t)$ is finally processed and obtained in the Display as follows.

$$S_{dB}(t) = 10 \cdot \log_{10}(I_S(t)^2 + Q_S(t)^2) \tag{3.37}$$

The parameter '*t*' (time) is translated into the frequency by Eq.(3.5).

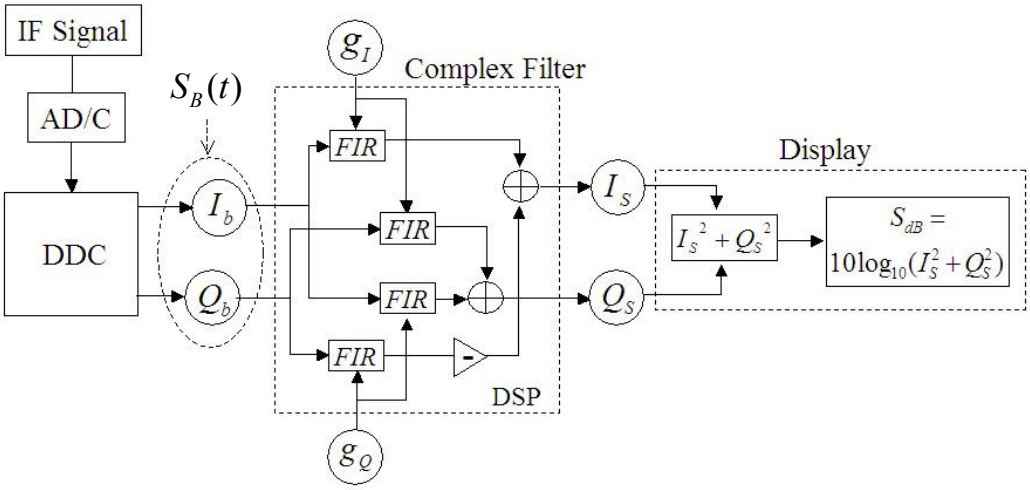

Fig. 3.10 Signal Flow of a Complex filter

We can design several ways to implement the complex filter, such as

$$\begin{aligned} I_S[k] + jQ_S[k] &= \sum_{i=0}^{N_G-1} (I_b[k+i] + jQ_b[\mathrm{k+i}]) * (g_I[i] + jg_Q[\mathrm{i}]) \\ &= \sum_{i=0}^{N_G-1} (I_b[k+i] \cdot g_1[i] - Q_b[k+i] \cdot g_Q[i]) + j(Q_b[k+i] \cdot g_I[i] + I_b[k+i] \cdot g_Q[i]) \end{aligned} \tag{3.38}$$

where N_G is the tap number. Equation (3.38) produces one sample of $I_S(t)+jQ_S(t)$ as a sum

of the product. Generally, it is efficient for a digital signal processor (DSP) to implement the operation in Fig.3.10 by four FIR filters. And we can implement the 'DSP' of Fig.3.10 into the circuit of FPGA.

Some discussion about the implementation and the performance of the filter are done in Chapter-6.

3.5 Summary

This chapter describes the theory of the super sweep method, inspects the operation of the negative chirp, and discusses the concept of the implementation of this method.

Through the discussion, we investigated that the sweep rate was in proportion to the rate *Flt* / *Rbw*.

3.6 Reference

[1] E.Oran Brigham, "The Fast Fourier Transform", Prentice-Hall,Inc.,1974

[2] Morris Engelson "Spectrum Analyzer Theory and Applications" Artech House publishers Oct. 1974

[3] Masao Nagano "Signal Processing of Sweep Spectrum Analyzer" S^2PATJ vol.3, No.4 Dec. 2000 pp.17-24

[4] George D. Tsakiris "Resolution of a spectrum analyzer under dynamic operations" Rev. Sci. Instrum., Vol.48, No.11, Nov. 1977 pp.1414-1419

[5] Masao Nagano "Spectrum Analyzer of Super Sweep IF Filter" S^2PATJ vol.4, No.2, June 2001 pp23-30

[6] F.J.Harris,"On the Use of Windows for Harmonic Analysis with the Discrete Fourier Transform", proceeding of the IEEE, Vol.66, No.1, JAN. 1978

Chapter 4

Experiments of new method

4.1 Introduction

This chapter describes the experimental system, set up to examine the theory of the super sweep method. We employed a conventional sweep spectrum analyzer as a RF down converter, which has 21.4MHZ IF output. We made a 'DSP unit', which has A/D converter, DDC and DSP. The operation of the new method is almost done on the DSP. This chapter describes the method and the condition of the experiment, and the result will be described in Chapter-5. Section 4.2 describe the overview of the experiment system and the implementation of the signal processing. Section 4.3 describes the digital filter in the DDC. Section 4.4 shows the essential specification of the experimental system.

4.2 Experimental system

4.2.1 Overview of the system

We set up the experimental system to examine the theory of the super sweep method. The system was designed based on the diagrams Fig.3.1, 3.2 and 3.10. The copy of Fig.3.1 is shown in Fig.4.1-(a). To realize the diagram, we employed a sweep spectrum analyzer as an RF down converter. The spectrum analyzer was R3264 produced by ADVANTEST Co. We made the DSP unit which took the operation from the AD/C to Complex filter in Fig.4.1-(a), and employed a conventional PC as a display system. The overview of the system is shown in Fig.4.1-(b).

By the concept of Fig.4.1, we designed the concept of the signal flow of the system, which is shown in Fig.4.3. This system was almost the same as the system of the sweep spectrum analyzer which has digital IF method, although this system had negative chirp filters.

The spectrum analyzer, R3264 has a local oscillator that generates sweep signal, mixers, IF band pass filters and output of '21.4MHz IF signal'. The architecture is shown in Fig.2-1, and described in section 2.2 and 2.3. The 21.4MHz IF signal is passed through the RBW filter of the R3264. The RBW filters can be changed by panel operation or GPIB operation. In Figure 4.3, the 'SWP' signal is made by the 'Sweep Generator'. And the voltage of SWP is corresponding to the frequency of the local oscillator, and the 'start to stop' frequency is corresponding to 0-5 Volt.

R3264 has output of 10MHz Reference clock signal. We used this signal as a reference clock of the DSP unit, which is duplicated into 80MHz, and it drives the AD/C, DDC, DSP and all circuit of the DSP unit. R3264 has BNC connectors, 21.4MHZ IF, SWP and 10MHz reference clock output from them. These connectors on the Real-Panel of R3264 are shown in Fig.4.2.

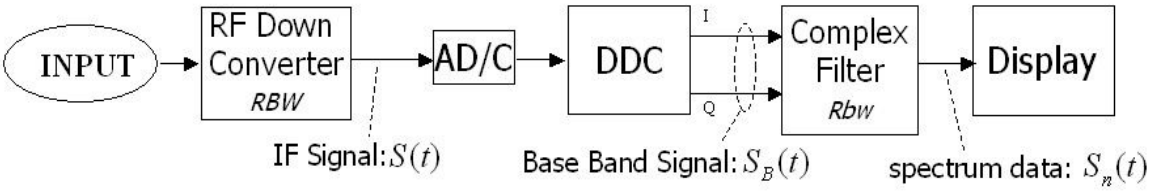

(a) The concept (Fig.3.1)

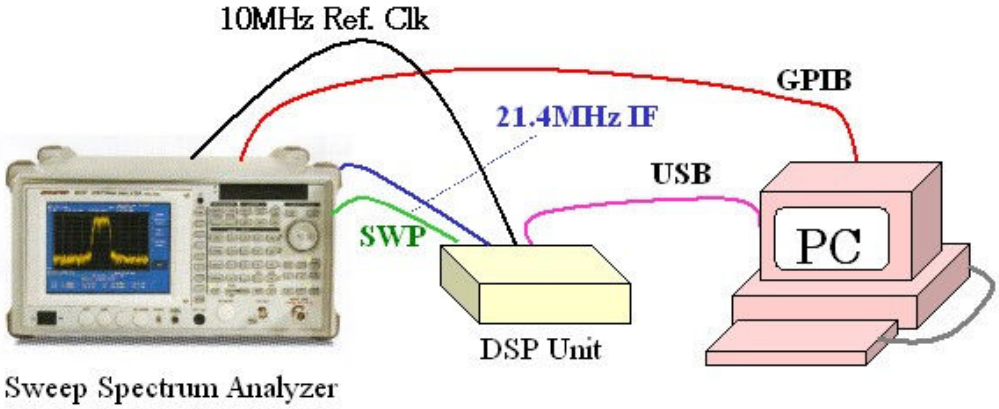

(b) Practical system, for a minimum development period and cost.

Fig. 4.1 Overview of Our Experimental System

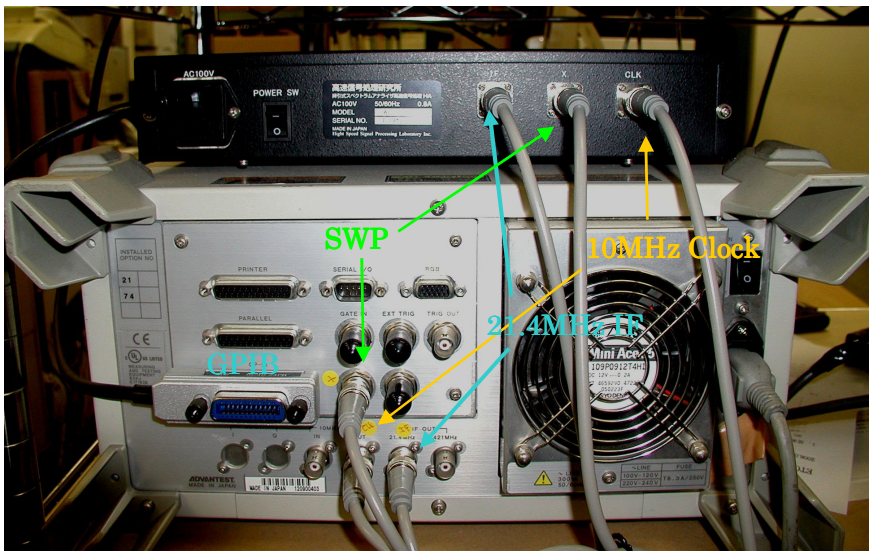

Fig. 4.2 Real Panel view of our Experimental System

Three signals are connected with the SPA to the DSP Unit

4.2.2 Signal flow of the system

The overview of the signal flow from input to the display of our experimental system is shown in Fig.4.3. The measured signal is inputted into the spectrum analyzer. The input signal is converted into the 21.4MHz IF signal. The condition of the spectrum analyzer was set to be adapted for our experiments, which is described in later sections.

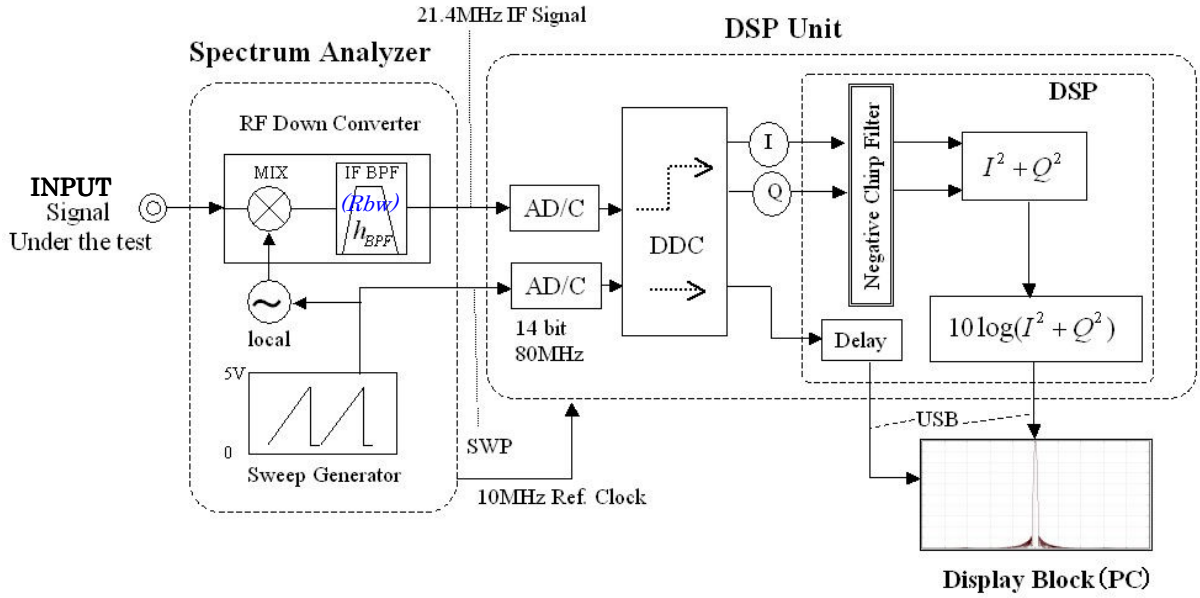

Fig. 4.3 Over view of Signal Flow of our Experimental System

We connected the 21.4MHz IF, the SWP signal, and the 10 MHz Reference clock of the analyzer to the inputs of the DSP unit. The IF and the SWP signal were digitized by the AD/C. We employed AD6645 produced by Analog Devices Co. as the AD/C of the DSP unit. They were operated by 80 MHz clock with 14-bit quantization. The digitized IF signal was finally converted into the spectrum data, and the SWP signal was used to synchronize the abscissa of the display with the sweep of the spectrum analyzer.

The DDC (digital down converter) was implemented using GC4016 supplied from the Texas Instrument Inc., which has CIC (Cascaded Integrator Com) and FIR digital filters to reduce the bandwidth and the sampling frequency. The description about the DDC is written in section 4.3.

The Complex Filter was composed of four independent numerical filters programmed on a DSP as the negative chirp filter. It is described in section 3.4. The DSP was TMS-320C6711, which is supplied from the Texas Instruments Inc. The output from the DSP was transferred to the

PC through the USB2.0 interface and the Display was figured on the PC. The PC controlled whole experimental system as well.

The SWP signal was passed thorough the same process with the IF signal to have the same latency with the IF signal, and it was registered with the IF signal. It gave the frequency value for each sample of the result as a spectrum data.

4.2.3 External view of the system

The external view of the experiment system is shown in Fig.4.4. The spectrum analyzer R3264 is shown at the left side. The black box above R3264 is the DSP unit. A spectrum is shown in the display of the PC in the right side.

Figure 4.5 is the internal view of the DSP unit. The power unit is shown in the upper side. The left lower side the AD/C board exists, and in the right side the DSP board which has DDC, MEM, DSP, and other logic circuits exits. The hardware diagram of the DSP unit is shown in Fig. 4.6.

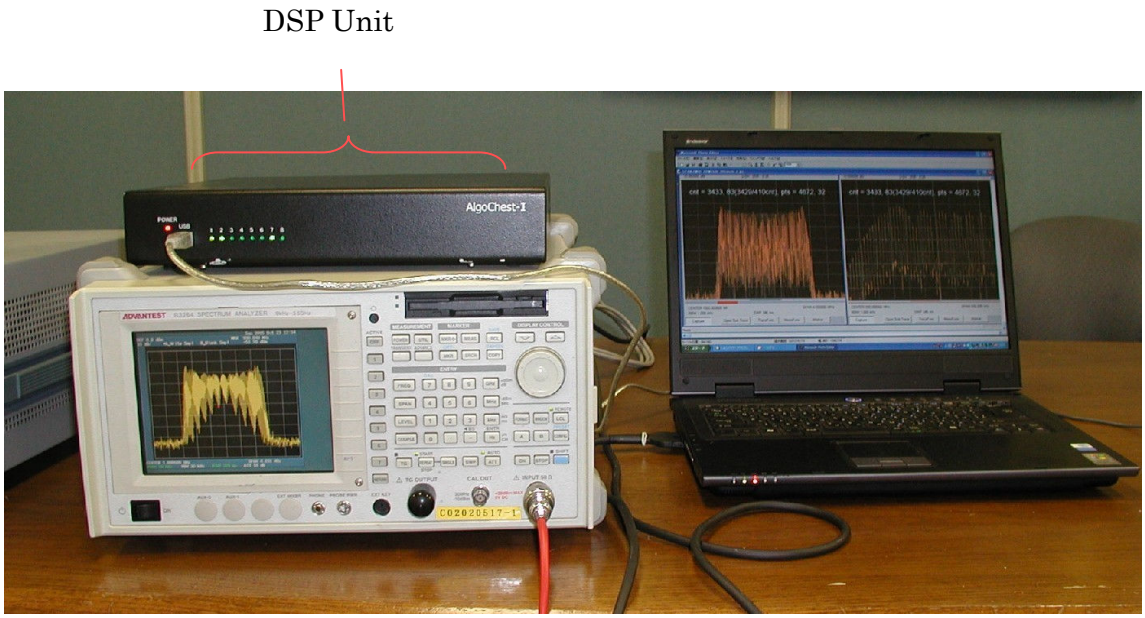

Fig.4.4 Over view of the Experimental System

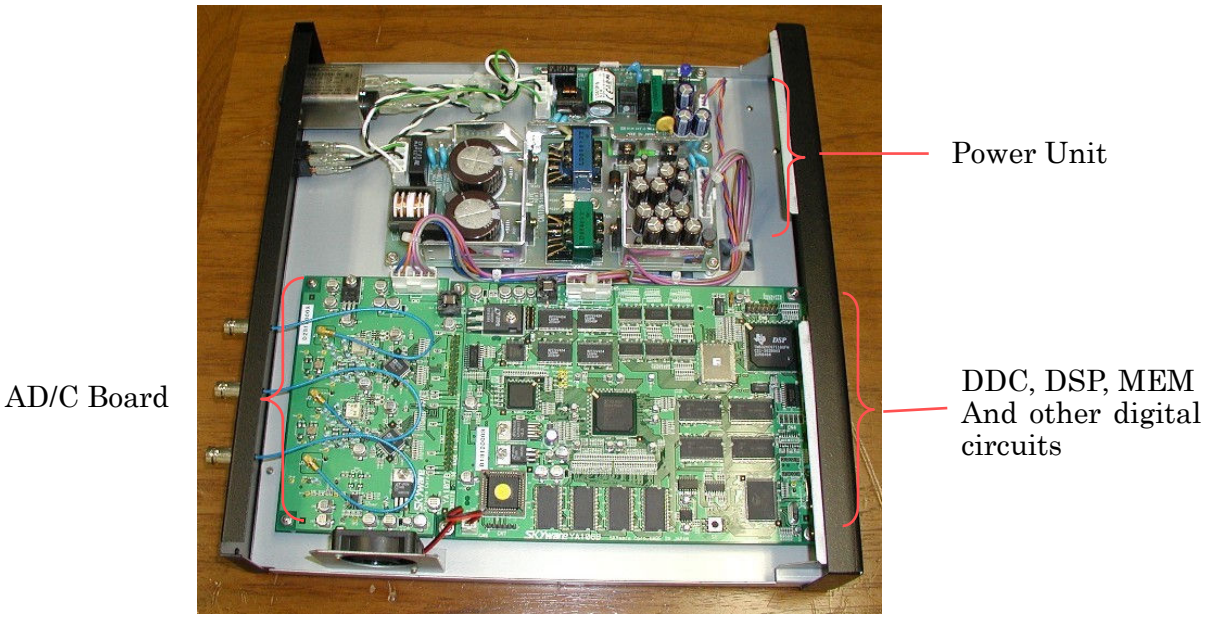

Fig.4.5 Internal view of DSP Unit

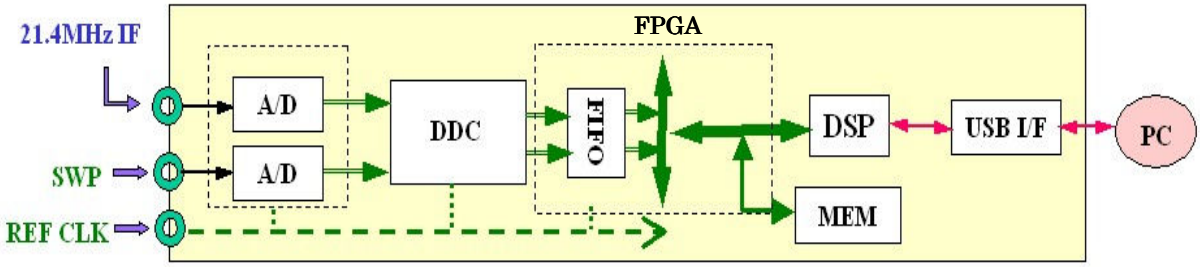

Fig.4.6 Internal block diagram of the DSP Unit

4.2.4 Chain of filters

The essence of the system is presented in Fig.4.7. The most important functions of the system are filters that are drawn in Fig.4.7. The function of this system is itemized as follows.

1. Input signal was mixed with the output of the sweeping local oscillator and transformed into the chirped IF signal by a few down-converters. In Figure 4.7, the down converters are drawn as single for a simplification.
2. The chirped IF signal was band limited by a few IF-BPFs. The narrowest BPF of the Spectrum analyzer (SPA) was the RBW filter, which should be selected adequately corresponding to the bandwidth of the negative chirp Gaussian filter, *Rbw*.
3. The DDC converted the digitized IF signal into the base band signal and limited the bandwidth of the signal. The bandwidth of output of the DDC is explained as 'Flt_{DDC}' (See Fig.3.9 and section 3.3.5). The DDC, GC4016 has the CIC filter whose decimation rate is controllable, and the FIR filter whose coefficient can be re-wrote. The sampling frequency of the input signal, f_0 and the decimation rate, N_D specifies the output rate f_S and the bandwidth Flt_{DDC}.
$$f_S = f_0 / N_D . \qquad (4.1)$$
In our system the configuration of the DDC was fixed except for the decimation of the CIC. *Flt* is the bandwidth of input signal of the negative chirp Gaussian filter, which is minimum bandwidth between RBW and Flt_{DDC}.
$$Flt = \min(RBW, Flt_{DDC}) \qquad (4.2)$$
Note) The detail of the DDC is shown in section 4.3.
4. The negative chirp Gaussian filter extracted the time when the frequency of the signal is 0 Hz. The bandwidth of the filter is *Rbw*, which is resolution bandwidth of the system as the spectrum analyzer. The coefficient of the negative chirp filter was calculated corresponding to the *Rbw* and σ, which is described in next section as Eq.(4.4).
5. $S_n(t)$ was a signal according with the spectrum as a convolution of the spectrum and resolution filter, Eq.(3.10), $|S_n(t)| = |F(\omega) * G(\omega)|$.

We assumed the experimental system to be a chain of the band-limit filters. The process of the band-limiting extracted the spectrum.

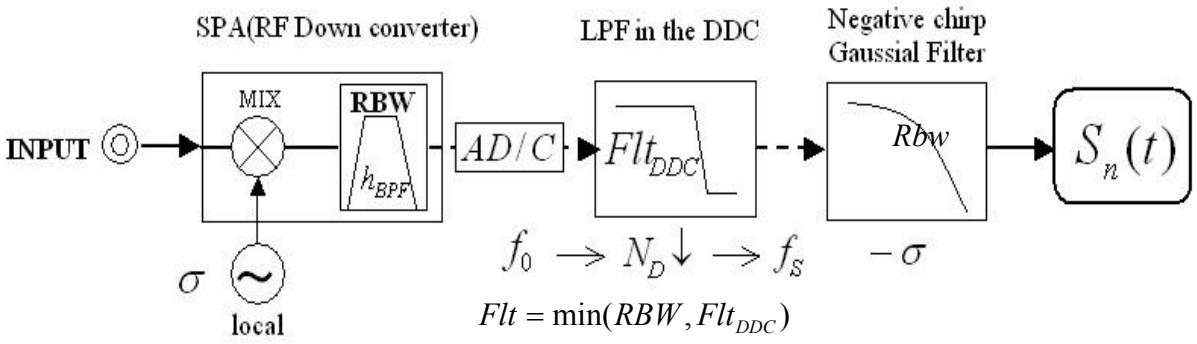

Fig.4.7 Chain of Band Limit Filters

4.2.5 Implementation of the Gaussian filter

The figure of the Gaussian filter (in dB scale) in frequency domain is shown in Fig.4.8. We designed the filter to have a dynamic range 100dB. The figure is a parabola and can be explained as

$$10\log(G(\omega)) = -a^2\omega^2 \qquad (4.3)$$

For the *Rbw* is 3dB down-bandwidth of the filter, the 100dB down-bandwidth is calculated as approximately 5.8 times as wider as the *Rbw*.

To achieve the high-speed sweep, the bandwidth of the input signal of the filter, the *Flt* have to be wider than the *Rbw*. The wider *Flt* is, the faster we can sweep. The sampling frequency of the input signal must be faster than the *Flt*. The configuration of the DDC specified the *Flt*.

The mathematical formula of the Gaussian filter is explain by Eq.(3.25).

$$g_n(t) = \exp\left[-\frac{(\pi \cdot Rbw)^2 t^2}{2\ln 2}\right] \times \exp[j(-\pi\sigma t^2)] \qquad (3.25)$$

The coefficients of $g_n(t)$ were computed with the discrete time as follows.

$$g_n[i] = \exp\left[-\frac{(\pi \cdot Rbw)^2}{2\ln 2}(i \times \Delta t)^2\right] \times \exp\left[-j\pi\sigma(i \times \Delta t)^2\right], \qquad (4.4)$$

where $i = -N_G/2, \cdots, 0, \cdots, N_G/2$ and $\Delta t = 1/f_S$. f_S is the sampling frequency of the input signal, which is given by Eq.(4.1). N_G was the sample (Tap) number, it was decided as

$$N_G = T_G \times f_S = \frac{\chi}{Rbw} \times f_S \ . \qquad (4.5)$$

T_G and χ were described in section 3.3.4.

Please note that Eq. (4.4) is independent of *Flt*.

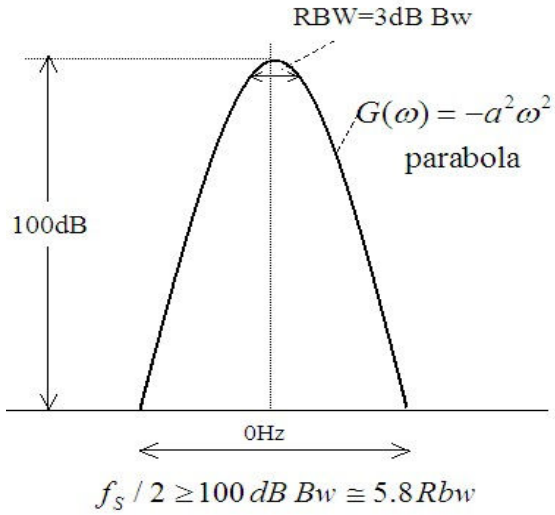

Fig.4.8 Figure of a Gauss filter (dB) and Minimum Sampling Rate

4.2.6 Sampling in the frequency domain

The example of discrete spectrum $S_n[i]$ is shown in Fig.4.9, and the mathematical formula is described in section 4.2.10. The abscissa indicates both frequency and time. Δf is the difference of the frequency between the sample. Δt is the period of the sampling as a time domain.

Δf is estimated by the following equation, which is modified from Eq(3.18).

$$\Delta f = \sigma \cdot \Delta t \qquad (4.6)$$

The two value, Δf and Δt are independent each other principally. We considered that Δf should be narrower than *Rbw/2* to keep the shape of the resolution filter.

$$\Delta f = \sigma \cdot \Delta t = \frac{\sigma}{f_S} \leq \frac{Rbw}{2} \qquad (4.7\text{-a})$$

This inequality can be modified as

$$\sigma \leq \frac{Rbw}{2} f_S \qquad (4.7\text{-b})$$

This inequality explains the relation among the three parameters. It needs higher sampling frequency to achieve faster sweep for same *Rbw*.

In the case that σ is slower than half of Eq.(4.7-b), we can decimate the spectrum data, and we can configure the Δf by choosing the adequate decimation rate.

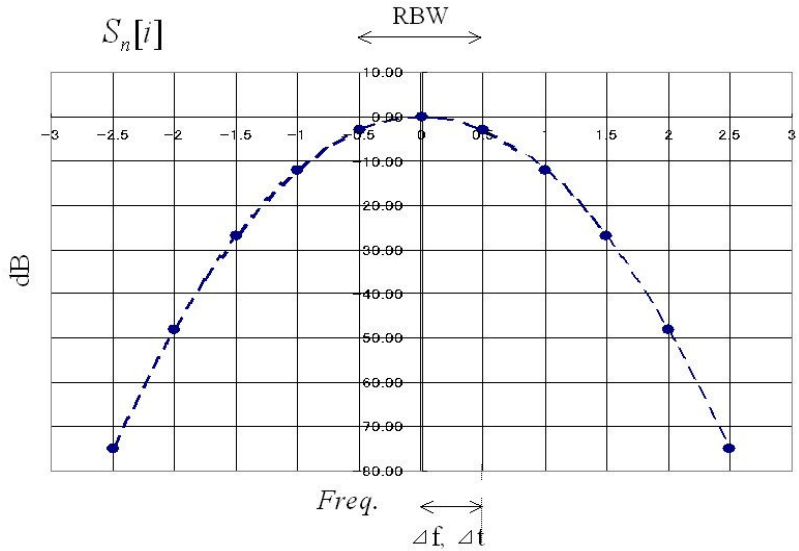

Fig.4.9 Sampling Rate of a spectrum data

4.2.7 Setting Up Parameters

This section describes the condition and parameters of our experiments. We made the system not only for experiment but also for practical use. The specification of the system is shown in section 4.4.

In the experimentation, the input-signal was a CW signal generated by a manufactured signal generator (SG), the frequency was 500 MHz and the power level was -10dBm.

The principal parameters are shown in Table 4.1. We made two configurations of the new method, '*S1'* and '*S2*'. The '*Cnv.*' is the configuration of the conventional method, the R3264 spectrum analyzer, for reference. In the case of *S1* and *S2*, the sampling frequency of the AD/C, f_0 was 80MHz, and the resolution bandwidth of the complex filter: *Rbw* was 300Hz. The *'RBW(SPA)'* was the RBW (resolution bandwidth) of R3264. And the Flt_{DDC} was the bandwidth of output signal of the DDC. The N_D was the total decimation rate of the DDC. f_S was the decimated sampling frequency, which was the input signal rate of the complex filter and was given by Eq.4.1. N_G was the sample (Tap) number of the negative chirp filter $g_n(t)$, it was decided by Eq.(4.4) with parameter χ and N_D as follows.

$$N_G = T_G \times f_S = \frac{\chi}{Rbw} \times \frac{80MHz}{N_D} \quad , \qquad (4.8)$$

where χ was 2.6.

And finally, R_S was defined by the following equation.

$$R_s \equiv \frac{\sigma_{\max\_S}}{\sigma_{\max}} = \frac{k_0}{\chi} \times \frac{Flt}{Rbw} \qquad (3.35)$$

We measured the input signal, and obtained the spectrums, which were averaged with over ten measurements. Then we obtained the peak level of the signals, and observed resolution bandwidth as '*Rbw*'', see Fig.2.19.

We obtained these data by changing the normalized sweep rate *1/k*, which was defined by Eq.(2.40) to compare with conventional method. In our experiment, the *1/k* were set as 0.1 to 75.0 as follows.

$$1/k = 0.1 \times 10^{n/8}, \qquad (4.9)$$

where '*n*' is an integer from 0 to 23, the all steps of *1/k* are shown in Table 4.2. For the given *1/k* we controlled the R3264 whose *Span* and the T_S (sweep time) was proper value, by referring to the Eq.(2.40).

Table 4.1 Principal parameters under the experiments

		Measurement configuration		
		Cnv	***S1***	***S2***
Parameter	*INPUT Frequency*	500MHz		
	INPUT Level	-10dBm		
	Rbw	300Hz		
	f_0	-	80MHz	
	RBW(SPA)	300Hz	1.0MHz	1.0MHz
	Flt(DDC)	-	2.44kHz	7.32kHz
	N_D	-	24756	8192
	f_S	-	3.255kHz	9.765kHz
	N_G	-	29	85
	χ	-	2.6	
	Flt/Rbw	-	8.1	24.4
	R_S	-	6.2	18.7

4.2.8 Coefficients of Negative Chirp Gaussianl Filters

The coefficient of the negative chirp filter is calculated by Eq.(4.4), where

$$\sigma = Span / T_S \quad \text{or} \quad \sigma = Rbw^2 \times (1/k). \qquad (4.10)$$

The coefficient of the Gaussian filter of *S1* and *S2* is shown in Fig.4.10-a and 4.10-b, where the σ were 4×10^5 (Hz/sec) and 1.33×10^6 (Hz/sec), respectively. There are three lines in each figure, the absolute value:$|g_n[i]|$, the real part: $\mathrm{Re}[g_n[i]]$, and the imaginary part: $\mathrm{Im}[g_n[i]]$. Each coefficient consists of two data array, $\mathrm{Re}[g_n[i]]$ and $\mathrm{Im}[g_n[i]]$.

The value of $|g_n[i]|$ does not change against *1/k*, but $\mathrm{Re}[g_n[i]]$ and $\mathrm{Im}[g_n[i]]$ have different value corresponding to *1/k*. We developed the system to calculate the value, $g_n[i]$ corresponding to *1/k* automatically. Figure 4.10-a and 4.10-b show the samples of these $g_n[i]$.

4.2.9 Span and Sweep time Corresponding to Plotted *1/k*

We made conditions of the system corresponding to the plotted 1/k, which is calculated by Eq.(4.9). Table 4.2 shows the important parameters of the measurement. These parameters were calculated by the following process.

①: Calculated the ideal 1/k using Eq.(4.9).
②: Decided the SPAN arbitrarily.
③: Estimated the rate, SPAN/RBW, which is decided to be under 3000.
（If this value was over 3000, it was difficult to observe the figure of the peak of a spectrum.）
④ Calculated the ideal sweep time T_S by modified Eq.(2.40).

$$T_{S\_ideal} = \frac{SPAN}{Rbw^2 \times (1/k)} \qquad (4.11)$$

⑤ Confirmed the sweep time of R3264. The significant figure of the value is only two.
⑥ Calculated the 1/k with the value ⑤.
⑦ Estimated the error of ⑥.

$$\delta(1/k) = 100\frac{⑥ - ①}{①} \ (\%) \qquad (4.12)$$

The maximum error of $\delta(1/k)$ was 4.1%. We considered this error is small enough for our experiment.

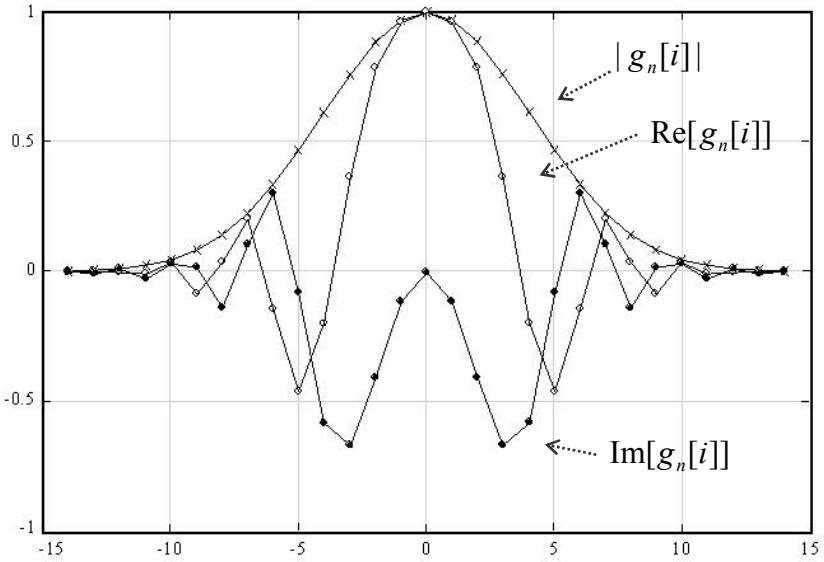

Fig.4.10-a Coefficients of the Gaussianl Filter of *S1*

$$\sigma = Span / T_S = 40 \cdot 10^3 / 0.1 = 4 \cdot 10^5$$

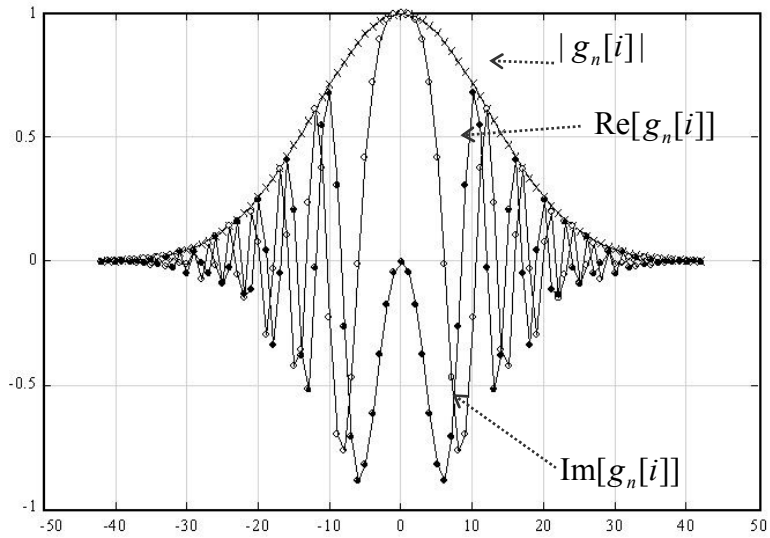

Fig.4.10-b Coefficient of the Gaussianl Filter of *S2*

$$\sigma = Span / T_S = 40 \cdot 10^3 / 0.03 = 1.33 \cdot 10^6$$

Table 4.2 Normalized sweep rate 1/k and the SPAN and Sweep time
RBW of all conditions are 300Hz

	①	②	③	④	⑤	⑥	⑦
n	1/k ideal	SPAN	SPAN/RBW	T_S ideal	T_S actual	1/k result	δ(1/k)%
0	0.1000	30000	100	3.3333	3.3	0.1010	1.01
1	0.1334	30000	100	2.4996	2.5	0.1333	−0.01
2	0.1778	30000	100	1.8745	1.9	0.1754	−1.34
3	0.2371	30000	100	1.4057	1.4	0.2381	0.40
4	0.3162	30000	100	1.0541	1.1	0.3030	−4.17
5	0.4217	30000	100	0.7905	0.79	0.4219	0.06
6	0.5623	30000	100	0.5928	0.59	0.5621	−0.04
7	0.7499	30000	100	0.4445	0.45	0.7491	−0.11
8	1.0000	30000	100	0.3333	0.33	1.0101	1.01
9	1.3335	30000	100	0.2500	0.25	1.3333	−0.01
10	1.7783	55300	100	0.3455	0.35	1.7556	−1.28
11	2.3714	100700	500	0.4718	0.47	2.3806	0.39
12	3.1623	150000	500	0.5270	0.53	3.1447	−0.56
13	4.2170	150000	500	0.3952	0.4	4.2194	0.06
14	5.6234	150000	500	0.2964	0.3	5.6306	0.13
15	7.4989	150000	500	0.2223	0.22	7.5075	0.11
16	10.0000	300000	2500	0.3333	0.33	10.1010	1.01
17	13.3352	300000	2500	0.2500	0.25	13.3333	−0.01
18	17.7828	300000	2500	0.1874	0.19	17.5439	−1.34
19	23.7137	450000	2500	0.2108	0.21	23.8095	0.40
20	31.6228	450000	2500	0.1581	0.16	31.2500	−1.18
21	42.1697	450000	2500	0.1186	0.12	42.0168	−0.36
22	56.2341	600000	2500	0.1186	0.12	56.0224	−0.38
23	74.9894	750000	2500	0.1111	0.11	75.0751	0.11

4.2.10 Discrete Integral to obtain a Spectrum

In the super sweep method, the spectrum was extracted by the algorithm of Eq.(3.2) or other equation in the section 3.22, such as

$$S_n(t) = g_n(t) * \{f(t) \times l(t)\}. \qquad (3.2)$$

Actually, in our experimentation, the integral is achieved by a discrete integral. The concept of the integral is shown in Fig.4.11. The discrete form of the $g_n(t)$ was presented by Eq.(4.4). In Figure 4.4, N_G is the tap number of $g_n(t)$, which was presented by Eq.(4.5). And $S_B(t)$ is the base band signal, which was a output of the DDC and explained by Eq.(3.12) and (3.13) or some other equation. At this stage, we operated the signal $S_B(t)$ as a discrete complex signal,

$$S_B[i] = I_b[i] + Q_b[i]. \qquad (4.13)$$

We defined N_B as the size of $S_B[i]$ at this stage which is shown in the upper side of Fig.4-11 as '$i = 0, N_B - 1$'. And it is corresponding to the product of the sampling rate f_S and the sweep time T_S,

$$N_B = T_S \times f_S, \qquad (4.14)$$

where f_S is defined by Eq.(4.1).

We obtained the spectrum as output of the discrete convolution of $S_B[i]$ and $g_n[i]$. The filter $g_n[i]$ has to be filled up by signal $S_B[i]$ to output the spectrum without the transitional response of the start and stop edge. Then, the size of the output was $N_B - N_G$, as shown in Fig.4.11. N_G is the tap number of $g_n[i]$ defined by Eq.(4.5).

Through the above considerations, the spectrum was explained by the next equation.

$$\begin{aligned} S_n[k_f] &= g_n[i] * S_b[i] \\ &= \sum_{i=0}^{N_G-1} g_n[i] \times \left\{ I\left[i + k_f + \frac{N_G}{2} \right] + jQ\left[i + k_f + \frac{N_G}{2} \right] \right\} \end{aligned} \qquad (4.15)$$

In Eq.(4.15), the parameter k_f corresponded to the frequency of each sample of $S_n[k_f]$. When the center frequency is f_{CF}, the frequency corresponding to k_f is given by,

$$f[k_f] = f_{CF} + \Delta f \times \left(k_f - \frac{N_B - N_G}{2} \right), \qquad (4.16)$$

where Δf is the difference of the frequency between each sample defined by Eq.(4.6) or (4.7), and $(N_B - N_G)/2$ was the sample number at the center.

We could obtain the spectrum discretely by the above two equations.

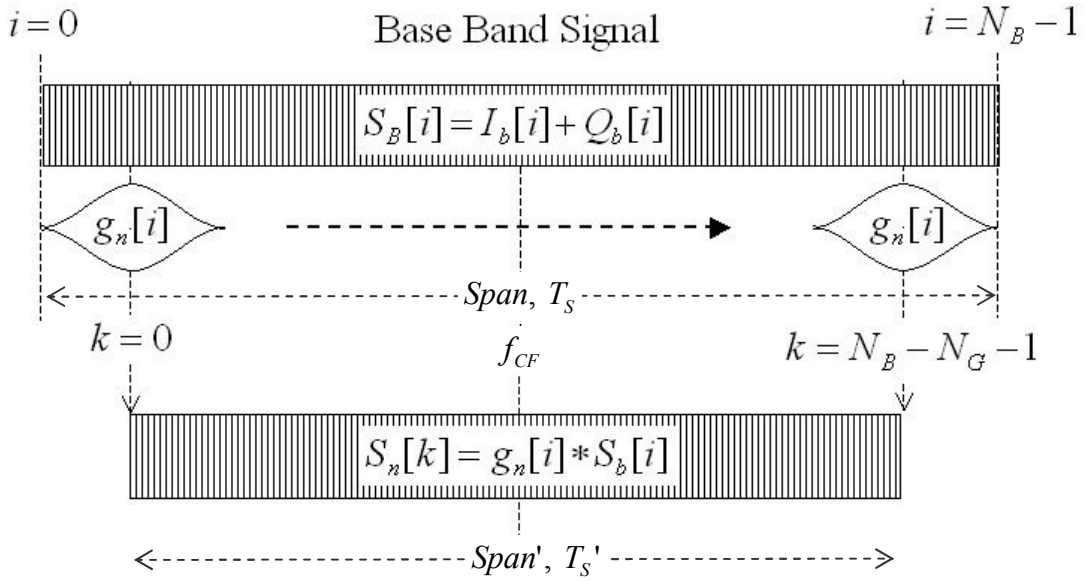

Fig.4.11 Discrete Integral to extract a Spectrum

4.3 Property and Configuration of DDC (GC4016)

The property and the configuration of the DDC that we employed in our experimental system are described in this section.

We employed GC4016 as the DDC supplied from Texas Instrument Inc. It was one of the most important devices in our system. Actually, we made the several conditions of measurement by changing the configuration of GC4016.

4.3.1 Outline of Digital Down Converter Channels

GC4016 has four down converter channels on a chip. The one channel is shown in Fig.4.12. The description of this chip is given in [7]. This section describes the essential function and our application on this chip as follows.

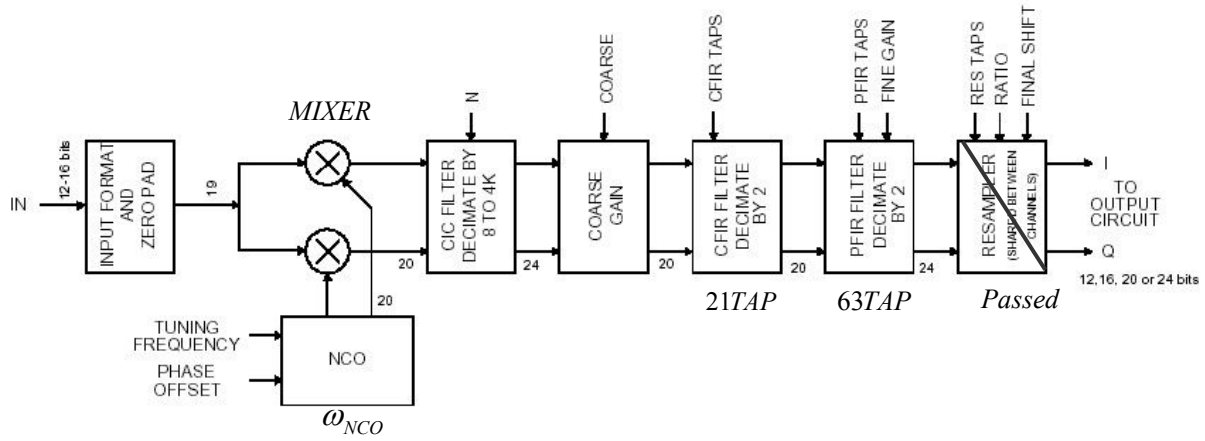

Fig.4.12 Down Converter Channels; from [7]

1. The input signal is band limited such as

$$f(t) = A(t) \cdot \exp[j\omega_{IF}t + \theta(t)], \qquad (4.17)$$

where *A(t)* is an amplitude, ω_{IF} is an IF frequency and $\theta(t)$ is a phase factor.

2. The NCO generates the signal $\cos(\omega_{NCO}t)$ and $\sin(\omega_{NCO}t)$ whose frequency is controllable. We tuned the frequency as $\omega_{NCO} = \omega_{IF}$.

3. The two mixers generates the signal as follows.

$$f_{mix\_out}(t) = A(t) \cdot \exp[j(\omega_{IF} \pm \omega_{IF})t + \theta(t)] \qquad (4.18)$$

There are two frequency factors, $2\omega_{IF}$ and zero. The three stages of filters reject the factor '$2\omega_{IF}$' and pass the factor 'zero' frequency (base band).

4. The CIC filter of GC4016 can decimate by arbitrary rate from 8 to 4096. But the pass band has a significant ripple.
5. The CIC filter has a gain that is adjusted coarsely by the 'COARSE GAIN' stage. It is usually set by [7]

$$COARSE\,GAIN = \sqrt{N} \qquad (4.19)$$

where N is the decimation rate of the CIC.

6. The CFIR filter is a FIR filter of 21TAP whose coefficient is programmable. The pass band of CIC is not flat, which is equalized by the CFIR filter. The decimation rate of CFIR is two unchangeably.
7. The PFIR filter is a FIR filter of 63 TAP whose coefficient is programmable. The decimation rate of PFIR is two which is unchangeable.
8. We did not use the 'RESAMPLER' stage.

4.3.2 CIC Filter

A CIC (Cascade In Comb) filter is a kind of digital filter whose function is both decimation and interpolation. The description about a CIC filter was presented by Hogenauer [9]. The structure of the CIC filter in GC4016 is shown in Fig.4.13. Essentially, the CIC filter is constructed with an addition and a division. The division is realized by a bit-shifter. The frequency response of the CIC filter has many side lobes, which are called 'comb'. The sample of the response referred from [8] is shown in Fig.4.14. The abscissa of Fig.4.14 is a relative frequency with the sampling frequency (after a decimation) which is corresponding to one. The response has null zone around the frequency which is a multiple of the sampling frequency. After the decimation, these null points will move around the zero frequency by an aliasing (imaging). And the area around zero frequency can escape the disturbance of an imaging noise. The CIC filter of GC4016 can decimate by arbitrary rate from 8 to 4096.

An example of the frequency response of a CIC filter around zero frequency is shown in Fig.4.15. Usually, the response has some possibility to have aliasing noise on the side of Nyquist frequency ($\pi = f_S / 2$). The filters on the next stage reject the aliasing noise, which is shown as 'Frequency Response of FIR' in the figure.

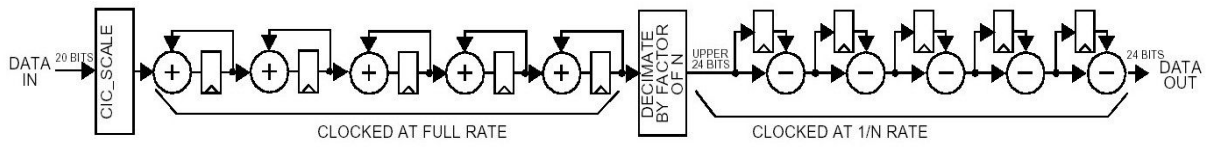

Fig.4.13 CIC Decimation Filter [8]

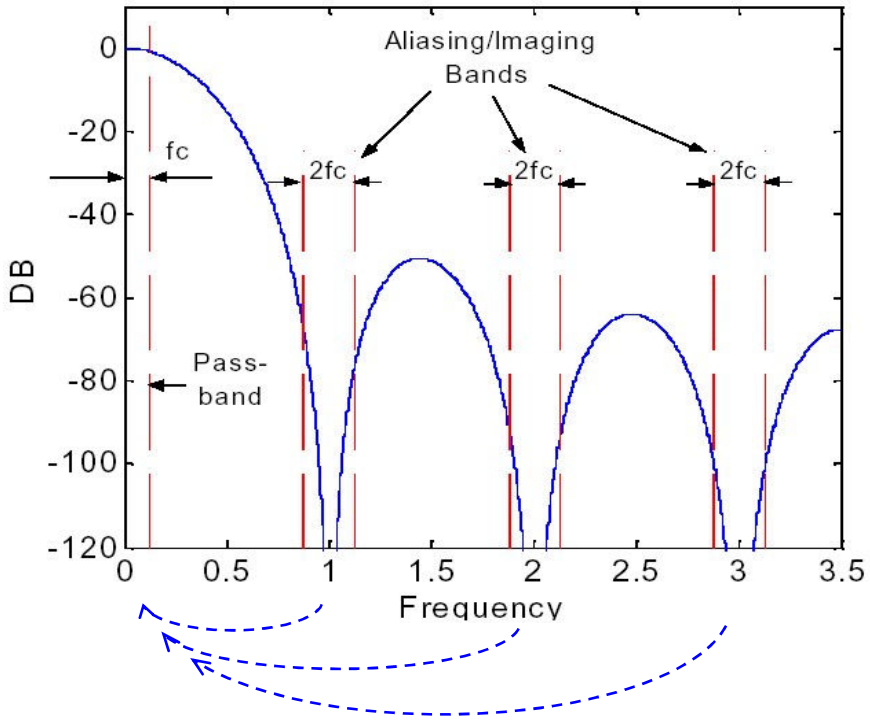

Fig.4.14 CIC Filter Frequency Response for N=4,M=1,R=7 and fc=1/8 [8]

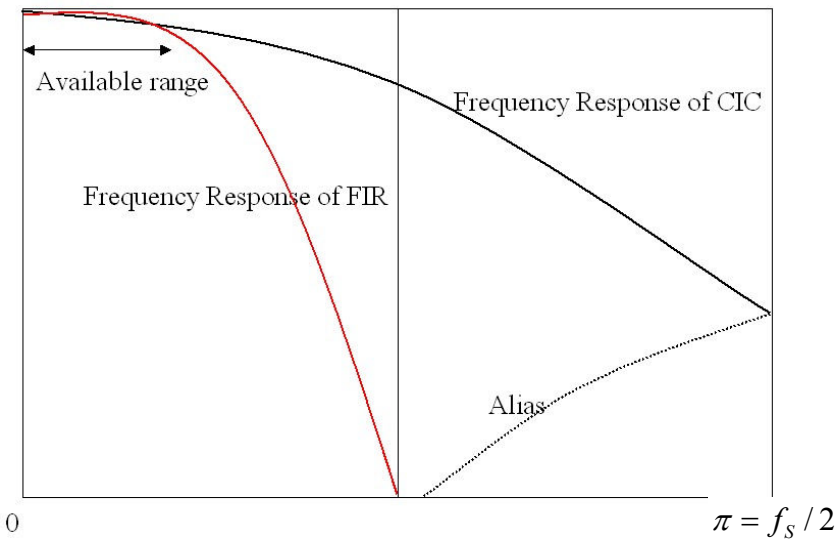

Fig.4.15 Frequency Response of CIC Filter around zero frequency [8]

4.3.3 Distribution Arithmetic (DA) method FIR Filter

The algorithm of the FIR filter is a product sum, which is illustrated in Fig.4.16. If we designed the FIR filter by this figure, it had many multipliers and the size of the circuit became very large. The GC4016 or other DDC, actually, employs another method. It is called "Distribution Arithmetic", which is shown in Fig.4.17. It uses a look up table to operate the product sum instead of the many multipliers. The description about the Distribution Arithmetic method is written in [10] and [11].

This method has almost no time to process a product sum, but it has tiny latency. The latency of the PFIR (63tap) filter of GC4016 is corresponding to 63-clock of the PFIR's input signal.

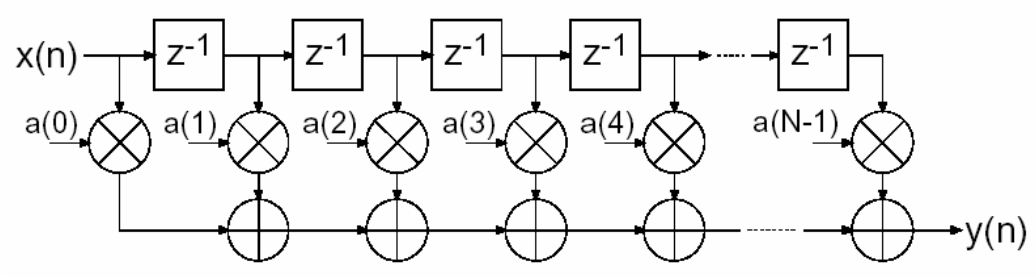

Fig.4.16 Illustrated algorithm of an FIR filter [8]

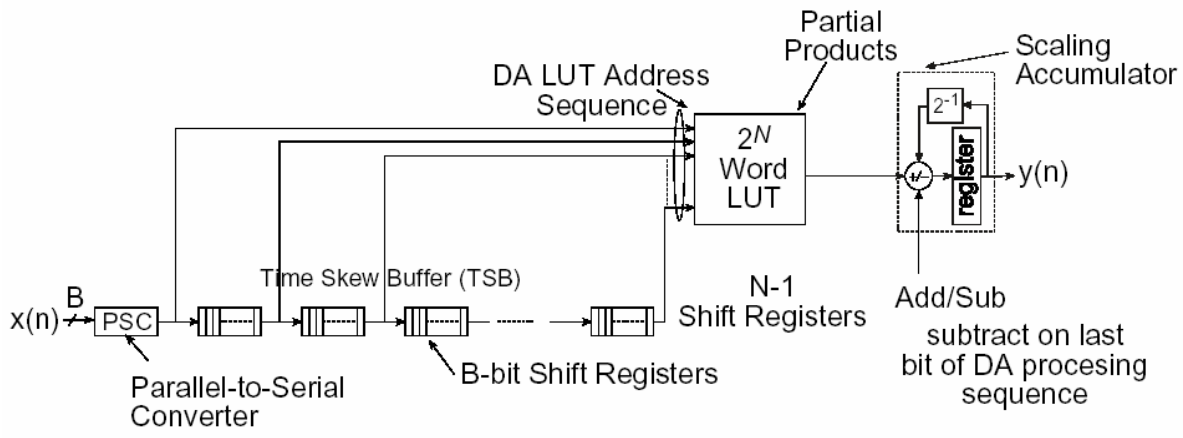

Fig.4.17 Concept of an FIR filter in DA method [8]

4.3.4 Apportionment of Decimation (--の配分)

The apportionment of the decimation in the DDC channel is described in this section.

GC4016 achieves the decimation by the three filters, CIC, CFIR and PFIR. The decimation rate of the two FIR filters is two which is unchangeable. We controlled the total decimation rate of GC4016 by the rate of CIC. The decimation rates of each stage in the mode ***S1*** and ***S2*** in Table 4.1 are given in Table 4.3. In the mode ***S1***, we added a decimation stage in the software of the DSP, which was done by a fir filter of 27 TAP.

We were able to control the bandwidth of the output signal by changing the decimation rate of the DDC.

Table 4.3 Apportionment of Decimation

		Mode	
		S1	S2
Stage	CIC	3072	2048
	CFIR	2	2
	PFIR	2	2
	DDC total	12288	8192
	DSP	2	1
	Total (N_D)	24576	8192

4.3.5 Coefficients of FIR filters

The coefficients of the CFIR and the PFIR, which are implemented by us, are shown in Table 4.4 and 4-5, and Figure 4.18 and 19 shows them graphically. These coefficients, ‘cfir_68’ and ‘pfir_68’ are supplied by Texas Instruments Inc., and are given in the data sheet [7].

The set of ‘cfir_68’ and ‘pfir_68’, in the data sheet, provided the frequency response which is shown in Fig.4.20. The pass bandwidth of this set of filters was 68% of the output sample rate of the DDC channel [7]. And the 3dB bandwidth was 75% experimentally. The *Flt* of Table 4.1 are 75% of f_S.

This filter set is used not only for ***S1*** and ***S2*** but also for the rest of conditions in the experimental system.

Table 4.4 Coefficients of the CFPR filter 'cfir_68' (21TAP) from [7]

i	CFIR[i]
−10	12
−9	−93
−8	−62
−7	804
−6	1283
−5	−1273
−4	−5197
−3	−3512
−2	8332
−1	24823

i	CFIR[i]
0	32767
1	24823
2	8332
3	−3512
4	−5197
5	−1273
6	1283
7	804
8	−62
9	−93
10	12

Table 4.5 The Coefficient of the PFPR filter 'pfir_68' (63TAP) from [7]

i	PFIR[i]
−31	2
−30	1
−29	−11
−28	−23
−27	−2
−26	45
−25	43
−24	−48
−23	−117
−22	−8
−21	191
−20	155
−19	−189
−18	−375
−17	26
−16	579

i	PFIR[i]
−15	358
−14	−601
−13	−918
−12	248
−11	1469
−10	618
−9	−1680
−8	−1995
−7	1104
−6	3690
−5	845
−4	−5354
−3	−5506
−2	6574
−1	24277

i	PFIR[i]
0	32767
1	24277
2	6574
3	−5506
4	−5354
5	845
6	3690
7	1104
8	−1995
9	−1680
10	618
11	1469
12	248
13	−918
14	−601
15	358

i	PFIR[i]
16	579
17	26
18	−375
19	−189
20	155
21	191
22	−8
23	−117
24	−48
25	43
26	45
27	−2
28	−23
29	−11
30	1
31	2

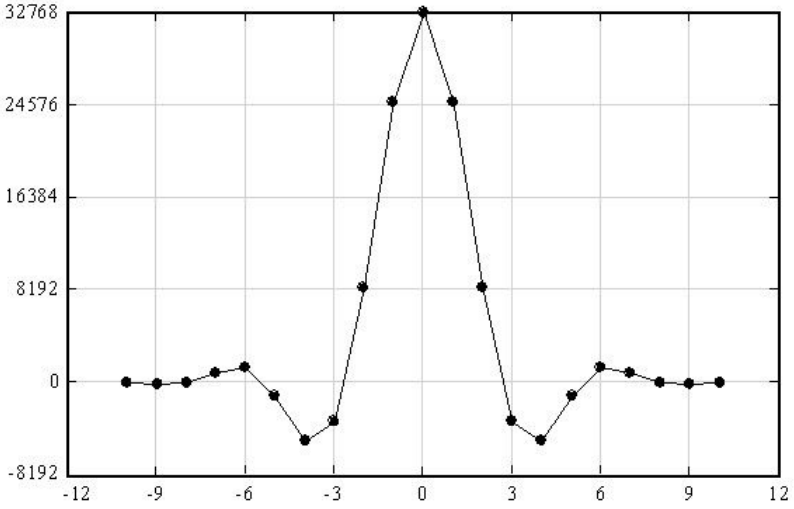

Fig.4.18 Figure of 'cfir_68' (21TAP) from[7]

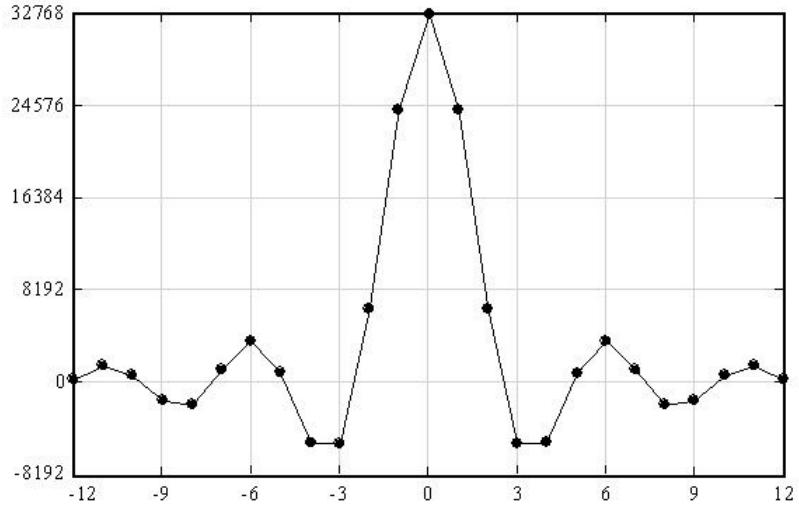

Fig.4.19 Figure of 'pfir_68' (63TAP) from[7]

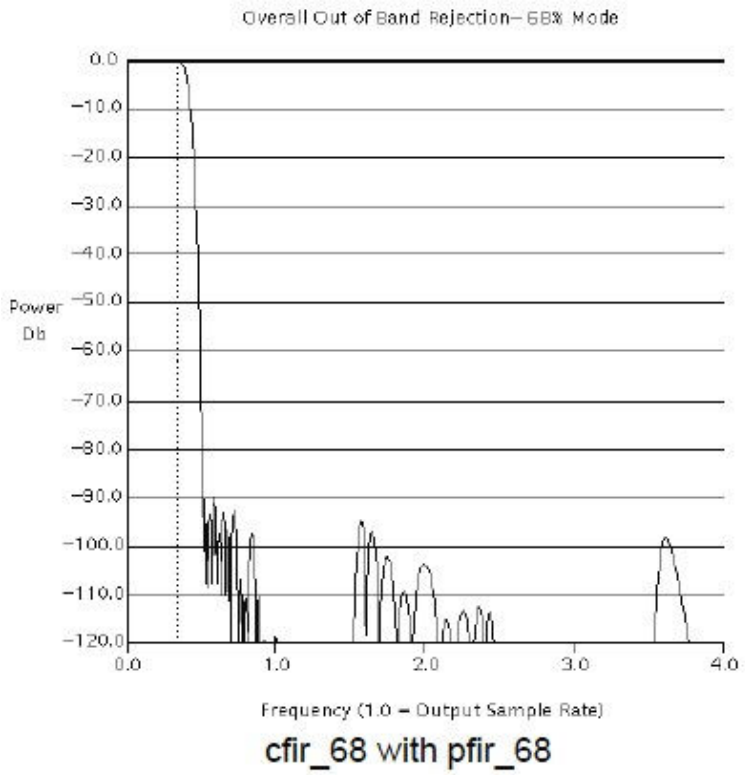

Fig.4.20　Frequency response of CFIR with PFPR：　from[7]

4.4 Specification of the experimental system

The rearranged essential parameters of our experimental system are given in Tables 4.6. Other specifications as a spectrum analyzer are dependent on the employed spectrum analyzer, R3264.

Table 4.6 Primary specification of the experimental system

Input of DSP Unit

IF	21.4MHz, 50Ω, BNC
Reference Clock	10MHz, 50Ω, BNC
SWP	-5~5V, 1kΩ, BNC (adjustable)

Frequency

Frequency range	Dependent on the attached spectrum analyzer
Maximum frequency Span	Dependent on the attached spectrum analyzer
Resolution bandwidth	1Hz ~ 100kHz, Digital Gaussian

Level

Display range	10~150dB, 10,5,2,1dB/div
Maximum Dynamic Rage	130dB (at RBW=1Hz)

Output/Interface of the DSP Unit

USB 2.0	Spectrum data with specialized format

Hard ware of the DSP Unit

AD/C	ADS6645S (Analog devices), Driven by 80MHz
DDC	GC4016 (Texas Instruments) ,Driven by 80MHz
DSP	TMS6711, Driven by 80MHz

2007.02.02, 2007.04.08, 5.08, 10.07

4.5 Summary

It needed a complicated system to achieve the super sweep method, which was described in this chapter. We employed the conventional sweep spectrum analyzer as a RF down converter. We developed the DSP unit included in the digital signal processing system that had an A/DC, a DDC and a DSP. We achieved the super sweep method in the DSP unit. The algorithm of the super sweep method was achieved on the DDC and the DSP. There were so many parameters that were concerned in the system, and they should be harmonized each other to achieve the super sweep method. This chapter described the samples of the parameters. We took the parameter 1/k to estimate the new method. We intended to estimated the over sweep-rate response against the 1/k. The result is given in Chapter 5.

4.6 Reference

[1] E.Oran Brigham, “The Fast Fourier Transform”, Prentice-Hall,Inc.,1974

[2] Morris Engelson “Spectrum Analyzer Theory and Applications” Artech House publishers Oct. 1974

[3] Masao Nagano “Signal Processing of Sweep Spectrum Analyzer” S^2PATJ vol.3, No.4 Dec. 2000 pp.17-24

[4] George D. Tsakiris “Resolution of a spectrum analyzer under dynamic operations” Rev. Sci. Instrum., Vol.48, No.11, Nov. 1977 pp.1414-1419

[5] Masao Nagano “Spectrum Analyzer of Super Sweep IF Filter” S^2PATJ vol.4, No.2, June 2001 pp23-30

[6] F.J.Harris,”On the Use of Windows for Harmonic Analysis with the Discrete Fourier Transform”, proceeding of the IEEE, Vol.66, No.1, JAN. 1978

[7] Texas Instruments Inc. “GC4016 MULTI-STANDARD QUAD DDC CHIP DATA SHEET REV 1.0”, SLWS133A, August 27, 2001, Dallas, Texas 75265

[8] Xilinx, Inc. “Cascaded Integrator-Comb (CIC) Filter V3.0”, March 14, 2002

[9] E.B.Hogenauer,”An Economical Class of Digital Filters for Decimation and Interpolation”, IEEE. Trans. Acoust.,Speech Signal Processing,Vol.29,No.1,pp.155-162 April 1981

[10] Peled and B. Liu, "A New Hardware Realization of Digital Filters", IEEE Trans. on Acoust., Speech, Signal Processing, vol. ASSP-22, pp. 456-462, Dec. 1974.

[11] S. A. White, ``Applications of Distributed Arithmetic to Digital Signal Processing", IEEE ASSP Magazine, Vol. 6(3), pp. 4-19, July 1989.

4.7 Appendix: Latency:

GC4016 has a value of latency with filter: CIC, CFIR, and PFIR. Each value of latency is given in the following table.

Filter	Latency ; clocks (N is the CIC decimation)
CIC	2.5N
CFIR	0.5N×Ctap
PFIR	N×Ptap
Total	N×(2.5+0.5Ctap+Ptap)
Our system	76×(N=8~3600)=7.6 μ sec~3.89msec

Chapter 5

Result and Discussion

5.1 Introduction

This section reported the result of our experiment and verified the theory of the super sweep method. The experiment was achieved by measuring the peak level and observed resolution bandwidth (Rbw') against the normalized sweep rate *1/k*, which is plotted from 0.1 to 75. We estimated the spectrum as two parameters, one was the peak level reduction and another was the broadening of the RBW. Section 5.2 shows the over view of the measured spectrum of the new method and the way to estimate the spectrum. Section 5.3 describes the result of the experiment as the peak level reduction and the broadening of the RBW. Section 5.4 discussed the result and analyzed the result.

5.2 Measured Spectrums

5.2.1 Sample of measurements

The results of spectrums corresponding to the condition that was described in section 4.2.7~4.2.9 is shown in Fig.5.1 (a) and 5.1 (b). We measured the CW signal, which was generated by a manufactured signal generator (SG), whose frequency was 500MHz, and the level was –10dBm, by changing the sweep rate *1/k* from 0.1 to 74.0 with 24 steps. Figure 5.1 (a) and 5.1 (b) were the results of that *1/k* were 0.562, 5.62 and 56.2 and the *Span* was 30kHz, 150kHz and 600kHz.

The spectrums in Fig.5.1 (a) were measured by conventional sweep spectrum analyzer, R3264. The peaks of the spectrum of *1/k*=5.62 and *1/k*=56.2 had large level reduction and frequency shift. These phenomenons were called 'over sweep-rate response' (see section 2.5.2). The spectrums in Fig.5.1 (b) were samples measured by the conditions of ***S1*** and ***S2*** (described in section 4.2.7), where the over sweep-rate response were shown in the spectrums of *1/k*=56.2.

The noise floor of Fig.5.1 (b) were higher than them of Fig.5.1 (a), this problem was finally resolved and will be discussed in Chapter 6.

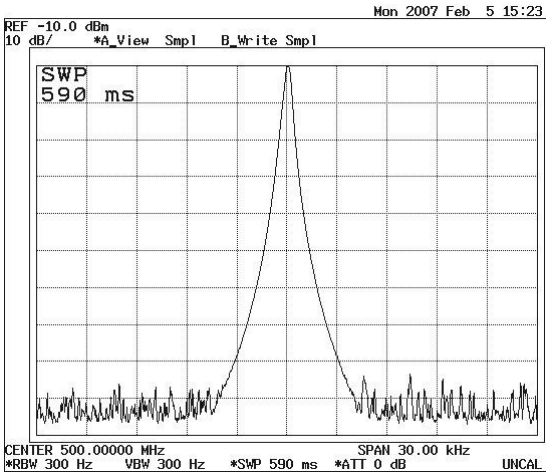

1/k=0.562
SPAN=30kHz
St=590msec
RBW300Hz

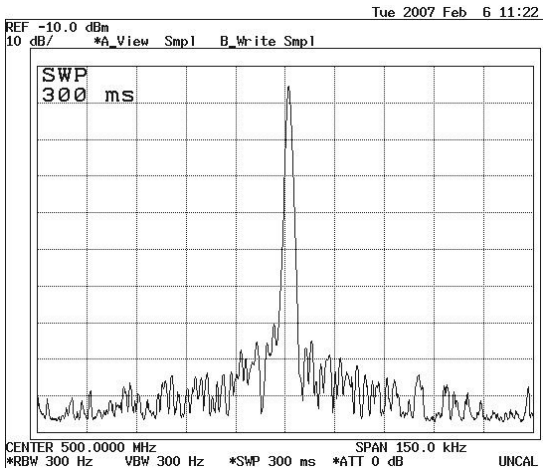

1/k=5.62
SPAN=150kHz
St=300msec
RBW300Hz

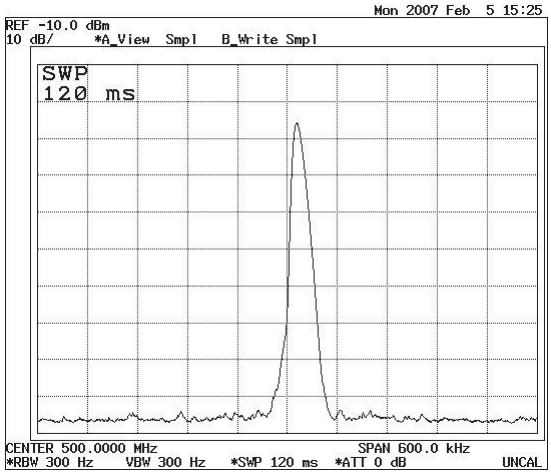

1/k=56.2
SPAN=600kHz
St=120msec
RBW300Hz

Figure 5.1 (a) Spectrums with various *1/k* of sweep method

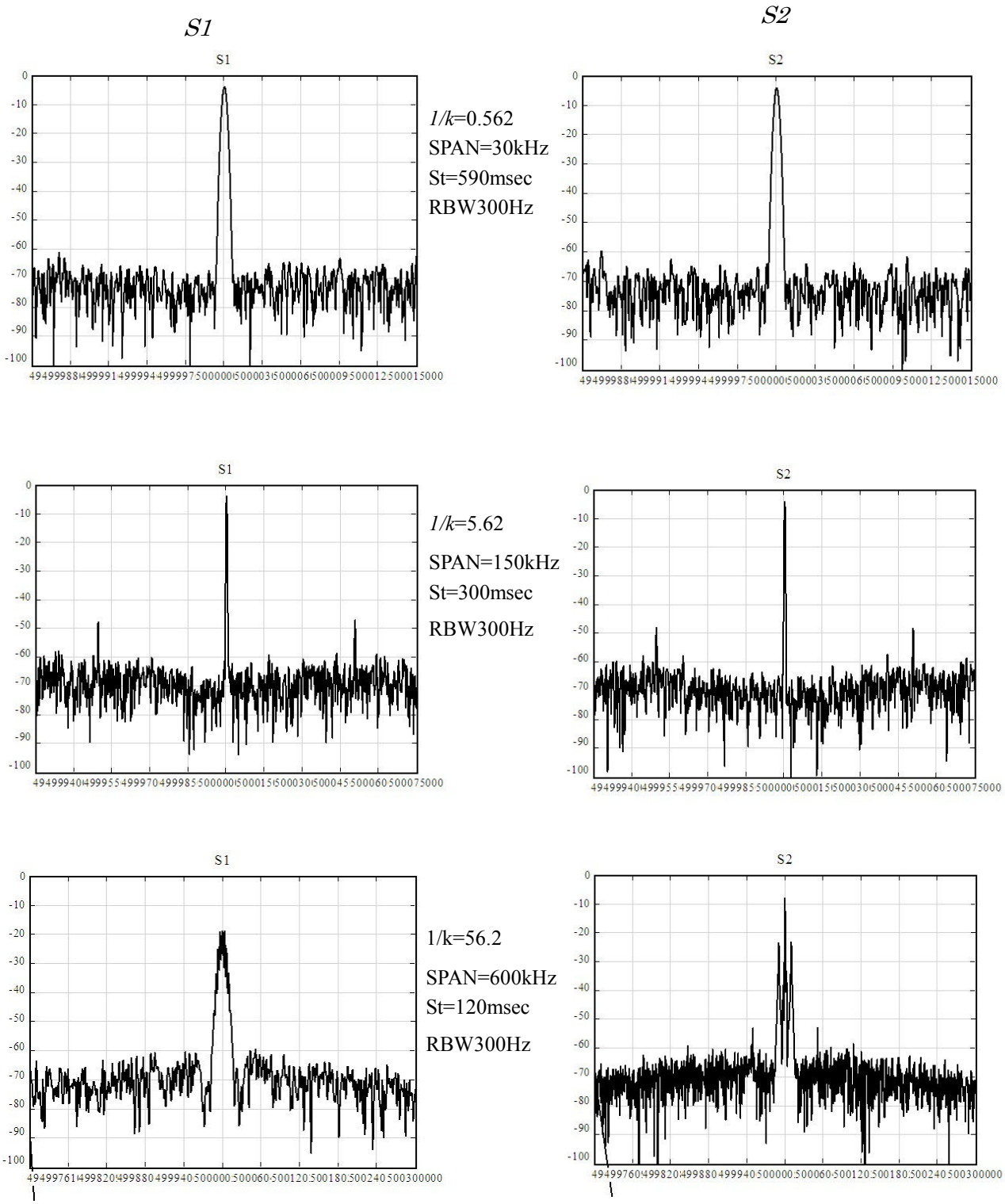

Figure 5.1 (b) Spectrums with various *1/k* of Super Sweep method

5.2.2 Verification of Over sweep-rate response

Generally, the over sweep-rate response is estimated as a peak level reduction and the broadening of the resolution bandwidth. These response are explained by following equation (see section 2.5.2).

$$\frac{A'}{A} = \left\{ 1 + \left(\frac{2}{\pi} \ln 2 \right)^2 \left(\frac{1}{k} \right)^2 \right\}^{-\frac{1}{4}} \qquad (2.41)$$

$$\frac{Rbw'}{Rbw} = \left\{ 1 + \left(\frac{2}{\pi} \ln 2 \right)^2 \left(\frac{1}{k} \right)^2 \right\}^{\frac{1}{2}} \qquad (2.42)$$

We did not take the peak shift as a subject, which is forecasted and corrected in the super sweep method.

We took the amplitude 'A' as a peak level, and '*Rbw*' as an indicated 3dB bandwidth of the peak when *1/k*=0.1, respectively. The indicated amplitude 'A'' was the peak level of the each measurement, simply. The indicated resolution bandwidth 'Rbw'' is estimated by the method described in next section.

5.2.3 Estimation of 3dB bandwidth of peaks

We conceived the way to estimate the observed 3dB bandwidth, *Rbw'*, which is described in this section.

1. The condition

We assumed that the figure of the peak was a parabolic corresponding to the Gauss function as the resolution filter. And we assumed that we could estimate the quadric function when we got level and frequency value of three points.

We took the difference of level between peak and other point as 2~10dB. It was better to take the distance larger to reduce the error of result.

2. The equation

We defined the coordinates of the three points around a peak as shown in Fig.5.2. The coordinate of the peak, the left side point of the peak, and the right side are (x_0, y_0), (x_{-1}, y_{-1}) and (x_1, y_1), respectively. '*x*' and '*y*' corresponds to the frequency (Hz) and the level (dB), respectively.

The quadric function corresponding to the three points is assumed

$$y = ax^2 + bx + c. \qquad (5.1)$$

The three points are explained by

$$\left.\begin{aligned} y_{-1} &= ax_{-1}^{\ 2} + bx_{-1} + c \\ y_0 &= ax_0^{\ 2} + bx_0 + c \\ y_1 &= ax_1^{\ 2} + bx_1 + c\,. \end{aligned}\right\} \qquad (5.2)$$

Following matrix explains these equations.

$$\begin{pmatrix} y_{-1} \\ y_0 \\ y_1 \end{pmatrix} = \begin{pmatrix} x_{-1}^{\ 2} & x_{-1} & 1 \\ x_0^{\ 2} & x_0 & 1 \\ x_1^{\ 2} & x_1 & 1 \end{pmatrix} \begin{pmatrix} a \\ b \\ c \end{pmatrix} \qquad (5.3)$$

Equation (5.3) is modified as

$$\begin{pmatrix} a \\ b \\ c \end{pmatrix} = \begin{pmatrix} x_{-1}^{\ 2} & x_{-1} & 1 \\ x_0^{\ 2} & x_0 & 1 \\ x_1^{\ 2} & x_1 & 1 \end{pmatrix}^{-1} \begin{pmatrix} y_{-1} \\ y_0 \\ y_1 \end{pmatrix} \qquad (5.4)$$

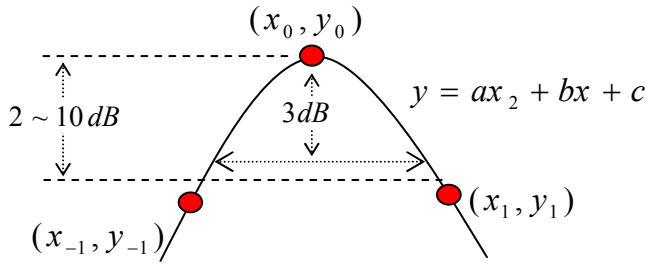

Fig.5.2 Three point data that decide the 3dB bandwidth, *Rbw*'

We can estimate *a*, *b* and *c* uniformly by Eq.(5.4). The three points can be selected arbitrarily, theoretically.

Equation (5.4) needs much complicated calculation. In the case that (x_0, y_0) is the peak, we can assume (x_0, y_0) =(0,0), and another two points assume relative coordinate as follows.

$$x_{-1} = x_{-1} - x_0$$
$$y_{-1} = y_{-1} - y_0$$

$$x_1 = x_1 - x_0$$
$$y_1 = y_1 - y_0$$

Then, Eq.(5.2) is modified

$$\left.\begin{aligned} y_{-1} &= ax_{-1}^{\ 2} + bx_{-1} \\ y_1 &= ax_1^{\ 2} + bx_1 \end{aligned}\right\} \qquad (5.5)$$

From Eq.(5.5), *a* and *b* is solved,

$$a = \frac{y_1 x_{-1} - x_1 y_{-1}}{x_1 x_{-1}(x_1 - x_{-1})} \qquad (5.6)$$

$$b = \frac{y_{-1} - ax_{-1}^{\ 2}}{x_{-1}} \qquad (5.7)$$

The quadric function whose peak is origin point (0,0), which is explained

$$y = ax^2 \qquad (5.8)$$

3. The observed resolution bandwidth, *Rbw'*

In the case that the unit of *y* is dB, the *y* value of the 3dB down point from the peak is –3, and Eq.(5.8) is modified that $-3 = ax^2$. Then the *x* value is given by

$$x = \sqrt{\frac{-3}{a}} . \qquad (5.9)$$

The 3dB bandwidth is twice of Eq.(5.9).

$$Rbw' \equiv 3dB\_BW = 2\sqrt{\frac{-3}{a}} \qquad (5.10)$$

The observed resolution bandwidth *Rbw*' is dependent on '*a*', which is estimated by Eq.(5.6).

5.2.4 Estimation of peak Level

The spectrum obtained by digital signal processing such as the FFT method has a scallop loss of the peak level as described in section 2.8.3. The super sweep method cased same loss on the spectrum. We assumed it was a not exact peak level to measure maximum level simply.

We conceived the way to estimate the peak level of the spectrum from the three points around the maximum level sample, which is described in this section.

We defined the coordinates of the three points around a peak as shown in Fig.5.3. We took tha three points whose differences of x value were same. And the coordinate of the three points were same to section 5.2.3, but x_{-1}, x_0, x_1 were assumed it –1, 0, and 1. The quadric function was assumes as $y = ax^2 + bx + c$, similarly to last section.

The coordinates give following three equations.

$$\left.\begin{aligned} y_{-1} &= a - bx + c \\ y_0 &= c \\ y_1 &= a + bx + c \end{aligned}\right\} \qquad (5.11)$$

Equation (5.11) give *a, b*, and *c* as follows.

$$\left.\begin{aligned} a &= \tfrac{1}{2}y_1 - y_0 + \tfrac{1}{2}y_1 \\ b &= \tfrac{1}{2}y_1 - \tfrac{1}{2}y_1 \\ c &= y_0 \end{aligned}\right\} \qquad (5.12)$$

By the way, the differential at the peak point is zero that gave following equation.

$$0 = 2ax_P + b\,. \qquad (5.13)$$

Then the x value of the peak point x_P is given by

$$x_P = \frac{-b}{2a} \qquad (5.14)$$

And the y value of the peak y_P is given by replacing the *a*, *b*, and *c* with Eq.(5.11) as

$$y_P = -\frac{b^2}{4a} + c \qquad (5.15)$$

We estimated the peak level by Eq.(5.15), which is independent on the *x* value.

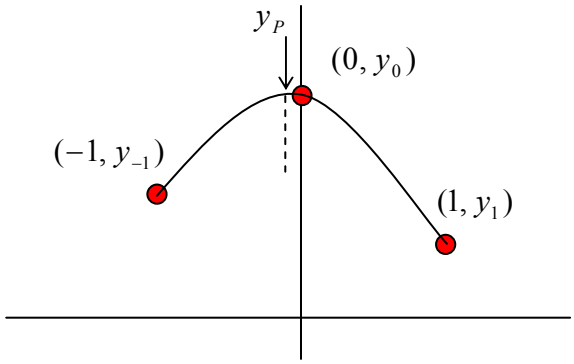

Fig.5.3 Three points around the peak

2007.5.08, 2007.09.16

5.3 Result

5.3.1 Numerical result

Table 5.1, 5.2, and 5.3 show the numerical results of the condition *S1, S2,* and conventional spectrum analyzer (*Cnv*) R3264, respectively. These conditions are described in section 4.2. The normalized sweep rate *1/k* : *Span* per Sweep time of each row is according with Table 4.2.

Table 5.1,5.2, and 5.3 show the frequency and level of the three points, Peak (x_0, y_0), L (x_{-1}, y_{-1}), R (x_1, y_1) and the indicated resolution bandwidth, *Rbw'*, which were calculated by Eq.(5.10). The normalized peak value shown in the column 'Peak (x_0, y_0) : Nmlzd dB' is difference of the level of *n=0* in dB unit. The normalized *Rbw'* shown in the column, '*Rbw':* Nmlzd', is the ratio of each value and it of *n=0*.

Table 5.1 Results of *S1*

(The unit of frequency is Hz and level is dB)

n	1/k	Peak (x_0, y_0)			L (x_{-1}, y_{-1})		R (x_1, y_1)		*Rbw'* (Hz)	
		Freq.(Hz)	Level (dBm)	Nmlzd (dB)	Freq (Hz)	Level (dBm)	Freq (Hz)	Level (dBm)	RBW'	Nmlzd
0	0.100	799999895	−12.36	0	799990709	−21.63	799991187	−21.86	270.3	1.00
1	0.133	799999897	−12.36	0	799990711	−21.66	799991190	−21.69	271.8	1.01
2	0.178	799999900	−12.36	0	799990705	−22.34	799991222	−24.25	271.1	1.00
3	0.237	799999902	−12.36	0	799990709	−21.96	799991196	−22.25	270.2	1.00
4	0.316	799999903	−12.36	0	799990709	−21.88	799991195	−22.15	270.9	1.00
5	0.422	799999906	−12.36	0	799990708	−22.19	799991194	−22.15	268.8	0.99
6	0.562	799999911	−12.36	0	799990708	−22.18	799991194	−22.02	269.7	1.00
7	0.750	799999914	−12.36	0	799990707	−22.08	799991193	−22.03	270.3	1.00
8	1.000	799999922	−12.35	0.01	799990716	−21.6	799991194	−21.48	273.1	1.01
9	1.33	799999931	−12.35	0.01	799990716	−21.72	799991202	−21.86	274.0	1.01
10	1.78	800000023	−12.39	−0.03	799990810	−21.69	799991286	−21.82	269.4	1.00
11	2.37	800000188	−12.39	−0.03	799990950	−20.45	799991396	−20.11	275.0	1.02
12	3.16	800000360	−12.38	−0.02	799991117	−21.36	799991584	−21.51	268.6	0.99
13	4.22	800000392	−12.38	−0.02	799991128	−21.26	799991594	−21.65	267.9	0.99
14	5.62	800000423	−12.42	−0.06	799991138	−21.18	799991604	−21.33	271.5	1.00
15	7.50	800000470	−12.55	−0.19	799991206	−17.55	799991571	−17.7	280.5	1.04
16	10	800001009	−12.49	−0.13	799991654	−18.01	799992014	−17.81	267.8	0.99
17	13.3	800001098	−14.37	−2.01	799991706	−18.07	799992022	−17.35	299.1	1.11
18	17.8	800001218	−15.93	−3.57	799991765	−17.92	799992022	−17.81	320.0	1.18
19	23.7	800001856	−18.42	−6.06	799992172	−20.93	799992641	−20.6	522.0	1.93
20	31.6	800002045	−20.32	−7.96	799992220	−23.03	799992756	−23.26	550.7	2.04
21	42.2	800002356	−22.89	−10.53	799992212	−25.19	799992966	−25.45	833.3	3.08
22	56.2	800003341	−25.42	−13.06	799992901	−27.37	799993639	−27.97	852.2	3.15
23	75.0	800004629	−28.07	−15.71	799993824	−29.77	799996857	−30.56	3631.1	13.44

Table 5.2 Results of *S2*

n	1/k	Peak (x_0, y_0)			L (x_{-1}, y_{-1})		R (x_1, y_1)		*Rbw'* (Hz)	
		Freq.(Hz)	Level (dBm)	Nmlzd (dB)	Freq (Hz)	Level (dBm)	Freq (Hz)	Level (dBm)	RBW'	Nmlzd
0	0.100	799991657	−12.61		799991377	−24.99	799991922	−23.99	273.9	1.00
1	0.133	799991656	−12.61	0	799991400	−23.18	799991907	−22.8	272.6	1.00
2	0.178	799991658	−12.61	0	799991382	−24.84	799991913	−23.24	272.2	0.99
3	0.237	799991656	−12.61	0	799991384	−24.76	799991928	−24.5	271.8	0.99
4	0.316	799991657	−12.61	0	799991385	−24.64	799991929	−24.43	272.9	1.00
5	0.422	799991658	−12.61	0	799991383	−25.01	799991934	−24.78	272.3	0.99
6	0.562	799991664	−12.66	−0.05	799991397	−24.23	799991931	−23.98	273.4	1.00
7	0.750	799991667	−12.66	−0.05	799991400	−23.92	799991934	−24.01	275.1	1.00
8	1.000	799991671	−12.67	−0.06	799991406	−23.68	799991934	−23.61	276.1	1.01
9	1.33	799991675	−12.67	−0.06	799991404	−24.25	799991943	−24.32	273.9	1.00
10	1.78	799991675	−12.66	−0.05	799991404	−24.61	799991943	−24.13	272.8	1.00
11	2.37	799992070	−12.65	−0.04	799991780	−26.58	799992360	−26.89	267.7	0.98
12	3.16	799992071	−12.65	−0.04	799991869	−19.33	799992274	−19.14	273.4	1.00
13	4.22	799992078	−12.65	−0.04	799991885	−18.69	799992289	−19.96	271.1	0.99
14	5.62	799992081	−12.64	−0.03	799991898	−18.36	799992265	−17.85	271.9	0.99
15	7.50	799992096	−12.64	−0.03	799991884	−19.89	799992309	−20.25	270.1	0.99
16	10	799992271	−12.66	−0.05	799992077	−18.72	799992464	−18.78	271.6	0.99
17	13.3	799992601	−12.66	−0.05	799992398	−19.39	799992804	−19.34	271.6	0.99
18	17.8	799992619	−12.72	−0.11	799992356	−23.76	799992882	−23.85	273.6	1.00
19	23.7	799992671	−12.92	−0.31	799992424	−22.34	799992914	−22.58	274.8	1.00
20	31.6	799992709	−13.51	−0.9	799992436	−22.69	799992981	−22.87	310.0	1.13
21	42.2	799993104	−14.64	−2.03	799992886	−19.32	799993307	−19.17	339.7	1.24
22	56.2	799993872	−16.78	−4.17	799993607	−21.06	799994152	−21.76	439.0	1.60
23	75.0	799993975	−18.86	−6.25	799993668	−23.15	799994318	−23.49	532.8	1.95

Table 5.3 Results of conventional spectrum analyzer (*Cnv*), R3264

n	1/k	Peak (x_0, y_0)			L (x_{-1}, y_{-1})		R (x_1, y_1)		*Rbw'* (Hz)	
		Freq.(Hz)	Level (dBm)	Nmlzd (dB)	Freq (Hz)	Level (dBm)	Freq (Hz)	Level (dBm)	RBW'	Nmlzd
0	0.100	799999892	−10.95	0.00	799999823	−16.03	799999970	−17.16	107.3	1.0
1	0.133	799999894	−10.97	−0.02	799999824	−16.09	799999984	−18.85	109.3	1.0
2	0.178	799999904	−10.93	0.02	799999816	−17.38	799999979	−17.73	109.2	1.0
3	0.237	799999907	−10.96	−0.01	799999815	−18.04	799999994	−19.42	111.0	1.0
4	0.316	799999912	−10.96	−0.01	799999826	−17.16	799999991	−18.15	110.2	1.0
5	0.422	799999923	−11.05	−0.10	799999829	−17.69	799999997	−18.21	109.7	1.0
6	0.562	799999931	−11.16	−0.21	799999830	−18.57	800000003	−17.64	112.7	1.1
7	0.750	799999946	−11.34	−0.39	799999853	−17.2	800000021	−18.48	112.9	1.1
8	1.000	799999964	−11.49	−0.54	799999868	−17.27	800000036	−18.05	115.4	1.1
9	1.33	799999982	−11.83	−0.88	799999894	−16.57	800000059	−18.39	119.3	1.1
10	1.78	800000021	−12.23	−1.28	799999915	−17.04	800000091	−18.55	124.8	1.2
11	2.37	800000049	−12.91	−1.96	799999948	−17.46	800000130	−17.7	144.8	1.3
12	3.16	800000088	−13.62	−2.67	799999984	−17.93	800000173	−17.29	163.7	1.5
13	4.22	800000162	−14.61	−3.66	800000024	−19.13	800000254	−18.38	193.5	1.8
14	5.62	800000247	−15.91	−4.96	800000076	−20.86	800000385	−19.83	254.3	2.4
15	7.50	800000352	−17.25	−6.30	800000120	−23.57	800000551	−21.17	331.9	3.1
16	10	800000485	−18.61	−7.66	800000275	−27.36	800000735	−21.56	321.3	3.0
17	13.3	800000700	−19.98	−9.03	800000360	−25.55	800001054	−23.48	563.0	5.2
18	17.8	800000960	−21.32	−10.37	800000516	−27.62	800001414	−24.37	717.9	6.7
19	23.7	800001380	−22.69	−11.74	800000880	−26.48	800001850	−24.95	969.3	9.0
20	31.6	800001876	−24.07	−13.12	800001192	−28.73	800002450	−25.95	1223.3	11.4
21	42.2	800002640	−25.52	−14.57	800001710	−29.61	800003350	−27.52	1651.6	15.4
22	56.2	800003510	−26.97	−16.02	800002420	−30.59	800004580	−29.19	2191.7	20.4
23	75.0	800005160	−28.63	−17.68	800003720	−31.41	800007120	−32.18	3302.1	30.8

5.3.2 Result of the Peak level reduction

The normalized peak level reductions against the *1/k* of each measurement mode are shown in Table 5.4 and Fig.5.4. These data ware pick upped from Table 5.1~5.3. The data named '*Thr*' corresponds to the theory, Eq.(2.41).

The values of *1/k* at 0.1 dB reductions in each configuration are listed in Table 5.5. The data named '*Ratio vs. Thr*.' are the value normalized by the '*Thr*'. We assumed this ratio was a parameter that corresponded to the fastness of the super sweep method against the conventional sweep method.

Table 5.4 Peak Level Reduction vs. Normalized sweep rate

n	1/k	Thr.	Cnv.	S1	S2
0	0.10	0.00	0.00	0.00	0.00
1	0.13	−0.01	−0.02	0.01	0.00
2	0.18	−0.01	0.02	0.01	0.00
3	0.24	−0.02	−0.01	0.01	0.00
4	0.30	−0.04	−0.01	0.00	0.00
5	0.42	−0.07	−0.10	0.01	0.00
6	0.56	−0.13	−0.21	0.01	−0.05
7	0.75	−0.22	−0.39	0.01	−0.05
8	1.01	−0.39	−0.54	0.01	−0.06
9	1.33	−0.62	−0.88	0.01	−0.06
10	1.76	−1.02	−1.28	0.01	−0.05
11	2.38	−1.62	−1.96	0.01	−0.04
12	3.14	−2.30	−2.67	0.01	−0.04
13	4.22	−3.20	−3.66	0.01	−0.04
14	5.63	−4.17	−4.96	−0.03	−0.03
15	7.51	−5.29	−6.30	−0.17	−0.03
16	10.1	−6.46	−7.66	−0.96	−0.05
17	13.3	−7.65	−9.03	−1.72	−0.05
18	17.5	−8.92	−10.37	−3.57	−0.11
19	23.8	−10.18	−11.74	−5.82	−0.31
20	31.3	−11.18	−13.12	−7.97	−0.90
21	42.0	−12.42	−14.57	−10.62	−2.03
22	56.0	−13.82	−16.02	−12.94	−4.17
23	75.1	−15.00	−17.68	−15.81	−6.25

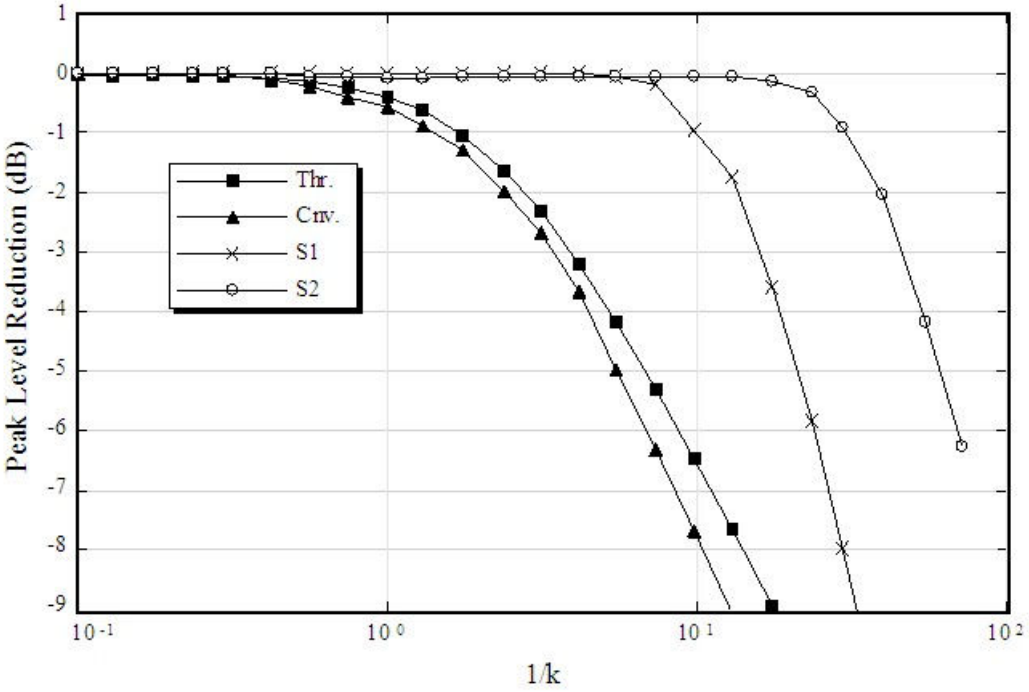

Fig.5.4 Peak Level Reduction vs. Normalized sweep rate

Table 5.5 1/k : Peak Level reduction corresponds to -0.1dB

	Thr.	*Cnv.*	*S1*	*S2*
1/k ：-0.1dB	0.5	0.42	6.9	17.1
Ratio vs. Thr.	1.0	0.84	13.8	34.2

5.3.3 Result of the broadening of RBW

The ‘ *Rbw*' ’ were observed as the 3dB bandwidth of the measured spectrum, and the configured *Rbw* was constantly 300Hz. The increase of the ratio ‘ *Rbw*'/*Rbw* ‘ against the *1/k* is shown in Table 5.6 and Fig.5.5. The column and line ‘*Thr*’ is theoretically calculated by Eq.(2.42).

In Table 5.7, ‘*1/k: 1.1*’ is the value of the *1/k*, which gives the *1.1* times broadening. The ‘*Ratio vs. Thr.* ’ is the values normalized by the *Thr.* We assumed this ration was the parameter that corresponded to the fastness of the new method against a conventional sweep method.

Table 5.6 Broadening of RBW vs. Normalized sweep rate *1/k*

n	1/k	Thr.	Cnv.	S1	S2
0	0.1	0	1	1	1
1	0.13	−0.01	1	1.01	1
2	0.18	−0.01	1	1	0.99
3	0.24	−0.02	1	1	0.99
4	0.3	−0.04	1	1	1
5	0.42	−0.07	1	0.99	0.99
6	0.56	−0.13	1.1	1	1
7	0.75	−0.22	1.1	1	1
8	1.01	−0.39	1.1	1.01	1.01
9	1.33	−0.62	1.1	1.01	1
10	1.76	−1.02	1.2	1	1
11	2.38	−1.62	1.3	1.02	0.98
12	3.14	−2.3	1.5	0.99	1
13	4.22	−3.2	1.8	0.99	0.99
14	5.63	−4.17	2.4	1	0.99
15	7.51	−5.29	3.1	1.04	0.99
16	10.1	−6.46	3	0.99	0.99
17	13.3	−7.65	5.2	1.11	0.99
18	17.5	−8.92	6.7	1.18	1
19	23.8	−10.18	9	1.93	1
20	31.3	−11.18	11.4	2.04	1.13
21	42	−12.42	15.4	3.08	1.24
22	56	−13.82	20.4	3.15	1.6
23	75.1	−15	30.8	13.44	1.95

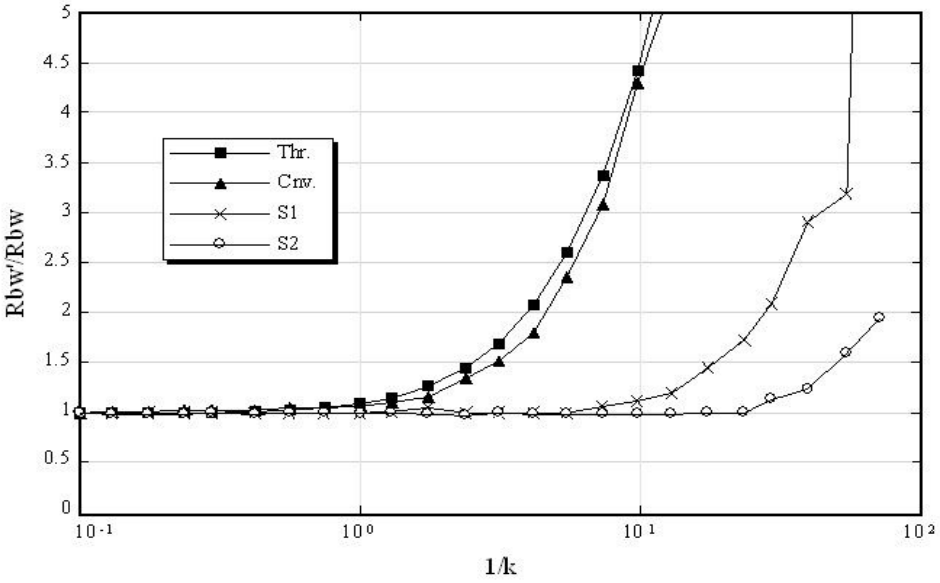

Fig.5.5 Broadening of the RBW vs. 1/k

Table 5.7 1/k corresponds to *Rbw'/Rbw=1.1*

	Thr.	*Cnv.*	*S1*	*S2*
1/k: 1.1	1.0	1.2	9.0	29
Ratio vs. Thr.	1.0	1.2	9.0	29

5.4 Discussion

A sweep spectrum analyzer has a property that is called 'over sweep-rate response'. This property was mentioned by many authors [1][2][3] and expressed by Eq.(2.41) and (2.42). In the super sweep method, the IF signal was digitized and converted into the base band signal whose bandwidth was wider than the resolution bandwidth, *Rbw*. The base band signal was inputted into the negative chirp filter. We expected that the negative chirp filter reduced the over sweep-rate response even in the faster sweep rate than the sweep method. In our experiment, we confirmed that the over sweep-rate response was reduced with changing the normalized weep rate *1/k*.

5.4.1 Peak level Reduction

The permissible limit of the peak level reduction of the conventional spectrum analyzer is generally 0.1dB [3]. By considering the second line of Table 5.5, *'Ratio vs. Thr.'*, we confirmed that the maximum sweep rate achieved of 13.8 and 34.2 times faster than the conventional theory, in the cases of *S1* and *S2*, respectively. And we calculated the following ratio.

$$\frac{Ratio\ vs\ Thr.;S2}{Ratio\ vs\ Thr.;S1}=\frac{34.2}{13.8}=2.48\ . \qquad (5.16)$$

The theoretical estimation of this ratio was given by the ratio of R_S between the cases of *S2* and *S1* in Table 4.1, that was 18.7/6.2≒3.0. And this was the ratio of the *Flt* (see Fig.3.9) between the cases of *S2* and *S1*.

5.4.2 Broadening of the resolution bandwidth

The typical permissible difference of the RBW for a conventional spectrum analyzer is $\pm 15\sim 20\%$ (by R3264). We measured the maximum sweep rate as the normalized sweep rate *1/k* which gave the resolution broadening of 1.1. By considering the second line of Table 5.7, *'Ratio vs. Thr.'*, we confirmed that the maximum sweep rate was 9.0 and 29 times faster than the conventional theory, in the cases of *S1* and *S2*, respectively. And we calculated the following ratio.

$$\frac{Ratio\ \ vs\ Thr.;S2}{Ratio\ \ vs\ Thr.;S1}=\frac{29}{9.0}=3.2\ . \qquad (5.17)$$

The theoretical estimation of this ratio was 3.0, similar to the case of Eq.(5.16).

5.4.3 Total consideration of the maximum sweep rate:

We studied the maximum sweep rate by focusing the two points, peak level reduction and broadening of the *Rbw*. We estimated that the level reduction was more critical than the broadening of the *Rbw*. By considering the Eq.(5.16) and (5.17), we confirmed that the maximum sweep rate was proportional to the ratio of *Flt/Rbw*.

The condition, which we estimated the $\sigma_{\max\_S}$ (maximum sweep rate in the new method) by Eq.(3.34-b),

$$\sigma_{\max\ S} = Rbw \times (Flt / \chi) ,$$

intended the integration of Eq.(3.4),

$$S_n(t) = l(t) \int_{-\infty}^{\infty} g(\tau) f(t-\tau) \times \exp[-j\omega\tau] d\tau ,$$

to operate perfectly. But the result of our experiments gave that $\sigma_{\max\_S}$ had a margin for the peak level reduction reaching 0.1 dB. Equation (3.35),

$$R_s \equiv \frac{\sigma_{\max\_S}}{\sigma_{\max}} = \frac{k_0}{\chi} \times \frac{Flt}{Rbw} ,$$

where $\sigma_{\max}$ is the maximum sweep rate of the sweep method. And R_S can be rewritten as

$$True\ R_s \cong \alpha \cdot R_S = \alpha \frac{k_0}{\chi} \frac{Flt}{Rbw} = \beta \frac{Flt}{Rbw}, \qquad (5.18)$$

where $True\ R_s$ was given as the second line of Table 5.5, α is an unknown constant, and *Flt/Rbw* was given in Table 4.1. Then the value of β were 1.4 and 1.7 in the case of *S1* and *S2,* respectively.

If we make the system, Fig.3-10, and configured it to have wider *Flt* and *Rbw*, we could obtain more fast sweep and wider *Rbw* measurement.

5.5 Summary

The result and discussion verified that the super sweep method achieved the first sweep measurement on the sweep spectrum analyzer. We argue that we made the break-through in the restriction of the sweep rate of a spectrum analyzer by using the super sweep method. Our further work is to study the over sweep-rate response of the new method in further detail.

5.6 Reference

[1] Morris Engelson, “Spectrum Analyzer Theory and Applications” Artech House publishers Oct. 1974

[2] George D. Tsakiris, “Resolution of a spectrum analyzer under dynamic operations” Rev. Sci. Instrum., Vol.48, No.11, Nov. 1977 pp.1414-1419

[3] R.A.Witte, “Spectrum and Network measurement”, 1993 Prentice-Hall,Inc

Chapter 6

Additional discussions

6.1 Introduction

Until last chapter, we investigated the theory of the super sweep method. In this chapter, the additional discussion about the method is described.

Our experimental system needed many processes to achieve its function. About 30 parameters (such as sampling frequency, data size etc.) played a role in the system. We had to configure these parameters optimally. Section 6.2 and 6.4 describe a few theory of the optimization. Section 6.2 describes the characteristics of the display system.

The super sweep method had a merit against not only the sweep method but also the FFT method. The merit was the property about the appearance of the IF filter response, which is described in section 6.5.

We had an attention about the similarity between the Chirp Z-transform and the new method. Section 6.6 describes the discussion about the similarity.

In section 2.5, we have some numerical analysis about the two-tone response of the spectrum on the sweep method. In section 6.7, we investigated the same analysis on the super sweep method,

In actual measurement system, there are several sources of a noise, and the results are under the influence of the noise. Section 6.8 discuss about the noise and the influence.

In section 6.9, we presented some samples of spectrum that was obtained by the super sweep method, and we described the merit of the method.

In section 6.10, we investigated the 'view of spurious peaks' in the new method. It is one characteristic of the new method.

In section 6.11, we discussed the characteristics of some methods of spectrum measurement.

6.2 Required condition for fast sweep

In this section, we analysis and discusses the processing time and the requirements to achieve fast sweep.

6.2.1 Operation time

Table 6.1 shows the relations between sweep time and operation time against the three conditions of the super sweep method.

In the measurements which gave the result of Table 6.1, the complex filter (see section 3.4 and Fig.3.10) were processed by the DSP, TMS3206711 80MHz; produced by Texas Instruments Inc. The sweep times of the measurements were 22.2, 16.7 and 7.7 times faster than the traditional sweep method. But the all processing times of the DSP were longer than the sweep times. R_{SO} are the ratio between the processing times and the sweep times. R_{SO} became as larger as wider the *Rbw*. The ratio R_{S_OP} explains the practical fastness of the new method. When *Rbw* was 100kHz, R_{S_OP} was 0.7 and the processing time was longer than the traditional sweep time, T_{S_trd}.

Table 6.1 Operation time of the experimental system (DSP complex filter)

		A	B	C	A/B	A/C	C/B
***Rbw* (kHz)**	***Span* (MHz)**	T_{S_trd} **(msec)**	T_{S_spr} **(msec)**	T_{DSP} **(msec)**	R_S	R_{S_OP}	R_{SO}
10	**100**	**2000**	**90**	**344**	**22.2**	**5.8**	**3.8**
30	**200**	**500**	**30**	**218**	**16.7**	**2.3**	**7.3**
100	**1000**	**230**	**30**	**309**	**7.7**	**0.7**	**10.3**

T_{S_trd} : A = The sweep time in a traditional sweep method
T_{S_spr} : B = The sweep time in the super sweep method
T_{DSP} : C = The operation time of the DSP (TMS320C6711 80MHz)
R_S : A/B = The ratio T_{S_trd} / T_{S_spr}, Ratio of the sweep time.
R_{S_OP} : A/C = The ratio T_{S_trd} / T_{DSP}, Ration of the sweep time and the operation time
R_{SO} : C/B= The ration T_{DSP} / T_{S_spr}, Ratio between the processing time and the sweep time

If the DSP had enough performance, the new method could sweep in the time T_{S_spr}. By considering R_{SO}, it assumed that the DSP required faster processing with wider *Rbw*.

Note: In our experiment system, the design of the DSP system did not optimized and the memories on the circuit were not so fast.

6.2.2 Operation time of each sample of a spectrum

This section analyzes the processing time that achieves the real time operation.

We investigated the operation time to obtain one sample of the spectrum. Figure 6.1 shows the simplified spectrum that is obtained by digital IF method, where Δf and Δt is the frequency and time between each sample of the spectrum. We had not any precise rules to decide the Δf. But we considered that Δf had to be equal or narrower than *Rbw*/2 to obtain the exact spectrum, experimentally.

$$\Delta f \le Rbw/2 \qquad (6.1\text{-a})$$

$$\Delta f_{\max} = Rbw/2 \qquad (6.1\text{-b})$$

Usually Δf equals $\Delta f_{\max}$ to achieve a fast measurement.

The relation between Δf and Δt is given by

$$\Delta f = \sigma \cdot \Delta t \ . \qquad (6.2)$$

The maximum sweep rate σ is explained by Eq.(3.34-b) as

$$\sigma_{\max} = Rbw \cdot Flt / \chi \ . \qquad (6.3)$$

By above three equations, Eq.(6.1-b)~(6.3), the minimum Δt is explained as follows.

$$\Delta t_{\min} = \frac{\Delta f_{\max}}{\sigma_{\max}} = \frac{Rbw/2}{Rbw \cdot Flt / \chi} = \frac{\chi}{2 \cdot Flt} \qquad (6.4)$$

$\Delta t_{\min}$ is in inversely proportion to the *Flt*.

We tried to replace the *Flt* of Eq.(6.4) by *Rbw* and other parameter. We can know the relation between *Flt* and *Rbw* by Eq.(3.35).

$$R_s \equiv \frac{\sigma_{\max\_S}}{\sigma_{\max}} = \frac{k_0}{\chi} \times \frac{Flt}{Rbw} . \qquad (3.35)$$

where R_S is the rate of sweep rate against a traditional sweep method. By modifying this equation *Flt* is given by

$$Flt = R_S \cdot RBw \cdot \chi / k_0 \ . \qquad (6.5)$$

Eq.(6.4) can be modified as

$$\Delta t_{\min} = \frac{\chi}{2 \cdot Flt} = \frac{\chi \cdot k_0}{2 \cdot R_S \cdot Rbw \cdot \chi} = \frac{k_0}{2 \cdot R_S \cdot Rbw} . \qquad (6.6)$$

$\Delta t_{\min}$ is in inversely proportional to the product of R_S and *Rbw*.

In the case that the operation time of each sample of the spectrum is shorter than $\Delta t_{\min}$, the measurement time is dependent on the sweep time, which is product of Δt and the sample-number. But in the case the operation time is longer than $\Delta t_{\min}$, the measurement time is dependent on the processing time.

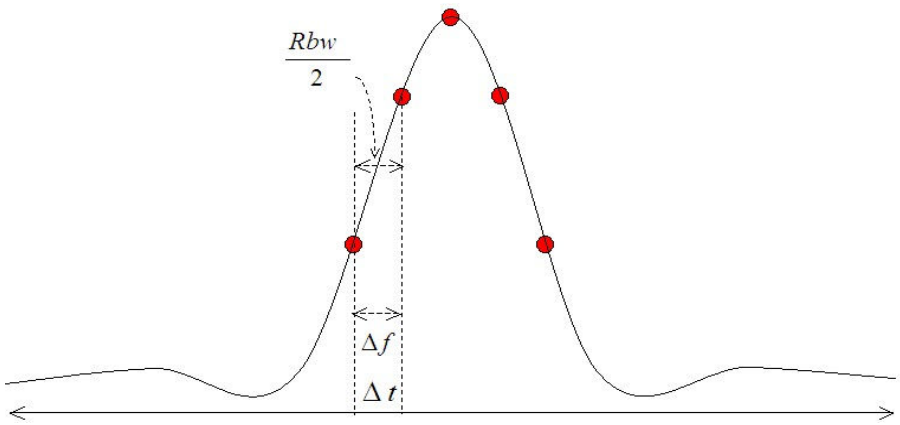

Fig.6.1 Interval of frequency and time between each sample of a spectrum

6.2.3 Required performance of the operation

We considered that the negative chirp (complex) filter was the most significant factor of the operation and the amount of the operation was in proportion to the number of the tap. We considered how the number of tap of the filter is decided.

N_G is the tap number, it was already given by Eq.(4.5).

$$N_G = T_G \times f_S = \frac{\chi}{Rbw} \times f_S \quad . \qquad (4.5)$$

where f_S is the sampling frequency of the input signal of the filter. The relation of f_S and *Flt* is described in next section, [1], and [2]. Practically, *Flt* is in proportional to f_S.

$$Flt = \gamma \cdot f_S \qquad (6.7)$$

The constant γ is decided by the property of the IF filter, usually γ is 0.5~0.8.
The relation between *Flt* and R_S is given by Eq.(3.35) and (5.13).

$$R_s \equiv \frac{\sigma_{\max\_S}}{\sigma_{\max}} = \frac{k_0}{\chi} \times \frac{Flt}{Rbw} \cong \alpha \frac{k_0}{\chi} \frac{Flt}{Rbw} \equiv \beta \frac{Flt}{Rbw} \qquad (6.8)$$

From Eq.(6.7) and (6.8), f_S can be explained as $f_S = \frac{Flt}{\gamma}$, and *Flt* is in proportion to R_S, as,

$Flt = \frac{R_S \cdot Rbw}{\beta}$. Then f_S is given by

$$f_S = \frac{Flt}{\gamma} = \frac{R_S \cdot Rbw}{\gamma \cdot \beta} \qquad (6.9)$$

By substituting f_S with Eq.(6.9) into Eq.(4.5), N_G is explained as

$$N_G = \frac{\chi}{Rbw} \times f_S = \frac{\chi}{Rbw} \frac{R_S \cdot Rbw}{\gamma \cdot \beta} = \frac{\chi}{\gamma \cdot \beta} R_S \, . \qquad (6.10\text{-a})$$

By Eq.(6.10-a), N_G is in proportion to R_S. In our experiment system, χ=2.6, γ=0.68 (see section 4.3.4) , and β=1.5 (see section 5.4.3), and N_G was approximately

$$N_G = 2.6 \cdot R_S \, . \qquad (6.10\text{-b})$$

We defined the rate R_O as the number of complex product sum to be operated within one second to obtain a spectrum within the sweep time. It is given by

$$R_O \equiv \frac{N_G}{\Delta t_{\max}} = \frac{\frac{\chi}{\gamma \cdot \beta} R_S}{\frac{k_0}{2 \cdot R_S \cdot Rbw}} = \frac{2 \cdot \chi}{k_0 \gamma \cdot \beta} Rbw \cdot {R_S}^2 \, . \qquad (6.11\text{-a})$$

In the case that k_0=2.0,

$$R_O = 2.6 \times Rbw \cdot {R_S}^2 . \qquad (6.11\text{-b})$$

R_O is in proportion to product of *Rbw* and square of R_S .

6.2.4 Relation between the IF bandwidth and the sampling frequency

This section is base on the argument of section 2.4 and investigates the relation between the IF filter and the sampling frequency. An example of the relation is shown in Fig.6.2, where the abscissa indicates frequency and the ordinate indicates a power, and a spectrum of base band signal is shown in this figure.

The large trapezoid represents the simplified frequency response of the low pass filters (LPF), which generates the base band signal. We can observe a spectrum of minus frequency as an analytic signal. In the figure, 'D (dB)' is the desired dynamic range of the signal passed thorough the LPF. '*Flt*' is the flat pass band of the LPF. The slanting slopes of the both side is the transitional area of the LPF. The frequency f_S is the sampling frequency, and $\pm f_S / 2$ is the Nyquist frequency. The tail ends of the transitional areas are extended out of the Nyquist frequency.

In the case that *Bwd* is the D dB down bandwidth of the LPF and the sampling frequency is given by

$$f_S = (Flt + Bwd)/2 , \qquad (6.12)$$

we can obtain the pass bandwidth *Flt* without the aliasing of transitional band [2][3].

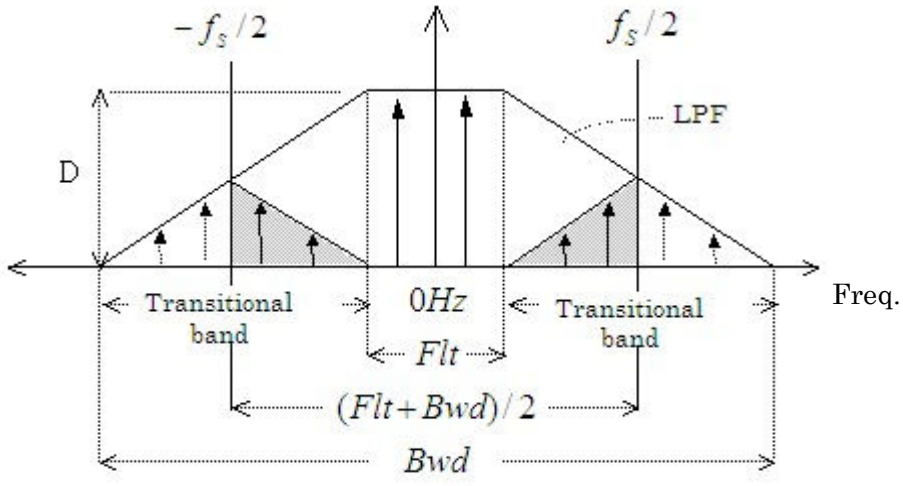

LPF: Pass band of the low pass filter before base band signal
D(dB) : Desired Dynamic range
Bwd: DdB down Bandwidth of the LPF
Gray zone: Frequency area that might has alias signal
f_S : Sampling frequency of I and Q signal

Fig.6.2 Relation between IF filter and sampling frequency

6.2.5 Implementation of the fast complex filter

This section investigates the implementation of the negative chirp filter. The architecture of the complex filter is presented in Fig.3.10. We implemented the complex filter as an operation of the DSP, which is described in chapter 4.

By the argument of Chapter 5, the required performance of the DSP was explained by Eq.(6.11-a) and (6.11-b). And the required operation rate is in proportion to the product of *Rbw* and square of R_S. In the case that the *Rbw* was narrower than 1kHz, the DSP of our experimental system could operate it within a sweep time. Table 6.1 shows the result of larger RBW than 1kHz. If the DSP had larger performance, the operation time was shorter than the result.

The operation of the complex filter is explained by

$$\begin{aligned} I_S + jQ_S &= (I_b + jQ_b) * (g_I + jg_Q) \\ &= (I_b * g_I - Q_b * g_Q) + j(Q_b * g_I + I_b * g_Q) \end{aligned} \quad , \qquad (3.36)$$

where $I_S + jQ_S$ is the output of the filter, $I_b + jQ_b$ is input signal, and $g_I + jg_Q$ is the coefficients of the complex (Gaussian negative chirp) filter. Equation (3.36) consists of four multiplexes, one subtraction and one addition. We implemented the system by modifying the system of chapter 4. It is shown in Fig.6.3, where the four multiplex were replaced by the four 'PFIR' filters.

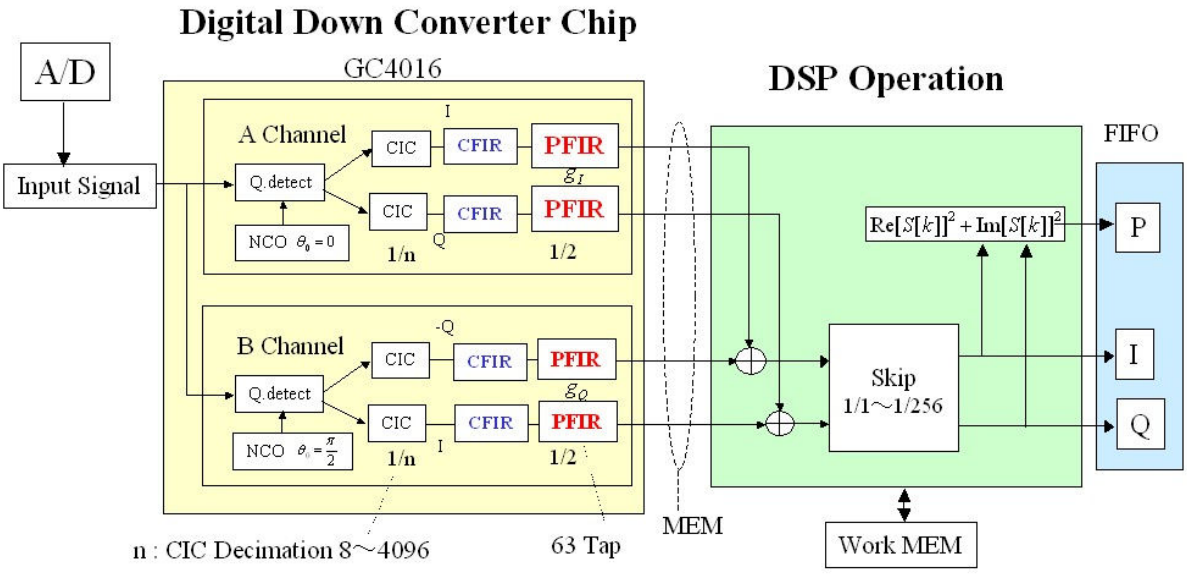

Fig.6.3 Complex filter using DA FIR filter of DDC: GC4016

We used the GC4016 (see section 4.3) as the Digital Down Converter (DDC), which has four channels of down converter. Each channel has two programmable FIR filter (PFIR), whose coefficient are common and 63 taps. We used two channels of GC4016, A and B, and configured the coefficient of PFIR of A and B channel with real and imaginary part and of the complex filter, respectively. We implemented the real part of the complex filter g_I in the PFIR of A channel, and the imaginary part g_Q is implemented into the B channel.

We configured the sign of the 'I' and 'Q' of the each channel by setting the initial phase, θ_0 of the NCO, of which A and B channel was 0 and $\pi/2$. In the case that the output of NCO in B Channel was

$$\{\cos(\omega+\pi/2), \sin(\omega+\pi/2)\} = \{-\sin(\omega), \cos(\omega)\}, \qquad (6.13)$$

the I and Q channel of B Channel operated as –Q and I, and the four output of the PFIR were the four convolutions of the right side of Eq.(3.36). The DSP operated the two additions only. The amount operation of the DSP was reduced from the method of chapter 4 drastically. Table 6.2 shows the result of this configuration.

Table 6.2 Operation time of the experimental system (complex filter of the DDC)

		A	B	C	A/B	A/C	C/B
Rbw **(kHz)**	***Span*** **(MHz)**	T_{S_trd} **(msec)**	T_{S_spr} **(msec)**	T_{DSP} **(msec)**	R_S	R_{S_OP}	R_{SO}
10	**100**	**2000**	**90**	**170**	**22.2**	**11.8**	**1.9**
30	**200**	**500**	**30**	**98**	**16.7**	**5.1**	**3.3**
100	**1000**	**230**	**30**	**139**	**7.7**	**1.7**	**4.6**

T_{S_trd} : A = The sweep time in a traditional sweep method
T_{S_spr} : B = The sweep time in the super sweep method
T_{DSP} : C = The operation time of the DSP (TMS320C6711 80MHz)
R_S : A/B = The ratio T_{S_trd}/T_{S_spr}, Ratio of the sweep time.
R_{S_OP} : A/C = The ratio T_{S_trd}/T_{DSP}, Ration of the sweep time and the operation time
R_{SO} : C/B= The ration T_{DSP}/T_{S_spr}, Ratio between the processing time and the sweep time

The filters included in the DDC (CIC, CFIR, and PFIR) have no operation time but a little latency time, from 7.6 μ sec to 3.9msec (see section 4.3). The operation time T_{DSP} was reduced approximately half of the Table 6.1, and the ratio R_{S_OP} and R_{SO} were improved. But the improvement was not corresponding to the reduction of the operation. We considered that the operation time was dependent on not only operation but also the accessing time of the memory.

The outputs signals of the four PFIR were sent to the DSP through a memory, and the DSP red the signals from the external memory. We considered that these accessing spent so much processing time. The design of the circuit of our experiment system was not optimized. The DSP was forced to spend so much accessing time for the memories. We expect that we can make the

operation time T_{DSP} to be shorter by optimization of the circuit design. On the other hand, we can design the circuit corresponding to the 'DSP Operation' in the Fig.6.3 using a FPGA. It is not difficult to make the circuit that has no operation time but some latency.

If we had optimized circuit, the operation time T_{DSP} would not be more than the sweep time T_{S_spr}, and the rate R_{S_OP} (A/C) would accord with R_S (A/B).

6.3 Display of new method

Many conventional spectrum analyzers have only one display and the spectrum is displayed with 1000 points (may be smaller or larger a little).

In the super sweep method, the spectrum analyzer can treat large data size of a spectrum and measure spectrum 10 or 30 times faster. We used a PC for the display as a Windows application, the example of a display is shown in Fig.6.4. The left side trace is 'Main trace' whose trace data was 4000 points, and the right side trace is 'Sub trace' which is extended trace of part of the Main trace whose area is indicated by orange colored cursor on the bottom of the Main trace.

Figure 6.5 shows the 'Artificial Analog display' of the R3264 (conventional), which displays 32times trace on a trace and each sample is displayed by a dot. The spectrum is displayed as light and shade, which corresponds to the probability of the spectrum. This trace takes 32time longer than the normal trace, but the new method will be able to display almost same time as traditional one trace. (We have not implement this function in the experiment system.)

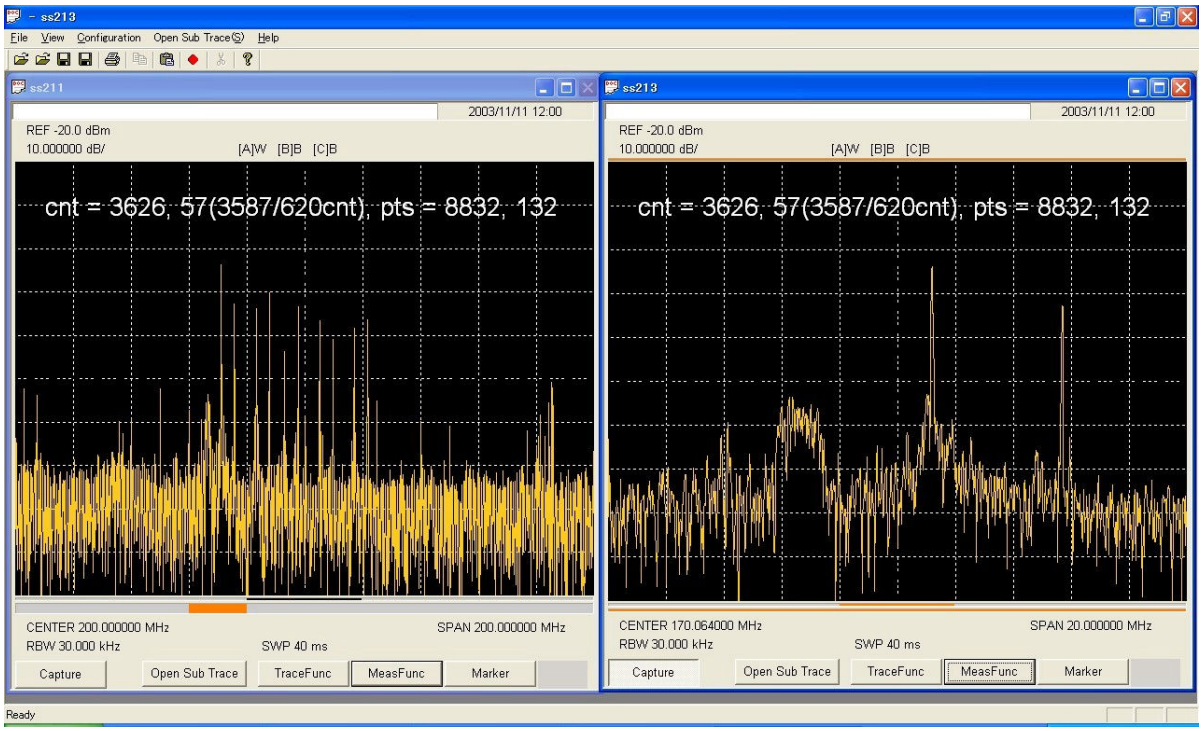

Fig.6.4 Multi trace Display on PC

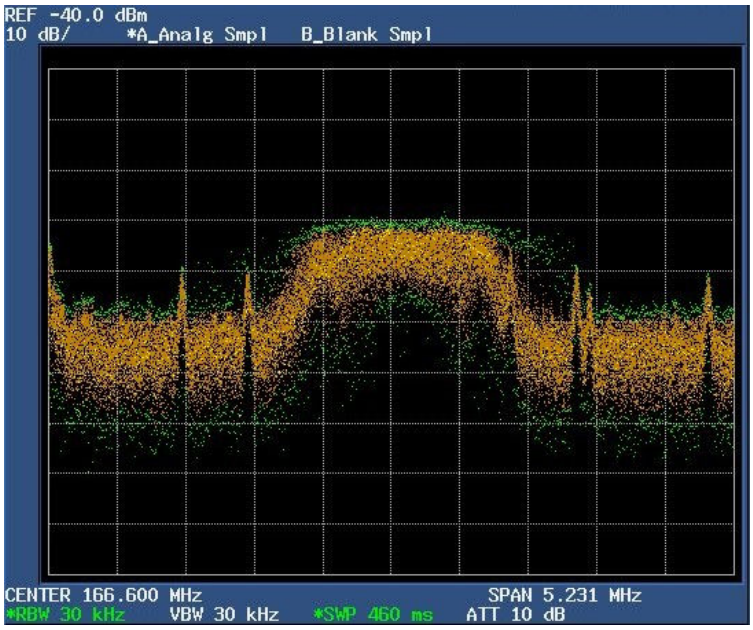

Fig.6.5 Artificial Analog trace Display of R3264

6.4 Filter margin and synchronization of frequency

The discussion of this section is standing on the system of Fig.6.6.

6.4.1 Over view of latency and synchronization of the system

A sweep spectrum analyzer (including a super sweep method) is a cyclic system as shown in Fig.2.5. Our experimental system consisted of the filter chain described in section 4.2.4. We had to consider the margin of the filters to obtain the spectrum with exact frequency.

We took the margin of the span and the sweep-time corresponding to the responses of the chain of the filters. And we achieved the synchronization between the spectrum and the ramp signal. The concept of the synchronization is shown in Fig.6.6, which shows the chain of the filter in the super sweep method and the position of the ramp signal.

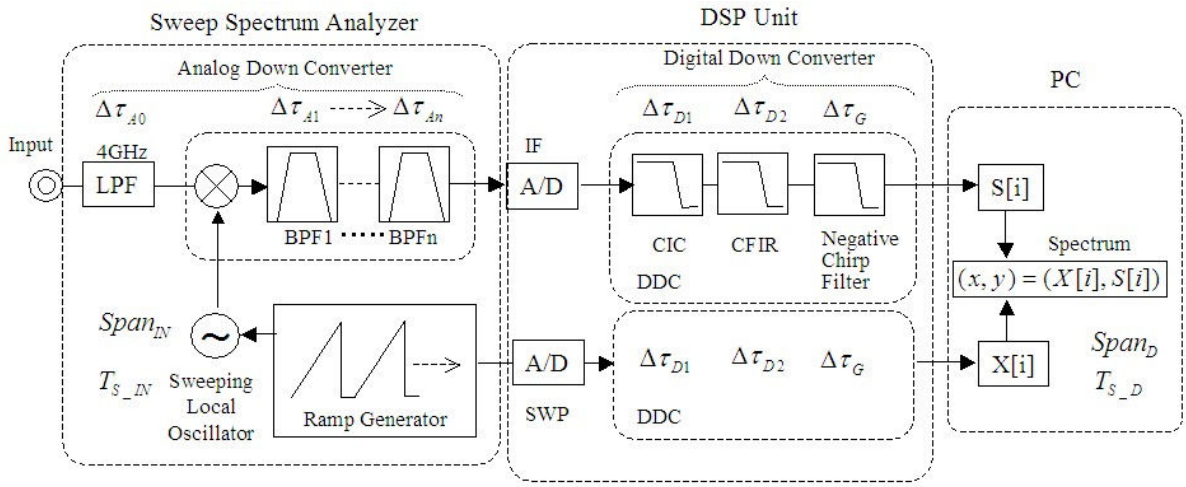

Fig. 6.6 Chain of Filters and its Latency

6.4.2 Margin corresponding to chain of filters

Most traditional sweep spectrum analyzers have no difference between $Span_{IN}$ and $Span_{D}$, and T_{S_IN} and T_{S_D}, where the sweep time is enough slow. In the super sweep method, sweep time was too short to ignore the difference.

In Fig.6.6, the signal of the spectrum is $S[i]$ (in the right square indicated as 'PC'), which is passed thorough the several filters in the system. Each filter has latency, which is according to its bandwidth. The bandwidth of the filters is wider at the left (input) side and narrower at the right (output) side. The narrowest filter has the longest latency; it is the 'Negative chirp' filter (in the center square).

An illustrated example of impulse response of a filter, input signal, and output signal is shown in Figure 6.7, where $\Delta\tau$ is the length of the impulse response, and T_{out} and T_{IN} is the time length of the input and output. T_{IN} is given by

$$T_{IN} \geq T_{OUT} + \Delta\tau, \qquad (6.13)$$

which provide the output without a transient response affected by the start and end of the input signal. T_{IN} is sum of the impulse response and time length of the output. We can consider that $\Delta\tau$ is a margin and latency.

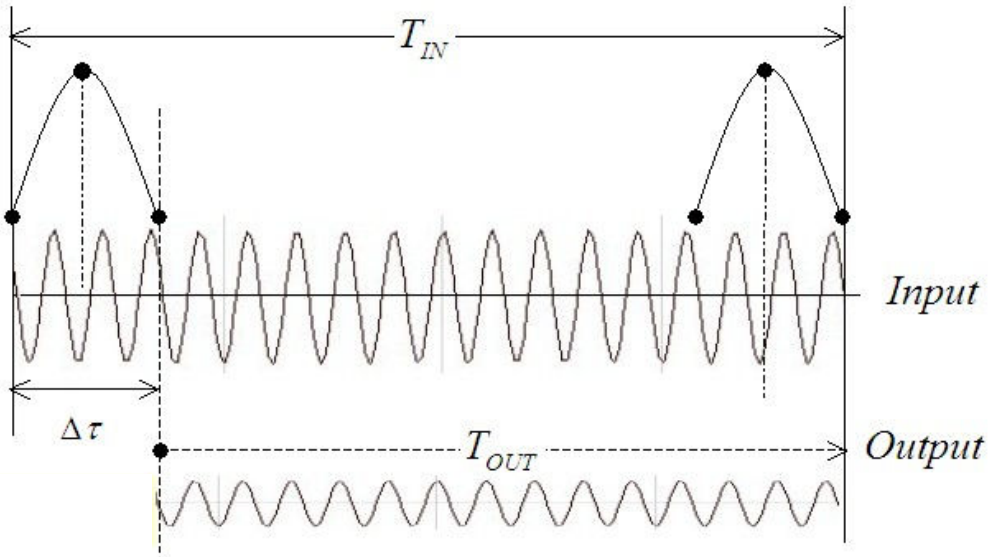

Fig. 6.7 Latency and Margin for a Filter

The total latency of the system figured by Fig.6.6 is given by

$$\tau = \sum_i \Delta\tau_i = (\Delta\tau_{A0} + \Delta\tau_{A1} + \cdots + \Delta\tau_{An}) + (\Delta\tau_{D1} + \cdots + \Delta\tau_G). \qquad (6.14)$$

The most critical latency depends on the filter whose bandwidth is narrowest; usually it is negative chirp (resolution) filter. But in the case that the video filter is implemented after the resolution filter, the most critical latency depends on the video filters. On the other hand, the latency of the BPF in the RF down converters is very short (usually, under one micro second), we can ignore it.

When we measure a spectrum whose span is $Span_D$ (Hz), the sweep time is T_{S_D}, the span and sweep time of the local oscillator (see Fig.6.6) is given by following equations.

$$Span_{IN} = Span_D \frac{T_{S\_D} + h}{T_{S\_D}} \qquad (6.15)$$

$$T_{S\_IN} = T_{S\_D} + h \qquad (6.16)$$

6.4.3 Synchronization between spectrums and ramp signals

In the case that we control the local oscillator in the system of Fig.6.6 exactly, the element number 'i' of the signal $S[i]$ has to correspond to the measured frequency. In our experiment system, we were not able to control the local oscillator directly. And we made the synchronization of the abscissa (frequency) by measuring the 'SWP' signal, $X[i]$ as shown in dot square of 'PC' in Fig.6.6.

The SWP (Sweep out) signal is one output signal of the spectrum analyzer R3264 (see section 4.2, especially Fig.4.2). The SWP is a nearly DC (Direct Current) signal whose voltage corresponds to the instantaneous frequency of the local oscillator. As shown in Fig.6.6, the SWP signal was digitized by the AD/C in the DSP Unit and passed through the digital filters whose properties were same to the filters that the IF signal were passed through. Then the latency was same to it of the IF signal, and we could obtain the spectrum as the pair of array, $X[i]$ and $S[i]$.

Figure 6.8 shows the illustration of our method how we made the synchronization. The upper side square is a simplified spectrum, the middle stage shows the SWP signal, and the bottom square shows the spectrum on the PC.

We made the three tone signals using a signal generator whose frequencies were as follows.

$$\left.\begin{aligned} f_{m4} &= f_{cf} - \frac{4}{10} Span_{IN} \\ f_{cf} &= Center\ \ Frequency \\ f_{p4} &= f_{cf} + \frac{4}{10} Span_{IN} \end{aligned}\right\}, \qquad (6.17)$$

where $Span_{IN}$ and f_{cf} were the conditions of the sweep spectrum analyzer.

We received the signal $(X[i], S[i])$ by the PC. The three signals were detected as peaks. The value of $X[i]$ corresponding to the three peaks were given by

$X_{m4} = X[i_{m4}]$, $X_{cf} = X[i_{cf}]$ and $X_{p4} = X[i_{p4}]$,

where i_{m4}, i_{cf} and i_{p4} were the element number. We could estimate the frequency of each sample of $S[i]$ as *F[i]* by following equation.

$$F[i] = f_{cf} + \frac{(X[i] - X_{cf}) \times 0.8 \cdot Span_{IN}}{X_{p4} - X_{m4}} \qquad (6.18)$$

The values of X_{m4}, X_{cf}, and X_{p4} were not change for the span and center frequency. Even if the center frequency and span are any other value, we can calculate the frequency *F[i]*.

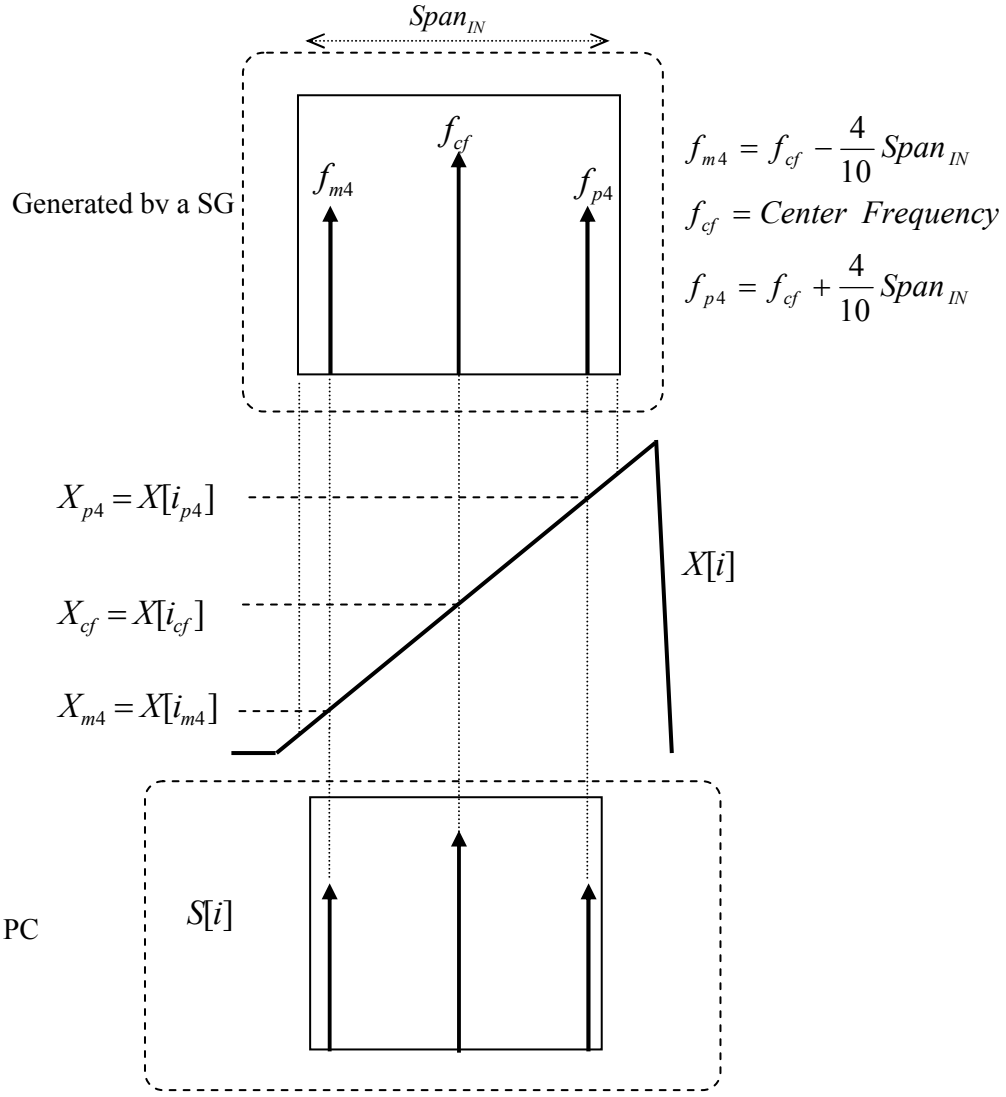

Fig. 6.8 Synchronization on abscissa

6.5 Response of IF filters

A diagram of the FFT method system is shown in Fig.6.9. The spectrum obtained by the FFT method is observed as a product of the true spectrum $F(\omega)$ and the frequency response of the system $H(\omega)$ as shown in Fig.6.10, where $F(\omega)$ and $H(\omega)$ are the Fourier transform of the measured signal and the impulse response of the system before A/D converter (especially the IF filter after the RF down converter) [4]. Usually, the pass band of the $H(\omega)$ is not completely flat and has some slope or ripple. The signal passed the outside of the pass-band is not suitable for measuring a spectrum. And we have to equalize the spectrum corresponding to the $H(\omega)$ to obtain an exact spectrum.

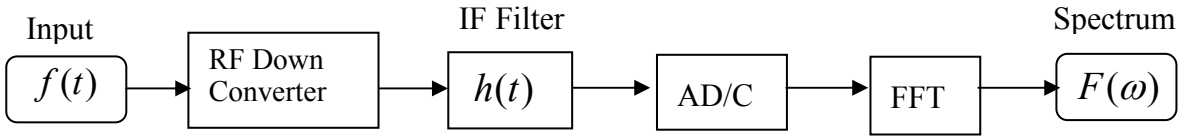

Fig. 6.9 Signal flow of Spectrum analyzers by FFT method

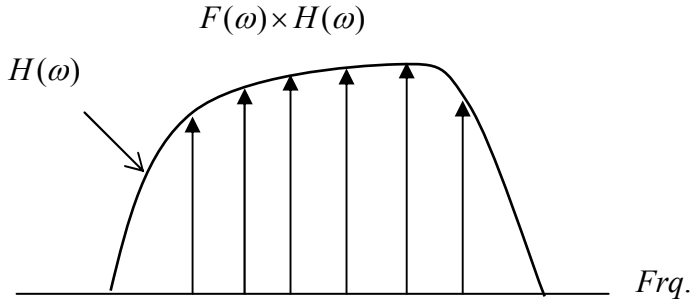

Fig. 6.10 Spectrum of FFT method with IF frequency response

The frequency resolution of the spectrum is decided by the window function of the FFT. The spectrum $S(\omega)$ is explained as following equation.

$$S(\omega) = \big(F(\omega)\times H(\omega)\big) * W(\omega), \qquad (6.19)$$

where $W(\omega)$ is the Fourier transform of the window function.

In the super sweep method, the spectrum is obtained as a convolution of $F(\omega)$ and $H(\omega)$, as Eq.(3.10) (see section 3.2).

$$S(\omega) = F(\omega) * H(\omega), \qquad (6.20)$$

where, $H(\omega)$ is a convolution of the total frequency response of the several stages of the system. $H(\omega)$ is dependent on the narrowest filter, usually it is the resolution filter. The spectrum is assumed as

$$S(\omega) = F(\omega) * G(\omega) \qquad (6.21)$$

where $G(\omega)$ is the frequency response of the resolution filter. In the super sweep method, we can obtain the spectrum with almost no influence of $H(\omega)$, it is one of the merit against the FFT method.

6.6 Super Sweep Method and Chirp Z-Transform

The super sweep method has a similarity between the Chirp Z-transform. This section discusses about the characteristics.

6.6.1 Theoretical Background

The chirp Z-transform is defined by following equation [3][6] (see Fig.6.11).

$$X(k) = c^{-1}(k)\sum_{n=0}^{N-1} y(n)\cdot c(k-n) \qquad (6.22)$$

where *k* is a discrete frequency, *n* is a discrete time. The function *c(n)* is called 'chirp signal' defined as

$$c(n) = W^{-\frac{n^2}{2}}, \qquad (6.23)$$

where *W* is a 'phase rotation factor' defined as

$$W = W_0 \cdot \exp[-j2\pi\sigma], \qquad (6.24)$$

where W_0 is a constant and σ is a chirp factor for quantified time *n*, which is corresponding to the sweep rate in a sweep spectrum analyzer. And y(n) is a product of *x(n)* and $A^{-n}\cdot c^{-1}(n)$,

$$y(n) = x(n)\cdot A^{-n}\cdot c^{-1}(n), \qquad (6.25)$$

where *x(n)* is discrete measured signal, and 'A' is defined by

$$A = A_0 \exp[-j\theta_0]. \qquad (6.26)$$

The Chirp-Z transform of *x(n)* is *X(k)* defined by Eq.(6.22). The concept of the Chirp-Z transform is drawn as a diagram of Fig.6.11.

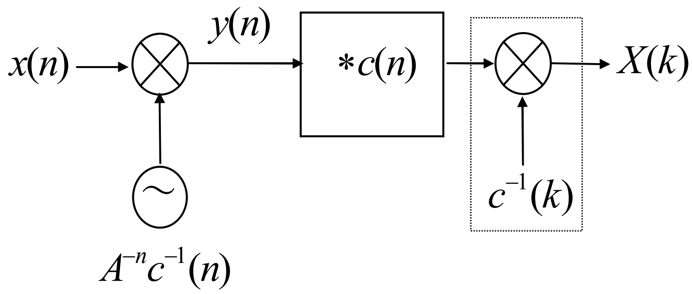

Fig.6.11 Concept of Chirp Z-Transform

The signal $A^{-n}c^{-1}(n)$ of Eq.(6.25) is corresponds to a output of the local oscillator of a sweep spectrum analyzer, *l(t)*, which is explained by

$$
\begin{aligned}
A^{-n}c^{-1}(n) &= A_0^{-n}\exp[-j\cdot n\cdot\theta_0]\times W_0^{\frac{n^2}{2}}\cdot\exp[j\pi\sigma n^2] \\
&= \exp\left[\tfrac{1}{2}n^2\ln(W_0)-n\ln(A_0)\right]\cdot\exp[j\cdot(\pi\cdot\sigma\cdot n^2-n\cdot\theta_0)] \qquad (6.27)\\
&= M(n)\cdot\exp[j\cdot(\pi\cdot\sigma\cdot n^2-n\cdot\theta_0)],
\end{aligned}
$$

where *M(n)* is the amplitude factor. The phase factor is a chirp signal, which has a frequency offset θ_0. In the case that W_0 is less than one, the magnitude takes a form of Gauss function, which has an offset on the time. In the case that $A_0=1$ and $W_0=1$, this signal has constant magnitude.

The signal $y(n)$ corresponds to the IF signal, which is chirped signal; $A^{-n}c^{-1}(n)$. The summation of Eq.(6.22) is assumed as a discrete convolution of $y(n)$ and $c(n)$, and the internal of the summation is explained by

$$
\begin{aligned}
y(n)\cdot c(k-n) &= x(n)A^{-n}\cdot c^{-1}(n)\cdot c(k-n) \\
&= x(n)\cdot M(n)\cdot\exp[j(\pi\sigma\cdot n^2-n\theta_0)]\cdot W_0^{-\frac{1}{2}(n-k)^2}\exp[-j2\pi\sigma(k-n)^2/2] \\
&= x(n)\exp\left(\tfrac{1}{2}n^2\ln(W_0)-n\ln(A_0)+(-\tfrac{1}{2}(n-k)^2)\ln(W_0)\right) \\
&\qquad\times\exp\left[j\left(\pi\sigma\cdot n^2-n\theta_0\right)-j(\pi\sigma(k-n)^2)\right] \\
&= x(n)\cdot\exp\left(-n\ln(A_0)+(nk-k^2)\ln(W_0)\right)\cdot\exp\left[j\left(-n\theta_0+2\pi\sigma\cdot k\cdot n-\pi\sigma k^2\right)\right] \\
&= \exp[-k^2\ln(W_0)]\exp[-j\pi\sigma\cdot k^2]\times x(n)\exp\left(-n\ln(A_0)+nk\ln(W_0)\right) \\
&\qquad\times\exp[-jn(2\pi\sigma k+\theta_0)] \\
&= c(k)\cdot M_1(n)\cdot x(n)\cdot\exp[-jn(2\pi\sigma k+\theta_0)].
\end{aligned}
$$

$\cdots\cdots\cdots\cdots\cdots\cdots\cdots\cdots\cdots\cdots\cdots$(6.28)

The factor dependent on not *n* but *k* is just replaced by $c(k)$, which is modified by Eq.(6.23) and (6.24) as

$$c(k)=\exp\left[-\tfrac{1}{2}k^2\ln(W_0)\right]\cdot\exp\left[-j\pi\sigma k^2\right]. \qquad (6.29)$$

In Eq.(6.22), the factor Eq.(6.29) is rejected by $c^{-1}(k)$, and the magnitude dependent on *n* is replaced by

$$M_1(n) = \exp\left[-n\ln(A_0) + nk\ln(W_0)\right]. \tag{6.30}$$

By above discussion, Eq.(6.22) can be rewritten as

$$X(k) = \sum_{n=0}^{N-1} M_1(n)\cdot x(n)\cdot \exp[-j\cdot n(2\pi\cdot\sigma\cdot k + \theta_0)] \tag{6.31}$$

This equation is a discrete Fourier transform of $M_1(n)\cdot x(n)$, which has frequency offset θ_0, and we could assume $M_1(n)$ to be weighting function. The frequency corresponding to *k* is σk. In the case that $\sigma = 1/N$, $X(k)$ is corresponding to the result of FFT. In the FFT method, the difference between each sample of a frequency is dependent on *N*, and it is *1/N*. In the Chirp Z-transform, the difference is not dependent on *N*. We can decide the difference corresponding to the condition of the system such as the sampling frequency and sweep rate. This ability is one of a merit of the Chirp Z-Transform against the FFT method.

Our experimental system described in chapter 4 was assumed the modified system of Fig.6.11 except for the product of $c^{-1}(k)$. In the experimental system, the mixer and the signal $A^{-n}c^{-1}(n)$ were implemented as an analog mixer and a local oscillator. The convolution of $y(n) * c(n)$ corresponded to the negative chirp filter. The result of the super sweep method had chirp phase factor as shown in Eq.(3.9), which corresponded to the lack of the product with $c^{-1}(k)$. But it is no problem to estimate amplitude of the spectrum. In the most case of measuring a spectrum, the phase factor is not object of the consideration.

We considered that the super sweep method was a derivative processing of the Chirp Z-Transform.

6.6.2 Numerical Analysis

We made a numerical analysis about the phase, Figure 6.12(a) to (e) are the results. The spectrum and I and Q part of the base band signal are shown in Fig.6.12 (a), which corresponds to a CW signal whose frequency was the center of the figure. The vertical full scale is 100dB for the spectrum, and from –1.0 to 1.0 for I and Q part. The measuring condition were SPAN=10kHz, Sweep Time=2msec, and RBW=1kHz.

The I and Q part of the output of the resolution filter (Gaussian negative chirp filter) is shown in Fig.6.12 (b) whose significant level is remained around the center. We obtained the phase factor of (b) by

$$\theta(t) = \tan^{-1}(Q_g(t)/I_g(t)) \ . \qquad (6.32)$$

This phase factor is shown in the figure (c). The line describes a parabola.

The differentiation of the phase is drawn in Fig.(d), it is nearly a line.

The 2nd differentiation of the phase is shown in Fig.(e). It was 5MHz/sec at the center that corresponded to the sweep rate, *Span/Sweep_time*. It was –4.95MHz at the both sides, which was 1% reduction of the sweep rate. We considered the reduction caused by a computing error, because I and Q had not enough accuracy without a error at the both side to operate Eq.(6.32).

By the discussion section 3.2.2 especially Eq.(3.9), we investigated that the phase of the spectrum measure by the new method was chirped, which was caused by the sweep of the local oscillator.

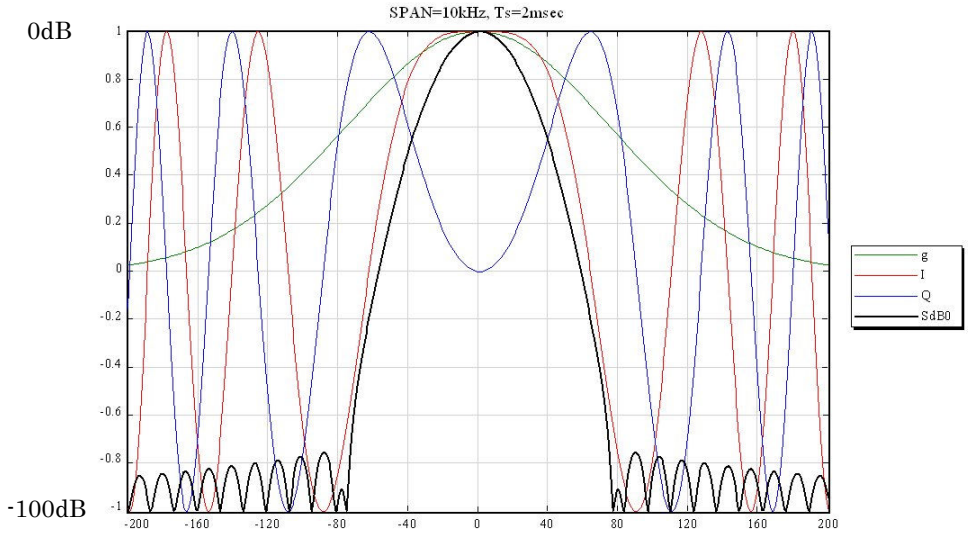

Fig.6.12 (a) Spectrum by Super Sweep Method (SdB), Gaussian Filter (g) And Base Band signal (I and Q)

Measuring condition:

SPAN=10kHz, Sweep Time=2msec, RBW=1kHz

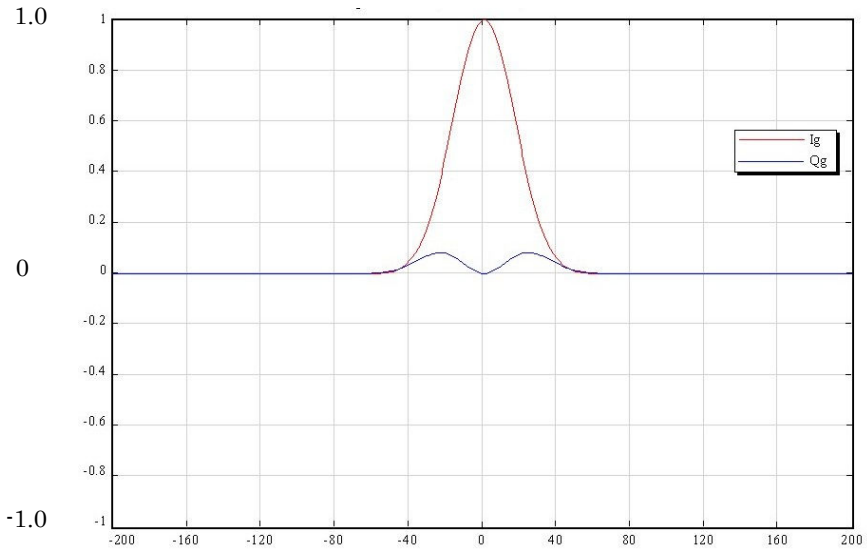

Fig.6.12 (b) I and Q part of the Spectrum in (a)

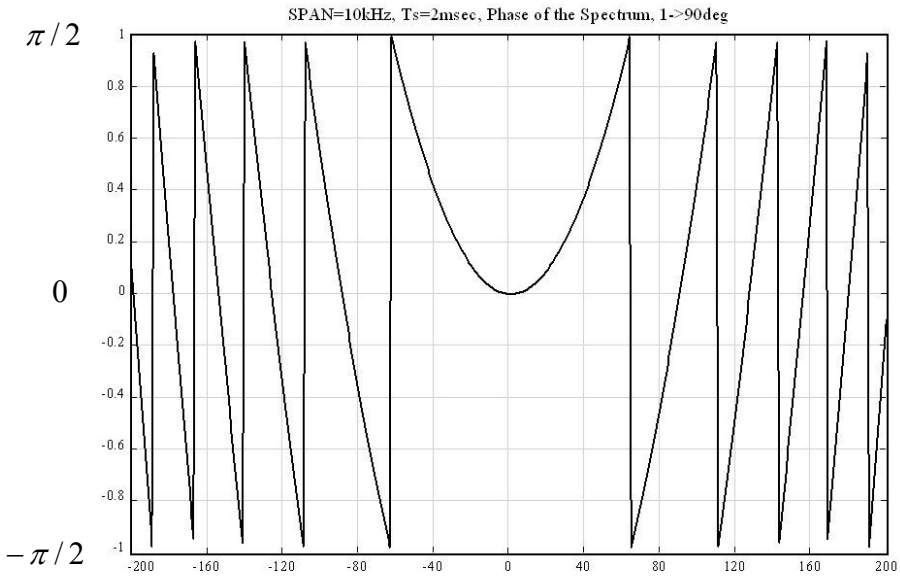

Fig.6.12 (c) Transition of phase of Spectrum in (a)
$\tan^{-1}(Q/I)$ **of (b)**

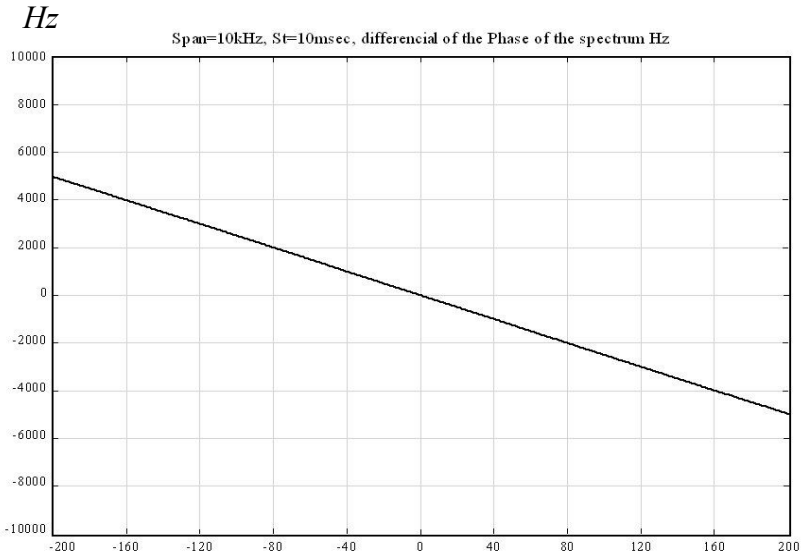

Fig.6.12 (d) Differentiation of phase in (b)

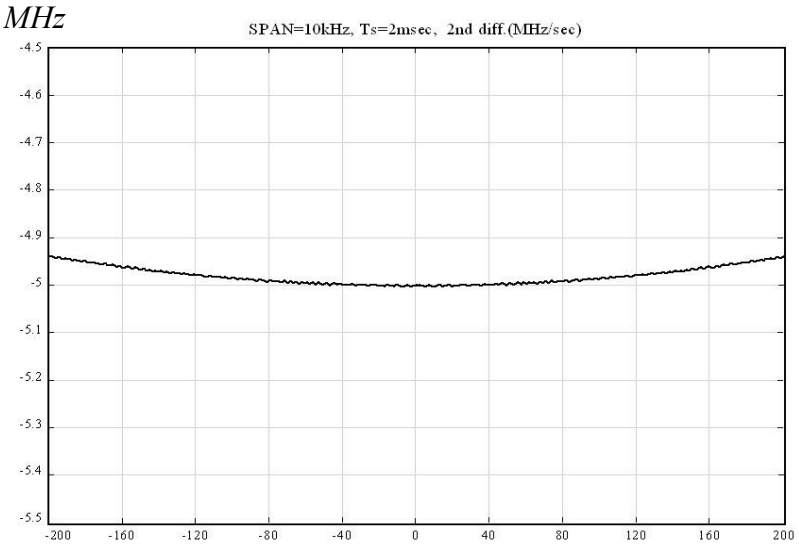

Fig.6.12 (e) Second differentiation of phase in (b)

6.6.3 Numerical Analysis of a Sweep Method

In a conventional sweep method, the spectrum is assumed to have chirp factor as shown in Eq.(2.31-c).

$$S(t) = \exp[\,j(\pi\sigma t^2 + \omega_0 t + \theta_0)] \times \int_{-\infty}^{\infty} g(\tau) f(t-\tau) \times \exp\left\{j\left(\pi\sigma\ \tau^2 - 2\pi\sigma\ t - \omega_0\tau\right)\right\} d\tau$$
$$= l(t) \int_{-\infty}^{\infty} g(\tau) f(t-\tau) \times \exp\left\{j\left(\pi\sigma\ \tau^2 - 2\pi\sigma\ t\tau - \omega_0\tau\right)\right\} d\tau \qquad \text{(2.31-c)}$$

We achieved a numerical analysis for the sweep method and verified the existence of the chirp factor as shown in Fig.6.13(a) to (c). The second differentiation of the phase is obtained by the same processing of Fig.6.12 (e), it was 500kHz per one second and it accorded with the sweep rate σ ,

$$\sigma = \frac{Span}{Sweep\ Time} = \frac{10kHz}{2m\,\mathrm{sec}} = 500kHz\,. \qquad (6.33)$$

The property of spectrum of two method, sweep and super method were similar, such as phase factor and the parabolic figure. While the sweep method has a restriction on the sweep rate, the super sweep method has not it.

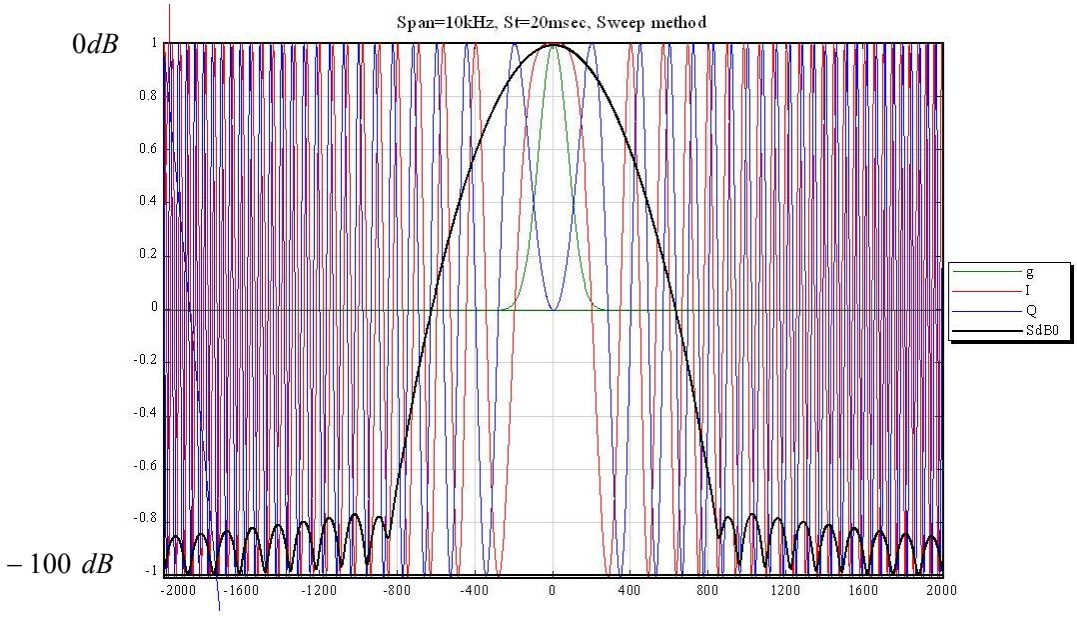

Fig.6.13 (a) Spectrum by Sweep Method (SdB), Gaussian Filter (g) and Base Band signal (I and Q)

Measuring condition:

SPAN=10kHz, Sweep Time=20msec, RBW=1kHz

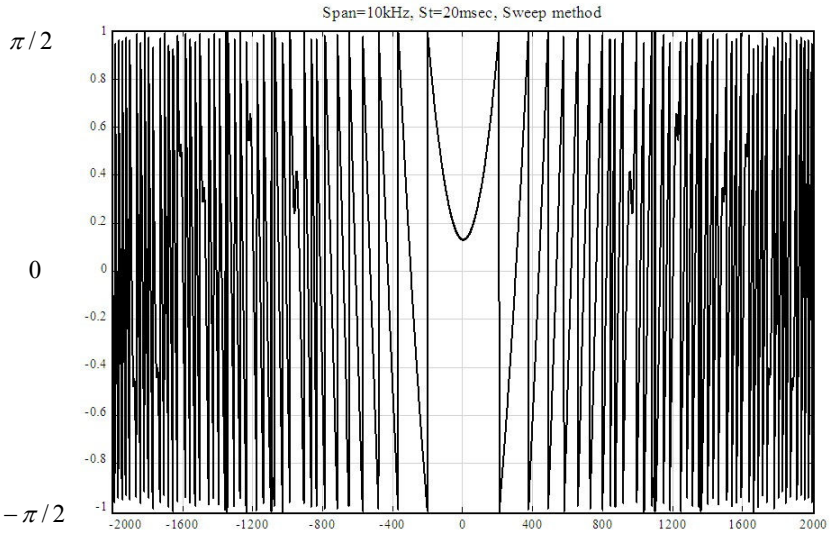

Fig.6.13 (b) Transition of phase of Spectrum of (a)

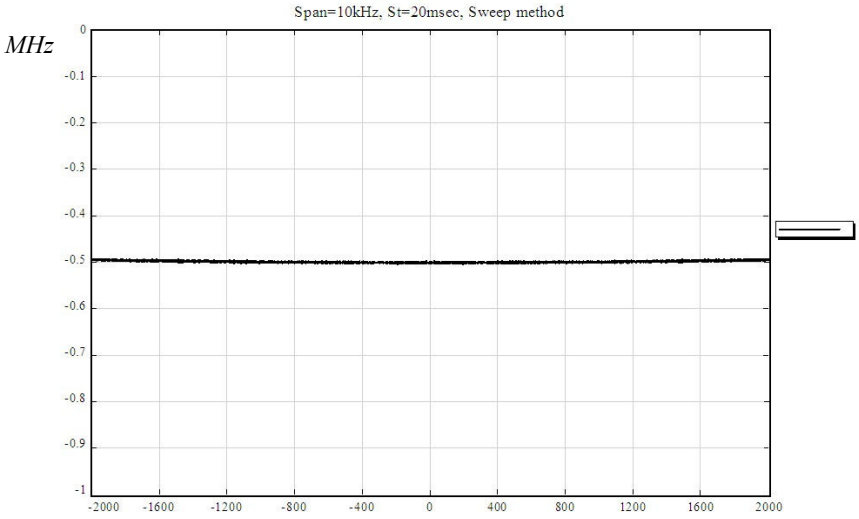

Fig.6.13 (c) Second differentiation of phase in (b)

6.7 Response against two-tone signals

The analysis of the spectrum of two-tone signals in the sweep method is described in section 2.5.7. This section describe the result of the experiment whose condition were same to section 2.5.7 except for measurements by the super sweep method.

The experiments were done by a numerical analysis. The measured signals were assumed as Eq.(2.59).

$$f(t) = \frac{1}{2}\left(\exp[-j(\omega_0 t + \pi\Delta f \times t + \theta_0)] + \exp[-j(\omega_0 t + \pi\Delta f \times t)]\right) \qquad (2.59)$$

where the frequency differences of the two-tone signal were $\Delta f(Hz)$, ω_0 was the carrier frequency. The spectrum were obtained as

$$S_n(t) = g_n(t) * \{f(t) \times l(t)\}, \qquad (3.2)$$

where *l(t)* is the swept signal, which is given by

$$l(t) = \exp[\, j(\pi\sigma \cdot t^2 + \omega_0 t)]$$

Then Eq.(3.2) is explained by

$$S_n(t) = g_n(t) * (1/2)\{\exp[\, j(\pi \cdot \sigma t^2 + \pi\Delta f\, t + \theta_0)] + \exp[\, j(\pi \cdot \sigma t^2 - \pi\Delta f\, t)]\} \qquad (6.34)$$

The experiment conditions of Fig.6.14 are shown in Table 6.3.

Table 6.3 Experimental conditions of Fig.6.12

	Sweep Time	Frequency differences of two tone signals	Span	Rbw
(a)	2 msec	1500Hz	10kHz	1kHz
(b)	2 msec	1000Hz		
(c)	10 msec	1500Hz		
(d)	10 msec	1000Hz		

We computed two spectrums for each figure. The spectrums are indicated by two bold black lines whose difference of initial phase between the two tones are 0 and π radian, they are indicated as “SdB 0” and “SdB 1”, respectively. The most part of two lines are overlapped together except around the center. The real part and imaginary part of the measured signal, which is corresponding to Eq.(6.34) are indicated in red and blue lines, and they correspond to “SdB1”. The green lines indicate the impulse response of Gaussian filters (RBW=1kHz).

In a traditional sweep method, the sweep rate is restricted and the sweep time was 20msec in the condition of Fig.2.25. In the condition of Table 6.3 and Fig 6.14, the sweep rate were 10 times faster in (a) and (b), and 2 times faster in (c) and (d) than the cases of Fig.2.25, respectively. In Fig.6.14, we obtained same spectrums with Fig.2.25. The frequency of the beat note in Fig.6.14 is fewer as faster as the sweep rate faster. We observed the same spectrums with the different sweep rates. The results of Fig.6.14 verify the new method that broke the restriction of the sweep rate.

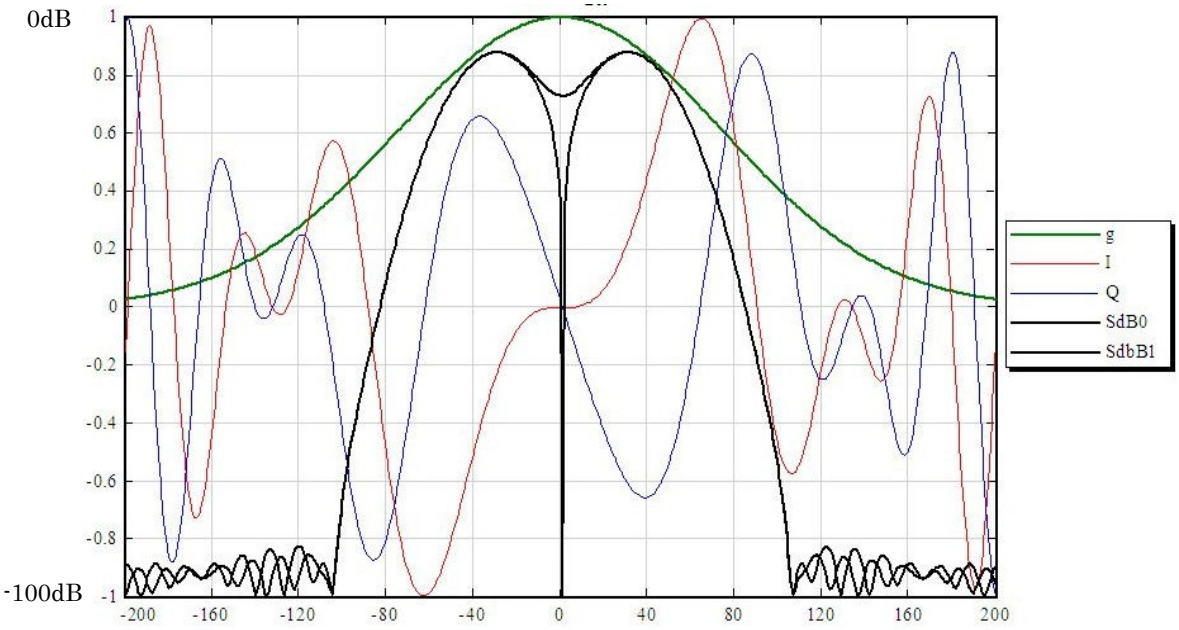

Fig.6.14 (a) Spectrums of two signals, ⊿f=1500Hz

Sweep Time 2msec

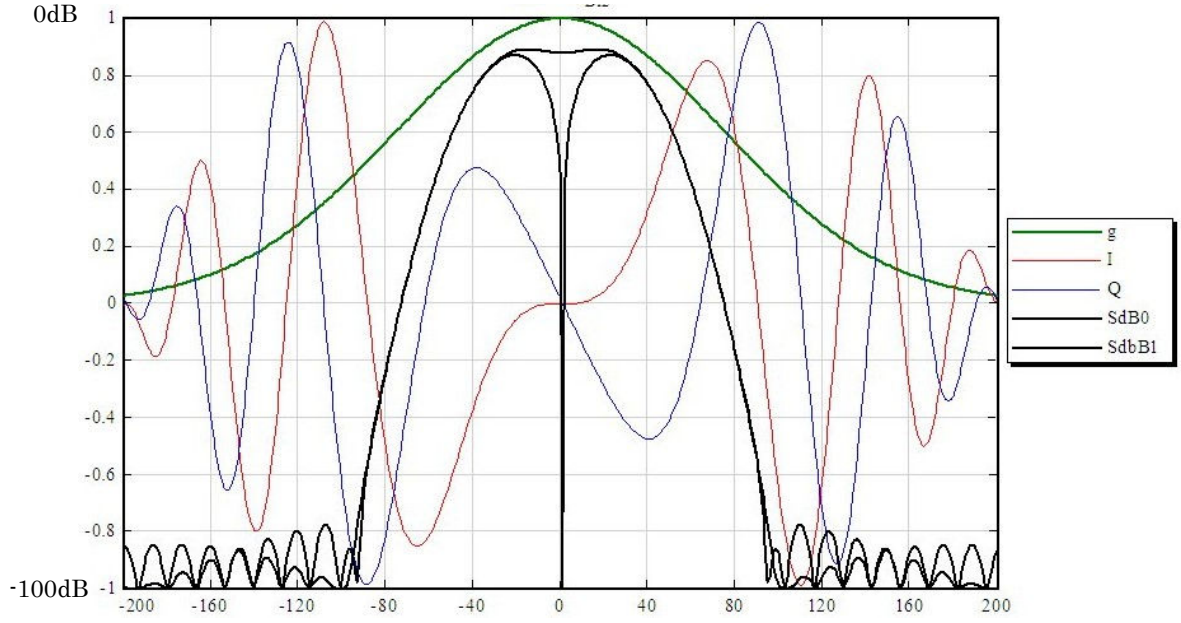

Fig.6.14 (b) Spectrums of two signals, ⊿f=1000Hz

Sweep Time 2msec

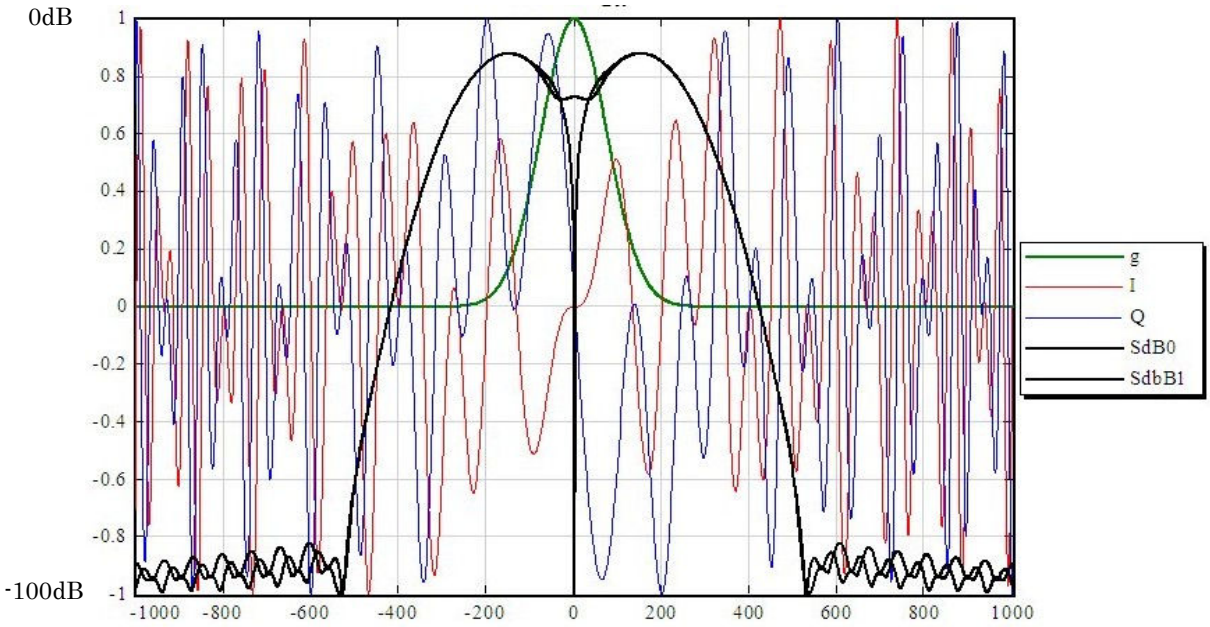

Fig.6.14 (c) Spectrums of two signals, ⊿f=1500Hz

Sweep Time 10msec

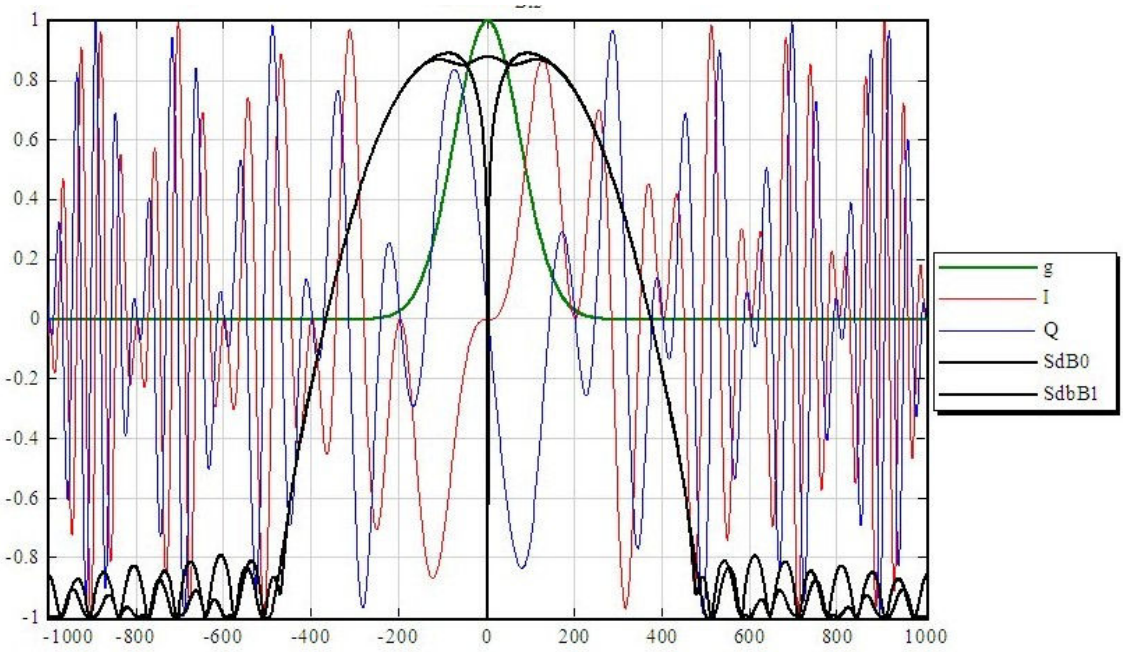

Fig.6.14 (d) Spectrums of two signals, ⊿f=1000Hz

Sweep Time 10msec

6.8 Influence of the noise

6.8.1 Noise in Spectrum analyzers

In a spectrum analyzer, the signal before the A/D converter thorough passes several analog circuits such as mixers (MIX), amplifiers (AMP) and some filters. These analog circuits produce noise, which appears on the spectrum. The concept of the noise produced in the analyzer is shown in Figure 6.15, which shows the signal process from the input to the RBW BPF. The phase noise produced by the local oscillator is a one of the representative noise. The influences upon the spectrum were difference corresponding to the sources of the noise; local oscillator, before or after the mixer, and before or after the Amplifier etc.

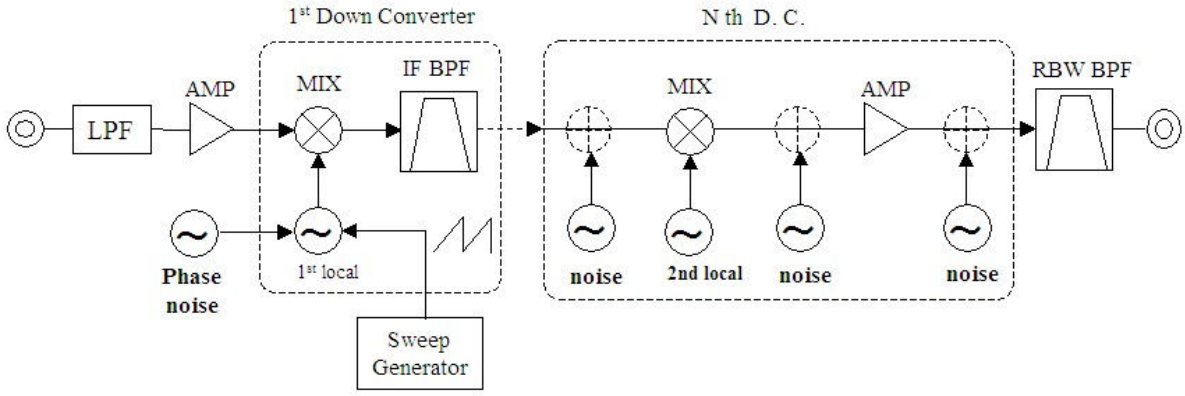

Fig.6.15 Model of noise of spectrum analyzers

6.8.2 Phase Noise of the local oscillator

In some measurement conditions of sweep spectrum analyzers, we can observe the phase noise of local oscillator on the sideband of the peak. One example is shown in Fig.6.16. The mathematical model of spectrum measured by a sweep spectrum analyzer is Eq.(2.31-b).

$$S(t) = \int_{-\infty}^{\infty} g(\tau) f(t-\tau) \times \exp\left\{- j\left(\pi \cdot \sigma(t-\tau)^2 + \omega_0 (t-\tau) + \theta_0\right)\right\} d\tau \qquad (2.31\text{-b})$$

We can make the noise as $\theta(t)$ instead of θ_0. The spectrum with the noise is explained by

$$S(t) = \int_{-\infty}^{\infty} g(\tau) f(t-\tau) \times \exp\left\{j\left(\pi \cdot \sigma(t-\tau)^2 + \omega_0 (t-\tau) + \theta(t)\right)\right\} d\tau \quad (6.35\text{-a})$$

This equation can be modified as

$$S(t) = \int_{-\infty}^{\infty} g(\tau) f(t-\tau) \times \exp[j\theta(\mathrm{t})] \times \exp\left\{j\left(\pi \cdot \sigma(t-\tau)^2 + \omega_0 (t-\tau)\right)\right\} d\tau \qquad (6.35\text{-b})$$

We cannot distinct whether the phase noise is including in the local oscillator or the signal *f(t)* by watching the spectrum.

The two overlaid spectrums are shown in Fig.6.16, one is obtained by SPAN=60kHz, and another is obtained by SPAN=59.9kHz whose noise-level is lower. The level of the phase noise of local oscillator was changed corresponding to the configuration of the oscillator [8]. The super sweep method has high sensitivity for the phase noise. The system that employs the super sweep method should be configured to have a lower phase noise.

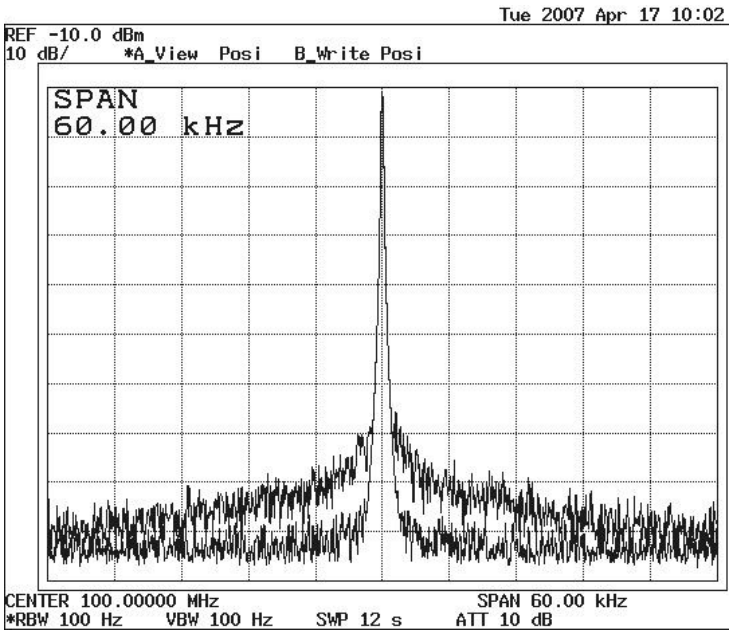

Fig.6.16 Phase noise of Sweep Spectrum Analyzers

6.8.3 Noise in the IF signal

This section reports and discusses about the noise of the IF signal. The deformed diagram of our experimental system is shown in Fig.6.17, which was described in chapter 4, where a few examples of the measurement are shown.

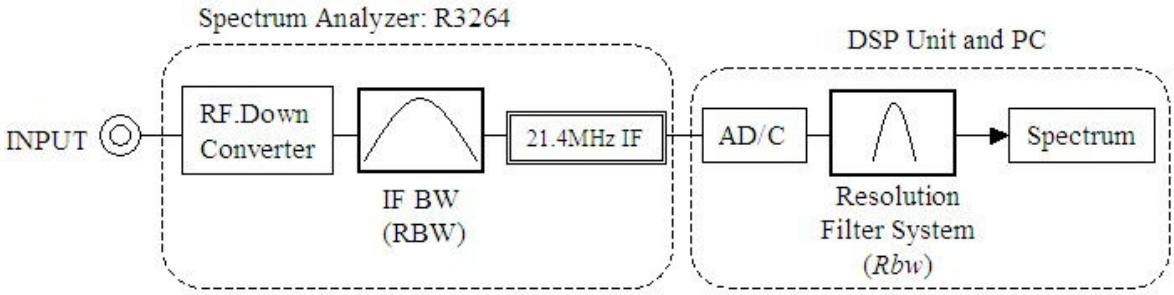

Fig.6.17 Deformed diagram of our experimental system

In Figure 6.18, the SPAN was 3MHz. In Fig.6.18 (a) and (b) the RBW was 3kHz. In Fig. (c) the RBW was 30kHz. The IF-bandwidth (RBW of R3264) was 30kHz in (a), 300kHz in (b) and (c), respectively. The sweep time of (a) and (b) were 70msec and it of (c) was 20msec.

In the case that the IF-bandwidth was 300kHz, the spectrum had high level of noise around its peak. The bandwidth and figure of these noise were according with the IF band pass filter (RBW of the R3264). If the noise was caused by a phase noise of the local oscillator, the figure of the noise was not dependent the IF band pass filter.

We considered that some very wide band noise existed in the IF-signal front of the IF band pass (RBW) filter, and the IF-signal included the wideband noise. The negative chirp filter pass the part of signal whose frequency was under the pass band. If the SNR of the IF signal was not enough for the dynamic range required on the measurement, the noise would remain in the spectrum as shown in Fig.6.19. This discussion has not been verified. It is our task for the future.

By the above discussion, we considered that we should choose the IF-bandwidth (RBW of the spectrum analyzer R3264) as narrower as we can to reduce the noise around the peak. But it needs wider IF-bandwidth to obtain faster sweep rate but the noise would enlarge. It is essential solution to develop the signal pass with satisfactory SNR.

In our experimental system, the pass band of the DDC was configured to be wider than the IF-bandwidth and the *Flt* was decided by the IF-bandwidth.

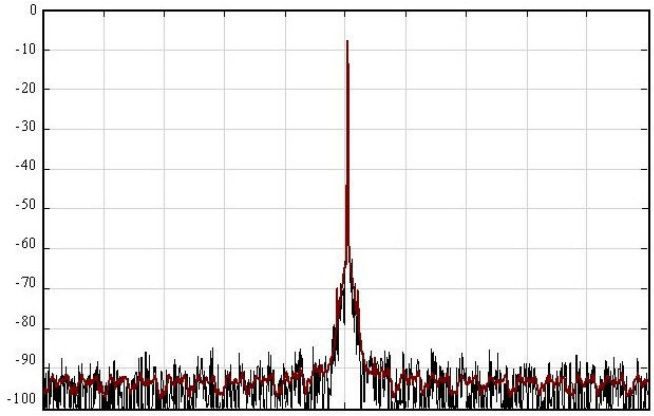

(a) SPAN=3MHz, RBW=3kHz, IF-Bandwidth=30kHz, St=70msec

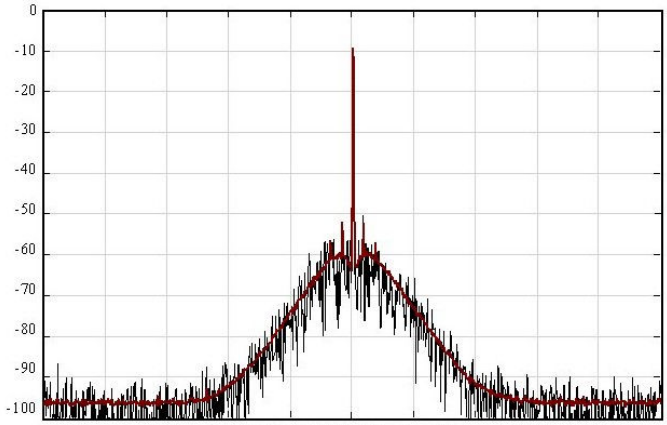

(b) SPAN=3MHz, RBW=3kHz, IF-Bandwidth=300kHz, St=70msec

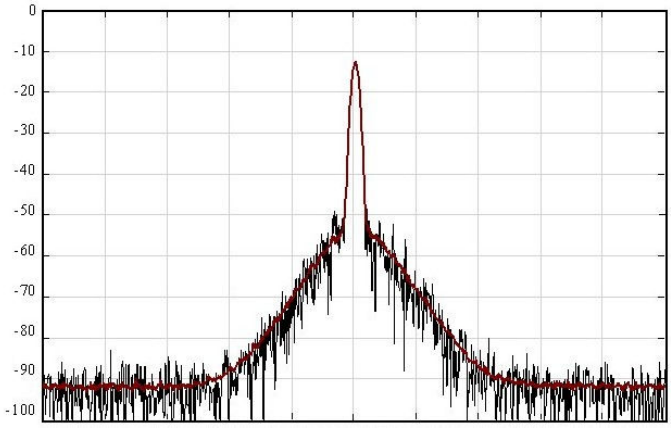

(c) SPAN=3MHz, RBW=30kHz, IF-Bandwidth=300kHz, St=20msec

Fig.6.18 Obtained Spectrums using Super Sweep Method

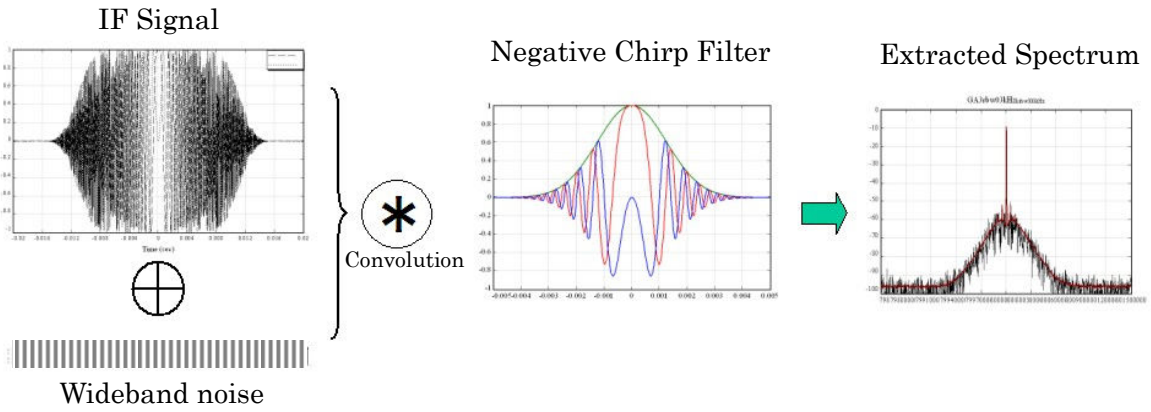

Fig.6.19 Noise of IF signal and Spectrum

6.9 Examples of Spectrums

To demonstrate the special feature of the new method, some result of measurements are presented in Fig.6.20～6.23(b). These results were obtained as the numerical data from the experimental system. We took four samples of the RBW were 1Hz, 100Hz, 1kHz and 100kHz and describes their futures in following sections.

6.9.1 RBW 1Hz

It is difficult to make the RBW filter of 1Hz by analog circuit. We achieved the filter as a digital filter of the new method. In traditional sweep method, the sweep time of the conditions, whose *Span* is 500Hz and *Rbw* is 1Hz, are approximately 1000 sec. In the super sweep method it was 2.88sec, which is about 350 times faster than the sweep method. The one result of measurement is shown in Fig.6.20.

In Fig.6.20, three spectrums, A, B, and C are results of measuring a CW signal. The spectrum A has some spurious peaks called 'Ham noise', which was caused by the frequency 50Hz of the AC power supply. The spectrum B is the result of no input, which shows the noise floor of the system. The spectrum C is the averaged (32 times) data of B. The data C indicated the noise floor approximately –124dBm. The to level the scale was 0dBm. This result investigated that the dynamic rage of the system was larger than 120dB.

It needs large margin of the sweep time and span to achieve the fast sweep (see section 6.4.2). The span and sweep time of the local oscillator was approximately twice for the result of the spectrum.

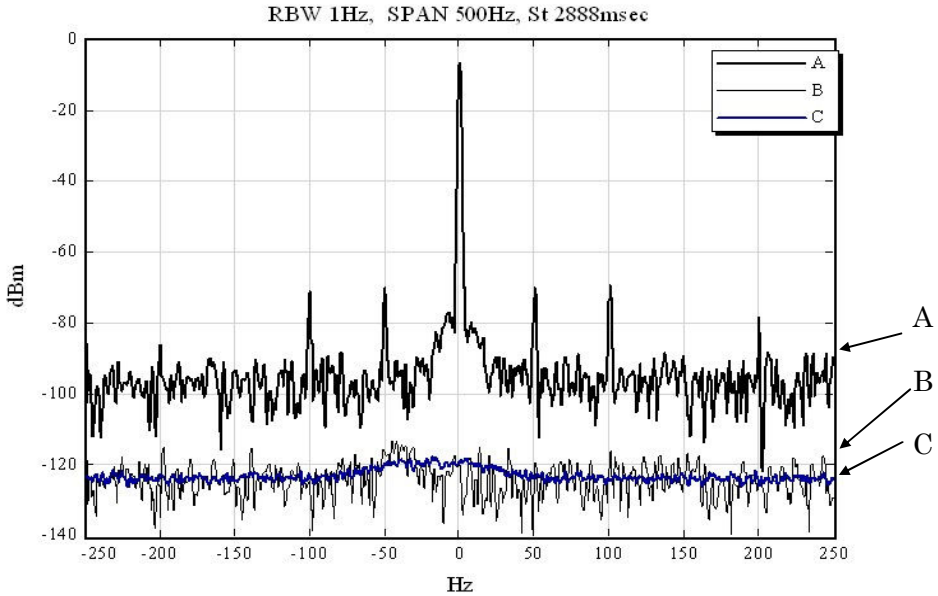

Fig.6.20 Spectrum with RBW 1Hz

SPAN=500Hz, St=2888msec, IF-bandwidth=300Hz,
(R3264 Set up: SPAN=1kHz, RBW=300Hz, St=5.8sec, CF=500MHz)
In a traditional method, it needs approximately 1000sec of the sweep time.

6.9.2 RBW 100Hz

This section shows the improvement of the dynamic range. In Figure 6.21, four spectrums are shown. The spectrum ①~③ were the result of measuring a CW signal, ④ was result with no input signal. The spectrums ① and ② were measured by the spectrum analyzer R3264 with RBW 1kHz and 100Hz, respectively. The sweep time of ① and ② was 0.2sec and 20sec. The spectrum ③ and ④ were measured by the super sweep method, whose RBW was 100Hz and the sweep time was 665msec. In the case that RBW was 100Hz, the new method achieved 30 times faster than R3264.

These spectrums were obtained with average mode (32 times) to get a comparison of the noise level. In the super sweep method, level of the noise were –100dBm or under. The noise floor of ② is limited at –97dBm.

When the reference level was -10dBm, the noise floor of R3264 were larger than –97dBm. It corresponded to specification of the LOG amplifier included in the R3264. The new method improved the limit of noise floor by the digital signal processing. The level of ③ indicated the noise floor with RBW 100Hz. It was approximately –112dBm.

Note) Unfortunately, it seemed there were non-Gaussian noise, which caused a cyclic noise waves on ③ and ④.

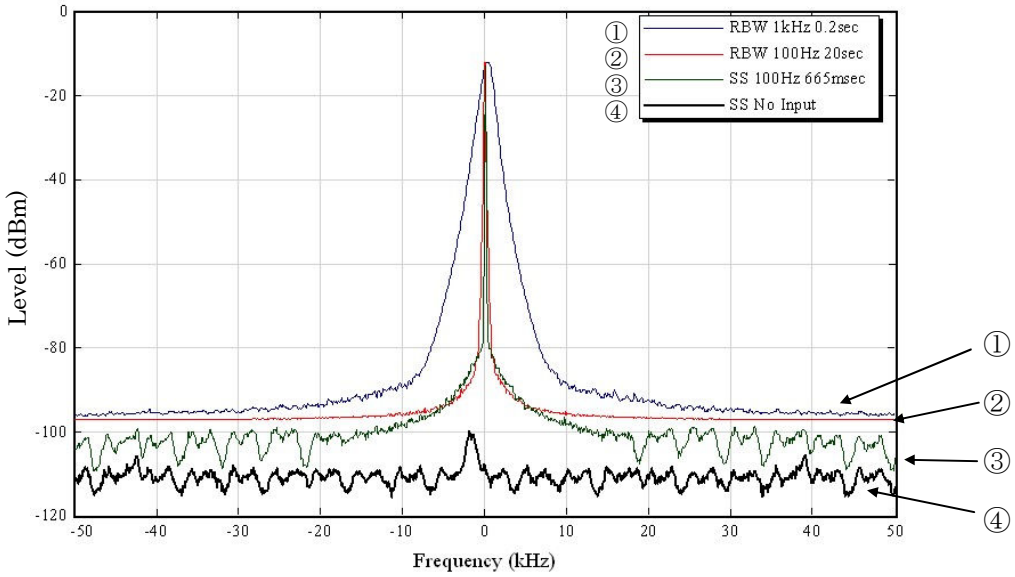

Fig.6.21 Spectrum with RBW 100Hz and 1kHz, SPAN100kHz

(R3264 Set up of ③and ④ : SPAN=111.1kHz, RBW=3kHz, St=740msec, CF=500MHz)

6.9.3 RBW 1kHz

Figure 6.22 (a) shows a spectrum of a FM signal; the deviation was 2MHz and the modulation frequency was 30kHz, the Span was 4MHz, RBW was 1kHz, and the sweep time was 693msec. The sweep time of R3264 for same SPAN and RBW is 8.4sec. New method was 12 times faster than R3264.

The signal consisted of many side lobes whose intervals were 30kHz. The spectrum shown in Fig.6.22 (b) is an extended spectrum of Fig.6.22 (a), whose span was 400kHz. The sweep time of (a) was 693msec.

In a traditional spectrum analyzer, the condition RBW 1kHz is too fine for SPAN 4MHz, because the displays of these analyzers are usually 1001 points. Our experimental system was designed that the display point were 30,000 point in maximum. The spectrum of (a) was given enough size of data and the resolution to drew the spectrum (b), which is drawn from the data of (a). We were able to observe the two spectrums in one measurement (see section 6.3). Traditional spectrum analyzers cannot measurements of (a) and (b) in one time.

Note: The setup of R3264 for Fig.6.22 is shown in the supplementation. The Span and Sweep Time had a margin, which were about 5 percent wider and longer than Fig.6.22(a). See section 6.4.2.

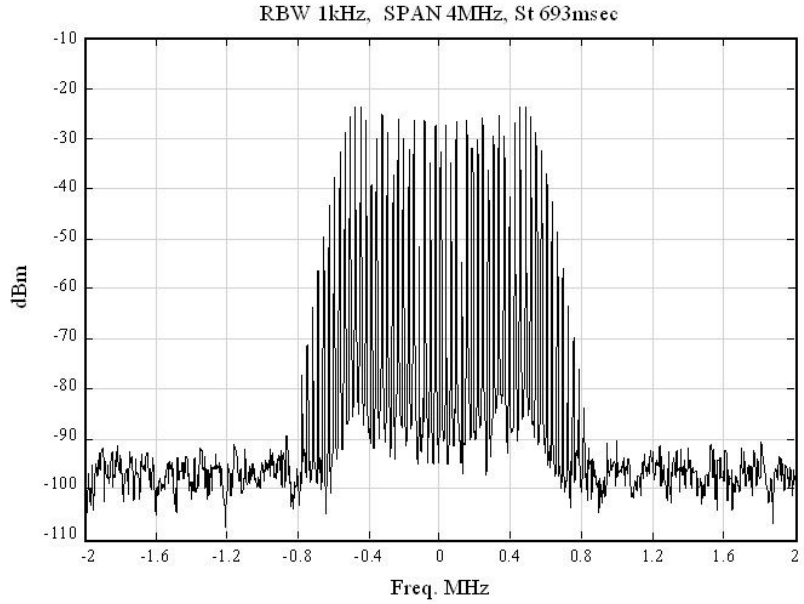

Fig.6.22 (a) Spectrum with RBW 1kHz , SPAN4MHz

St=693msec, IF-bandwidth=10kHz,
(R3264 Set up: SPAN=4.176MHz, RBW=10kHz, St=730msec, CF=500MHz)
The sweep time of R3264 for same SPAN and RBW is 8.4sec.

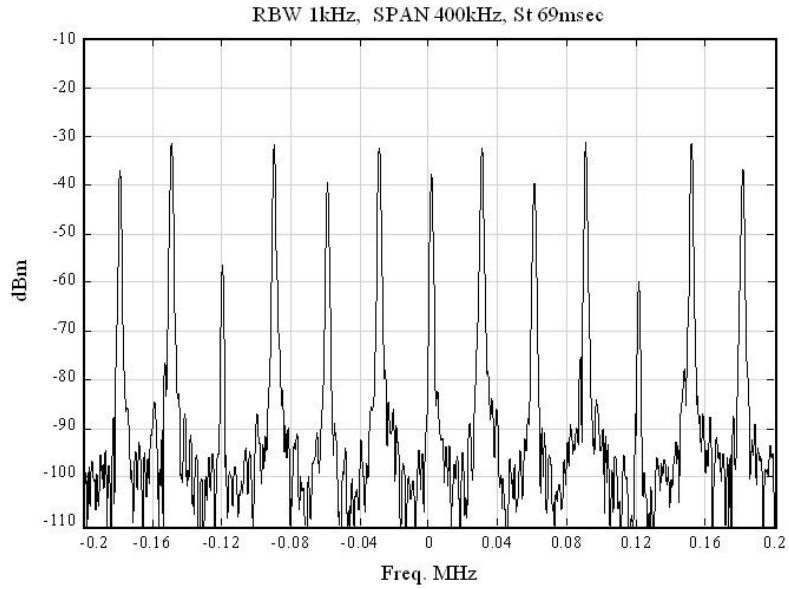

Fig.6.22 (b) Spectrum with RBW 1kHz , SPAN400kHz

Around the center of Fig.6.21(a)

6.9.4 RBW 100kHz

The maximum RBW of our experimental system was 100kHz. An example of spectrums measured with RBW 100kHz is shown in Fig.6.23 (a) and (b). The sweep time of (a) was 14msec. In the same condition, the sweep time of R3264 is 200msec. The new method achieved the sweep 10 times faster than the conventional way.

In the FFT method described in section 2.9, it needs several times of stepping up the local oscillator to measure for such a wide span, and it needs the so long setting time and operation time of the DSP. Some spectrum analyzers implemented the FFT method using a DSP, such as FSU series produced by R&S Co., achieves the fast sweep up to RBW 1kHz or 3kHz. For wider RBW than 3kHz, the measurement rate is not faster than the sweep method.

Our experimental system achieved not only a fast sweep rate with RBW 100kHz but also obtained the sufficient and seamless information of the spectrum. Figure 6.23 (b) shows the part of (a), whose span is 100MHz and the center frequency is 500MHz. In Figure (b), the sample points are indicated by small dots. We can see the spectrum with the resolution of 100kHz as any part of (a).

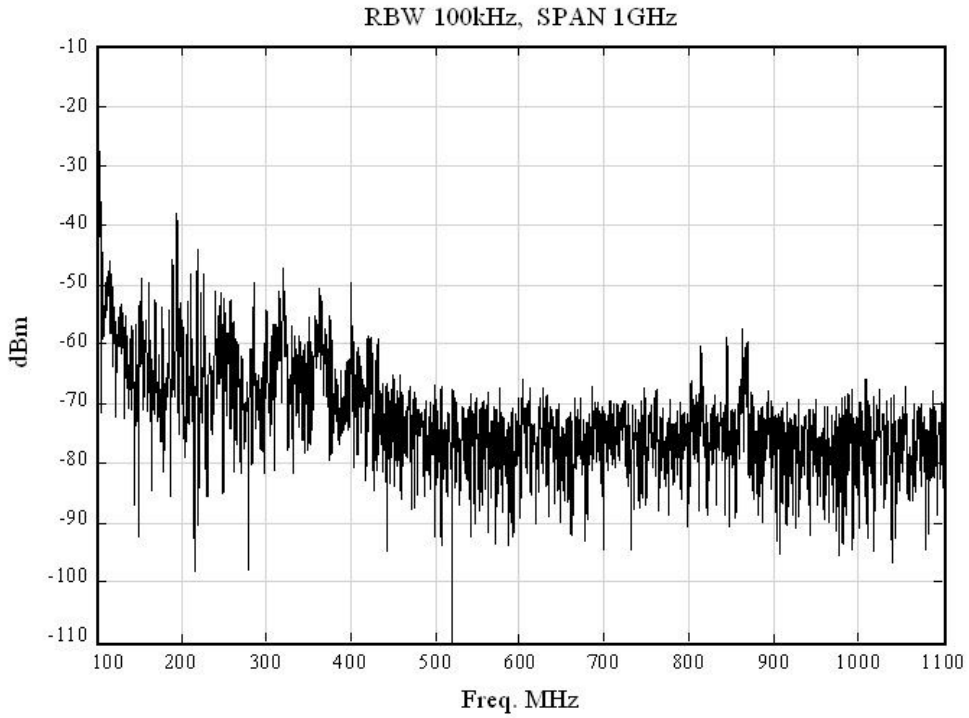

Fig.6.23 (a) Spectrum with RBW 100kHz , SPAN 1GHz

St=34msec, IF-bandwidth=1MHz,
(R3264 Set up: SPAN=1.18GHz, RBW=1MHz, St=40msec, CF=500MHz)
The sweep time of R3264 for same SPAN and RBW is 200msec.

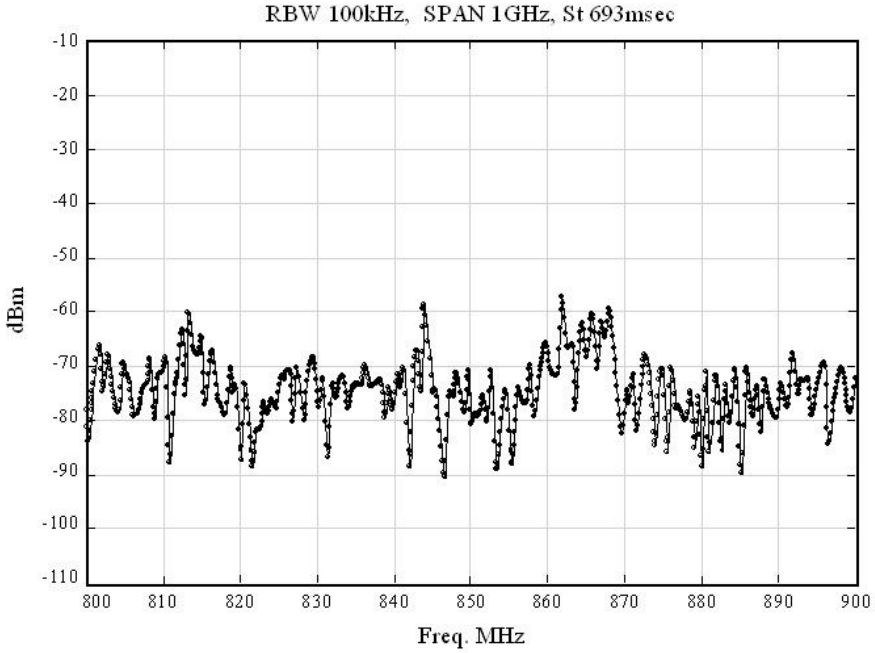

Fig.6.23 (b) Spectrum with RBW 100kHz , SPAN 100MHz

6.10 View of spurious peaks

The spectrum analyzer used in our experiment had some spurious peaks at the condition as shown in Fig.6.24 (a). In the super sweep method the spurious peaks existed too, but the levels were lower and the observed bandwidth were broader than the peaks of Fig. (a) as shown in Fig. (b).

Figure 6.24 (c) shows the overlapping spectrums as a part of (a) and (b). The start frequency is –1kHz, and stop frequency is 13 kHz, where the spectrum of (b) is drawn as bold line and (a) is drawn as thin line.

The peaks at the center frequency of (a) and (b) had no broadening of the resolution and had no level reduction. But the spurious peaks of (b) were broadened and the levels were reduced. These figure of the spurious peaks are similar to the over sweep-rate response.

We hypothesized that the input signal or the output of the local oscillator had some harmonics and the frequency of them were given by

$$\omega_{spurious} = n \cdot \omega_l + m \cdot \omega_{IN} , \qquad (6.36)$$

where ω_l was the frequency of the local oscillator, ω_{IN} was the frequency of input signal, and n and m are arbitrary whole numbers. In the model of Fig.2.5, n was one and m was minus one. The new method worked on the assumption that the value n and m were known. Especially in our experiment, n and m were one and minus one. In the case that any signal produced by another value of n and m, the negative chirp filter could not cancel the chirp factor of the input signal and the Eq. (3.10);

$$| S_n(t) | = | G^*(\omega(t) - \omega_s) * F(\omega(t)) | \quad ; \qquad (3.10)$$

could not be accomplished.

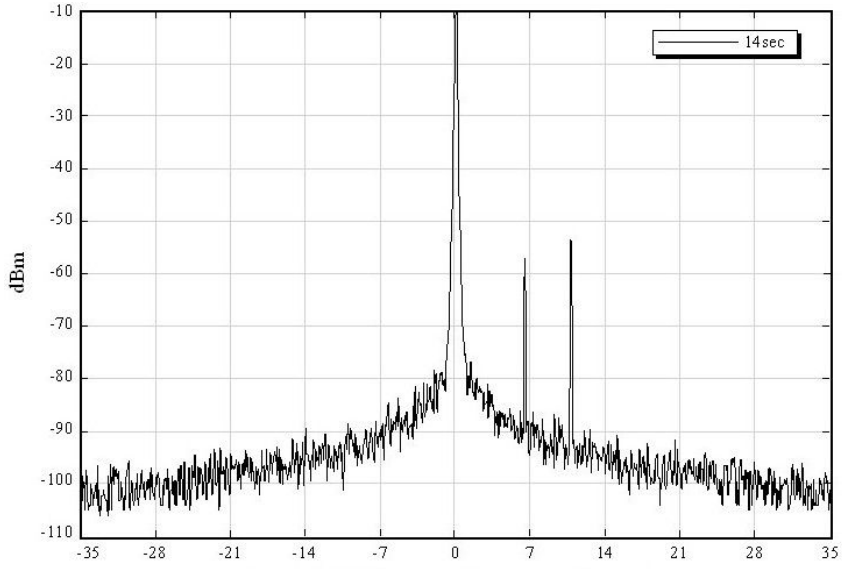

Fig.6.24 (a) Spectrum measured by R3264

CF 30MHz, RBW 100Hz, SPAN 70kHz, T_S 14sec

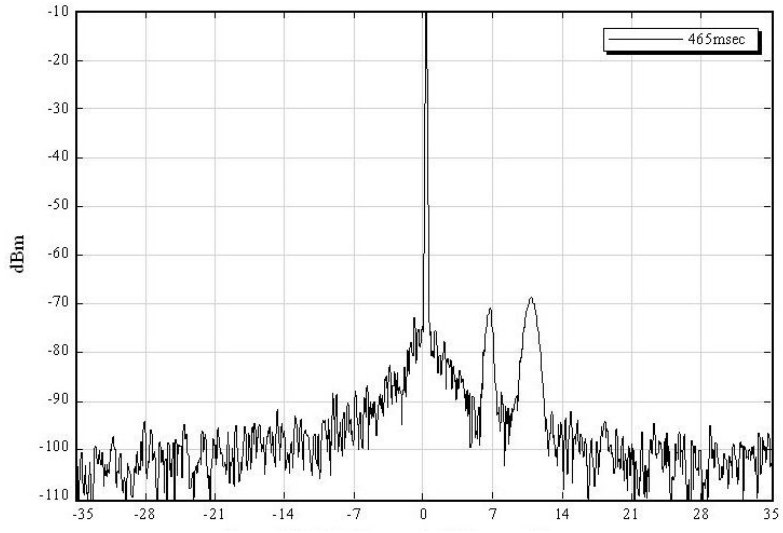

Fig.6.24 (b) Spectrum measured by Super sweep method

CF 30MHz, RBW 100Hz, SPAN 70kHz, T_S 465msec

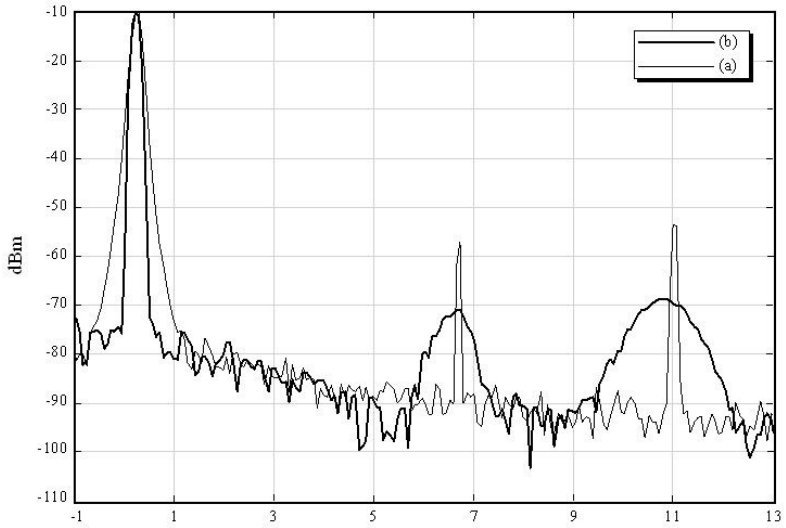

Fig.6.24 (c) Over lay of Spectrums of (a) and (b)

The expanded spectrum around the spurious peaks
whose frequency was –1kHz to 13kHz (Span 14kHz) of (a) and (b)

We assumed that n of the spurious signal in Eq.(6.36) was –1 and the frequency was given by

$$\omega_{Spurious} = -\omega_l + m \cdot \omega_{IN} \quad . \tag{6.37}$$

And the signal, $f_{SP}(t)$ which corresponds to this frequency, is explained by

$$f_{SP}(t) = A_{SP}(t) \cdot \exp[j(-\sigma \cdot t^2 + m \cdot \omega_{IN} t)], \tag{6.38}$$

where $\sigma \cdot t^2 = \omega_l$. The time-frequency diagram of the signal is shown in Fig.6.25. There are two types of the chirp signals, a normal chirp and an inversed chirp. In a sweep method, both signals give same response thorough the RBW filter, because the chirp rates of both signals are same. In the super sweep method, we obtained the spectrum $S_{SP}(t)$ from the signal $f_{SP}(t)$ as the convolution of $f_{SP}(t)$ and the negative chirp filter, $g_n(t)$. And the convolution is explained by

$$\begin{aligned}
&S_{SP}(t) = g_n(t) * f_{SP}(t) \\
&S_{SP}(t) = \{g(t)\exp[-j\pi\sigma t^2]\} * \{A_{SP}(t) \times \exp[j(-\pi\sigma t^2 + m\omega_{IN} t)]\} \\
&\quad = \int_{-\infty}^{\infty} \{g(\tau) \cdot \exp[-j\pi\sigma\tau^2]\} \\
&\qquad \times \{A_{SP}(t-\tau)\exp[j(-\pi\sigma(t-\tau)^2 + m\omega_{IN}(t-\tau))]\} d\tau \\
&\quad = \exp[j(-\pi\sigma t^2 - m\omega_{IN} t)] \\
&\qquad \times \int_{-\infty}^{\infty} g(\tau) A_{SP}(t-\tau) \times \exp[j(-2\pi\sigma\tau^2 + (2\pi\sigma t - m\omega_{IN})\tau)] d\tau \, .
\end{aligned} \tag{6.39}$$

Where the amplitude of the term of τ^2 is twice in comparison with Eq.(2.31-c). These terms were causes of the over sweep-rate response. As a result, in the super sweep method, we were able to distinguish the spurious peaks. This characteristic does not exist in a traditional sweep method.

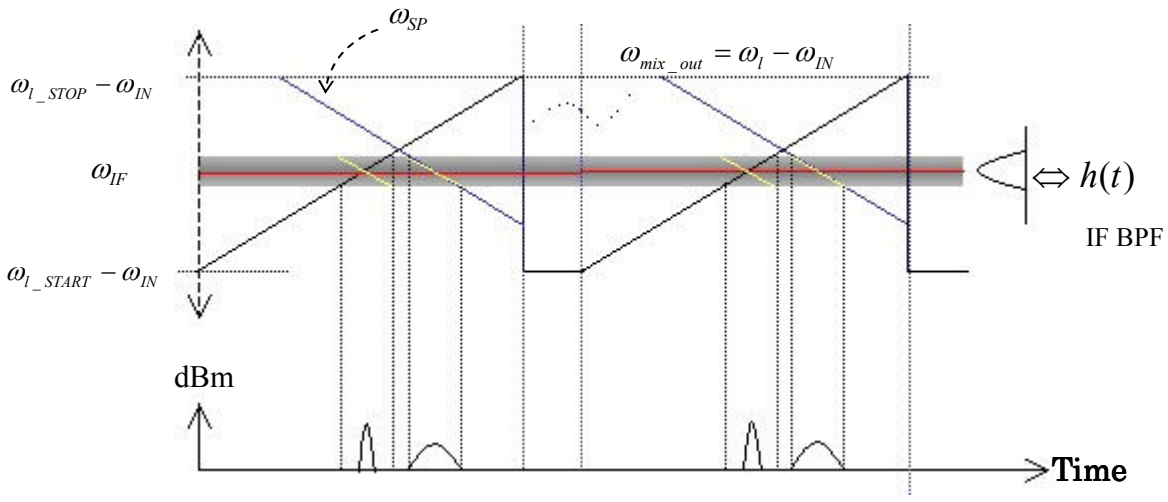

Fig.6.25 Time/Frequency Diagram of IF signal and resolution filter

6.11 Comparison of the methods

This thesis describes the three methods to measure a spectrum, the FFT, the sweep, and the super sweep. Chapter 2 described about the sweep method. Some sub-sections of Chapter 2 described about the FFT method. Chapter 3 and the following chapters described the future of the super sweep method. Some representative features of the methods are shown in Table 6.4. This table compares the parameters of columns on the assumption that the RBW is same.

Table 6.4 Comparisons of spectrum measurement methods

<table>
<tr><th rowspan="2"></th><th rowspan="2">Final Analog IF Bandwidth (α >1)</th><th colspan="2">Measurement Time</th><th rowspan="2">Influence Of the IF Filter</th><th rowspan="2">Abscissa</th></tr>
<tr><th>Narrow SPAN</th><th>Wide SPAN</th></tr>
<tr><td>Sweep Analog IF</td><td>RBW</td><td rowspan="2">SPAN/ σ
$\sigma \propto RBW^2$</td><td rowspan="2">SPAN/ σ
(Single Sweep)</td><td rowspan="2">None</td><td rowspan="2">Frequency and Time</td></tr>
<tr><td>Sweep Digital IF</td><td rowspan="3">$\alpha \cdot RBW$</td></tr>
<tr><td>Super Sweep</td><td rowspan="2">SPAN/ σ
$\sigma \propto RBW$</td></tr>
<tr><td>FFT With RF Down-converter</td><td>Span/ σ + β
(Multi Sweep)</td><td>Ripple on Spectrums</td><td>Frequency</td></tr>
</table>

Final Analog IF Bandwidth and Dynamic Range: *1)

At the points of the dynamic range, the three sweep methods of Table 6.4 (Analog IF, Digital IF, Super Sweep) have an advantageous against the FFT method [9][10]. In these sweep methods, signals are passed thorough IF band pass filters, and the power of the spectrum are detected as narrow band signals.

Generally, the FFT method digitizes the input signal using high speed A/D converter to achieve the high-speed measurement, and the bandwidth of the input signal is configured sufficiently wider than the RBW. In the case that the signal is wideband and wider than the RBW, the total power of the signal is inputted into the A/D converter, and the full range level of the converter must be fit for the total power. A low power signal inputted with such a signal may be behind under the noise floor of the A/D converter. On the other hand, in the three sweep method, the input signal of the A/D converter is band limited by the narrow IF filter and we can take the full range level lower than it if the FFT method. But, in the case that the bandwidth of the IF bandwidth of the Digital IF and Super Sweep method are same to the FFT method, the full range level should be same, and the dynamic range become same to the FFT method.

*1) In this section, ‘Dynamic range’ means the difference of the level between full range of the system (i.e. A/D converter) and the noise floor of the system.

Measurement Time (Narrow SPAN):

In the analog and digital sweep methods, the sweep time is inversely proportional to the square of the RBW. The maximum sweep rate σ is shown in Eq.(2.38)

On the other hand, in the FFT method, σ is inversely proportional to the RBW as shown in Eq.(2.81). In the Super Sweep method, σ is inversely proportional to the RBW too, as shown in Eq.(3.34-b). In the case that both bandwidth of the final IF of these two methods are same, the maximum sweep rate became almost same.

As narrower as the RBW, the difference of the measurement time between them becomes larger.

Measurement Time (Wide SPAN):

In the FFT method, the frequency span of one measurement obtained by one FFT operation depends on the sampling frequency [4]. In the case that the span is wider than the Nyquist frequency, we can step up the receiving frequency band and joint the result of the multiple measurements. In this case, 'blanking time" is added to the measurement time. The blanking time is needed between sweep-end and the start of the next sweep. It is usually 5msec to 100msec that is different corresponding with specification of each analyzer. When the SPAN is wider and the large number of times of the sweep is needed, sum of the blanking time becomes significant and the control of the system will be complicated.

On the other hand, in the sweep methods, we can measure 3 or 4 GHz Span in one sweep ***2)**. Generally, for wide span measurement, sweep methods have an advantage at the point of measurement time.

*2) In 2006, Anritsu Co. produced the spectrum analyzer whose measurement bandwidth was 8GHz.

Influence of the IF Filter:

This feature is described in section 6.5. In the FFT method, a spectrum is obtained as a product of the Fourier transform of the signal and the frequency response of the IF BPF. This response is mostly dependent on the characteristic of the narrowest IF filter. It is not easy to make IF filter which has flat pass band of wide bandwidth. Then some ripples of the IF filter appear on the spectrum as sown in Fig.2.45.

On the other hand, in the three sweep methods, the spectrum is obtained as not the product, but the convolution of them. Usually, the bandwidth of the IF filter is sufficiently wider than the RBW filter, therefore influence of the IF filter almost do not appear on the spectrum.

Abscissa：

In section 2.6, it is described that the abscissa of the sweep method has a factor of time. By changing the sweep time, we can obtain useful and various information from the spectrum.

On the other hand, in the FFT method the abscissa has not a factor of time. The frequency difference of the each sample of the spectrum: Δf is dependent on the sampling frequency and the time length of the window function (see Eq.2.75-b). To shorten Δf we must take the time length of the window function long. The long window function gives a fine RBW. And we have no arbitrariness for the ratio between Δf and RBW. But in the sweep methods, we have the arbitrariness by changing the sweep time.

This section describes the some feature of the methods as shown in Table 6.4. Each of the method has some merits and demerits against each other. We have not any methods that have no demerit. We should select the method corresponding to the purposes of the measurement and properties of the signal.

6.12 Reference

[1] Masao Nagano, "The fundamental of the signal processing in a digital radio communications", Interface Sep 2002, CQ Pub. Tokyo Japan

[2] Masao Nagano, "The theory and fundamentals of digital modulations and demodulations", Interface Sep 2004, CQ Pub. Tokyo Japan

[3] Masao Nagano "Spectrum Analyzer of Super Sweep IF Filter" S^2PATJ vol.4, No.2, June 2001 pp23-30

[4] E.Oran Brigham, "The Fast Fourier Transform", Prentice-Hall,Inc.,1974

[5] N.Kojima, T.Shinozaki, "Introduction to the Z-Transform", Tokai University Publish, Tokyo Japan, 1983.

[6] Oppenheim, Schafer, "Digital Signal Processig", Prentice-Hall,Inc. New Jersey, USA.

[7] L.R.Rabiner R.W.Schafer, "The Chirp z=Transform Algorithm", IEEE Transaction on Audio and Electroacpustics, Vol.Au-17, No.2, pp86-92, JUNE 1969.

[8] Agilent Technologies, Spectrum Analysis Basics, Application Note 150, August 2,2006

[9] Agilent Technologies, Spectrum Analyzer Measurements and Noise Application Note 1303, Dec.16 2006.

[10] Agilent Performance Spectrum Analyzer Series Swept and FFT Analysis Application Note, 2004-1-19

Chapter 7

Application in Radio Astronomy

7.1 Introduction

In radio astronomy, the power of the observed signal is very low, and the signal is observed almost as a noise. Therefore, in many case we cannot observe these signals from one time measurement of FFT processes and sweep spectrum analyzers. The signals are detected through a correlation processes such as XF, FX and FFX algorithm [1]. In these methods, on the assumption that the signal is observed under an ergodic process, and spectrums are obtained from a time average of many results of FFT operations.

On the other hand, it is an accepted view that a sweep spectrum analyzer is not suitable for observations of radio astronomy for its slow speed of measurements. But conventional spectrum analyzer is used to tune and maintain the system indispensably. One of the reasons is that the spectrum analyzer has tunable down-converter and can measure variable measurement conditions. If sweep spectrum analyzer can measure faster, it will be useful in radio astronomy.

In section 7.2, author investigated the SNR (signal noise ratio) against a measurement time for super sweep and sweep method, and reported the result.

In section 7.3, author reported the observation of radio astronomical body W49N, which is measured by author's experimental system and the built-in FFT system in VERA-Mizusawa observatory.

In section 7.4, author reported the results of the observation of radio astronomical body G9.62+0.20.

In section 7.5, some discussions for the observations of section 7.2,7.3 and 7.4 are reported.

In section 7.6, author reviewed a papers which is reported about a radio telescope which is applied CZT (chirp Z transform) as a spectrometer. And author reported the relation to the super sweep method and CZT.

In section 7.7, under the discussion of section 7.2 to 7.6, author considered the product of receptive bandwidth and acquisition-time.

Section 7.8 is the conclusion.

7.2 Improvement of SNR against sweep method

In radio astronomy, signal from an astronomical object is recognized as a weak peak from the noise floor in the measured spectrum, where an SNR is defined as follows.

$$R_{SN} \equiv \frac{(P_p - \mu_n)}{\sigma_n} \quad , \qquad (7.1)$$

where P_p is a peak level of the signal, μ_n is an averaged noise level and σ_n is a standard deviation of the noise, the unit of these parameters are watt (W).

Author simulated the observation of astronomical object using the system as shown in Fig.7.1, and the conditions of the measurement are shown in Table 7.1. Author observed the spectrums using sweep spectrum analyzer; R3264, 'SPA' in Fig.7.1, and the super sweep system, and estimated the SNR by changing the average times, which is according with the measurement times.

The two spectrums of Fig.7.2(a) and (b) were obtained using the sweep spectrum analyzer. Figure 7.2 is the result of three sweeps average, three-second integral time, where the peak of the signal (should be in the center) is covered in the noise floor. Figure 7.2 (b) shows the spectrum with 30 sweeps average, 30-second measurement, where the peak of the signal is clearly shown from the noise floor.

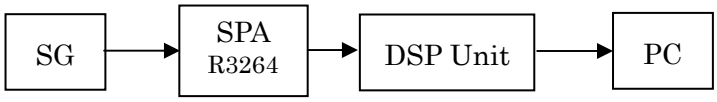

Figure 7.1 System for estimating SNR

Table 7.1 Conditions of Measurements

Input Signal Level	−113dBm	−105dBm
SPAN	500kHz	
RBW	1kHz	
Sweep Time (Sweep)	1sec	
Sweep Time (Super Sweep)	41msec	

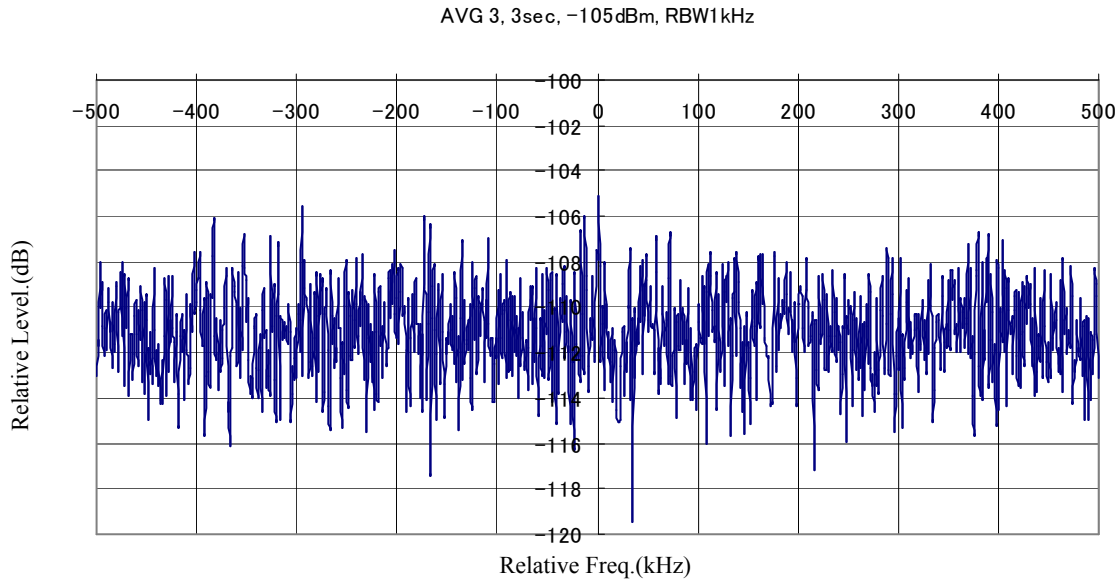

Input Power	SPAN	RBW	VBW	ST	AVG	Integral time	R_{SN}	σ_n
-105dBm	500kHz	1kHz	1kHz	1.0 sec	3	3 sec	0.493	3.30E-12

Fig. 7.2 (a) Measured Spectrum using sweep spectrum analyzer with AVG 3

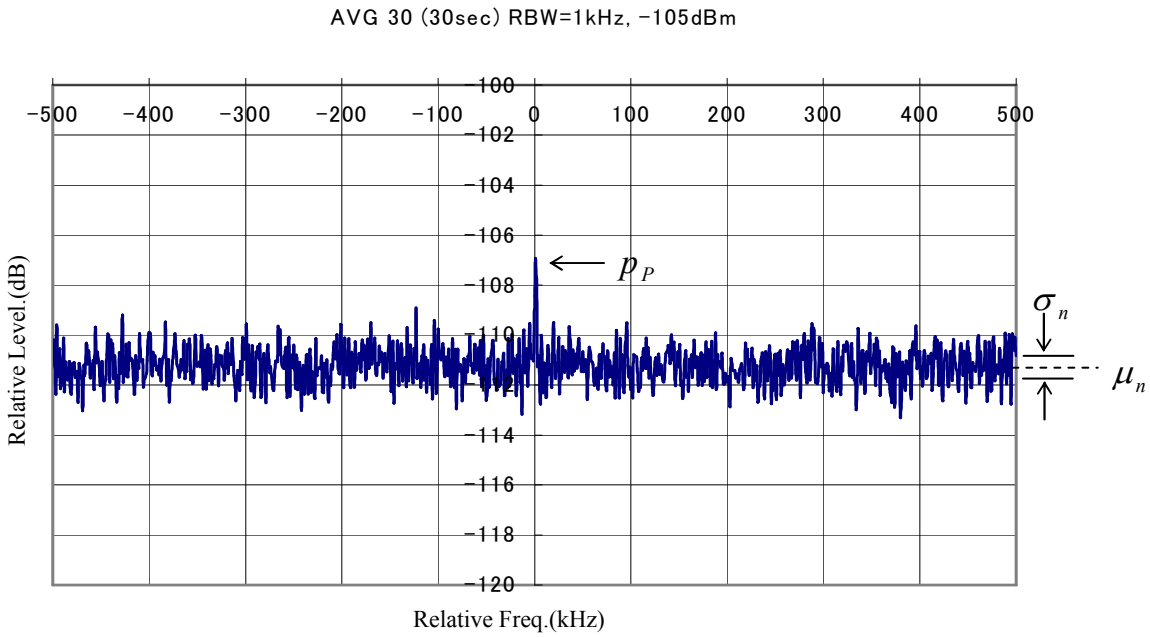

Input Power	SPAN	RBW	VBW	ST	AVG	Integral time	R_{SN}	σ_n
-105dBm	500kHz	1kHz	1kHz	1.0 sec	30	30sec	1.63	1.24E-12

Figure 7.2 (b) Spectrum measured with AVG 30

The spectrums measured through the super sweep method, which were configured 30 times faster than the sweep method, are shown in Fig.7.3 (a) and Fig.7.3(b), they were measured same integral time of average with Fig.7.2 (a) and (b), respectively. In these cases, the sweep time of one sweep were 41 msec and the average time were 73 and 732 (the integral time were 3 and 30 sec), the SNR R_{SN} is so much greater than Fig.7.2 and the deviation σ_n is so smaller. The transition of SNR and the deviation is shown in Fig.7.4, Fig.7.5, Table 7.2 and Table 7.3. The parameters R_{SN} and σ_n are not dependent on the integral time but the average times, then the fast sweep of the super sweep improved the R_{SN} and σ_n in the same integral time.

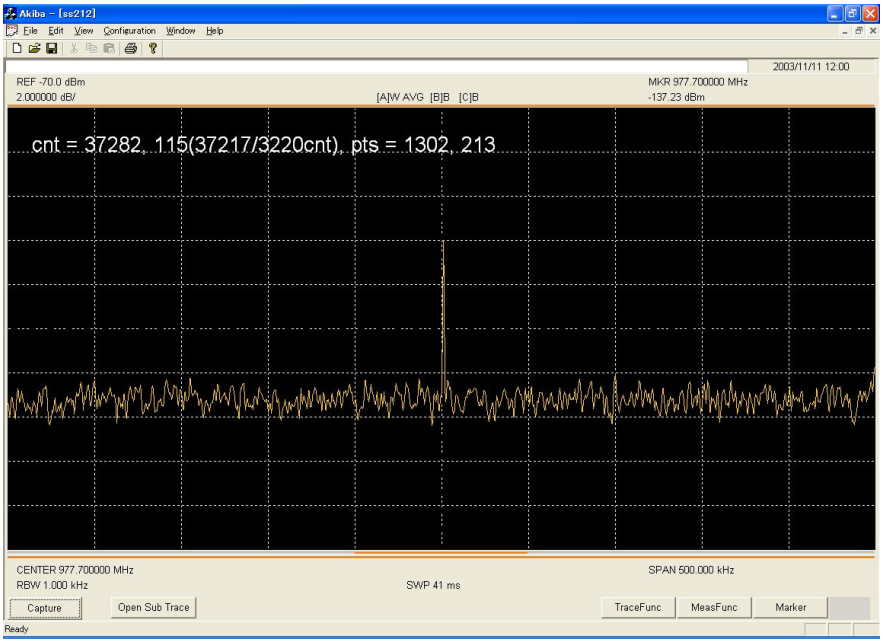

Input Power	SPAN	RBW	VBW	ST	AVG	Integral time	R_{SN}	σ_n
-105dBm	500kHz	1kHz	1kHz	41msec	73	3 sec	35	0.023

Fig. 7.3 (a) Spectrum measured using Super sweep method with AVG 73

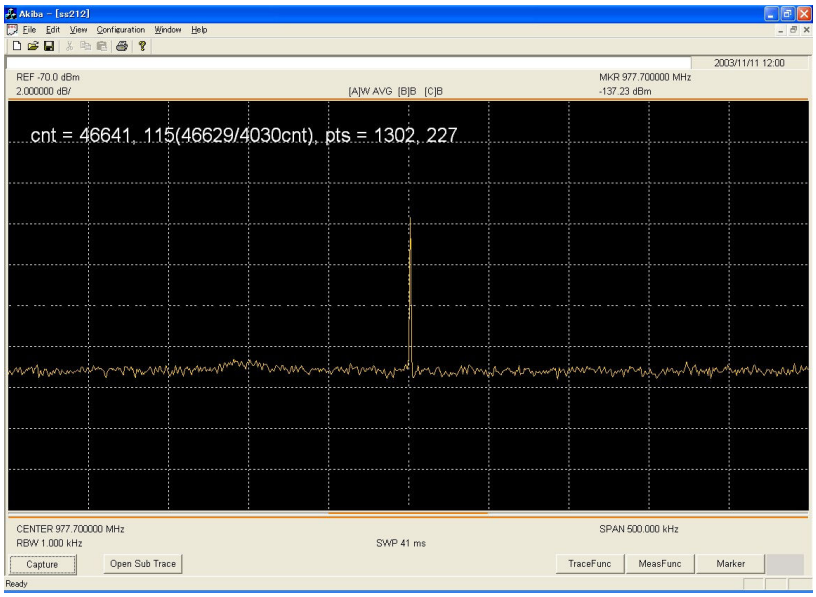

Input Power	SPAN	RBW	VBW	ST	AVG	Integral time	R_{SN}	σ_n
-105dBm	500kHz	1kHz	1kHz	41msec	732	30 sec	94	0.00779

Fig. 7.3 (b) Spectrum measured using Super sweep method with AVG 732

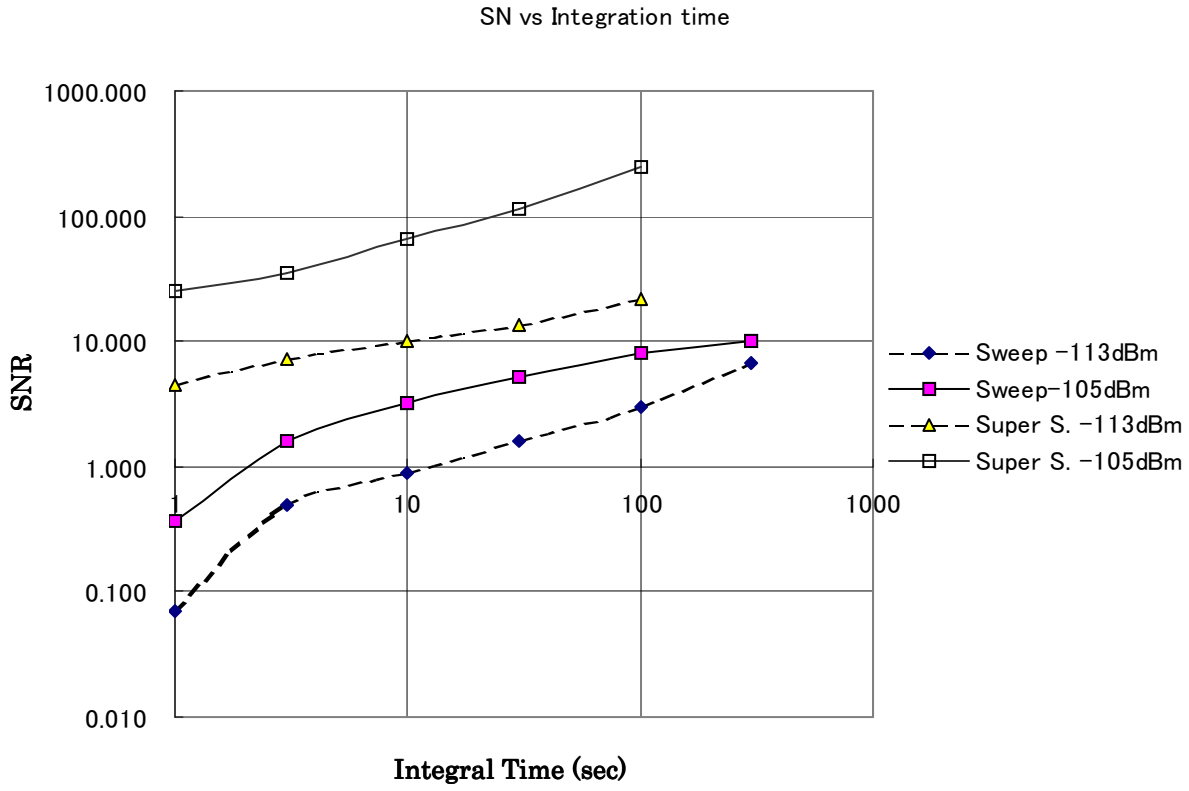

Fig. 7.4 SNR against Integral time

Table 7.2 SNR against Integral time

		Sweep		Super Sweep			
		A: -113dBm	A': -105dBm	B: -113dBm	B':-105dBm	B/A	B'/A'
Ti	1 sec	-0.129	0.36	4.5	25	--	69.4
	3	0.493	1.60	7.23	35	14.7	21.9
	10	0.900	3.20	9.97	65	11.1	20.3
	30	1.63	5.28	13.4	115	8.2	21.78
	100	3.00	7.96	22.1	250	7.37	31.4
	300	6.71	9.96	--	--	--	--

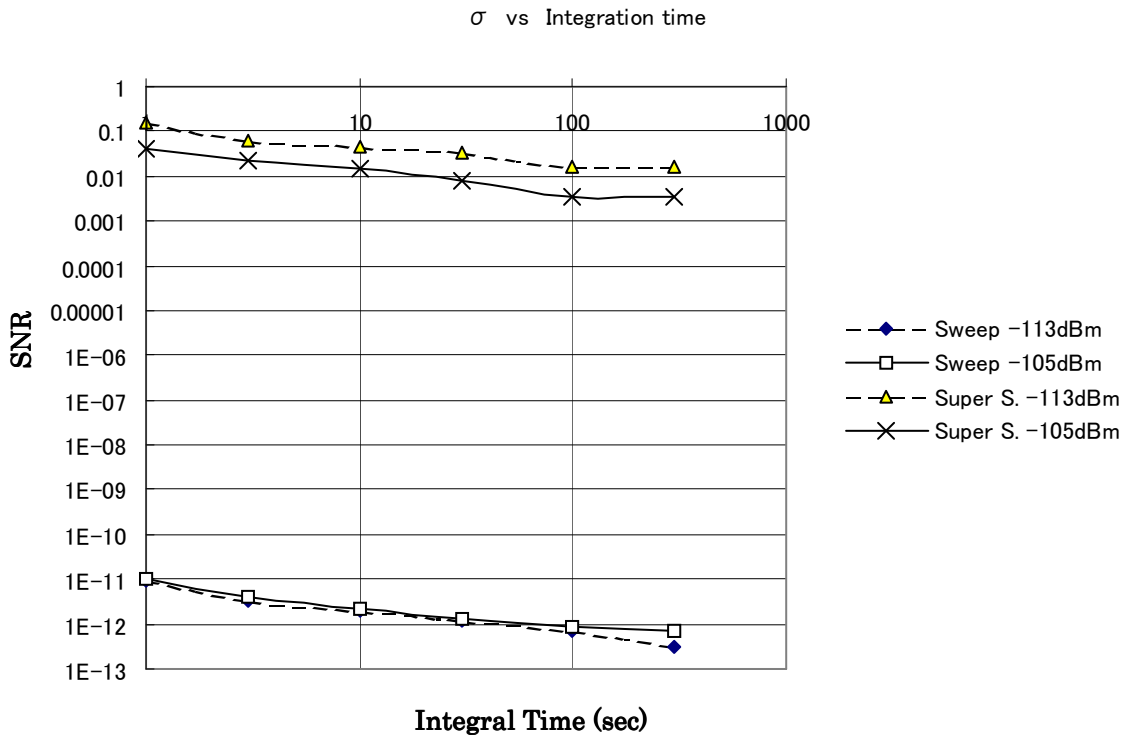

Fig. 7.5 Standard deviations against Integral times

Table 7.3 Standard deviations against Integral times

Ti	A: AVG -113dBm	A': AVG -105dBm	B: SSDI -113dBm	B': SSDI -105dBm	B/A	B'/A
1	9.59E-12	1.0197E-11	0.15	0.04	1.56E+10	3.92E+9
3	3.30E-12	3.91058E-12	0.063	0.023	1.91E+10	5.88E+9
10	2.02E-12	2.19366E-12	0.045	0.015	2.23E+10	6.84E+9
30	1.24E-12	1.34483E-12	0.033	0.0078	2.66E+10	5.80E+9
100	7.01224E-13	9.08595E-13	0.016	0.0035	2.28E+10	3.85E+9
300	3.16E-13	7.27233E-13	--	--	--	--

7.3 Observation of W49N

On 27th Dec. 2007, author's group observed the hydrogen maser of an astronomical body W49N using the 22m ϕ radio telescope of VERA-Mizusawa observatory. The spectrum of Fig.7.6 was measured using the built-in FFT, and the condition of the measurement is shown below the spectrum. This spectrum is the result of the correlation, which was 31250 times average. The slopes of noise floor around right and left sides were caused through the digital filter, which is implemented before the FFT operation. The difference of the level between the maximum peak and the noise floor was 12.1dB.

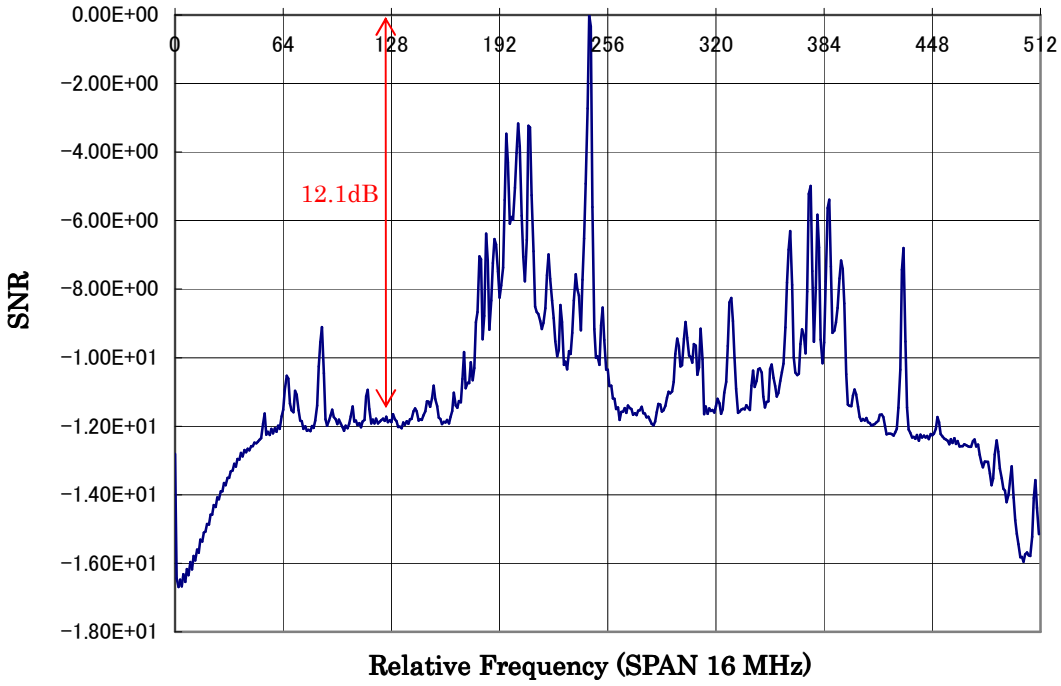

Center Frequency	5437MHz
Frequency-SPAN	16MHz
Size of the spectrum and FFT	512
Δ f	31.25kHz
Integral time	1.0sec (31,250 times average)
μ_n	-11.8dB
σ_n	0.0024
R_{SN}	392
WindownFunction	Hamming
RBW	1.3bin, 40.6kHz

Fig. 7.6 Spectrum of Hydrogen Maser of W49N

Author observed the spectrum using the super sweep system and the results are shown in Fig.7.7(a) ~ Fig.7.7(c). The integral time of Fig.7.7(a) was 1.0 sec that is same to Fig.7.6. The figure of this spectrum was almost same to Fig.7.6. The difference of the level between the maximum peak and the noise floor was approximately 13.2dB, which is 1.1dB better than Fig.7.6, and the SNR was approximately 2/3 of Fig.7.6.

The sweep rate of Fig.7.7(a) was only 3.1 times faster than the sweep method. Author measured spectra with another two condition as shown in Fig.7.7(b) and Fig.7.7(c). They are approximately 30 times faster than the sweep method.

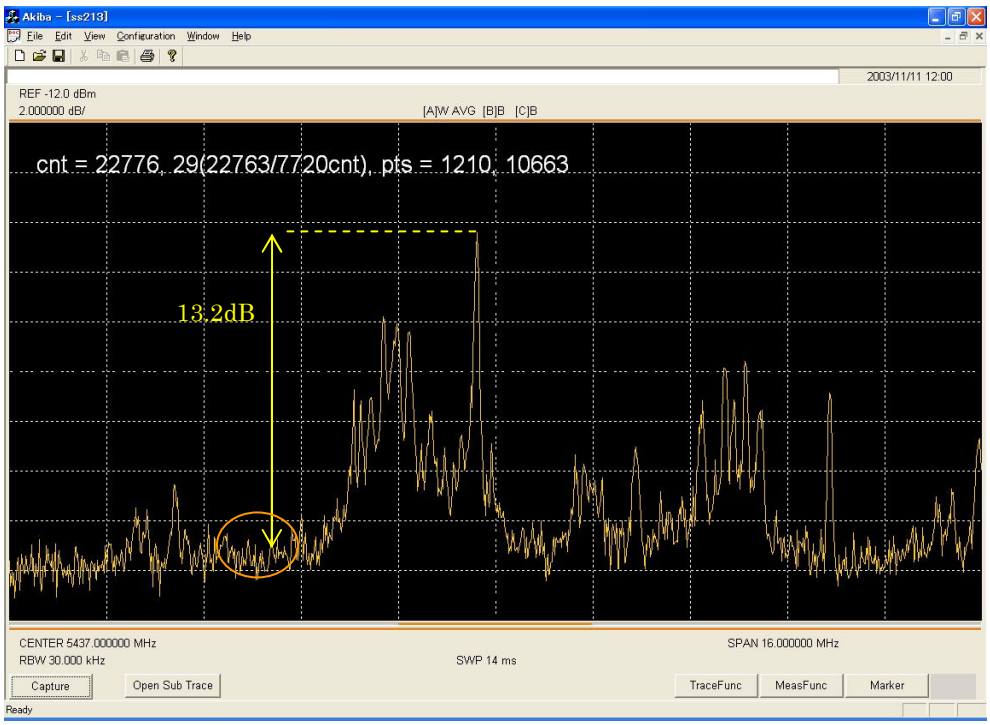

Center Frequency	5437MHz
Frequency-SPAN	16MHz
Bbw	30kHz
Integral time	1.0sec (73 times average)
St	14msec
St of sweep method	44msec
μ_n	-13.3dB *)
σ_n	0.00392 *)
R_{SN}	243 *)

Fig 7.7 (a) Spectrum measured using Super sweep method

*) These parameters were estimated from the circled part of the figure.

The resolution bandwidth (*Rbw*) of Fig.7.7(b) was 10kHz, the integral time was 3.4 sec, the average time was 244, the sweep rate was 30 times faster than the sweep method, the level difference between the peak and noise was 14.0dB, and the SNR was 80% of Fig.7.6. If we took the integral time so longer, the deviation of the noise floor should be so narrower and obtain better SNR.

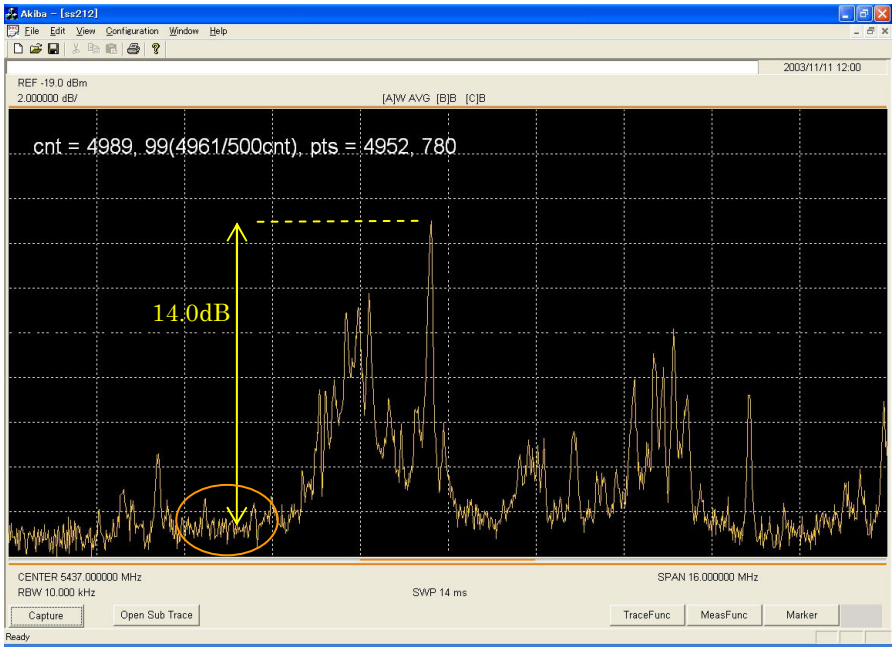

Center Frequency	5437MHz
Frequency-SPAN	16MHz
Bbw	10kHz
Integral time	3.4sec (244 times average)
Sweep time	14msec
Sweep time of sweep method	400msec
μ_n	-13.75dB *)
σ_n	0.00263 *)
R_{SN}	364 *)

Fig 7.7 (b) Spectrum measure with 3.4 sec integral

*) These parameters were estimated from the circled part of the figure

The resolution bandwidth (*Rbw*) of Fig.6.7-c was 3kHz, the integral time was 29.4 sec, the average time was 200, the sweep rate was 30 times faster than the sweep method, the level difference between the peak and noise was 14.0dB, and the SNR 497 was superior to it of Fig. 7.6.

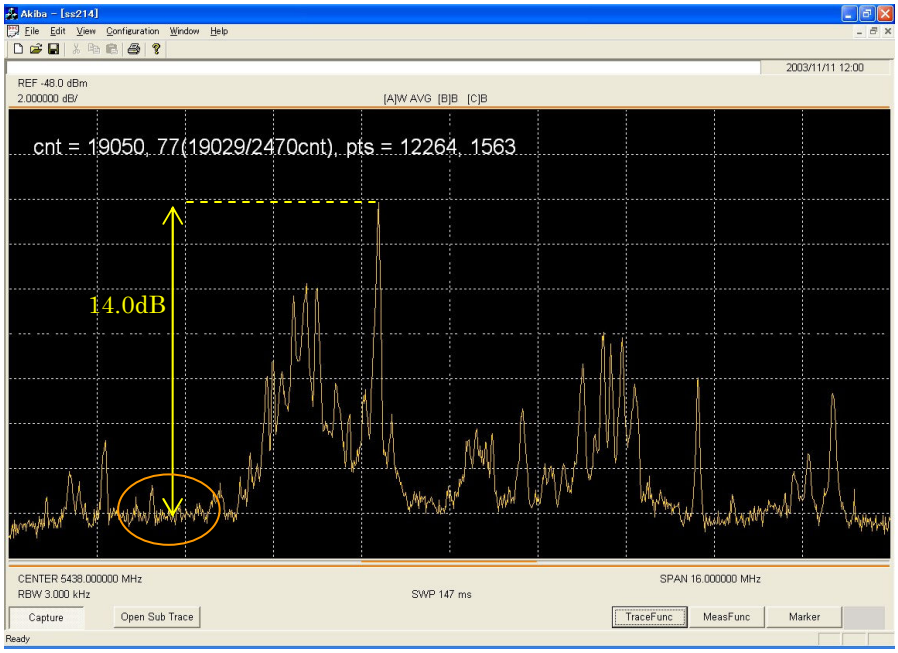

Center Frequency	5438MHz
Frequency-SPAN	16MHz
Bbw	3kHz
Integral time	29.4sec (200 times average)
St	147msec
St of Sweep method	4.44 sec
μ_n	-14.1dB *)
σ_n	0.0019 *)
R_{SN}	497 *)

Fig 7.7 (c) Spectrum measured with 29.4 sec integral

*) These parameters were estimated from the circled part of the figure

The relation SNR and measurement integral time is shown in Fig.7.8, where the plotted data is obtained from Fig.7.6～7.7(c). It is assumed from Fig.7.8 that our experimental system could achieve same SNR with approximately 5.3 times long integral time. If our experimental system could measure 5.3 times faster, it was superior to the FFT system. By the discussion of section 6.2, it is possible to make the system whose performance is superior the FFT system by the super sweep method.

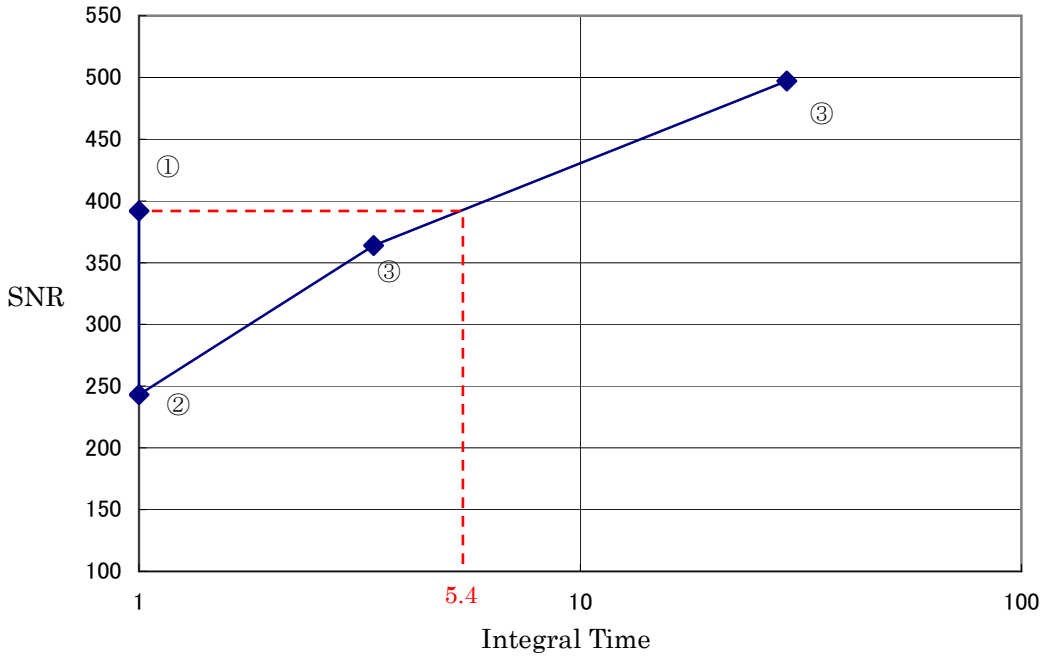

	Fig	Δ f/RBW	SNR	Integral Time
①	7.6	Δ f =31.25kHz	392	1.0 sec
②	7.7(a)	RBW=30kHz	243	1.0sec
③	7.7(b)	RBW=10kHz	364	3.4sec
④	7.7(c)	RBW=3kHz	497	29.4sec

Fig 7.8　SNR against Average time length

7.4 Observation of Methanol Maser at Yamaguchi

On 13th Oct 2007, we observed a methanol (CH_3OH) maser signal of the radio astronomical body 'G9.62+0.20' at the satellite relay center of KDDI that is located in Yamaguchi Prefecture. We used the 32m ϕ radio telescope parabola antenna, where the spectrum analyzer ESA, provided by Agilent Technology Co, was used as a monitor. Figure 7.9 show the spectrum measured by the ESA analyzer. The measuring conditions were Center Frequency=9.67GHz, SPAN=4MHz, RBW=10kHz, VBW=100Hz and Sweep Time=3.3sec. The ratio between the peak level and the noise floor was approximately 4.7dB and the SNR was 11.3.

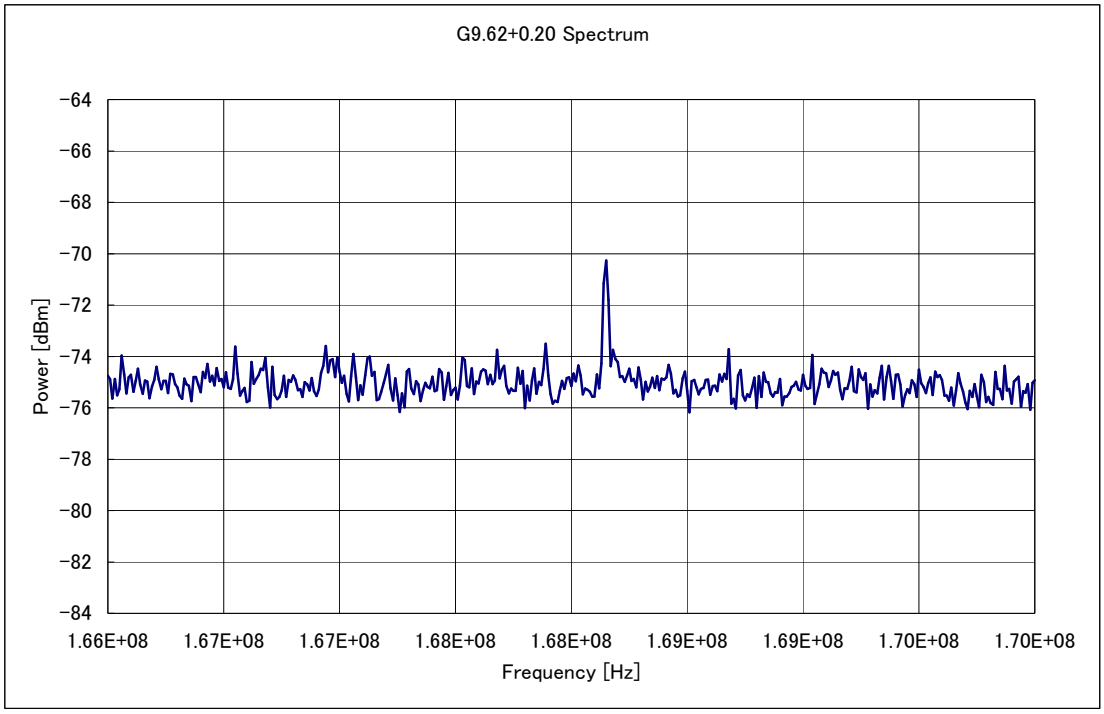

Center Frequency	9.67GHz
Frequency-SPAN	4MHz
Bbw	10kHz
VBW	100Hz
Integral time	3.3sec (no average)
St	3.3sec
μ_n	-4.72dB
σ_n	0.0586
R_{SN}	11.3

Fig. 7.9 Signal raised by methanol maser of 9.67GHz.
This signal is measured by using the sweep spectrum analyzer ESA (produced by Agilent Technology Co).

We measure the signal using our experimental system described in Chapter 4. In this case, we used an average function of the system instead of using the video filter (VBW). The average times was 100, and it was according to the video bandwidth 100Hz. We intended to set up the same condition with Fig.7.9, measured by the ESA analyzer. The measure spectrum is shown in Fig.7.10.

The sweep time was 14msec which is approximately 200times faster that the sweep time of the ESA. Even if we considered the average time 100, it was two times faster. The level difference between the peak and the noise floor was approximately 6.0dB, and the SNR was 17.2.

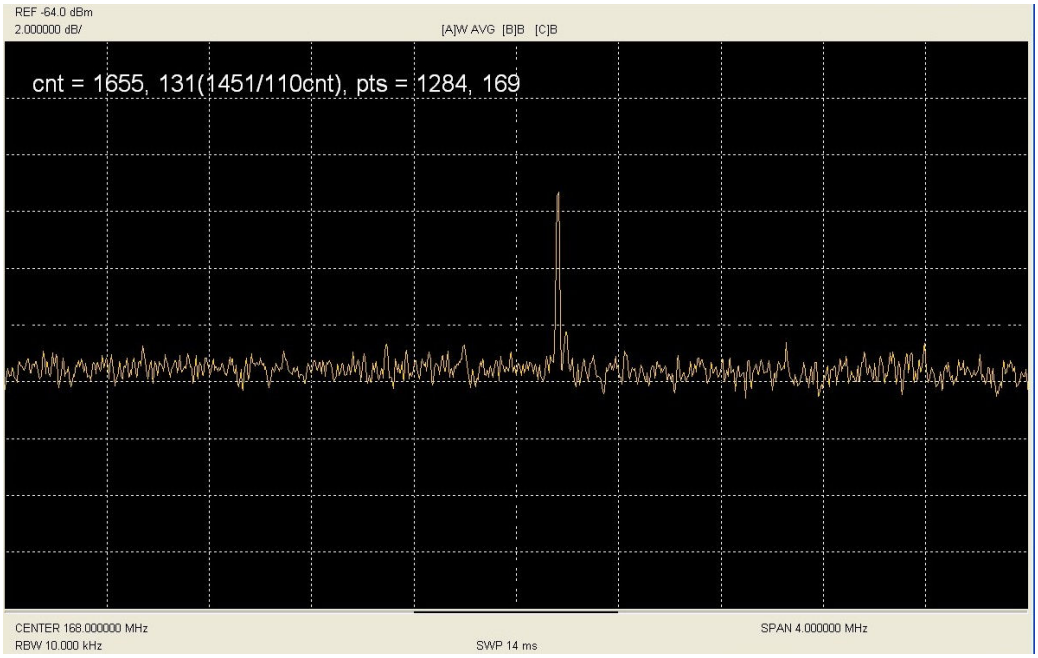

Center Frequency	9.67GHz
Frequency-SPAN	4MHz
Bbw	10kHz
Integral time	1.4sec (100times average)
St	14msec
μ_n	-6.00dB (from the peak)
σ_n	0.0435
R_{SN}	17.2

Fig 7.10 Same signal with Fig.7.9 measure by Super sweep method

7.5 Discussion about Observations of 7.2, 7.3 and 7.4

In section 7.2, author estimated the SNR against some condition, where the measured signals were obtained using the signal generator. Author obtained the result under weaker external disturbances. In the results of the section, the SNR were in proportion to the square root of the integral time and the number of the sweeps as shown in Fig.7.4.

The numerical results are shown in Table 7.2. The two columns in the right side show the ratio of the SNR of super sweep method to the sweep method as “B/A” and “B’/A”. The average value of “B/A” was approximately 10, and “B’/A’ “ was 24. In the measurements in section 7.2, the sweep time of the sweep method were 1.0 sec, and the sweep time of the super sweep were 41msec. The ratio of the sweep time was 24.4 that is corresponds to the result of “B’/A’ “ of Table 7.2. Author thought that the result of the signals whose level was –113dBm were not exact, where it was difficult to measure exact peak level.

The result of section 7.3 is shown in Fig.7.8, where the SNR of the super sweep method was almost proportional to the square root of the integral time. In the case that the RBW was narrower, the sweep time was longer and the SNR became larger corresponding to the RBW. The SNR of the built-in FFT system of VERA-Mizusawa observatory was 392. This SNR 392 is corresponds to the integral time 5.4sen as shown in Fig.7.8. If we made the experimental system to be 5.4 times faster, the system achieved same SNR with the FFT system. It is possible to make the system using recent AD/C and other devices such as a FPGA. Although, the results of super sweep method were not superior it of the FFT system in the same measurement time. The level difference between peak and noise floor were larger than the FFT method, and the SNR measured with longer integral time was better than the FFT result.

Section 7.4 shows the comparison of the SNR between sweep method and the super sweep method by measuring the maser signal from the real celestial body. The two results of Fig.7.9 and Fig.7.10 were stood on same condition except the sweep time on the assumption that the VBW corresponds to the average. The integral time of Fig.7.10 was 100times of the sweep time 14msec. On the principal of the super sweep method, the sweep time should be shorter than 14msec. But the sweep time was restricted by the minimum sweep time of the spectrum analyzer R3265, which is used in the experimental system. Although the two SNR should be same, the SNR of the super sweep method was 1.52 times larger. The reason of this advantage was assumed that the resolution filter of the super sweep method was digital and the grade of the R3265 was superior against the analyzer ESA.

In conclusion, it was verified that the super sweep method could obtain better SNR of a measured signal against the sweep method, and had a possibility to obtain better SNR more than the result of the FFT method.

7.6 Chirp Z-Transform System of GREAT

In Chapter 6, author described that the super sweep method is a kind of the Chirp Z-transform (CZT) [4]. This algorithm has been already applied on radio astronomy. The spectrometer applied CZT is a part of the GREAT (German REceiver for Astronomy at Terahertz frequencies) instrument onboard SOFIA, the Stratospheric Observatory For Infrared Astronomy [3][5]. In the system GREAT, CZT is used as a high-resolution spectrometer as shown in Fig.7.11.

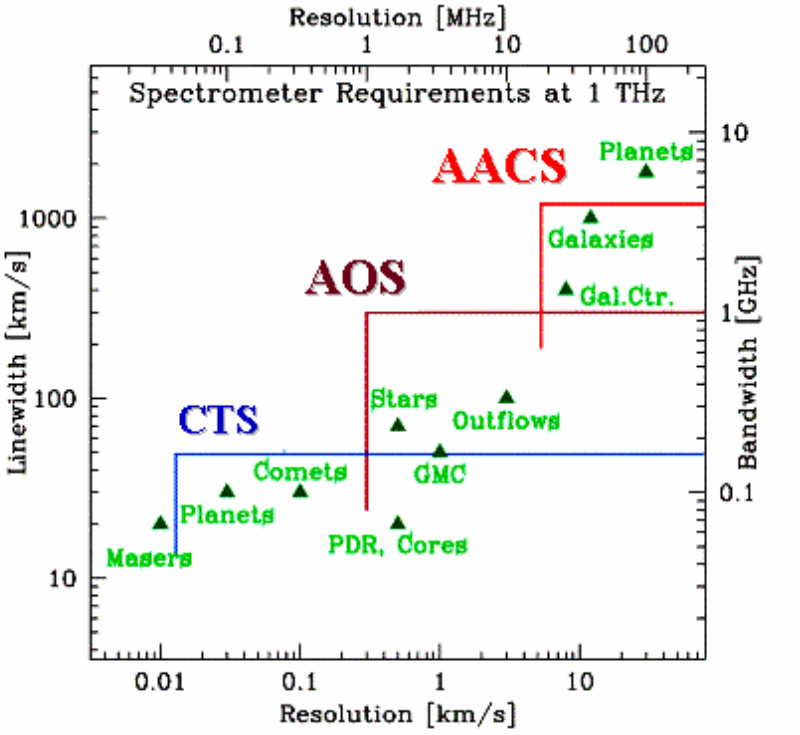

Fig 7.11 Astronomical requirements on spectral resolution and bandwidth (Referred from [5])

AACS: Wideband analog Auto-correlator
AOS: Acoustics Optical Spectrometoer
CTS: Chirp Z-Transform Spectorometer

The simplified block diagram of SOFIA-GREAT-CTS is shown in Fig.7.12 [3][5]. In [5], the 'Chirp Generator' of Fig.7.12 is constructed with SAW device. In [3], the Generator is implemented as 'Adaptive Digital Chirp Processor (ADCP)'. In the Fig7.12, 'SAW Compressor' corresponds to the negative chirp filter of the super sweep method. The configuration of this system is fixed, which corresponds to the SAW Compressor.

The duty of useful part of the output signal from the SAW Compressor is 50%. The other part, 50% is the transitional response of the compressor as shown in Fig.7.13.

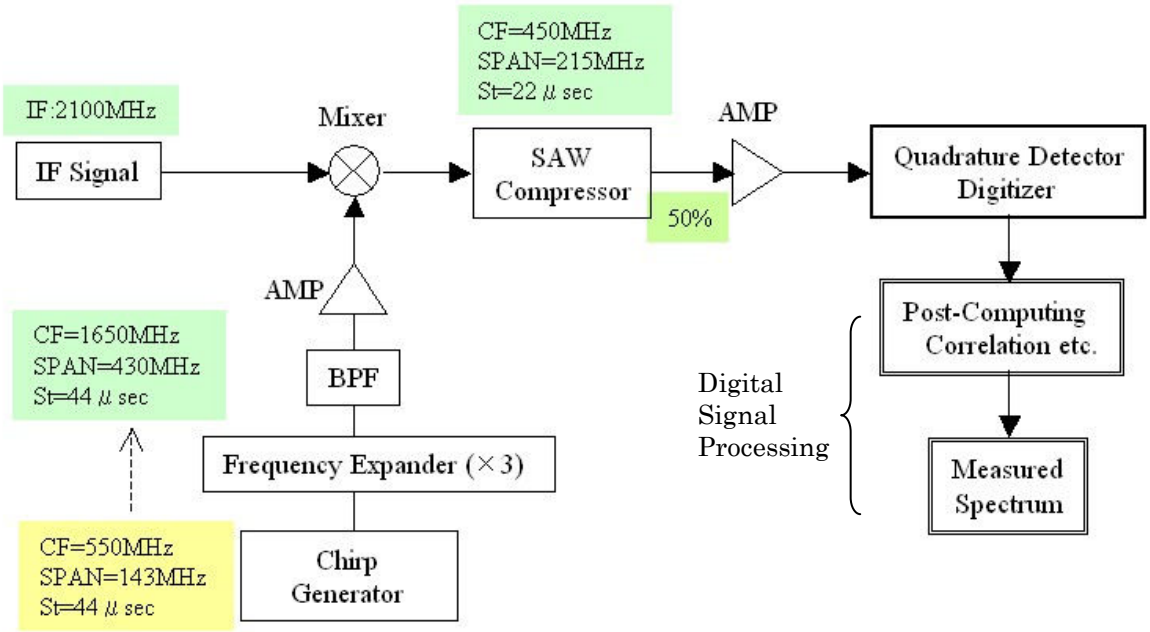

Fig 7.12 Diagram of SOFIA-GREAT-CTS spectrometer [3][5]

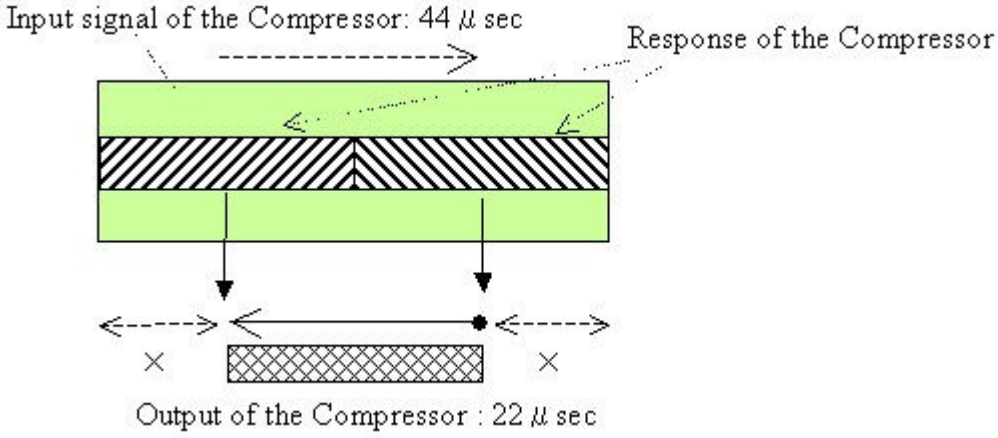

Fig 7.13 Output of SAW compressor of SOFIA-GREAT-CTS spectrometer [3][5]

The fundamental algorithm of SOFIA-GREAT-CTS is same to it of the super sweep method. But the configuration of the system is fixed; it is adapted to the SAW compressor. This system measure spectrum whose span is 215MHz every 22 μ sec. It is very high-speed measurement as a spectrometer. But there is not any flexibility for variable measurement condition.

Author considered it is important that a measurement system had flexibility. The system described in Chapter 4 and other chapters was designed to have flexibility that can be configured corresponding to any measurement condition which was allowed by the sweep spectrum analyzer (SPA) as shown in Fig.7.14. There were many parameters over 30 ('Processing condition in Fig7.14), which were decided automatically to drive the system with best condition through the software included in the PC. Author developed the software, which was the core part of the experimental system, and it was the most difficult work through the development of the system. For instance, the software computed the coefficients of the negative chirp filter $g_n[N_G]$, which were corresponded to all conditions of the system and a measurement. The SOFIA-GREAT-CTS system has no flexibility what our experimental system had.

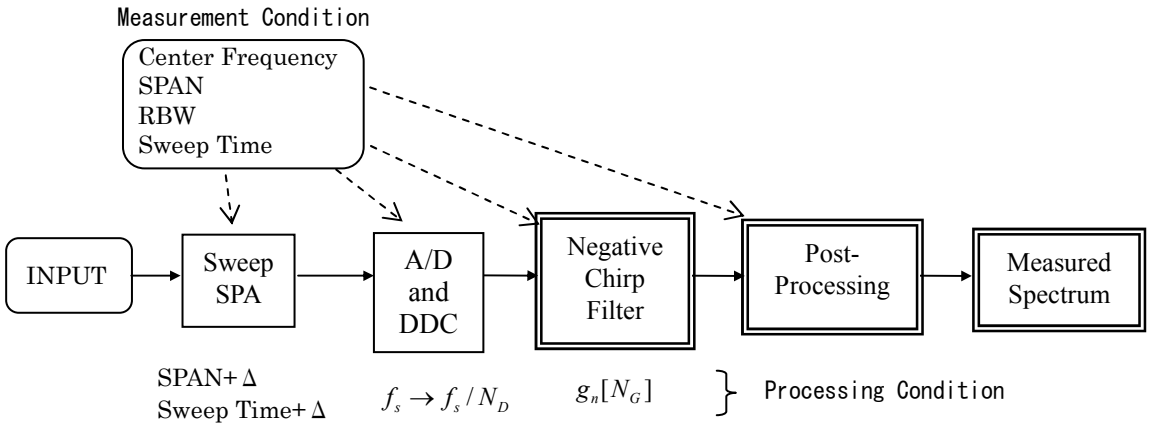

Fig 7.14 Adaptive Configuration Corresponding to the Measurement Condition

7.7 Characteristic of each method

The FFT method is the best way to measure spectrum with higher rate. But the super sweep method and chirp z-transform spectrometer (CTS) has some merit against the FFT method.

7.7.1 Maximum sweep rate

The discussion of section 2.9.2 and 3.3.5 the sweep rate of FFT method and super sweep method is explained as Eq.(2.81) and (3.34-b) as follows.

$$FFT: \quad \sigma_{\max\_FFT} = \frac{Flt}{T_W} = \frac{1}{k_W} Flt \cdot Rbw, \quad (2.81)$$

$$SuperSweep \quad : \quad \sigma_{\max\ S} = Rbw \times (Flt / \chi), \qquad (3.34\text{-b})$$

where σ is the sweep rate Hz/second, *Flt* is the bandwidth of the IF signal, T_W is time length of the window function, k_W and χ are constants defined by Eq.(2.80) and (3.27). In the case that the

resolution filter and windows function are same function such as Gauss, k_W and χ are same value such as 2.0～3.0.

Theoretically, the super weep method can achieve the same sweep rate with the FFT method. Practically, in some case, the sweep rate is dependent on the performance of the local oscillator. For example, when *Flt = 1GHz, Rbw=10kHz* and χ*=2.5,* $\sigma_{\max S}$ is 4000GHz/sec, which is according to the sweep time 250 μ sec. Until 1980's, many spectrum analyzers achieved this speed sweep without a PLL system, but local oscillators of most recent analyzers after 1980's are controlled by PLL synthesizer whose minimum sweep time are 1~20mse *).

In the case that we record the digitized signal continuously, the efficiency of the data acquisition of the FFT method is perfect and ideal. The super sweep method cannot be superior to it, but can approach it almost same to it.

In the FFT method, the SPAN bandwidth is limited under the *Flt* or the Nyquist frequency. But the Super sweep method and CTS has no limitation. In the case that we use same A/D converter and signal processing system, the super sweep method and CTS can measure wider span-bandwidth than the FFT method with same sweep (measurement) rate.

*) note: The minimum sweep time of R3273 (produced by ADVANTEST Co.) is 20msec, and it of PSA series, ESA4440 made by Agilent Co, is 1msec.

7.7.2 Sample data on a spectrum

The some characteristics of the FFT method are already described in section 2.8. The significant difference between the FFT method and the super sweep method included the CTS is the frequency difference between each sample of a spectrum.

In the super sweep method and CTS, the frequency difference is explained by Eq.(6.2).

$$\Delta f = \sigma \cdot \Delta t \ ,$$

where Δt is the inverse of the sampling rate f_s, and σ is the sweep rate. This parameter Δf is independent against the resolution: RBW.

On the other hand, in the FFT method Δf is decided by Eq.(2.75-c).

$$\Delta f = f_S /(2N) \ ,$$

where *N* is the size of the FFT. The RBW is dependent on the sample rate and the window function as shown in Table 2.4 (in section 2.8.3). In the case that *N* is increased to improve the resolution, the 3dB bandwidth (RBW) become narrower and the relation of Table 2.4 is not changed.

Author considers it is significant disadvantage of the FFT method, which has the 'scallop loss [9]' as shown in Table 2.4. Especially the rectangle window has the loss of 3.92dB. It should be corrected by some post-processing. In the super sweep method and CTS, this loss can be avoided to take Δf enough smaller than the RBW.

7.7.3 Product of Receptive Bandwidth and Aquisition-Time

In a radio astronomy, the value of the SNR is defined by Eq.(7.1).

$$R_{SN} \equiv \frac{(P_p - \mu_n)}{\sigma_n} \quad , \qquad (7.1)$$

In radio astronomy, it is very important matter to observe a signal with larger SNR and measure it as fast as we can. There are three ways to obtain better SNR.

1. Reduce the σ_n (standard deviation of the noise)
2. Increase the level P_p (peak level of the signal)
3. Decrease the level μ_n (averaged noise level)

In the most case that P_p is increased, the noise level would be up and the value μ_n and σ_n would increase. In radio astronomy, many observation systems take the FFT method and obtain spectrum data as fast as they can to reduce the value μ_n and σ_n.

Figure 7.15 shows a diagram, which indicates a condition of spectrums on the frequency-time diagram. In a FFT method which is so called 'Real-Time FFT', the measured signal is recorded without discontinuance, and the data is translated into the spectrum. In Figure 7.15, the *Flt* is assumed as 1MHz, and the data acquisition time is assumed 20msec. Where T_W is the time length of the window function to obtain the resolution the RBW. In the case that the RBW equals 10kHz, T_W is approximately 0.2msec. We can obtain 100 independent spectrums within the time 20msec. There are no data that do not take a part to make the spectrums as shown in the figure 'Non Response Area: 0%'. As described in section 7.5.1, the FFT method is a perfect and ideal method that has no response area.

On the other hand, the bandwidth of the acquisition data in the sweep method equals to RBW. Figure 7.16 shows the frequency-time diagram, which corresponds to Fig.7.15. In this case, the minimum sweep time is 20msec by Eq.(2.14), and we obtain only one spectrum.

We can consider a parameter that is product of a receptive bandwidth and acquisition time, 'bandwidth-time product' as following equation.

$$S_{BT} \equiv Flt \times T_W \qquad (7.2)$$

In the FFT method of Fig.7.15, the product is approximately 200 (1MHz×0.02sec). In the sweep method of Fig.7.16, the product is approximately 200 (10kHz×20msec). In both method, (FFT and sweep), the bandwidth-time product takes same value.

One sample of the time frequency diagram in the super sweep method is shown in Fig.7.17. Where the *Flt* is assumed 100kHz, and RBW is assumed 10kHz. The maximum sweep rate is given by Eq.(3.34-b), and the sweep time $T_{S\_\min}$ is given as

$$T_{S\_\min} = \frac{Span}{\sigma_{\max\_s}} = \frac{Span}{Rbw \cdot Flt / \chi} \cong 2m\sec \qquad (7.3)$$

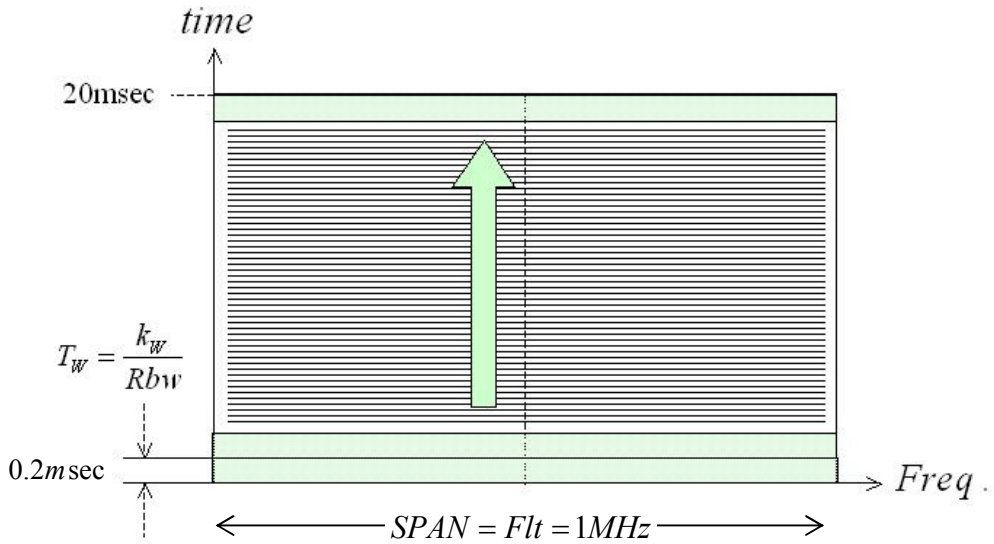

Fig.7.15 Time Frequency Diagram of Measured Spectrum and Processing Bandwidth: Real-Time FFT Method

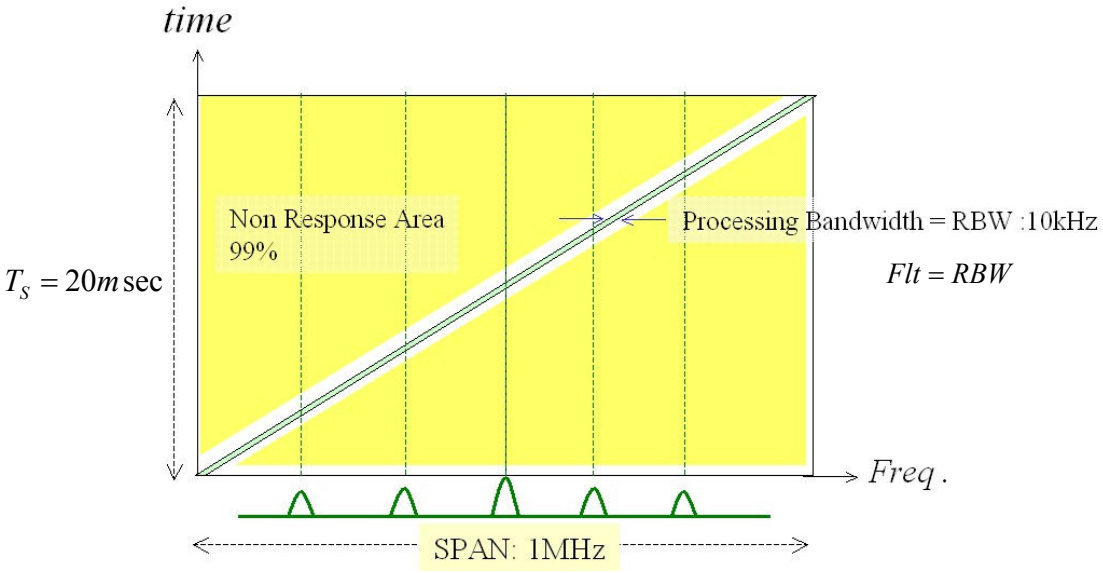

Fig.7.16 Time Frequency Diagram of Measured Spectrum and Processing Bandwidth: Sweep Method

The sweep time is 1/10 of the sweep method in Fig.7.15. The bandwidth-time product is given by Eq.(7.2) and it is 200 (100kHz×2msec).

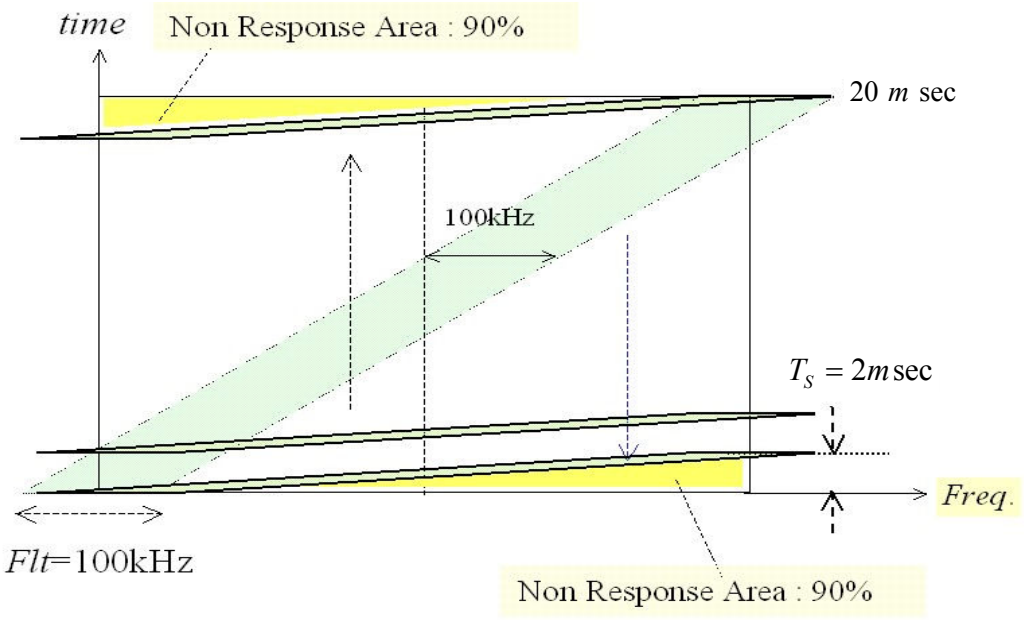

Fig.7.17 Time Frequency Diagram of Measured Spectrum and Processing Bandwidth: Super Sweep Method

By above discussion, author investigated as follows. In the case that the RBW and SPAN are common to the three methods, the bandwidth-time product is constant. Then by taking the *Flt* wider we can achieve the sweep time shorter.

On the point of efficiency of the data acquisition, the sweep method of Fig.7.16 has very low efficient. The non-response area of Fig.7.16 is shows as yellow zone, which is 99% of the area, frequency-time product of the SPAN and the sweep time. In the super sweep method of Fig.7.17, the non-response area is reduced into 90%. This efficiency is 1/10 to the FFT method.

By taking the *Flt* as wider and wider, we can obtain better efficiency acquisition. Figure 7.18 (a) and (b) is a sample of a time frequency diagram. In the figure (a), the *Flt* equals the Span, and the non-response area is 25%. In the figure (b), the *Flt* is twice as the Span, and the non-response area is 0%. It is possible to make the efficiency 100% by this way. But in this case, the sampling frequency of the AD/C should be four times wider than the SPAN, which is twice of the FFT method. At the point of efficiency in all systems, the efficiency is half of the FFT method.

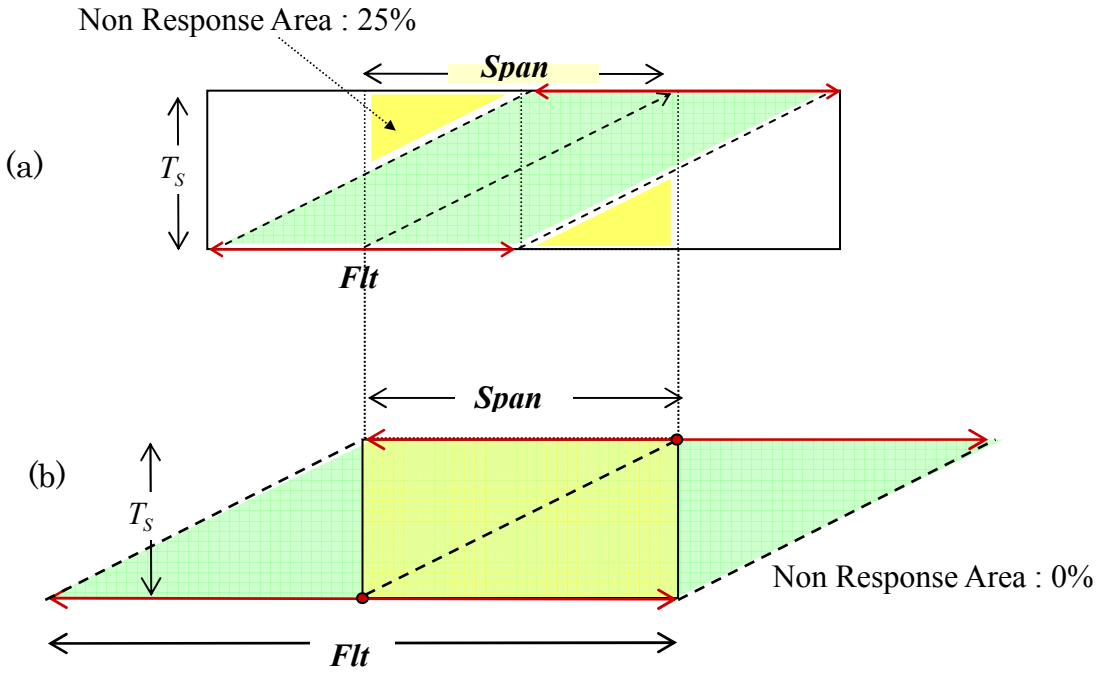

Fig.7.18 Super Sweep with very wide-band *Flt*

Author suggest the suitable configuration of the super sweep method as follows.

1) The measurement SPAN is sufficiently wider than the Nyquist frequency of the AD/C.
2) The *Flt* should be as wider as the Nyquist frequency.

In this condition, the system could measure wider SPAN of a spectrum than the FFT method, and the efficiency of the data acquisition would be half to the FFT method.

The receptive bandwidth of a conventional sweep spectrum analyzer is fixed as its RBW. The super sweep method broke the restriction, and gave the sweep method a freedom to change the receptive bandwidth independently from an RBW. By this freedom, the sweep spectrum analyzer (including the super sweep method) became not only to be able to measure high-speed measurement with narrow RBW but also obtain a variety of a measurement condition.

7.8 Conclusion

We confirmed that it needs larger number of average to obtain better SNR in spectrum measurements. Although author's system could not be superior the optimized FFT system in Mizusawa, the level differences between peak and noise floor were better than the FFT system.

The super sweep method has characteristics as follows.

a) In theoretically, the super sweep method can measure as fast as the FFT method .

b) No restriction between RBW and bin on the frequency domain
c) Better dynamic range because of a narrow band system

By the discussion of this chapter, author suggests application of super sweep method in radio astronomy as follows.

1) As a high performance monitor:

Sometimes, the monitor may be used as a spectrometer for the observation.

2) In the case that the spectrometer is demanded lightweight, high resolution or a low-cost:

Generally, a high-speed FFT system demands much large size of memory. In the super sweep method, the sampling frequency of the acquisition data is decimated appropriately, and the size of the memory can be reduced corresponding to the sampling rate.

3) As a very wideband spectrometer:

It measure wideband spectrum, which is wider than the Nyquist frequency of the fastest AD/C.

7.9 Reference

[1] S.Iguchi, T.Okuda, "The FFX Correlator", Publ.Astron.Soc.Japan, 2007, Astronomical Society of Japan

[2] Agilent Performance Spectrum Analyzer Series Swept and FFT Analysis Application Note, 2004-1-19

[3] G.Villanueva, P.Hartogh,"THE HIGH RESOLUTION CHIRP TRANSFORM SPECTROMETER FOR THE SOFIA-GREAT INSTRUMENT", Experimental Astronomy, Springer 2006

[4] L.R.Rabiner, R.W.Schafer,"The Chirp z-Transform Algorithm", IEEE Transactions on Audio And Electroacoustics, Vol.AU-17,No2 JUNE 1969

[5] R.Gusten, P.Hartogh,Heinz-Wilhelm Hübers, Urs Graf b, Karl Jacobs,Hans-Peter Röser, Frank Schäfer, Rudolf Schieder, Ronald Stark, Jürgen Stutzki,Peter van der Wal, Achim Wunsch," **GREAT – The First-Generation German Heterodyne Receiver For SOFIA**", http://www.sofia.usra.edu/Science/publications/spie_2000/ Great.pdf

[6] S. Gulkis', M. Frerkin ', M. Janssen', P. Hartogh',G . Beaudin', T. Koch, Y. Salinas', and C. Kahn1, "MICROWAVE INSTRUMENT FOR THE ROSETTA ORBITER (MIRO)", http://en.scientificcommons.org/20367287

[7] Hartogh, P.: Messung der 142 GHz Emissionslinie des atmosph¨arischen Ozons, PhD thesis, University of Goettingen (1989)

[8] F.J.Harris, "On the Use of Windows for Harmonic Analysis with the Discrete Fourier Transform", Proceeding if the IEEE, Vol.66, No.1, January 1978.

[9] F.J.Harris "On the Use of Windows for Haramonic Analysis", Proceedings of the IEEE, Vol66, No.1, Jan, 1978

Chapter 8
Conclusions

8.1 Conclusions

A conventional sweep spectrum analyzer has the property that is called 'over sweep-rate response'. This property was mentioned by many authors [1][2][3] and expressed in Eq.(2.41) and (2.42). In the super sweep method, the IF signal was digitized and converted into the base band signal whose bandwidth was wider than the resolution bandwidth (RBW). The base band signal is inputted into the negative chirp filter. Author expected that the negative chirp filter would reduce the over sweep-rate response even in the case of the faster sweep rate than that of the conventional method. In our experiment, author confirmed that the over sweep-rate response was reduced.

In Chapter 1, the outline of spectrum analyzers is summarized. The purpose of this thesis described here is to reduce the over sweep-rate response and achieve faster measurement.

In Chapter 2, author investigated the signal processing and mathematical model of the sweep method of spectrum analyzers. Author described the cause of the over sweep-rate response. The analysis of this chapter introduces the idea of the super sweep method. Some characteristics of the FFT method were mentioned in this chapter.

In Chapter 3, the theory and the signal processing system of the super sweep method are described. Author employed the negative chirp filter as the resolution filter, which reduced and canceled the over sweep-rate response.

In Chapter 4, author described the experiment system. In the system, author used a conventional spectrum analyzer as the RF down converter, and designed and made the DSP unit, and used the PC as a display and a controller. Author provided the optimized environment to drive the negative chirp filter, and measured the spectrum of CW signal by changing the normalized sweep rate *1/k*.

In Chapter 5, the results of the experiment produced from chapter 4 were described. The results plotted the peak level and the broadening of the resolution bandwidth against the *1/k*. Author verified that the new method reduced the over sweep-rate response, and achieved the fast sweep rate 10 or 30 times faster than traditional sweep methods. Author confirmed that the sweep rate was proportional to the bandwidth *Flt*, which is the bandwidth of the IF signal just front of the resolution filter.

In Chapter 6, several interesting properties and characteristics of the new method were described. Author verified that the new method was a derivation of the Chirp Z-transform. A comparison of spectrum measurement methods is described at the end of this chapter.

In Chapter 7, author investigated the characteristics of the super sweep method as a spectrometer used in a radio telescope. Author observed some radio astronomical body using the experimental

system, and described result and discussion. Author suggested that the super sweep method has a possibility of a spectrometer in a radio astronomy.

In conclusion, author and his group made break through in the restriction of the sweep rate of a spectrum analyzer using the super sweep method. Our further work is to study the characteristics of the new method in further detail.

8.2 The representative contributions

Author invented and verified the architecture of the super sweep method, which is a method to measure spectrum of a signal. The new method kept the merits of the sweep method and achieved the fast measurement. The measurement rate (sweep rate) was proportional to the IF bandwidth, *Flt*.

The abscissa of the spectrum obtained through the new method showed not only a frequency but also a time. This property is a merit of the sweep method against the FFT method, and it can provide operators more information of measured signals changing conditions such as sweep time and the RBW.

The dynamic range of the experimental system was superior to the conventional spectrum analyzer R3264. The level of the noise floor was –120dBm or under at RBW 1Hz. The new method did not reduce the performance of the system, but improved them.

Author suggested the system to achieve the fast operation in section 6.2.5. We took attention to the noise of the system to achieve the performance of the system in section 6.8.3. In the super sweep method, we need to reduce the noise of IF signal. In traditional analog IF method, the noise does not remain on the spectrums.

Author expect that the super sweep method should be used to measure spectrum for test of EMI (Electro Magnetic Interference), detecting unlicensed radio stations and tests of a spurious of radio set, which demands to measure a wideband spectrum and an adequate resolution. In conventional sweep method, these measurements would need long measurement time. The new method is suitable to measure a purity of CW oscillators, which need fine resolution such as RBW=1Hz.

Author used the experimental system to observe the radio signal of W49N and G9.67+2.0 as the radio telescope spectrometer, and verified the advantage against a sweep spectrum analyzer. The SNR of the results were approximately half of the built-in FFT system at the integral time, one sec. These were satisfied as a monitor.

A spectrum of a signal is presented by Fourier transform of the signal. But we cannot escape from the principle of the ‘uncertainty principle’. The Fourier transform of the signal exists as an ideal and imaginary measurement. Although we can never observe the spectrum of the signal, we can observe it under the restriction of the uncertainty principle; the product of the resolution and measurement time is constant; $\Delta f \times \Delta t = \text{constant}$.

We have several methods using digital signal processing to obtain a spectrum such as FFT, Chirp Z-Transform, MEM etc. A sweep method is popular to measure radio frequency signal. But the

sweep method has the restriction which is called the over sweep-rate response described in Chapter2. This restriction is not cased by the uncertainty principle. Therefore, the sweep method needs longer measurement time than the FFT method and other methods at fine frequency resolution.

By the super sweep method, we can cancel the over sweep-rate response and approach the restriction of the measurement to the uncertainty principle.

Finally, the idea and architecture is under the protection of the patent [4]. This patent was applied to U.S.A and other primary nations.

Reference

[1] Morris Engelson “Spectrum Analyzer Theory and Applications” Artech House publishers Oct. 1974
[2] George D. Tsakiris “Resolution of a spectrum analyzer under dynamic operations” Rev. Sci. Instrum., Vol.48, No.11, Nov. 1977 pp.1414-1419
[3] R.A.Witte “Spectrum and Network measurement”, 1993 Prentice-Hall,Inc
[4]Japanese Patent office, Patent Number ３３３８３７０（Ｐ３３３８３７０）

Chapter 9
List of Publications

【Journal Paper：First Author】

1. 「掃引式ｽﾍﾟｸﾄﾗﾑ･ｱﾅﾗｲｻﾞの信号処理」（長野昌生）
   高速信号処理応用技術学会誌　Vol.3 No.4　pp.17-24 (2000.12)

2. 「FFT を用いたスペクトラム・アナライザの IF フィルタ」（長野昌生）
   高速信号処理応用技術学会誌　Vol.4 No.1　pp.20-27 (2001.3)

3. 「超掃引方式のｽﾍﾟｸﾄﾗﾑ･ｱﾅﾗｲｻﾞ」
   高速信号処理応用技術学会誌　Vol.4 No.2　pp.20-27 (2001.6)

4. N.Nagano, T.Onodera, M.Sone, “Experimental Evaluation of the Super Sweep Spectrum Analyzer”, IEICE TRANS. FUNDAMENTALS, VOL. E91-A, No. 3 MARCH 2008

【International Conference】

1．“Approximation polynomial for Discrete Signal” （Masao Nagano）
   International Workshop on Signal Processing Applications & Technology,2000 , October 20-21, 2000

【Conference】

1. 「超掃引方式スペクトラム・アナライザの提案」(長野昌生、中田寿一)（㈱アドバンテスト）
   高速信号処理応用技術学会 2000 年春季研究会 講演論文集

2. 「周波数ドメインによる高速クロックジッタの測定法」（長野昌生）（㈱ディスクウェア）
   高速信号処理応用技術学会 2001 年秋季研究会 講演論文集

3. 「各種スペクラム演算法の処理時間と演算量の検討」(長野昌生)（㈱ミッシュインターナショナル）
   高速信号処理応用技術学会 2002 年春季研究会 講演論文集 pp.15-21

4. 「DA 方式の FIR フィルタによる複素フィルタの高速化」(長野昌生)（㈱高速信号処理研究所）
   高速信号処理応用技術学会 2005 年研究会 講演論文集 pp.30-31

5．「車載型 ETC 電界強度測定装置の開発」(長野昌生)（㈱高速信号処理研究所）
   高速信号処理応用技術学会 2006 年研究会 講演論文集 pp.53-54

【Commercial Magazine】

1. 「スペクトラム・アナライザによる隣接チャンネル漏洩電力測定について」（長野昌生）
自衛無線ネットワーク　第 18 号　1996-3　　自営無線ユーザ協会

2. 「処理ポイント無制限の DFT」（長野昌生）（超電導工学研究所）
超電導応用研究所(東京電機大学)/ハイテク・リサーチ・センター研究報告(1999)　pp91-92

3. 「ソフトウェア無線に必要な超伝導 A/D 変換器の性能」長野昌生
平成 11 年度　新エネルギー・産業技術総合開発機構委託
－超電導応用基盤技術研究開発－ 総合調査研究
超電導応用基盤技術動向調査委員会　第 4 小委員会報告「デジタル応用」
平成 12 年 5 月　p23-p30　　財団法人 国際超電導産業技術研究センター

4. 「ソフトウェア無線実現のキーデバイス」　長野昌生
MPP(Microwave Photonics Products) No3. 2002 JUN COSMO Liberty Co.

5. 「ディジタル無線通信における信号処理の基礎」　（長野昌生）
Interface Sep. 2002 p161-p175 CQ 出版

6. 「デジタル無線通信における高速演算デバイス　解説論文」(長野昌生)
高速信号処理応用学会誌　vol.6 No.1 (2003.3)

7. 「ディジタル変調／復調の基礎と原理」（長野昌生）（㈱高速信号処理研究所）
Interface Sep. 2004 pp.90-p104 CQ 出版

8. 「信号処理から理解するスペクトラム・アナライザの原理
第１回　掃引式スペクトラム・アナライザ編」（長野昌生）
Interface June. 2005 pp.132-139 CQ 出版

9. 「信号処理から理解するスペクトラム・アナライザの原理
第２回　FFT 式スペクトラム・アナライザの基礎的な使い方編」（長野昌生）
Interface Aug. 2005 pp.146-152 CQ 出版

10. 「信号処理から理解するスペクトラム・アナライザの原理
第３回　FFT 式スペクトラム・アナライザーマニアックス編」（長野昌生）
Interface Sep. 2005 pp.196-203 CQ 出版

11. 「もっとつかいこなしたい人のためのスペクトラム・アナライザのメカニズム
第１回　ディジタル IF 方式の原理と問題」（長野昌生）
Interface Jan. 2006 pp.161-172 CQ 出版

12. 「もっとつかいこなしたい人のためのスペクトラム・アナライザのメカニズム
第２回　過掃引現象を解決－ “超”掃引式スペクトラム・アナライザ」（長野昌生）
Interface Feb. 2006 pp.143-150 CQ 出版

13. 「もっとつかいこなしたい人のためのスペクトラム・アナライザのメカニズム
第 3 回(最終回) 過掃引現象の解決－ 実装と実験」(長野昌生)
Interface Mar. 2006 pp.118-127 CQ 出版

【Seiminor】

1. 「ディジタル無線通信における信号処理の基礎」長野昌生
MST2000 DSP シンポジウム D3
2000 年 11 月？日 東京ファッションタウンにて
高速信号処理応用技術学会主催

２.「ディジタル無線通信における高速演算デバイス」長野昌生
Embedded Technology 2002 DSP シンポジウム
D3 2002 年 11 月 20 日
パシフィコ横浜 アネックスホール F206 にて
高速信号処理応用技術学会主催

【Conference Collaboration】

1. 「超掃引方式による高速スペクトラム・アナライザの製作」(小野寺俊雄、長野昌生)
高速信号処理応用技術学会 2003 年春季研究会 講演論文集

2. 「高速掃引を可能にするスペクトラム・アナライザの開発」
2004 年 3 月 電子情報通信学会 総合大会（小野寺俊雄、長野昌生）

【International Conference 共著】

"Development of High Speed Sweep Spectrum Analyzer by Complex Filters" GSPx 2004 Conference（Toshio Onodera, Masao Nagano）
GSPx 2004 Santa Clara, California, September 27-30, 2004